



Department of Applied Chemistry

**ELABORATION OF A KINETIC MODEL IN ORDER TO PREDICT THE
MOLECULAR AND ISOTOPIC COMPOSITION OF NATURAL GAS GENERATED
DURING THE THERMAL CRACKING OF HYDROCARBONS**

Luc FUSETTI

This thesis was presented as part of the French-Australian scientific 'co-tutelle' scheme to
obtain the Degrees of Doctor of Philosophy of:

Curtin University of Technology (Perth, Australia)

And

Pierre et Marie Curie University (Paris, France)

The thesis was defended in IFP headquarters (Rueil-Malmaison, France) on the 5th of June 2009
in front of the following jury:

Reporter 1 : **Prof. Pierre CARTIGNY**, IPG Paris

Reporter 2: **Prof. Éric VILLENAVE**, Bordeaux I University

Examiner 1 : **Dr. François MONTEL**, TOTAL

Examiner 2: **Prof. François BAUDIN**, Pierre et Marie Curie University

Australian Academic Supervisor: **Prof. Kliti GRICE**, Curtin University of Technology

Industry Supervisor: **Dr. Françoise BEHAR**, IFP

French Academic Supervisor: **Prof. Sylvie DERENNE**, Pierre et Marie Curie University

DECLARATION

To the best of my knowledge and belief, this thesis contains no material previously published by any other person except where due acknowledgement has been made.

This thesis has been undergone under the co-tutelle scheme for French-Australian scientific cooperation (*c.f.* appendix IV of the manuscript for copies of the agreements). It is this scheme that has enabled the double Degree of Doctor of Philosophy of Curtin University of Technology (Perth, Australia) and Pierre et Marie Curie University (Paris, France) to be awarded.

This thesis contains no material which has been accepted for the award of any other degree or diploma in any university.

Luc Fusetti

Date: 20/07/2009

Signature:

ABSTRACT

The scope of the present study was to validate an approach that could be used to elaborate a model that would predict the $\delta^{13}\text{C}$ of the gases generated during thermal cracking of oil. The attention was focused on C_{14} methylaromatics and alkylaromatics but the entire methodology was demonstrated on one component *i.e.* 1,2,4-trimethylbenzene.

Pyrolysis experiments at temperatures of 395, 425, 450, and 475 °C and at a pressure of 100 bar were performed in order to study the whole range of conversions. All pyrolysis fractions were recovered and quantified. All identified products were also quantified individually. A free-radical mechanism until 70% conversion of 1,2,4-trimethylbenzene was achieved. This mechanism was then used to characterize some CH_4 generation pathways at 425 and 200 °C. In both cases the identified pathways included: (i) demethylation of 1,2,4-trimethylbenzene into xylenes (and to a lesser extent demethylation of xylenes into toluene), (ii) dimerization of monoaromatics, (iii) intramolecular ring closure reaction of dimers into triaromatics.

In a second step, the free-radical mechanism was used to constrain the chemistry of a simpler lumped kinetic model predicting CH_4 generation under laboratory and geological conditions for the whole range of conversions. The resulting scheme was composed of four pathways P_i for methane generation: Reactant \rightarrow Dimers (P_a), Reactant \rightarrow Xylenes (P_b), Dimers \rightarrow {Prechar + Char} (P_c), and Xylenes \rightarrow Dimers + Toluene (P_d). Optimization yielded activation energies in the range of 50-60 kcal/mol, and frequency factors in the neighbourhood of 10^{12} s^{-1} . Simulations revealed that P_b and P_c led to the greatest amounts of CH_4 below 5% conversion, followed by P_a . Above 5% conversion, CH_4 generated *via* P_c became dominant but P_a and P_b were also found to be of importance. Contribution of P_d was found to be negligible, except for when 100% conversion was almost reached. Simulations under geological heating rates revealed that significant amounts of CH_4 were generated by methylated monoaromatics in deeply buried reservoirs and that methylated monoaromatics thus had a higher thermal stability than their polyaromatic counterparts but lower than the saturated hydrocarbons. CH_4 yield was also modelled using a unique stoichiometric equation ($\text{CH}_{4\text{max}} = 7.6 \text{ wt\%}$ per methyl group) associated with $E_a = 58.5 \text{ kcal/mol}$ and $A = 10^{11.96} \text{ s}^{-1}$, showing relative similarities to other reported values for methylated polyaromatics.

In the final stage, P_a , P_b , and P_c were selected as relevant contributions to $\delta^{13}\text{C}_{\text{CH}_4}$ until 100% conversion. Kinetics for the generation of $^{12}\text{CH}_4$ and $^{13}\text{CH}_4$ were then expressed separately and implemented into the lumped model. Optimization yielded a ratio of frequency

factors $\Omega = 1.028$, variations of activation energy ΔE_i in the range of 36-79 cal/mol (kinetic effect); and a $\delta^{13}\text{C}_p$ of CH_4 precursor groups equal to -32.7‰ (precursor effect). Simulations performed under geological heating rates illustrated the greater isotopic fractionation of CH_4 generated under geological conditions compared with laboratory conditions. The comparison at high maturity with $\delta^{13}\text{C}_{\text{CH}_4}$ during thermal cracking of 1-methylpyrene and mature kerogen under the same simulation conditions emphasized the need to determine the magnitude of the precursor effect for natural compounds.

FRENCH SUMMARY

ELABORATION D'UN MODELE CINETIQUE EN VUE DE PREDIRE LA COMPOSITION MOLECULAIRE ET ISOTOPIQUE DES GAZ NATURELS ISSUS DU CRAQUAGE DES HYDROCARBURES

L'objectif de cette étude était de valider une approche qui pourrait permettre l'élaboration d'un modèle prédisant le $\delta^{13}\text{C}$ des gaz générés durant le craquage de l'huile. L'attention était focalisée sur les aromatiques méthylés et alkylés mais la méthodologie complète a été démontrée dans le cas du 1,2,4-triméthylbenzène.

Des pyrolyses à $T = 395, 425, 450, \text{ et } 475\text{ }^\circ\text{C}$ ($P = 100\text{ bar}$) ont été menées afin d'étudier toute la gamme de conversions en 1,2,4-triméthylbenzène. Toutes les fractions issues de la pyrolyse ont été récupérées et quantifiées. Tous les produits identifiés ont été quantifiés individuellement.

Un modèle mécanistique a ensuite été validé pour des conversions allant jusqu'à 70%. Ce modèle a été utilisé pour caractériser des voies de genèse de CH_4 à 425 et à 200 $^\circ\text{C}$. Dans ces deux cas, les voies identifiées ont été : (i) la déméthylation du réactif en xylènes et dans une moindre mesure celle des xylènes en toluène, (ii) la dimérisation des monoaromatiques, (iii) la cyclisation intramoléculaire des dimères en triaromatiques.

Dans un deuxième temps, le modèle mécanistique a été utilisé pour contraindre la chimie d'un modèle lumpé plus simple mais permettant de prédire la genèse de CH_4 en conditions de laboratoire et en conditions géologiques pour toute la gamme de conversions. Le schéma cinétique obtenu était composé de 4 voies de genèse: Réactif \rightarrow Dimères (P_a), Réactif \rightarrow Xylènes (P_b), Dimères \rightarrow {Préchar + Char} (P_c), et Xylènes \rightarrow Dimères + Toluène (P_d). L'optimisation a abouti à des énergies d'activation dans la gamme 50-60 kcal/mol et des facteurs de fréquence dans le voisinage de 10^{12} s^{-1} . Les simulations ont montré que P_b et P_c , suivis de P_a , produisaient les plus importantes quantités de CH_4 en dessous de 5% de conversion. Au-delà de 5% de conversion, le CH_4 généré *via* P_c était majoritaire mais les contributions de P_a et P_b restaient non négligeables. La part de P_d était en revanche toujours anecdotique excepté en approchant 100% de conversion. D'autres simulations réalisées pour des conditions géologiques montrèrent que des quantités importantes de CH_4 étaient générées par les monoaromatiques méthylés dans les réservoirs profondément enfouis (HT) et que les monoaromatiques méthylés avaient donc une stabilité supérieure à leurs homologues polyaromatiques mais inférieure aux hydrocarbures saturés. La genèse du CH_4 a également

été simulée au moyen d'une équation stoechiométrique unique ($\text{CH}_{4\text{max}} = 7,6 \text{ wt}\%$ par groupe méthyle) associée à $E_a = 58,5 \text{ kcal/mol}$ et $A = 10^{11,96} \text{ s}^{-1}$, montrant une relative similitude avec d'autres valeurs publiées pour des polyaromatiques méthylés.

Dans la dernière étape, P_a , P_b , et P_c ont été conservées comme les voies régissant $\delta^{13}\text{C}_{\text{CH}_4}$ jusqu'à 100% de conversion. Les cinétiques de genèse de $^{12}\text{CH}_4$ et $^{13}\text{CH}_4$ ont été exprimées individuellement et incorporées au modèle cinétique lumpé. L'optimisation a abouti à un rapport des facteurs de fréquence $\Omega = 1,028$, à des variations d'énergie d'activation ΔE_i dans la gamme 36-79 cal/mol (effet cinétique) et à un $\delta^{13}\text{C}_p$ des groupes précurseurs de CH_4 égal à -32,7‰ (terme source). D'autres simulations réalisées pour des conditions géologiques ont illustré le caractère plus prononcé du fractionnement isotopique par rapport aux conditions de laboratoire. La comparaison à haute maturité avec $\delta^{13}\text{C}_{\text{CH}_4}$ durant le craquage thermique du 1-méthylpyrène et du kérogène mature a montré la nécessité de quantifier le terme isotopique source pour les composés naturels.

A mes proches et tout spécialement à ma mère, à ma soeur et à mon père pour leur soutien inconditionnel durant mes études.

ACKNOWLEDGEMENTS

For this PhD I was officially funded by the IFP (France). I thus want to thank Dr Françoise Béhar, my industry supervisor from the Geochemistry Department of the IFP, who guided me through this scientific challenge. Her constant expectations in terms of scientific rigour and innovation played the role of making me the scientific person I am today. There were some hard times and arguments but there were also unforgettable moments of satisfaction, especially when the three successive models showed accuracy in their predictions. I also thank Françoise for her tremendous personal investment during the writing of this thesis and the writing of the three papers.

I can not miss out Prof. Kliti Grice from Curtin University of Technology (Australia) in this series of acknowledgments. As my co-supervisor during this joint PhD, Kliti managed to organise the full availability of the isotopic analysis equipment in her group during each of my stay there. This material comfort enabled me to fit the mountain of required analyses in the tight schedule and thus undeniably played a major role in the success of this work. On the personal side, Kliti provided tireless effort, tremendous encouragement, and pertinent scientific guidance over the past three years. She will no longer be my supervisor but will remain a very close friend after this PhD.

To conclude with my three supervisors, I thank Prof. Sylvie Derenne from Université Pierre et Marie Curie, my academic supervisor in France. Since I was located most of the time either at IFP or at Curtin University, it has not been easy for Sylvie to keep in touch with the progress of this work but she successfully managed to do it. My full access to the GCMS facilities of her laboratory also played a strategic role with the identification of the compounds that enabled the elaboration of the mechanistic model.

Apart from the ‘official’ track of supervisors, Paul-Marie Marquaire (ENSIC), Roda Bounaceur (ENSIC), and François Lorant (IFP) are gratefully acknowledged. Their technical training, their enthusiasm, and their tremendous scientific competence, were a substantial added value to the papers for which they are co-authors.

Regarding the lab side, I would like to thank all the persons directly involved in this work: Christelle Anquetil (Université Pierre et Marie Curie), Raymond Berthou (IFP), Geoff

Chidlow (Curtin University), Claudette Leblond (IFP), Carole Vivargent (IFP trainee) and Sue Wang (Curtin University) for their technical assistance which was the indefectible foundation of this work.

I would like to thank Bernard Colletta and Rémi Eschard who successively welcomed me within the Geology-Geochemistry-Geophysics Division of the IFP. I also thank Frank Haeseler, the head of the Geochemistry Department, who brought me support and motivation on a daily basis.

I would like to thank Prof. Robert Kagi who welcomed me to the Centre of Applied Organic Geochemistry (Curtin University), which has now grown into the Western Australian Organic and Isotope Geochemistry Centre under the direction of Prof. Kliti Grice.

I am indebted to the Australian Academy of Science and the French Embassy in Australia for financial support *via* the PhD-Cotutelle Travel Award.

I address a huge thank to all the former colleagues and people I met in different occasions who, even they were not directly involved in this work, provided me the punctual assistance, advices, and encouragements that undeniably played a major role in the success of this three-year race. I am too scared to forget some names so I will not attempt writing them down but please be sure that you all have my best feelings.

Eventually, I would like to conclude this section of acknowledgements by thanking François Baudin (Université Pierre et Marie Curie), Pierre Cartigny (IPG Paris), François Montel (TOTAL S.A.), and Éric Villenave (Université Bordeaux I) who made me the honour to examine this work.

SCIENTIFIC COMMUNICATIONS ARISING FROM THIS STUDY

Publications:

Fusetti, L., Behar, F., Bounaceur, R., Marquaire, P.M., Grice, K., Derenne, S., 2009a. New insights into secondary gas generation from oil thermal cracking: methylated monoaromatics. A kinetic approach using 1,2,4-trimethylbenzene. Part I: A free-radical mechanism. *Organic Geochemistry*, *accepted and revision in progress*.

Fusetti, L., Behar, F., Grice, K., Derenne, S., 2009b. New insights into secondary gas generation from oil thermal cracking: methylated monoaromatics. A kinetic approach using 1,2,4-trimethylbenzene. Part II: A lumped kinetic scheme. *Organic Geochemistry*, *accepted and revision in progress*.

Fusetti, L., Behar, F., Lorant, F., Grice, K., Derenne, S., 2009c. New insights into secondary gas generation from oil thermal cracking: methylated monoaromatics. A kinetic approach using 1,2,4-trimethylbenzene. Part III: A stable carbon isotope fractionation model. *Submitted to Organic Geochemistry*.

Patents:

Fusetti, L., Behar, F., Lorant, F., 2007. Méthode pour déterminer l'origine compositionnelle d'un gaz issu d'une dégradation thermique de matières carbonnées. French patent FR2915807 and European patent EP1988393.

Fusetti, L., Behar, F., Lorant, F., 2008 Method for determining a gas compositional origin from carbon material thermal degradation. US patent US20080306695.

Conferences:

Fusetti L., Behar F., Grice K. and Derenne S., 2007. Methane and ethane generation from oil cracking: first isotopic modelling based on ¹³C-labelled compounds. 23rd International Meeting on Organic Geochemistry (IMOG), Torquay, UK.

Fusetti L., Behar F., Grice K. and Derenne S., 2007. Elaboration of a kinetic model to predict the carbon isotope fractionation of hydrocarbon gases produced during oil cracking. Energy Day, Edmonton, Canada.

Fusetti L., Behar F., Grice K. and Derenne S., 2007. Methane and ethane generation from oil secondary cracking in high pressure-high temperature reservoirs: isotopic modelling based on ^{13}C -labelled compounds. AAPG Hedberg Conference; Basin Modelling Perspectives, The Hague, The Netherlands.

TABLE OF CONTENTS

Abstract	1
French summary	3
Acknowledgements	5
Scientific communications arising from this study	7
Table of contents	9
General introduction	11
Chapter I: Framework	
<i>Part A: The generation, migration and accumulation of petroleum fluids in sedimentary basins</i>	
1. Formation of kerogen	17
2. Generation of petroleum fluids	20
3. Migration and accumulation of petroleum fluids	21
4. Composition of petroleum fluids in natural reservoirs	
4.1 Crude oils	22
4.2 Gases	23
<i>Part B: Kinetic modelling of the thermal cracking of oil and related components</i>	
1. Principles of kinetic modelling	24
2. Thermal cracking of model compounds	
2.1 Thermal cracking of saturated hydrocarbons	24
2.2 Thermal cracking of aromatic compounds	27
3. Thermal cracking of oils	
3.1 Kinetic models	30
3.2 Influence of pressure	32
3.3 Chemical interaction between oil components	32
4. Use of kinetic models in basin modelling	33
<i>Part C: Modelling carbon isotope fractionation occurring during thermal cracking</i>	
1. Stable isotope geochemistry	
1.1 Stable isotopes	35
1.2 Standards and notations	35
1.3 Stable isotope analysis	36
1.4 Stable carbon isotopes in organic matter	36
2. Stable carbon isotope fractionation of gases	
2.1 Equilibrium isotopic effect	38
2.2 Kinetic isotopic effect	39
<i>Part D: Research strategy</i>	44
Chapter II: Experimental and Choice of the initial chemical system	
<i>Part A: Experimental</i>	
1. Pyrolysis conditions	49
2. Recovery and analysis of pyrolysis products	
2.1 Gaseous products	49
2.2 Liquid and solid products	51

3. Data processing	
3.1 Mass balances	55
3.2 Conversion	56
3.3 ¹³ C balances	56
Part B: Choice of the initial chemical system	
1. C ₁₄ -aromatics: first step to a kinetic model predicting δ ¹³ C of secondary gases	58
2. A chemical system composed of methylaromatics and alkylaromatics	58
3. From a chemical system of 7 model compounds to a system of 2 model compounds	60
Chapter III:	63
Fusetti, L., Behar, F., Bounaceur, R., Marquaire, P.M., Grice, K., Derenne, S., 2009a. New insights into secondary gas generation from oil thermal cracking: methylated monoaromatics. A kinetic approach using 1,2,4-trimethylbenzene. Part I: A free-radical mechanism. <i>Organic Geochemistry, accepted and revision in progress.</i>	
Chapter IV:	111
Fusetti, L., Behar, F., Grice, K., Derenne, S., 2009b. New insights into secondary gas generation from oil thermal cracking: methylated monoaromatics. A kinetic approach using 1,2,4-trimethylbenzene. Part II: A lumped kinetic scheme. <i>Organic Geochemistry, accepted and revision in progress.</i>	
Chapter V:	135
Fusetti, L., Behar, F., Lorant, F., Grice, K., Derenne, S., 2009c. New insights into secondary gas generation from oil thermal cracking: methylated monoaromatics. A kinetic approach using 1,2,4-trimethylbenzene. Part III: A stable carbon isotope fractionation model. <i>Submitted to Organic Geochemistry.</i>	
Chapter VI: Conclusions and Perspectives	
Part A: Conclusions	155
Part B: Suggestions for further work	159
Appendix I: Experimental data	163
Appendix II: Synthesis of new model compounds	171
Appendix III: References	181
Appendix IV: PhD co-tutelle agreements between <i>Université Pierre et Marie Curie</i> and <i>Curtin University of Technology</i>	205

GENERAL INTRODUCTION

Natural gas, a key source of energy for the future

Despite the fact that gaseous hydrocarbons have been historically identified as a possible energy resource for about 1800 years, the first industrial natural gas business only started during the 19th century, in the United States of America. The important increase in energy demand after the First World War mainly benefited the oil industry; the interest for gas remained limited for many years particularly because of its high transport cost. However, since the 80's, the popularity of natural gas as an energy source has increased. Technological improvements enabling the storage of Liquefied Natural Gas (L.N.G.) or the conversion of natural gas into synthetic fuel *via* Gas to Liquid (G.T.L.) processes have led to a reduction in transportation costs and high energy efficiency in power generation. Moreover, since gas combustion produces less carbon dioxide than oil and coal and thus poses less environmental concerns, natural gas is regarded as a key source of energy for the future.

Natural gases are ubiquitous products generated at different stages of organic matter burial. Biogenic methane can be generated in shallow sediments where bacterial activity is still possible ($T < 80\text{ }^{\circ}\text{C}$), whereas at higher depths thermal cracking of organic matter (kerogen or oil) can lead to thermogenic gas production. Tools to improve and help to predict the origin of natural is vital in a period facing an exponential increase of exploration costs in parallel to a huge volatility in the price of the barrel.

Layout of the thesis

$\delta^{13}\text{C}$ analysis of individual gases such as methane, ethane, propane, and carbon dioxide is regarded as a key analytical tool to classify natural gas with respect to its origin and post genetic history. Recent studies have been employed to establish models predicting the $\delta^{13}\text{C}$ of gases generated during thermal cracking of kerogen.

The scope of the present study was to validate an original integrated approach that could be applied to elaborate a model that would predict the $\delta^{13}\text{C}$ of the gases generated during the thermal cracking of oil. This thesis report comprises six chapters.

Chapter I consists of four parts (A, B, C, and D) which set the framework of the thesis. Part A describes the processes which influence the composition (molecular and isotopic) of the gas fraction found in reservoir-rocks. Part B tackles kinetic modeling associated with the thermal cracking of oil or individual components of oil. The fundamental principles behind isotopic fractionation and associated models that are used to predict stable carbon isotope fractionation for gases generated from the thermal cracking of organic matter are discussed in

part C. Based on observations described in parts A, B, and C; part D describes the purpose of the research strategy and overall aims of the thesis.

The following four chapters report the results which were obtained following the methodology described under the research strategy section. Chapter II summarises all the experimental conditions and also reports on how the initial chemical system considered for this study was determined. Chapters III, IV, and V actually represent three papers submitted to peer-reviewed international journals. Chapter III presents the elaboration and calibration of a free radical mechanism describing the thermal cracking of a chosen chemical system under laboratory conditions. The simplification of this mechanism into a lumped kinetic model was then extrapolated to other temperatures and these form the results and discussions in Chapter IV. Finally in Chapter V, the isotope fractionation was implemented into equations obtained from the previous kinetic model to obtain a new model to predict the $\delta^{13}\text{C}$ of methane generated at all temperatures.

Chapter VI consists of the overall conclusions of the thesis. In addition some suggestions for further work are recommended.

All experimental data as well as results obtained from calculations for all compounds quoted in this report are shown in Appendix I.

All quoted references are listed in Appendix III.

CHAPTER I:

Framework

PART A: THE GENERATION, MIGRATION AND ACCUMULATION OF PETROLEUM FLUIDS IN SEDIMENTARY BASINS

Organic geochemistry is the study of organic matter in sedimentary rocks. It attempts to understand its composition, origin, formation, modes of deposition and distribution, as well as its interaction with minerals. More specifically, petroleum organic geochemistry is concerned with the processes involving sedimentary organic matter leading to the formation and accumulation of crude oil and natural gas. These processes include the input, accumulation and preservation of organic matter in depositional environments, its burial history in the sediment, and eventually its alteration under thermal stress (maturation) in the subsurface which can lead to the formation of liquid and gaseous hydrocarbons.

The following paragraph summarizes the basic concepts and terms used by petroleum organic geochemists to describe processes leading from the deposition of organic matter to the generation, migration, and accumulation of petroleum fluids found in reservoir-rocks.

1. Formation of kerogen

Life consists of three domains: Prokaryotes, Eukaryotes, and Archeae. When these organisms die the lipids, lignin (in land plants only), proteins and carbohydrates they contain (De Leeuw and Largeau, 1993) sink through the water column. The majority of this organic matter is reincorporated into the biological carbon cycle and only 0.1% to 1% of the organic carbon (especially lipids and lignin) becomes preserved in sediments (Durand, 1980 and 2003; Tissot and Welte, 1984). However, the residential time of carbon present in sediments beneath the subsurface is much longer (several million to several hundred of millions of years) than that of carbon that exists in the oceanic-atmospheric system of the surface of the Earth (several years and still on-going). The mass of carbon contained in sediments is consequently very substantial and estimated to about 10^{16} tons compared to the estimated 10^{12} tons of carbon that exists in living biomass at the surface of the Earth (Durand, 1980; Waples, 1981; Tissot and Welte, 1984).

After deposition, sediments are progressively buried. Sediments rich in organic matter are deposited in environments with anoxic bottom water conditions *i.e.* less than 0.1 ml/l of dissolved oxygen (Demaison and Moore, 1980). Anoxic bottom waters exist in enclosed seas, bays, lagoons, lakes, where the access of oxygen to the sedimentation environment is restricted, and coastal zones with upwelling. River deltas installed in areas of abundant vegetation are also very favourable environments, because the very abundant plant debris are

quickly buried and therefore escape the action of aerobic bacteria. The phenomenon of burial and lithification of sediments is called subsidence. The accumulation of sediments strata leads to the formation of a sedimentary basin. During burial, pressure increases because of the weight of accumulated sediments which provokes a compaction and a reduction of porosity. Moreover, temperature also increases due to a temperature gradient within the sediment column, the average of which is 30 °C/km and the range between 10 °C/km to 50 °C/km approximately (Sallé and Debyser, 1976) depending on the basin and its history.

The first stage describing the evolution of freshly deposited organic matter is referred to as diagenesis (Tissot and Welte, 1984). A main characteristic of diagenesis is the loss of functional groups, of nitrogen, and of oxygen within organic matter (Huc, 1980). It differs from the succeeding stages since it occurs in a restricted depth range of subsidence (usually less than a kilometre below the water-sediment interfaces) and at low temperatures (below 60 °C). The transformations undergone by sedimentary organic matter during diagenesis are thus related to physico-chemical and biochemical processes rather than thermal processes. Under such conditions, bacterial activity is still substantial and engenders the generation of biogenic methane (Rice and Claypool, 1981; König, 1992). Polycondensation reactions within organic matter lead to the formation of fulvic and humic acids. Some living organisms such as microalgae generate insoluble macromolecules which are very resistant to physico-chemical and biochemical degradation processes, keeping their outer walls structure intact while the other components of organic matter undergo degradation and mineralization. Such selective preservation has been recently demonstrated to play a key role in the formation of some kerogens containing thin lamellar structures (Berkaloff et al., 1983; Largeau et al., 1986; Derenne et al., 1991). In sulfate-rich and anaerobic depositional environments, sulfur incorporation may take place. Indeed, sulfate-reducing bacteria can generate H₂S which in turn reacts with lipids and carbohydrates (Sinninghe Damsté and De Leeuw, 1990; Sinninghe Damsté et al., 1998). Sulfur incorporation is characterized by the reticulation of alkyl chains *via* sulfur atoms, generating complex kerogens which are very resistant to bacteria.

At the end of diagenesis, all the previous processes have led to the transformation of sedimentary organic matter into two fractions called kerogen and bitumen. Kerogen is a high molecular-weight residue and is defined (Durand, 1980; Tissot and Welte, 1984) as the fraction of macromolecular organic matter dispersed in sedimentary rocks that is solid and insoluble in usual organic solvents (*e.g.* chloroform, dichloromethane). Bitumen is thus the fraction of the resultant organic matter that is soluble in usual organic solvents. Three types of kerogens are generally distinguished, according to the nature of the organic matter they

contain and the depositional environment of the sediments which led to their formation (Durand and Espitalié, 1973; Tissot et al., 1974; Tissot and Welte, 1984). These kerogens types have different atomic ratios O/C and H/C whose evolution is represented in the van Krevelen (1961) diagram (Figure I.1).

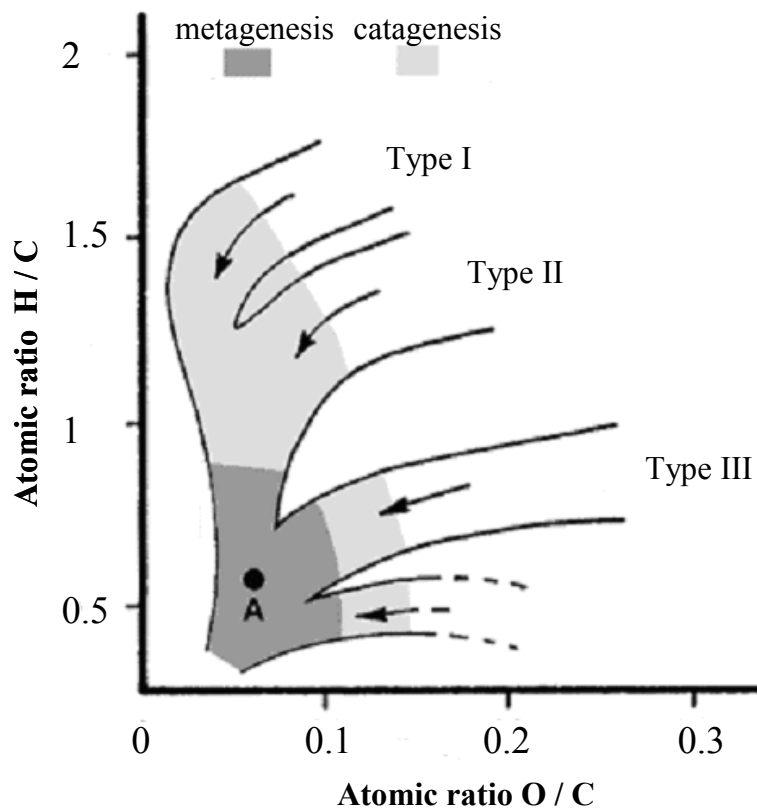


Figure I.1. van Krevelen diagram (after Durand and Monin, 1980)

- (i) Type I kerogen contains a high proportion of organic matter derived from the outer walls of microalgae found in evaporitic/lacustrine lakes. It consists of a highly of aliphatic structure rather than aromatic, and it is characterized by a high H/C (> 1.5) and a low O/C (between 0.03 and 0.1). This type of kerogen is quite rare (e.g. Green River shales, Utah, USA) and it possesses a high petroleum potential and it can produce hydrocarbons up to 80% of its weight during burial.
- (ii) Type II kerogen is very common and contains organic matter derived from marine phytoplankton, zooplankton and bacteria deposited in sags or epicontinental seas. It is more enriched in naphthenic and aromatic structures than Type I and thus its hydrogen index is lower ($H/C \approx 1.3$) as well as its petroleum potential. It also contains more oxygen than Type I ($O/C \approx 0.15$). It may contain a high proportion

of sulfur and is then called Type II-S (*e.g.* Miocene Monterey formation, California, USA) which is sometimes classified as a fourth type of kerogen. Type II kerogen (*e.g.* lower Toarcian shales, Paris Basin, France) may produce hydrocarbons up to 30 % of its weight during burial.

- (iii) Type III kerogen originates from debris of terrestrial higher plants accumulated in deltas of streams having a dense vegetation (equatorial areas for instance). It is thus highly enriched in aromatic structures (residues of lignin), oxygen ($0.2 < O/C < 0.4$) and depleted in hydrogen ($H/C < 0.9$). Such kerogen (*e.g.* shales from the Mahakam Delta, Indonesia) has a low oil potential but can generate substantial amount of gas if buried at high depths.

2. Generation of petroleum fluids

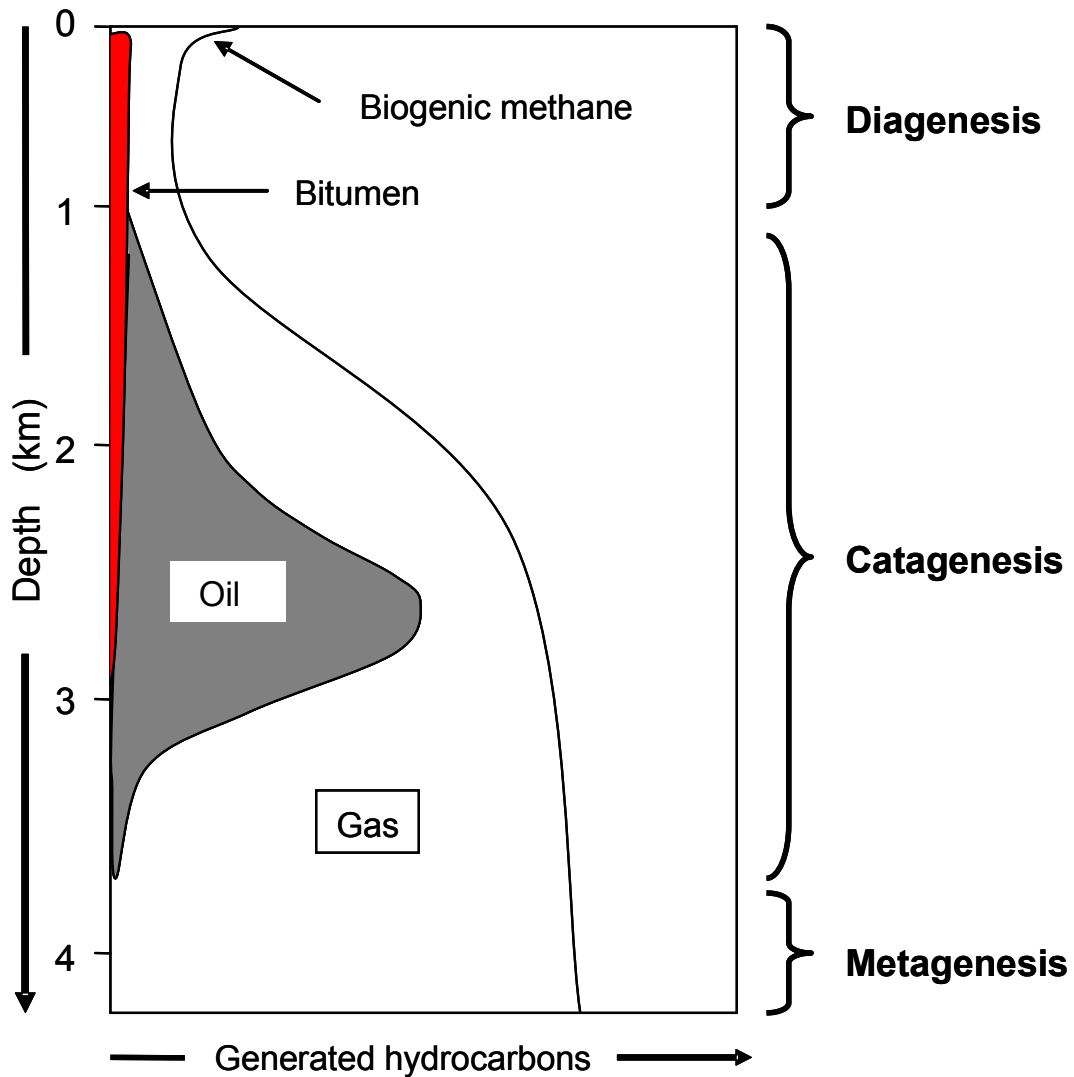


Figure I.2. Generation of oil and gas during thermal maturation of kerogen (after Tissot and Welte, 1984)

When subsidence proceeds kerogen undergoes increasing temperature and pressure. The first stage of thermal maturation is called catagenesis and takes place over a depth range that can reach (Figure I.2) nearly 4 kilometres below the sediment/water interface (temperatures are comprised approximately between 60 °C and 150 °C). As shown on the van Krevelen diagram (Figure I.1), catagenesis results in a sharp decrease in H/C, corresponding to the liberation of hydrocarbons (Durand, 1980) and an increase in aromatisation (Pelet, 1980; Vandenbroucke and Largeau, 2007). The kerogen, which loses between 50 wt% and 90 wt% during catagenesis, indeed generates oil and an associated gas (early primary cracking). Partial thermal cracking of the oil (secondary cracking) which has not yet been expelled may also occur to lead to gas generation. As shown on Figure I.2 catagenesis is characterized by an oil-window with the formation of oil passing through a maximum yield (Hunt, 1996). A source rock is a rock that can expel hydrocarbons during the stage of catagenesis (Durand, 1980; Tissot and Welte, 1984).

Metagenesis is the second stage of thermal maturation and takes place at temperatures higher than 150 °C. Residual kerogen undergoes high temperature thermal cracking (late primary cracking). Methane is the only gaseous product generated significantly (dry-gas window) and its yield decreases during this stage (Figure I.2). At the end of metagenesis (dot A Figure I.1), solid residues tend to have a structure resembling graphite (Hunt, 1996).

3. Migration and accumulation of petroleum fluids

Due to the increasing weight of the sedimentary column, the volume of the rock and its thickness decrease: this is called compaction. Oil and gas can be expelled when the quantity generated reaches a certain threshold of saturation within the porous network of the source-rock (*i.e.* a certain proportion of the porosity is occupied by hydrocarbons, the rest being occupied by water): this is called primary migration.

After expulsion from the source-rock, petroleum fluids can migrate away from the source-rock: this is called secondary migration. Pools of petroleum may be formed if hydrocarbons are eventually prevented from further migration reaching a permeability barrier (cap rock, faults which put an impermeable layer in front of the drain, strong decrease in grain size of the drainage layer) in a permeable reservoir-rock and therefore accumulate in this trap. Crude oils trapped in reservoir-rocks for several millions of years may be subjected to temperatures above 130-140 °C. In these conditions, some components of oil become thermally unstable. Such secondary cracking (as opposed to primary cracking of the kerogen)

generates compounds of lower and higher molecular-weight, the ultimate products being pyrobitumen and methane. Improving our understanding of the mechanisms generating secondary gas is the purpose of the present work and Part B of this chapter is thus a separate literature review dedicated to studies tackling this topic.

If oil fluids do not meet a barrier of permeability during secondary migration, they can migrate towards the surface. Petroleum fluids may also leak from the trap: this is called tertiary migration. Near the surface, petroleum undergoes biodegradation and water washing. Indeed, some bacteria brought up by meteoritic water can utilise some hydrocarbons as an energy source *via* their oxidation into carboxylic acids. Biodegradation increasingly alters molecules in quasi-step wise fashion: *n*-alkanes > *iso*-alkanes > alkylcycloalkanes > alkylbenzenes > bicycloalkanes > steranes > hopanes > diasteranes > tricyclic terpanes > triaromatic steroids and porphyrins (Hunt, 1996) and thus degrade the quality of crude oils by increasing their concentration of heavy compounds. Water-washing is due to the water soluble nature of certain components present in crude oils and is particularly important for light hydrocarbons such as benzene and toluene (Palmer, 1993).

4. Composition of petroleum fluids in natural reservoirs

4.1. Crude oils

Crude oils consist of saturated hydrocarbons, aromatic hydrocarbons, NSO compounds, and (in some cases) metal porphyrin complexes containing vanadium, nickel and occasionally iron (Hunt, 1996).

Saturated hydrocarbons can be further divided into aliphatic and cycloaliphatic hydrocarbons. Aliphatic hydrocarbons comprise normal and branched alkanes. Cycloaliphatic hydrocarbons comprise monocyclic (*e.g.* alkylcyclopentanes, alkylcyclohexanes), and multi-ring aliphatic compounds (*e.g.* hopanes, steranes).

Molecules classified in aromatic hydrocarbons comprise strictly aromatic compounds (ranging from benzene to polycyclic aromatic hydrocarbons containing up to five aromatic rings), their methylated and alkylated counterparts, hydroaromatic hydrocarbons, and aromatics containing heteroelements. Sulfur, which is mainly present in thiophenic type structures, account for 2 wt% of the aromatic fraction of Type II-S crude oils.

NSO compounds are polar compounds containing heteroatomic elements (mainly nitrogen, sulfur and oxygen) in addition to carbon and hydrogen. They comprise molecules

such as alcohols, phenols, fatty acids, resins, and asphaltenes. Resins and asphaltenes are polycyclic heteroatomic structures of high molecular weight in the range 300 g/mol to 1000 g/mol and around 10,000 g/mol, respectively (Tissot and Welte, 1984). Asphaltenes precipitate in contact with a non polar solvent (commonly *n*-heptane).

The composition of crude oil in the reservoir rock depends on the type of source rock and changes with time and geothermal conditions. Tissot and Welte (1984) classified crude oils according to the percentage of their main components and linked them to the depositional environment (Figure I.3).

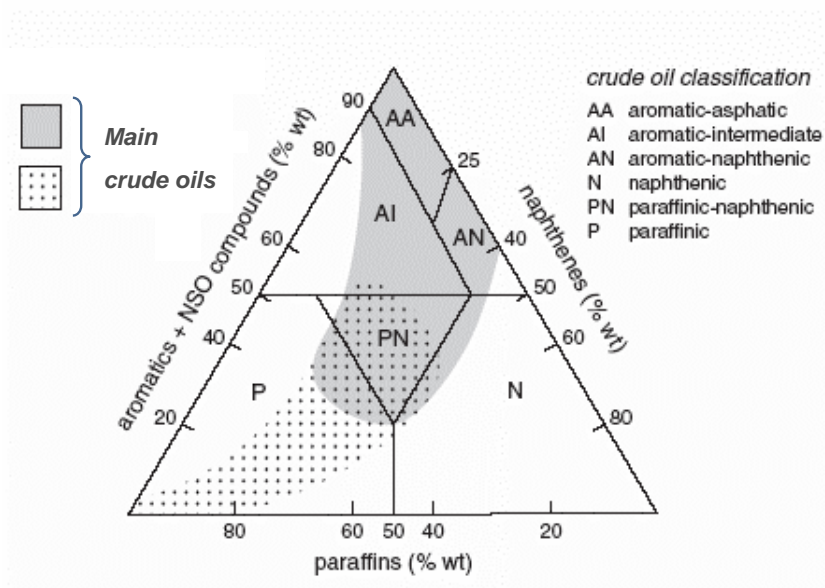


Figure I.3. Classification of crude oils according to their percentage of naphthenes, paraffins and aromatics + NSO (after Tissot and Welte, 1984).

4.2. Gases

Natural gas is the fraction of petroleum fluids in reservoir rocks which is gaseous under temperature and pressure conditions met at the surface. Natural gas is mainly made of methane (CH₄), carbon dioxide (CO₂) and molecular nitrogen (N₂). Some other chemical species such as C₂-C₄ hydrocarbons and hydrogen sulphide (H₂S) may account for substantial amounts in the composition of natural gas. Traces of inert gases (He, Ne, Ar) can also be reported. The presence of molecular hydrogen (H₂) and carbon monoxide (CO) is very rare.

The origin of such components can be multiple. We already evoked thermogenic gas (primary and secondary) and biogenic gas but inorganic sources (atmosphere, volcanoes, geothermal sources, and radioactivity) can also account for the generation of some species found in natural gas.

PART B: KINETIC MODELLING OF THE THERMAL CRACKING OF OIL AND RELATED COMPONENTS

1. Principles of kinetic modelling

Whether thermogenic gases are formed through primary or secondary processes, accumulations of these components are the result of a combination of thermal cracking reactions from several sources within the organic matter matrix. It is widely accepted (e.g. Tissot and Welte, 1984) that the thermal evolution of oil is controlled by the kinetics of these cracking reactions. To express rate constants k , the semi-empirical Arrhenius equation is commonly considered as an adequate approximation over the considered range of temperature:

$$k = A \cdot \exp(-E_a/R \cdot T)$$

Where A = frequency factor (or pre-exponential factor in s^{-1}), E_a = activation energy (in $J \cdot mol^{-1}$), $R = 8.314 J \cdot mol^{-1} \cdot K^{-1}$, and T = temperature (in K).

This allows petroleum geochemists to simulate the low temperature, long residence time of natural processes causing the generation of hydrocarbons ($60\text{ }^\circ\text{C} < T < 220\text{ }^\circ\text{C}$ for millions of years) by performing laboratory studies at higher temperatures ($250\text{ }^\circ\text{C} < T < 550\text{ }^\circ\text{C}$ for a few hours to a few weeks).

Some studies have focused on specific compounds present in crude oils whilst others have attempted to work on molecular fractions and in certain cases have worked on the whole oil alone.

2. Thermal cracking of model compounds

2.1. Thermal cracking of saturated hydrocarbons

a) Saturated model compounds

The thermal cracking of saturated hydrocarbons was first studied with pioneering publications of Rice (1931 and 1933), Rice and Herzfeld (1934), and Kossiakoff and Rice (1943). Tilicheev (1939), Voge and Good (1949), and Yu and Eser (1997a and 1997b) then attempted to empirically correlate the rate constant of thermal cracking of n -alkanes to the number of carbon of the aliphatic chain. Watanabe et al (2001) also estimated rates constants

for n -alkanes ranging from n -C₃ to n -C₃₂ using Kossiakoff and Rice theory (1943). They demonstrated that thermal instability of n -alkanes increased with their chain length (Figure I.4).

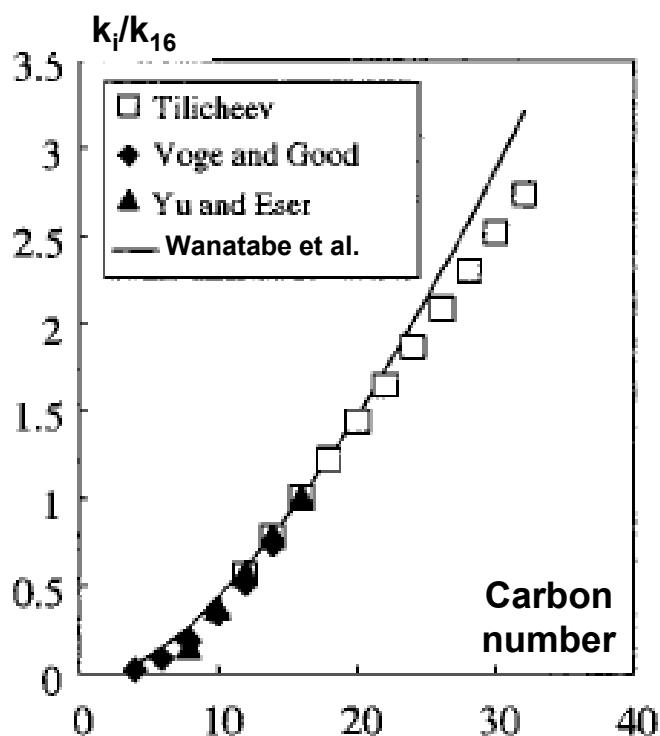


Figure I.4. Ratios of the rate constant k_i of thermal decomposition of n -alkanes (containing i carbon atoms) to the rate constant k_{16} of thermal decomposition of n -C₁₆ (after Watanabe et al., 2001).

Numerous studies were proposed on specific model compounds such as n -C₅ (Bonnier and Gaudemaris, 1962), n -C₆ (Dominé, 1989 and 1991; Dominé et al., 1990; Dominé and Enguehard, 1992), n -C₈ (Lannuzel, 2007), n -C₁₄ (Song et al., 1994), n -C₁₆ (Fabuss et al., 1962; Doué and Guiochon, 1968; Groenendyk et al., 1970; Ford, 1986; Khorasheh and Gray, 1993; Jackson et al., 1995; Wu et al., 1996; Watanabe et al., 2001; Burklé-Vitzthum, 2001), and n -C₂₅ (Behar and Vandenbroucke, 1996). Kinetic models were proposed with for example the mechanistic model of Dominé and Enguehard (1992) describing thermal cracking of n -hexane (n -C₆) and the empirical one of Behar and Vandenbroucke (1996) for thermal cracking of n -pentacosane (n -C₂₅). Table I.1 lists some available values of global activation energies E and frequency factors A for the thermal cracking of n -tetradecane (n -C₁₄), n -hexadecane (n -C₁₆) and n -pentacosane (n -C₂₅). Results show that the average range of activation energies is between 60 kcal/mol and 74 kcal/mol and that of frequency factors between 10^{14} s⁻¹ and 10^{19} s⁻¹.

Products generated from the thermal cracking of saturates are mainly constituted of saturated compounds of lighter molecular weight with minor traces of aromatic compounds (Rice, 1931 and 1933; Voge and Good, 1949; Doué and Guiochon, 1968; Ford, 1986; Zhou et al., 1987; Dominé, 1989; Bounaceur et al., 2002a).

Compound	Reference	E (kcal/mol)	A (s ⁻¹)
<i>n</i> -C14	Song et al., 1994	67.6	7.2*10 ¹⁸
<i>n</i> -C16	Ford, 1986	59.6	3.1*10 ¹⁴
<i>n</i> -C16	Khorasheh and Gray, 1993	61.2	1.5*10 ¹⁵
<i>n</i> -C16	Jackson et al., 1995	74.0	3.0*10 ¹⁹
<i>n</i> -C25	Behar and Vandenbroucke, 1996	68.2	6.1*10 ¹⁷

Table I.1: Global E and A obtained on the n-C₁₄, n-C₁₆ and n-C₂₅.

b) Influence of pressure

The role of pressure on thermal cracking is still a matter of debate. Voge and Good (1949) stated that an increase in pressure accelerated cracking reactions of paraffins at high temperature. On the contrary, Jackson et al (1995) observed a continuous retarding effect for *n*-hexadecane pyrolysis between 120 bar and 600 bar at low temperature. Dominé (1989 and 1991), Dominé et al (1990), Dominé and Enguehard (1992) also found out that the effect of pressure is not independent from the temperature stating that the inhibiting effect due to a pressure increase was all the more substantial as temperature was lower. However, thermal cracking of paraffins was found to be accelerated in many studies at P < 400 bar, a retardation effect was observed at higher pressures (Fabuss et al., 1964; Dominé, 1989 and 1991; Dominé et al., 1990; Dominé and Enguehard, 1992; Behar and Vandenbroucke, 1996; Yu and Eser., 1997a and 1997b; Lannuzel, 2007). Behar and Vandenbroucke (1996) calculated that in geological conditions, for depths less than 4000 m, the influence of pressure on thermal cracking of heavy paraffins was negligible. It only started to have an accelerating effect between 4000 m and 6000 m and in high-pressure/high-temperature reservoirs (6000 m, 200

°C, and 1000 bar) thermal cracking of those compounds was inhibited compared to laboratory conditions.

2.2. Thermal cracking of aromatic compounds

a) *Aromatic model compounds*

Thermal cracking of molecules classified as part of the aromatic fraction of oil (see Part A, §4.1) was investigated more recently (*e.g.* Smith and Savage, 1991, 1992, 1993, and 1994) but literature is rich in studies on various compounds like benzene (Louw and Lucas, 1973; Brooks et al., 1979; Bruinsma et al., 1988), toluene (Zimmerman and York, 1964; Gräber and Hüttinger, 1982; Brouwer et al., 1988; Bruinsma et al., 1988; Rao and Skinner, 1989; Jess, 1996; Taralas et al., 2003; McClaine and Wornat, 2007; Lannuzel, 2007), ethylbenzene (Crowne et al., 1969; Clark and Price, 1970; Brooks et al., 1982; Davis, 1983; Mizerka and Kiefer, 1986; Domke et al., 2001), butylbenzene (Freund and Olsmtead, 1989; Yu and Eser, 1998a), decylbenzene (Burklé-Vitzthum et al., 2003), dodecylbenzene (Behar et al., 2002), *n*-pentadecylbenzene (Savage and Klein, 1987), tetralin (Poutsma, 1990 and 2002; Grigor'eva et al., 1991; Yu and Eser, 1998b; Bounaceur et al., 2000), 2-ethyltetralin (Savage and Klein, 1988), 1-methynaphthalene (Yang and Lu, 2005; Leininger et al., 2006), 2-methynaphthalene (Yang and Lu, 2005), 1-, 2- and 9-methylanthracenes (Smith and Savage, 1993), 9,10-dimethylanthracene (Virk and Vlastnik, 1992), 9-methylphenanthrene (Behar et al., 1999), 1-methylpyrene (Smith and Savage, 1992; Lorant et al., 2000), 1-dodecylpyrene (Savage, 1995), 2-dodecyl-9,10-dihydrophenanthrene (Savage and Baxter, 1996), dibenzothiophene (Dartiguelongue et al., 2006). Table I.2 lists some available values of global activation energies and frequency factors for a series of aromatic compounds. Results show that, in contrast to saturated hydrocarbons, both E and A are shifted to lower values; *i.e.* 47 kcal/mol to 62 kcal/mol and 10^9 s^{-1} to 10^{14} s^{-1} , respectively.

Compound	Reference	E (kcal/mol)	A (s ⁻¹)
Tetralin	Yu and Eser, 1998b	58.0	3.5*10 ¹²
2-Ethyltetralin	Savage and Klein, 1988	53.5	5.0*10 ¹²
2-Dodecyl-9,10-dihydrophenanthrene	Savage and Baxter, 1996	54.5	4.0*10 ¹³
Ethylbenzene	Domke et al., 2001	62.3	4.7*10 ¹³
Butylbenzene	Freund and Olmstead, 1989	52.9	1.1*10 ¹²
Dodecylbenzene	Behar et al., 2002	53.3	1.3*10 ¹³
Pentadecylbenzene	Savage and Klein, 1987	55.5	1.1*10 ¹⁴
1-Methylnaphthalene	Leininger et al., 2006	47.4	7.9*10 ⁹
9-Methylphenanthrene	Behar et al., 1999	49.0	4.5*10 ¹⁰
Dibenzothiophene	Dartiguelongue et al., 2006	59.0	1.9*10 ¹¹

Table I.2: Global E and A obtained on various aromatic model compounds.

It is also worth noting that the two different ranges of A and E proposed in literature for saturates and aromatics lead to a reverse relative thermal stability between the high (> 300 °C-500 °C) and the low temperature range (< 200 °C). For example, when simulating (Behar and Vandenbroucke, 1996; Behar et al., 1999, 2002) thermal cracking of dodecylbenzene (DDB), 9-methylphenanthrene (9-MPh) and *n*-pentacosane (*n*-C₂₅), the Arrhenius plots cross each other at around 300 °C (Figure I.5). Dodecylbenzene is the most unstable compound under laboratory and geological conditions. In contrast, *n*-C₂₅ decomposes faster than 9-MPh under laboratory conditions, whereas it is much more stable at low temperature. This means that when increasing thermal stress saturates/aromatics ratio will continuously decrease under laboratory conditions whereas it will continuously increase under geological conditions. Moreover, as illustrated with the kinetic parameters proposed by Dartiguelongue et al (2006) for thermal cracking of dibenzothiophene, compounds containing sulfur are relatively stable

under geological conditions hence explaining the substantial quantities of such compounds found in mature oils (Marynowski et al., 2002).

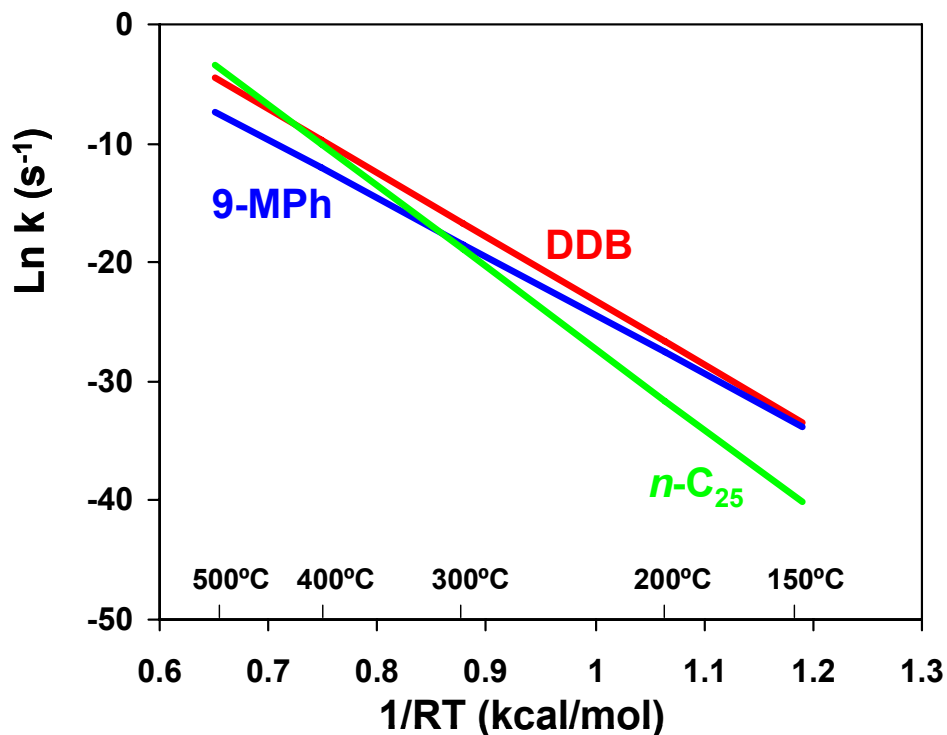


Figure I.5. Arrhenius diagram obtained on selected model compounds (Behar and Vandembroucke, 1996; Behar et al., 1999, 2002)

The extent of the delocalization of Π -electrons has an influence over the rate of decomposition of aromatics. Several studies showed a correlation between the rate of decomposition of the aromatic and its Dewar number (Smith and Savage, 1991; Leyssale, 1991). Indeed, as shown in Table I.2 the rate of decomposition increases when comparing alkylbenzenes with methylthalene and methylphenanthrene.

When aromatics possess a side-chain its length influences their rate of decomposition. The longer the chain, the faster the decomposition as the number of hydrogen atoms potentially able to be abstracted increases (*e.g.* Robaugh and Stein, 1981). This conclusion is illustrated with kinetic parameters giving increasing rates of decomposition for compounds ranging from tetralin to ethyltetralin and from ethylbenzene to pentadecylbenzene (Table I.2).

The main thermal reaction for alkyl aromatics is the breakdown of the side chain in β -position. The difference in bond-energies (Figure I.6) indeed preferably induces homolysis of the C_{α} - C_{β} bond. It leads to the generation of saturates on the one hand and of methylated aromatics on the other hand (Freund and Olmstead, 1989; Savage and Klein, 1987, Savage

and Korotney, 1990; Poutsma, 1990; Smith and Savage, 1993; Burnham et al., 1998; Behar et al., 2002; Burklé-Vitzthum et al., 2003). Then, methylated compounds lead to the subsequent demethylated and dimethylated aromatics and undergo polycondensation reactions through a complex reaction network (Smith and Savage, 1993; Dartiguelongue et al., 2006; Leininger et al., 2006) to form aromatic structures with heavier molecular weight than that of the reactant. With increasing thermal maturity, the number of aromatic rings of the generated aromatics increases leading to molecules more depleted in hydrogen. When the molecular size is large enough, the polyaromatic structures are no more soluble in organic solvent such as dichloromethane (DCM) and precipitate as a solid residue.

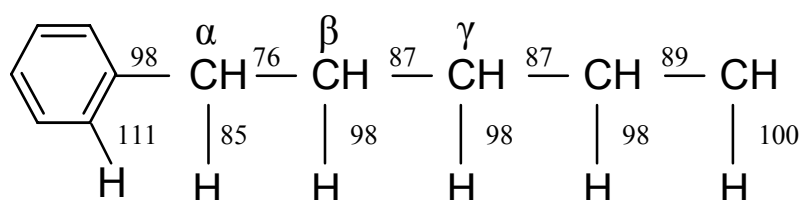


Figure I.6. Bond dissociation energies (in kcal/mol) for an alkylbenzene (after Savage, 2000).

b) Influence of pressure

The specific effect of pressure on aromatics is also a matter of debate. Dominé (1991) studied thermal cracking of *n*-butylbenzene at 305 °C and 357 °C with pressure ranging from 210 bar to 15,400 bar. The author found out that pressure hindered the cracking process. However, this conclusion was not confirmed by Al Darouich et al (2006b) when they pyrolysed a mixture of light aromatic compounds at 375 °C and at pressures of 400 bar, 800 bar and 1,200 bar. A slight acceleration of the global rates was observed with increasing pressure.

3. Thermal cracking of oils

3.1. Kinetic models

Burnham (1991) proposed a kinetic scheme for thermal cracking of oils generated from artificially matured kerogens. The model was based on parallel reactions including both Gaussian and discrete distributions of activation energies comprised between 55 kcal/mol and 63 kcal/mol. Frequency factors were ranging between 10^{14} s^{-1} and 10^{17} s^{-1} . In the approaches of Dieckmann et al (2000), and Braun and Burnham (1990 and 1992) the kinetics derived for

oil cracking were dependent on those derived for kerogen cracking. Moreover, the chemical distribution of the pyrolysis products was dependent on the heating rates chosen for experimentations.

In other studies, natural reservoir oils were directly subjected to pyrolysis experiments. Horsfield et al (1992) determined the global kinetics of the conversion of oil to gas and this study was completed with a study on 4 other oils by Schenk et al (1997). Resulting activation energies were ranging from 66 kcal/mol to 70 kcal/mol and a constant frequency factor of $1.1 \times 10^{17} \text{ s}^{-1}$ was assigned. For the global transformation of oil into gas, Pepper and Dodd (1995) however proposed the value of 10^{14} s^{-1} for their constant frequency factor. They pointed out that the optimised distribution of activation energies was highly dependent on parameters related to oil composition such as the ratio of saturates to aromatics. A compositional model was proposed by Behar et al (1991a and 1991b) to describe thermal degradation of oil conversion into gas, light hydrocarbons, polyaromatics, and prechar. The same frequency factor was assigned to all unstable classes. Despite being calibrated on experimental data, this model showed no accuracy to predict oil thermal cracking under laboratory conditions since even at such high pyrolysis temperatures (365 °C - 500 °C) only the thermal cracking of compounds present initially in the oil was considered but secondary cracking reactions were ignored. Moreover, the choice of a constant frequency factor (A) whatever the chemical class was too simplistic since recent published data on model compounds clearly showed different set of kinetic parameters for saturates and aromatics (Tables I.1 and I.2). An improved kinetic scheme was proposed by Vandenbroucke et al (1999) using various frequency factors. Kuo and Michael (1994) proposed a kinetic model for oil cracking which was calibrated on the experiments of Behar et al (1991a and 1991b). Unfortunately they did not take into account secondary cracking reactions. Complementary work providing an understanding of the main thermal reactions occurring during oil cracking was published by Hill et al (2003). A detailed study was performed on the thermal cracking of the light aromatic fraction of Type II oil (Al Darouich et al., 2006a). After fractionating such initial C₆-C₁₄ aromatic fraction into alkylaromatics (48 wt%), methylated aromatics (19 wt%), BTXN (14 wt%) and naphthenoaromatics (19 wt%), a kinetic scheme was proposed for each individual class. The optimised A and E values were in the same range as those previously proposed for model compounds, ranging from 10^{11} s^{-1} to 10^{13} s^{-1} and 49 kcal/mol to 60 kcal/mol, respectively. The most unstable aromatics (alkyl and naphtheno aromatics) were shown to be converted into gas and methylated aromatics. Polyaromatics of higher molecular-weight were observed and the kinetics for their thermal degradation into methane and char

were constrained by two distributions of activation energies (49.2-49.4 kcal/mol, 54.4-55.2 kcal/mol) and a single frequency factor ($5.1 \times 10^{11} \text{ s}^{-1}$). Behar et al (2008b) focused on the thermal stability of heavy chemical classes such as C_{14+} saturates, C_{14+} aromatics and NSOs (resins and asphaltenes) in Type II oil. Activation energies and frequency factors were respectively in the range 47-54 kcal/mol and 10^{10} - 10^{13} s^{-1} for the C_{14+} aromatics, 64-68 kcal/mol and 10^{16} s^{-1} for the C_{14+} saturates, and 50-54 kcal/mol and 10^{12} s^{-1} for the NSOs. The model gave satisfying results for predicting global conversions and yields of generated products obtained with laboratory experiments. When extrapolated to geological conditions, the prediction was not in contradiction with observed field data *i.e.* aromaticity increasing above 140 °C and C_{14+} saturates starting to decrease above 170 °C-180 °C.

3.2. Influence of pressure

Kressman (1991) showed that in the case of a binary mixture {*n*-hexane + 2,4-dimethylpentane} the reaction of thermal decomposition was accelerated when pressure increased from 100 bar to 2,000 bar. The opposite result was observed for a binary mixture {*n*-hexane + benzene}. However, in both cases it was found that pressure increased the formation of heavy products (C_5 - C_{13} and C_{14+}) but inhibited the formation of the light ones (C_2 - C_4). The author did not notice any correlation between pressure and temperature effects. Hill et al (1996) only found a relatively small influence of pressure over thermal cracking of the C_{9+} fraction of a Devonian oil from Alberta basin enriched in saturates and emphasized that temperature was the main parameter which influenced thermal cracking.

3.3. Chemical interaction between oil components

An oil being a complex mixture of various chemical structures, it is important to determine if chemical classes react independently from each other or if chemical interactions influence the global kinetics of the thermal cracking process.

It was demonstrated that saturated hydrocarbons do not influence each other during the thermal cracking process (Billaud et al., 1983; Yu and Eser, 1997b). Shah et al. (1973) reported an inhibition of *n*- C_9 thermal cracking in the presence of pent-2-ene. Burnham et al (1995 and 1998), labelled *n*-hexadecane and dodec-1-ene and mixed them with various natural oils. They observed a delay on the global conversion of *n*-hexadecane, the amplitude of which was dependent on the chemical composition of the oil in which it was mixed. The same experimental approach was followed by Mc Kinney et al (1998) for studying the global conversion of both labelled *n*- C_{25} and 9-methylphenanthrene mixed either in a marine or in

continental-derived oil. Despite delayed conversion of n -C₂₅ was also observed, the impact on the global activation energy was only a shift of 1 kcal/mol and no change for the frequency factor was observed. Results also demonstrated that the global conversion of 9-methylphenanthrene was only slightly accelerated. Smith and Savage (1994) found out that alkylphenanthrenes and alkylphenanthrenes did not influence thermal cracking of other aromatics, as opposed to alkylanthracenes which accelerated it. However, the latter being present in very low amounts in natural oils, their effect was concluded to be negligible. Other studies (Baronnet et al., 1971; Khorashesh and Gray, 1993; Razafinarivo, 2006; Lannuzel, 2007) showed that toluene may inhibit thermal cracking of paraffins, especially at low pressure. Bounaceur et al, (2002b) established a free radical mechanism based on experimental data of Burklé-Vitzthum (2001) who had found out a stabilizing effect of tetralin over hexadecane pyrolysis. Dominé et al (2002) confirmed such inhibitor effect of tetralin over alkanes and showed that it was lower than that of toluene. Burklé-Vitzthum et al (2003 and 2004) suggested that long-chain alkylbenzenes may inhibit rather than accelerate the cracking of alkanes in natural hydrocarbon mixtures. Dartiguelongue (2006) did not characterize any influence from dibenzothiophene over the rate of decomposition of n -C₁₆ and showed a slight acceleration when replacing dibenzothiophene with 4-methyldibenzothiophene. Behar et al (2008b) found kinetic parameters of heavy chemical classes of oil such as C₁₄₊ saturates and C₁₄₊ aromatics to be relatively close to those obtained for model compounds, showing that a potential mixture effect did not change the conversion of global chemical classes.

4. Use of kinetic models in basin modelling

As shown above, despite the huge variety of chemical components constituting crude oils, the development of kinetic models describing their thermal degradation passes through the simplification of the system by 'lumping' individual molecules bearing similar structural features and thermal reactivity, into same chemical classes which are very often represented by a single model compound. The next step is then the implementation of such models into basin simulators which reconstruct the geological and thermal events in sedimentary basins that lead to the formation of oil and natural gas fields. Improving such knowledge is indeed of tremendous importance since it reduces risk in hydrocarbon-potential assessment, especially with the current financial climate facing an exponential increase of exploration costs in parallel to a huge volatility in the price of the barrel. However, to be implemented into basin simulators, kinetic schemes need to be limited in reaction numbers and have to allow a

reliable extrapolation to their prediction for low temperatures met under geological conditions. Accordingly, two complementary types of kinetic models are generally proposed:

- (i) Mechanistic models are based on free-radical reactions (*e.g.* Dominé et al., 2002; Leininger et al., 2006; Dartiguelongue et al., 2006). These models describe chemical phenomena using elementary reactions (involving known compounds) associated with kinetic parameters which can thus be extrapolated to other temperatures, including those that occur under geological conditions. Unfortunately, despite simplification *via* the 'lump' of species of similar reactivity, the numerous free-radical chemical equations involved do not facilitate the implementation of these models into basin simulators.
- (ii) Empirical models are based on global stoichiometric equations associated with kinetic parameters calibrated on the basis of global observations obtained from laboratory experiments (*e.g.* Behar et al., 2008b). These models consist of a limited number of chemical equations which facilitate their implementation into basin simulators. However, the extrapolation of these models' prediction to geological conditions is controversial since the stoichiometric equations and their associated kinetic parameters represent global experimental results observed at high temperatures which are the sum of elementary processes. Consequently, if some chemical processes are inactive at high temperatures, this global description is unable to account for these processes' influence at low temperatures even though they might be of critical importance to properly model thermal cracking phenomena under geological conditions.

The aim of the present work was to take advantage of the complementarities offered by the two previous approaches.

PART C: MODELLING CARBON ISOTOPE FRACTIONATION OCCURRING DURING THERMAL CRACKING

1. Stable isotope geochemistry

1.1. Stable isotopes

Isotopes can be divided into two types; stable and unstable (radioactive species). Stable isotopes as opposed to radiogenic (unstable) isotopes do not decay, thus their overall natural abundances (Table I.3) generally remain relatively constant. Stable isotope geochemistry is based upon the relative and absolute concentrations of the elements and their stable isotopes on Earth. There are a number of stable isotopes of interest to organic geochemists but the stable isotopes of carbon and hydrogen are used the most frequently as natural tracers in sedimentary organic matter because they are usually the most abundant elements and the most easily analysed by compound specific isotope analyses (CSIA). This is a technique commonly used in organic geochemistry studies.

Carbon	Hydrogen	Oxygen	Sulfur	Nitrogen
¹² C (98.891)	¹ H (99.985)	¹⁶ O (99.759)	³² S (95.018)	¹⁴ N (99.634)
¹³ C (1.109)	² D (0.015)	¹⁷ O (0.037)	³³ S (0.750)	¹⁵ N (0.366)
		¹⁸ O (0.204)	³⁴ S (4.215)	
			³⁶ S (0.017)	

Table I.3. Natural abundances (atom %) of some stable isotopes

1.2. Standards and notation

Stable carbon isotope composition is determined not as an absolute isotopic abundance, but as a ratio of heavy isotope (¹³C) to light isotope (¹²C) relative to a standard: the international standard Pee Dee Belemnite (PDB), a marine limestone from the Pee Dee formation in South Carolina (USA). Stable carbon isotope composition is expressed as a delta ($\delta^{13}\text{C}$) in units of per mil (‰) or parts per thousand, and calculated using the following equation:

$$\delta = \left[\left(\frac{R_{\text{sample}}}{R_{\text{standard}}} \right) - 1 \right] \times 1000 \quad (\text{‰})$$

Where *R* is the ratio of heavy to light isotope.

The PDB international standard is thus assigned the value $\delta^{13}\text{C}_{\text{PDB}} = 0\text{‰}$. However, it should be noted that PDB went exhausted and was replaced by calibrating another carbonate (NBS-19) relative to PDB (Urey et al., 1951; Craig, 1957). The new calibration was termed 'VPDB' (Vienna PDB).

1.3. Stable isotope analysis

Stable isotopic compositions are most effectively determined using isotope ratio mass spectrometric (irMS) methods (Hoefs, 1987). The two general methods of analysis are bulk isotope analysis, and the aforementioned CSIA.

a) Bulk isotope analysis

Bulk isotope analysis involves measurement of the stable isotopic composition of the total carbon, hydrogen, oxygen, nitrogen or sulphur within a sample. It thus represents the average isotopic composition of all compounds in complex mixtures. The entire sample undergoes quantitative combustion, oxidation, reduction and/or pyrolysis to convert the element of interest into a gaseous analyte which is amenable to high-precision isotopic analysis by an irMS.

b) CSIA

CSIA involves measurement of the stable isotopic composition of individual compounds in a complex mixture. The development of gas chromatography-isotope ratio mass spectrometry (GC-irMS) allowed online GC separation of components of a complex mixture prior to combustion (or pyrolysis) and analysis of the gas analyte (CO_2 or H_2) by the irMS (Matthews and Hayes, 1978). GC-irMS instruments were developed with the capability of measuring $^{13}\text{C}/^{12}\text{C}$ (Matthews and Hayes, 1978), $^{18}\text{O}/^{16}\text{O}$ and $^{15}\text{N}/^{14}\text{N}$ (Brand et al., 1994), and D/H (Burgoyne and Hayes, 1998).

1.4. Stable carbon isotopes in organic matter

a) Living organisms

Carbon is the fundamental element of all organic compounds. It is an essential element for plants and animals, ultimately derived from atmospheric carbon dioxide assimilated by plants during photosynthesis. Photosynthetic carbon fixation favours ^{12}C . Therefore

biosynthesised organic compounds are in general depleted in ^{13}C relative to their carbon source. The present day environmental distribution of stable carbon isotopes in plants and phytoplankton are controlled by many factors (Hayes, 1993):

- (i) $\delta^{13}\text{C}$ of the carbon source, and its availability,
- (ii) The photosynthetic pathway involved in the uptake of carbon dioxide (*e.g.* Schouten et al., 1998),
- (iii) Isotopic fractionations associated with biosynthesis like lipids versus protein and carbohydrates biosynthesis (*e.g.* Schouten et al., 1998; Grice et al., 2005),
- (iv) Other physiological factors like cell size and geometry (Goericke et al., 1994; Popp et al., 1998), growth rates of phytoplankton (Laws et al., 1995), and the plant-water use efficiency of terrestrial plants (Ehleringer et al., 1993).

The measurement of $\delta^{13}\text{C}$ values of plants is useful in petroleum geochemistry because it can enable the reconstruction of ancient biogeochemical processes related to the carbon cycle in ancient depositional environments (*e.g.* Freeman et al., 1990), which would have played a major role in the production of the source organic matter for present-day reservoirised crude oils.

b) Petroleum

The stable carbon isotope composition ($\delta^{13}\text{C}$) of petroleum components has been used extensively in various areas of petroleum geochemistry such as oil-source rock correlation (*e.g.* Sofer, 1984; Chung et al., 1992; Murray et al., 1994), oil-oil correlation (*e.g.* Bjorøy et al., 1991; Whiticar and Snowdon, 1999; Santos Neto and Hayes, 1999; Harris et al., 2003; Dawson et al., 2007), and gas-source correlation (*e.g.* Stahl and Carey, 1975; Schoell, 1983; Whiticar et al., 1986; Palasser, 2000). Numerous studies have also shown that thermal maturity substantially alter the $\delta^{13}\text{C}$ value of petroleum components (*e.g.* Clayton, 1991b; Clayton and Bjorøy, 1994; Berner and Faber, 1996).

2. Stable carbon isotope fractionation of gases

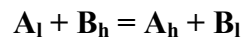
The $\delta^{13}\text{C}$ analysis gases such as methane, ethane, propane, and carbon dioxide is regarded as a key analytical to classify natural gas with respect to its origin and post genetic history (Schoell, 1988; Whiticar, 1994). Pioneering models have empirically linked $\delta^{13}\text{C}$ of gases to maturity (vitrinite reflectance) of respective source rocks (*e.g.* Stahl and Carey, 1975; Chung and Sackett, 1979; Schoell, 1983; Faber, 1987; Berner and Faber, 1996). These results

have provided the backbone of natural gas interpretation carried out in the oil and gas industry showing that the $\delta^{13}\text{C}$ of thermogenic gases was thermally less altered than the $\delta^{13}\text{C}$ of biogenic gases (Rice and Claypool, 1981) ranging from -60‰ to -25‰ and from -90‰ to -55‰, respectively. However, these empirical models faced limitations because they were not based on a fundamental understanding of what governs isotopic fractionation and therefore were not generally applicable to all types of sedimentary basins, gas sources, and thermal histories.

Variations in stable isotopic composition or 'isotopic fractionations' occur in nature as a result of chemical and physical processes, due to different isotopes of an element having subtly different chemical and physical properties (Urey, 1947; Bigeleisen and Mayer, 1947; Bigeleisen, 1949). Equilibrium and kinetic processes have been shown to govern isotopic fractionation.

2.1. Equilibrium isotopic effect

The equilibrium isotope effect occurs as a result of temperature-dependent equilibrium isotope-exchange reactions. These result in a change of the isotope distribution between different chemical substances, phases, or between individual molecules (Hoefs, 1987). For example the equilibrium reaction:



Where subscripts indicate that species A and B contain either the light (l) or the heavy (h) isotope.

In these cases, there is no net change in the chemical system, *i.e.* the products are molecularly identical to the reactants. The difference is that ^{13}C and ^{12}C are distributed differently between them.

The fundamentals of the equilibrium theory are based on β -factors (Urey, 1947; Bigeleisen and Mayer, 1947). At a given temperature, the β factor of a molecule A that contains n atoms X to be isotopically substituted, is defined as the ratio to the power of n between the two partition functions of the isotopically substituted and unsubstituted forms of A. Several formalisms, all based on quantum mechanical calculations, have been proposed to express the partition functions (Urey, 1947; Bigeleisen and Mayer, 1947; Botao and Casanova, 1964; Galimov et al., 1972; Galimov and Ivlev, 1973; Poljakov, 1996).

Regarding hydrocarbons generation, James (1983) considered that the difference between the $\delta^{13}\text{C}$ of generated hydrocarbon gases in sedimentary basins was due to the equilibrium isotope effect. He used the β -factors calculated by Galimov and Ivlev (1973) to establish a diagram by plotting the $\delta^{13}\text{C}$ of gases against a thermal maturity indicator, the Level of Organic Metamorphism (LOM). The LOM was defined by Hood et al (1975) as a function of both time and temperature but the model proposed by James (1983) only accounted for its temperature dependence. This model was questioned in many studies (Jenden et al., 1988; Jenden and Kaplan, 1989; Galimov, 1988; Clayton, 1991a) which considered that the assumption of an isotopic equilibrium to describe the generation of hydrocarbons was not justified.

2.2. Kinetic isotopic effect

a) Principles

According to Bigeleisen (1949), the phenomenon of isotope partitioning during chemical reactions without any further rearrangement is caused by differences between reaction velocities of individual isotope species and is called the ‘kinetic isotope effect’. In a reaction where a reactant A yields products B and C, there may be two (or more) competing unidirectional isotopic reactions to describe the isotope between B and A:



Where k_l and k_h are the rate constants of the reactions yielding to the isotopically light (B_l) and heavy (B_h) forms of B, respectively.

The isotopic fractionation factor α between A and B is then defined as the ratio of the rate constants:

$$\alpha = k_h / k_l$$

Normally, a unidirectional chemical reaction shows a depletion of the heavy isotope in the product compared to the reactant. This is due to the slower reaction rate of the heavier isotopic species. It is indeed easier to break the bonds that contain lighter isotopes because the vibration frequency of such bonds is higher.

Regarding the hydrocarbons generation, it is now widely accepted that stable carbon isotope fractionations (dynamic evolution of $\delta^{13}\text{C}$ as a function of temperature and time) of

thermogenic gases are due to the kinetic isotope effect (Sackett et al., 1966; Sackett, 1968; Frank and Sackett, 1969). Moreover, it was shown (Galimov, 1975) that another effect may influence the $\delta^{13}\text{C}$ of gases. The evidence of this so called 'precursor effect' is to be found when the stable carbon isotope composition of the cumulated gas at the end of the reaction ($\delta^{13}\text{C}_\infty$) differs from the bulk initial stable carbon isotope composition of the reactant ($\delta^{13}\text{C}_o$). The $\delta^{13}\text{C}$ of the generated gas indeed tends to reach the initial stable carbon isotope composition $\delta^{13}\text{C}_p$ of its precursor within the reactant. However, molecules are not isotopically homogeneous and it was for example demonstrated that in substituted aromatics, ^{13}C is preferentially concentrated in the aromatic rings rather than in the alkyl substituents (Galimov, 1975). Consequently, the initial stable carbon isotope composition $\delta^{13}\text{C}_p$ of the gas precursor might differ from the bulk initial stable carbon isotope composition $\delta^{13}\text{C}_o$ of the reactant, causing the precursor effect.

Regarding the dynamic description of $\delta^{13}\text{C}$, models based on a kinetic approach to predict the stable carbon isotope fractionation of hydrocarbon gases generated from thermal cracking of organic matter can be divided into three types.

b) Statistical approach

A first kinetic approach involved statistics. Waples and Tornheim (1978) established a theoretical model to predict the $\delta^{13}\text{C}$ of gases generated during the thermal cracking of *n*-alkanes. Carbon isotope fractionations were accounted using Poisson's statistic law in terms of spontaneous breaking probabilities of carbon-carbon bonds. The breaking probability q_i of a carbon-carbon bond versus time *t* was thus expressed as:

$$q_i = 1 - \exp(-k_i \cdot t)$$

Where k_i was the reaction rate constant ($i=1$ for a $^{12}\text{C}-^{12}\text{C}$, 2 for a $^{13}\text{C}-^{12}\text{C}$ and 3 for a $^{13}\text{C}-^{13}\text{C}$ bond; $k_1 > k_2 > k_3$).

However, the assumptions made by the authors on the isotopic homogeneity within molecules and on the random thermal cleavage of bonds along the carbon chain constituted strong simplifications that yielded to discrepancies between the model prediction and observed experimental data.

c) Distillation models

A second kinetic approach (Clayton, 1991a; Berner et al., 1992 and 1995; Rooney et al., 1995) was based on the distillation theory (Rayleigh, 1896) to predict stable carbon

isotope fractionations of gases generated during the thermal cracking of kerogen or oil. When considering the reaction:

Source --> gas

Stable carbon isotope ratios ($R = {}^{13}\text{C}/{}^{12}\text{C}$) were expressed as:

$$R_s = R_s^\circ \cdot F^{(\alpha-1)}$$

$$R_{ig} = \alpha \cdot R_s^\circ \cdot F^{(\alpha-1)}$$

$$R_{cg} = R_s^\circ \cdot (1-F^\alpha)/(1-F)$$

Where:

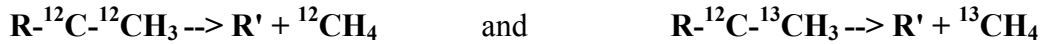
- (i) R_s is the stable carbon isotope ratio of the source S ,
- (ii) R_s° is the initial stable carbon isotope ratio of the source S ,
- (iii) R_{ig} is the stable carbon isotope ratio of the instantaneously generated gas,
- (iv) R_{cg} is the stable carbon isotope ratio of the cumulated gas,
- (v) F is the residual fraction of the source ($0 \leq F \leq 1$),
- (vi) $\alpha = R_{ig}/R_s$ is the isotopic fractionation factor between the instantaneously generated gas and its source.

In the distillation theory, the stable carbon isotope ratio of the generated gas thus depends on the initial stable carbon isotope ratio R_s° of its source, on the isotopic fractionation factor α , and on the progress F of the gas generation reaction. When the whole starting material was considered to be the gas source (Berner et al., 1992 and 1995) the use of the distillation theory thus caused the $\delta^{13}\text{C}_\infty$ of the cumulated gas when $F = 0$ (*i.e.* 100% conversion of the source) to be equal to the bulk initial $\delta^{13}\text{C}_0$ of the starting material. As it may happen that $\delta^{13}\text{C}_\infty \neq \delta^{13}\text{C}_0$ due to the aforementioned 'precursor effect', Clayton (1991a) and Rooney et al (1995) proposed improved models in which gases were considered to be produced by specific precursor moieties within the starting material. These gas precursor moieties were assigned an initial stable carbon isotope composition $\delta^{13}\text{C}_p \neq \delta^{13}\text{C}_0$ with $\delta^{13}\text{C}_p = \delta^{13}\text{C}_\infty$.

In the distillation theory, the isotope fractionation factor α is always taken as a constant whatever the temperature. The models quoted above (Clayton, 1991a; Berner et al., 1992 and 1995; Rooney et al., 1995) thus induced a direct comparison of laboratory data (high temperature processes) with observation made on sedimentary basins (low temperature processes). However, the isotope fractionation phenomenon is known (*e.g.* Lorant et al., 1998, Tang et al., 2000) to be of greater importance under geological conditions than under laboratory conditions.

d) *Compositional approach*

The third kinetic approach attempted to combine the reaction kinetic concept commonly used to describe gas generation and the fundamentals of the isotope fractionation phenomenon (Smith et al., 1971; Sundberg and Bennet, 1983; Galimov, 1988; Tang and Jenden, 1995; Poljakov 1996; Lorant et al., 1998 and 2000; Cramer et al., 1998 and 2001; Tang et al., 2000; Xiong et al., 2004; Cramer, 2004). When a molecule of methane is formed *via* the two following isotopic reaction pathways approximated to be of first-order:



The respective rates of these reactions are expressed as:

$$d[\text{R-}^{12}\text{C-}^{12}\text{CH}_3]/dt = -k_l[\text{R-}^{12}\text{C-}^{12}\text{CH}_3] \quad \text{and} \quad d[\text{R-}^{12}\text{C-}^{13}\text{CH}_3]/dt = -k_h[\text{R-}^{12}\text{C-}^{13}\text{CH}_3]$$

To express rate constants k , the semi-empirical Arrhenius equation is commonly considered as an adequate approximation over the range of temperature characterizing hydrocarbons generation in laboratory studies ($250\text{ }^\circ\text{C} < T < 550\text{ }^\circ\text{C}$) and under geological conditions ($60\text{ }^\circ\text{C} < T < 220\text{ }^\circ\text{C}$):

$$k = A \cdot \exp(-Ea/R.T)$$

Where A = frequency factor (or pre-exponential factor in s^{-1}), Ea = activation energy (in $J.mol^{-1}$), $R = 8.314\text{ } J.mol^{-1}.K^{-1}$, and T = temperature (in K).

Consequently, unlike the Rayleigh theory, the temperature dependence of the isotopic fractionation factor α can be accounted using this approach:

$$\alpha = k_h/k_l = (A_h/A_l) \cdot \exp(-\Delta Ea/R.T)$$

Where (A_h/A_l) and ΔEa are respectively the ratio of frequency factors and the variation of activation energy.

The temperature dependence of the isotopic fractionation factor α was however not accounted by several models. Smith et al (1971), Galimov (1988), and Lorant et al (1998) fixed α as a constant which was thus somehow equivalent to a distillation model combined with a compositional approach (Rooney et al., 1995). Xiong et al (2004) studied the stable carbon isotope fractionation of methane generated during coalification. They assumed either a uniform initial stable carbon isotope composition $\delta^{13}C_p$ for all methane precursors or a constant isotope fractionation factor α during the whole gas formation process. Sundberg and Bennet (1983) and Poljakov (1996) did consider α as temperature-dependent but used

respectively a second order polynomial function $\log(\alpha) = f(1/T)$ and complex mathematical equations rather than the Arrhenius equation to account for this dependency. Tang et al (2000) used the Arrhenius equation to mathematically model the $\delta^{13}\text{C}$ of methane generated during thermal cracking of several simple model compounds. Variation of activation energies ΔE_a were calculated using zero-point energy differences resulting from quantum mechanical calculation of a previous work (Tang and Jenden, 1995). Tang et al (2000) calibrated their model on data obtained during laboratory pyrolysis of *n*-octadecane and emphasized the need to well constrain the precision of experimental $\delta^{13}\text{C}$ values as the isotope fractionation phenomenon of greater importance under geological conditions than under laboratory conditions. Lorant et al (2000) proposed a temperature-dependent model to predict the $\delta^{13}\text{C}$ of methane generated during thermal cracking of 1-methylpyrene, taken as a model compound for the thermal cracking of kerogen. Unfortunately, part of the equation giving the rate of methane was a mathematical fitting function with no chemical meaning and thus restricted to the experimental conditions for which it was calibrated. An extended contribution to the development of theoretical principles of stable carbon isotope fractionations was brought by Cramer and co-workers (Cramer et al., 1998 and 2001; Cramer, 2004). Modelling stable carbon isotope fractionation of methane generated from thermal maturation of coal under non-isothermal pyrolysis experiments, their approach was successfully extrapolated to geological heating rates. Their studies concluded that the influence of the kinetic effect (α) and of the precursor effect ($\delta^{13}\text{C}_p$) over the $\delta^{13}\text{C}$ of generated gases should not be accounted separately and should instead be both included in a reaction kinetic picture of isotopic fractionation claiming any reference to reality.

PART D: RESEARCH STRATEGY

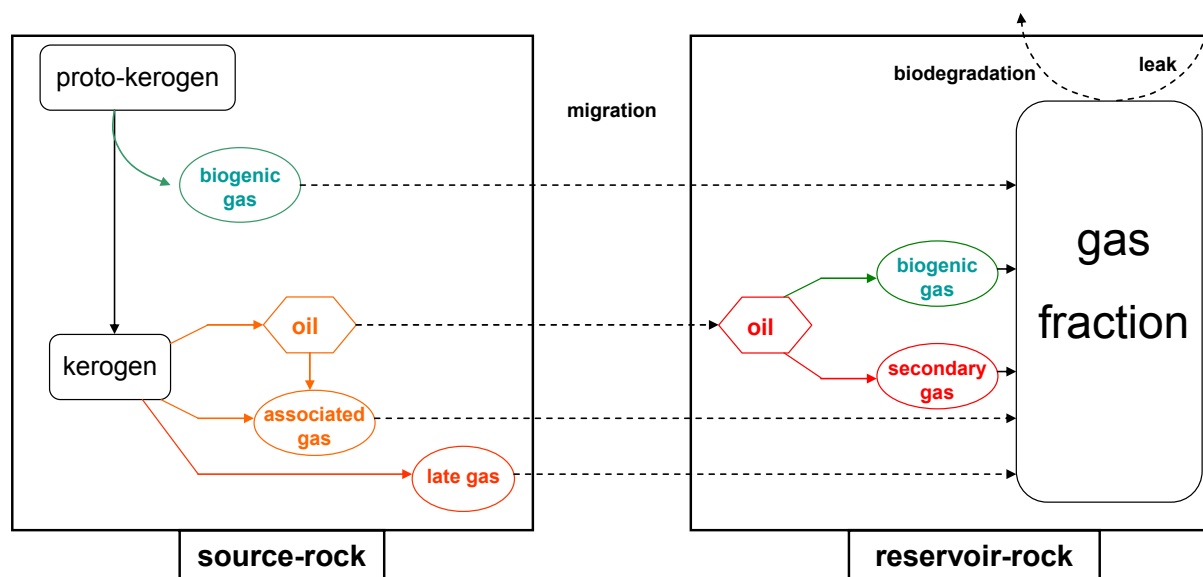


Figure I.7. Main sources of the gas fraction found in reservoir rocks.

As explained in the general introduction of this thesis, the scope of the present study was to validate an original integrated approach that could be applied to elaborate a model that would predict the $\delta^{13}\text{C}$ of the gases generated during the thermal cracking of oil.

Figure I.7 summarizes the main processes detailed in Part A which influence the composition (molecular and isotopic) of the gas fraction found in reservoir-rocks. As illustrated, the type of organic matter (depositional environment), the source (mature or immature kerogen, oil), the mode of generation (biogenic or thermogenic), the events faced during migration and storage (mixing, leakage, water-washing, biodegradation) thus affect the composition of this gas fraction.

Part B emphasized that even a further implementation of the model into a basin simulator would require a limited number of equations, it was scientifically more rigorous to identify a maximum of elementary pathways *via* a mechanistic model before lumping reactions. This way the extrapolation of the model prediction to geological conditions would be more accurate.

Part C demonstrated that the chemical and isotopic modifications during gas generation were related to the same genetic pathways and thus an isotopic fractionation model should be based on a kinetic model.

In regard to the previous observations, the following research strategy has been conducted:

(i) An initial chemical system was determined and an extensive set of experimental data (molecular and isotopic) was collected.

(ii) A free-radical mechanism was validated to describe the thermal cracking of this chemical system and the evolution of its products up to a maximum range of conversion.

(iii) Based on the chemistry constrained in the previous mechanism, a lumped kinetic scheme was derived to account for methane generation on the whole range conversion and for other temperatures.

(iv) Equations of stable carbon isotope fractionation were implemented into the previous lumped scheme to predict the $\delta^{13}\text{C}$ of the methane at all temperatures.

CHAPTER II:

**Experimental
and
Choice of the initial
chemical system**

PART A: EXPERIMENTAL

1. Pyrolysis conditions

Isothermal pyrolysis experiments at 395 °C, 425 °C, 450 °C, and 475 °C were performed at a constant pressure of 100 bar. Pyrolyses were performed in gold sealed-tubes (65 mm length, 9 mm i.d. and 0.5 mm thickness). Filling and ultrasonic-welding of the tubes were carried out under a nitrogen atmosphere in a glove-box to prevent contamination by oxygen and carbon dioxide (whose concentrations did not exceed 10 ppm). The charge was loaded in each tube and the exact mass of compound was accurately calculated by subtracting the weight of the tube before loading (one extremity being already welded) to the weight after loading it and welding the second extremity. The pyrolysis oven was pre-heated prior to each experiment at the chosen temperature. Gold tubes were then placed in pressurized autoclaves at 100 bar. Temperature (measured by a calibrated thermocouple, accuracy ± 1 °C) and pressure were maintained constant and continuously recorded. The pyrolysis time was initiated when the desired isothermal temperature was reached (± 1 °C), *i.e.* about 15 min to 20 min after placing the autoclaves in the oven. At the end of the desired reaction time, the autoclaves were cooled in a water bath, and slowly depressurized in order not to rupture the gold tubes.

When the analysis (molecular + isotopic) of all products and residual reactant was necessary, three tubes were used for each pyrolysis (temperature/time) experiment: one for molecular analysis of gaseous products, one for determination of stable carbon isotope composition of gaseous products, and one for analysis (molecular + isotopic) of liquid and solid products. In this case, special attention was paid to mass balances using different fractions: a gaseous fraction (H_2 ; C_1 - C_4 gases), a pentane extract (C_6 - C_{13} and C_{14+} compounds), a dichloromethane extract and the residue insoluble in dichloromethane. In our experimental procedure, C_5 compounds were not recovered and thus, not quantified.

2. Recovery and analysis of pyrolysis products

2.1. Gaseous products

a) Recovery

Gold tubes were pierced in a vacuum line equipped with a primary vacuum pump, a secondary vacuum pump and a Toepler pump. The latter pump was employed to isolate and measure the total quantity of gas (Behar et al., 1989). Condensable gases (C₂-C₄ alkanes) were trapped in a programmable-temperature cold trap filled with liquid nitrogen while permanent gases (N₂ from the glove-box, H₂ and C₁ products) remained volatilized in the line. Permanent gases were then transferred into a calibrated ampoule. The volume, pressure and temperature of the permanent gases were measured in order to estimate the recovered amount (total number of moles *n*). Thereafter, the programmable-temperature cold trap was warmed to -90 °C, allowing condensable gases to volatilize in the line (water remaining trapped). Their recovery and quantification was achieved as above for permanent gases. The whole gas fraction was transferred into a vacuumed ampoule for subsequent analyses.

b) Molecular analysis

The molecular characterization and quantification of all individual gases generated were performed by gas chromatography (GC). A Varian 3800 GC equipped with two thermal conductivity detectors (TCD) was used. The gas sample was introduced simultaneously into two 250 µl loops connected to a vacuum pump. Three columns were used during the same run: 1 (molecular sieve 13X, 80-100 mesh, 1.5 m x 1/8"), 2 (Porapack N, 60-80 mesh, 3.30 m x 1/8"), 3 (molecular sieve 13X, 45-60 mesh, 1 m x 1/8"). The first channel (carrier gas nitrogen) was used to analyze hydrogen. The second channel (carrier gas helium) was used to analyze the other permanent gases and the condensable gases. The GC was calibrated using a reference gas mixture (H₂, N₂, methane, ethane, propane, *iso*-butane and *n*-butane) to calculate relative response factors. When some oxygen was detected (due to an imperfect vacuum in the line during the previously described recovery of gaseous effluents or due to a leak in the connection between the ampoule and the GC), a correction was made on the nitrogen peak (using the ratio of response factors of N₂ and O₂ and their relative proportions in the atmosphere) to only take into account the nitrogen issued from the glove-box.

c) Stable carbon isotope analysis

Compound-specific stable carbon-isotope compositions ($\delta^{13}\text{C}$) of hydrocarbon (HC) gases were determined on a Micromass IsoPrime mass spectrometer interfaced to a GC. Conditions of the GC were similar as those described above for the molecular analysis of gases. $\delta^{13}\text{C}$ values were calculated by integration of the *m/z* 44, 45 and 46 ion currents of the

CO₂ peaks produced of the chromatographically separated compounds using copper oxide pellets (4mm x 0.5 mm, isotope grade, Elemental Microanalysis Ltd.) at 850°C. Compositions were reported relatively to CO₂ reference-gas pulses (Coleman Instrument grade, BOC Gases Australia Ltd.) of known ¹³C/¹²C content into the spectrometer. The ¹³C/¹²C content of the CO₂ reference gas was monitored daily *via* analysis of the gas mixture of reference compounds. At least three analyses were performed per sample. Carbon-isotope compositions were given in the delta notation relative to Vienna Peedee Belemnite (VPDB).

2.2. Liquid and solid products

a) Recovery

The volatile nature of some pyrolysis products required special care. Refrigeration was used and concentration/evaporation procedures were avoided whenever possible, or used under mild conditions. Tube opening was carried out at low temperature by cooling in dry ice under atmospheric pressure. Two successive extractions were performed by stirring under reflux for 1h before filtering.

The first extraction was carried out with *n*-pentane. Three aliquots were sub-sampled. Such procedure allowed concentrations of the residual reactant and different products to be adjusted adequately in order to enable accurate analyses. The first aliquot was used for molecular identification and for determination of compound-specific stable carbon-isotope compositions ($\delta^{13}\text{C}$) of the C₆-C₁₃ compounds on a GC coupled to a mass-spectrometer (GC/MS) and on an isotope ratio mass spectrometer interfaced to a GC (GC-irMS), respectively. An internal standard (*n*-C₂₅) was added to the second aliquot prior to GC-FID analysis for quantification of the above C₆-C₁₃ compounds. Solvent was evaporated from the third aliquot to quantify the total amount of C₁₄₊ compounds soluble in *n*-pentane by weight. A minimum quantity of *n*-pentane was then re-added to the third fraction and an aliquot was analysed by GC-FID (+ *n*-C₂₅ as internal standard) and GC-MS to individually quantify and identify C₁₄-C₁₈ products soluble in *n*-pentane and kept in solvent to allow the determination of the bulk stable carbon isotope composition of this fraction on an isotope ratio mass spectrometer interfaced to an elemental analyser (EA-irMS).

Thereafter, the fraction insoluble in *n*-pentane and the pieces of gold tube underwent a second extraction, carried out in dichloromethane (DCM) under a 1h reflux. The filtrate then underwent solvent evaporation and the remaining fraction was weighed and kept for analysis

on the EA-irMS. If no residue had been observed on the walls when looking at pieces of the gold tube after opening, zero was assigned to the value of the residue. If a black deposit of residue had been observed, quantification was performed by weighing the gold tube pieces (left to dry 1h at 60 °C in an oven) after this second extraction, and the analysis of the residue was performed on the EA-irMS.

b) Molecular analysis

Regarding the quantification of C₆-C₁₃ and C₁₄-C₁₈ products soluble in *n*-pentane a Varian 3800 GC was used. The programmable temperature vaporizing (PTV) injector was programmed from 20 to 320 °C at a heating rate of 200 °C/min. A DB-1 capillary column (60 m length, 0.32 mm i.d., 0.25 µm film thickness) was used. Helium was used as the carrier gas with a flow rate of 2.0 ml/min at the column outlet. CO₂ was used as a cryogenic gas to maintain the oven at 20°C for 10 min, before heating to 320 °C at a rate of 3 °C/min and holding this temperature for 30 min. The temperature of the flame ionization detector (FID) was 320 °C. Flame conditions were: air: 300 ml/min, H₂: 30ml/min and nitrogen was employed as a make-up gas with a flow rate of 25 ml/min. A volume of 1 µl was injected with a 10 µl syringe *via* a Varian 8400 auto-sampler (split/splitless injector) using pulsed-splitless mode.

Regarding the identification of C₆-C₁₃ products soluble in *n*-pentane, GC-MS was performed using a HP 5973 mass-selective detector (MSD) interfaced to HP 6890 GC fitted with a 60 m x 0.25 mm i.d. fused silica open tubular capillary column coated with a 0.25 µm (5%-phenyl, 95%-methyl)polysiloxane stationary phase (HP-5MS, Agilent J&W). The GC was programmed from 35 °C to 280 °C at 3 °C/min with initial and final hold times of 1 min and 10 min, respectively. Samples dissolved in *n*-pentane were injected (split/splitless injector) by a HP 6890 series auto-sampler using pulsed-splitless mode. Ultra-high purity (UHP) helium (further purified using an in-line OMI™ Indicating purifier, Supelco, Bellefonte, PA) was used as the carrier gas at a flow rate of 1.5 ml/min with the injector operating at a constant flow. In full-scan mode, the MS was typically operating at ionisation energy of 70 eV, a source temperature of 230 °C, an electron multiplier voltage of 1800 V and a mass range of 20 Dalton to 550 Dalton.

Regarding the identification of C₁₄-C₁₈ products soluble in *n*-pentane, GC-MS was performed using a Thermo Fisher MS DSQ (Dual Single Quadrupole) detector interfaced to a Thermo Fisher GC Trace gas chromatograph (GC) fitted with a 30 m x 0.25 mm i.d. fused silica open tubular capillary column coated with a 0.5 µm (5%-diphenyl, 95%-

dimethyl)polysiloxane stationary phase (RTX-5Sil MS, Restek). The GC was programmed from 50 °C to 320 °C at 3 °C/min with a final hold time of 60 min. Samples dissolved in *n*-pentane were manually injected (split/splitless injector) in splitless mode. Ultra-high purity (UHP) helium (Alphagaz 1) was used as the carrier gas at a flow rate of 1.0 ml/min with the injector operating at a constant flow. In full-scan mode, the MS was typically operating at ionisation energy of 70 eV, a source temperature of 220 °C, an electron multiplier voltage of 1100 V and a mass range of 40 Dalton to 600 Dalton.

c) Stable carbon isotope analysis

Compound-specific stable carbon-isotope compositions ($\delta^{13}\text{C}$) of $\text{C}_6\text{-C}_{13}$ products soluble in *n*-pentane were determined on a Micromass IsoPrime mass spectrometer interfaced to the same HP 6890GC as the one described above for the GC-MS analysis of $\text{C}_6\text{-C}_{13}$ products soluble in *n*-pentane. The carrier gas, injection, and temperature conditions were also identical to those described above for GC-MS analysis of $\text{C}_6\text{-C}_{13}$ products soluble in *n*-pentane. During the analysis of a mixture of reference compounds (decane, undecane, dodecane and methyldecanoate), the GC oven was programmed from 50 °C to 310 °C at 10 °C/min with initial and final hold times of 1 min and 10 min, respectively. $\delta^{13}\text{C}$ values were calculated by integration of the m/z 44, 45 and 46 ion currents of the CO_2 peaks produced of the chromatographically separated compounds using copper oxide pellets (4mm x 0.5 mm, isotope grade, Elemental Microanalysis Ltd.) at 850 °C. Compositions were reported relatively to CO_2 reference-gas pulses (Coleman Instrument grade, BOC Gases Australia Ltd.) of known $^{13}\text{C}/^{12}\text{C}$ content into the spectrometer. The $^{13}\text{C}/^{12}\text{C}$ content of the CO_2 reference gas was monitored daily *via* analysis of the gas mixture of reference compounds. At least three analyses were performed per sample. Carbon-isotope compositions were given in the delta notation relative to Vienna Peedee Belemnite (VPDB).

Regarding C_{14+} compounds soluble in *n*-pentane (*n*-C5), compounds insoluble in *n*-pentane but soluble in dichloromethane (DCM)}, and solid residue, bulk isotope analyses were performed on a Micromass Isoprime isotope ratio mass spectrometer interfaced to a EuroVector EuroEA3000 elemental analyser. The corresponding fraction was weighed into a small tin capsule which was then folded and compressed thoroughly to remove atmospheric gases. In the case of the residue, this solid was easily transferred into the tin capsule. C_{14+} compounds soluble in *n*-pentane and compounds insoluble in *n*-pentane but soluble in dichloromethane had to be transferred into the capsule in solution in a minimum amount of the respective solvent using a micro syringe. A tiny piece of combustion filter was used to

keep the liquid sample in the capsule during the further evaporation of the solvent. The capsule was then folded together with the filter. Each capsule was dropped by an auto-sampler into a combustion reactor at 1025 °C. The sample and tin capsule melted in an atmosphere temporarily enriched with oxygen, where the tin promoted flash combustion. The combustion products, entrained in a constant flow of helium, passed through an oxidation catalyst (chromium oxide). The now oxidized products passed through a reduction reactor at 650 °C containing copper granules, in which any oxides of nitrogen (NO, NO₂ and N₂O₂) were reduced to N₂ and the excess of oxygen was removed. The resulting gas species then passed through a magnesium perchlorate filter to remove water. The remaining CO₂, along with N₂ and SO₂ (if present) were separated on a 3 m chromatographic column (PoropackQ) at ambient temperature, before passing through a thermal conductivity detector (TCD), and into the isotope ratio mass spectrometer (irMS). The irMS was calibrated every 8 runs *via* the analysis of a reference compound (Beet Sugar) of known $\delta^{13}\text{C}$. At least three analyses were performed per sample. Carbon-isotope compositions were given in the delta notation relative to Vienna Peedee Belemnite (VPDB).

The above recovery and analysis procedures are summarized on Figure II.1. In cases where this full process was applied to a sample, additional calculations were performed as described in the following lines.

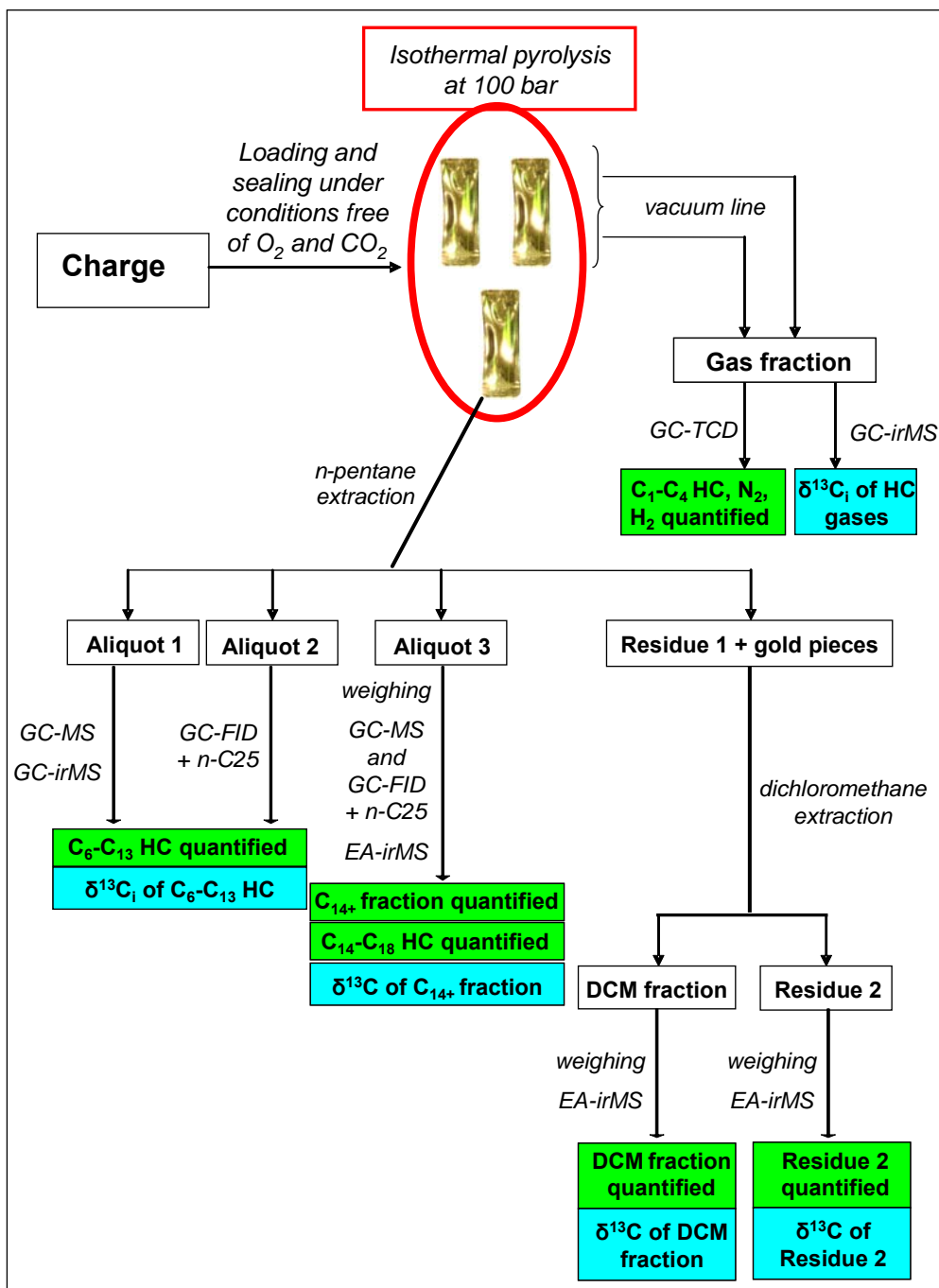


Figure II.1. Recovery and analysis of fractions resulting from isothermal pyrolysis experiment in gold sealed tubes.

3. Data processing

3.1 Mass balances

To calculate mass-balances, five fractions were distinguished: gaseous products, C_6 - C_{13} compounds which were soluble in n -pentane (n - C_5), C_{14+} compounds which were soluble

in *n*-pentane, non-volatile compounds which were insoluble in *n*-pentane but soluble in dichloromethane (DCM) and the experimental residue. Mass-balances (in mg/g of initial charge) were calculated as:

$$MassBalance(mg / g) = \frac{\sum \text{fractions masses (mg)}}{\text{initial mass of reactant (g)}} \quad (1)$$

All experiments with mass balances showing a deviation of more than 20 mg/g compared with 1000 mg/g were discarded.

3.2 Conversion

At low thermal stress (*i.e.* below 5% conversion), the reactant global conversion was derived from the overall mass of recovered pyrolysis products (excluding the residual reactant) as:

$$Conv1(\%) = \frac{\sum \text{products masses}}{\text{initial mass of reactant}} * 100 \quad (2)$$

Indeed, the experimental uncertainty in the quantification of residual reactant by GC-FID could generate a substantial error at such low conversions. For higher thermal stress, the reactant global conversion was derived from the estimation of its residual quantity using GC-FID (equation 3).

$$Conv2 (\%) = 100 - \%(residual \text{ reactant}) \quad (3)$$

3.3 ¹³C balances

To calculate an overall ¹³C-mass balance, the δ¹³C of the initial reactant as well as the δ¹³C all products (including residual reactant) and fractions were needed. Indeed, as shown above in equation (4), the δ¹³C_{*i*} of a given entity *i* (fraction of individual compound) was linked to the ratio of heavy isotope (¹³C) to light isotope (¹²C):

$$R_i = \frac{N_i(^{13}C)}{N_i(^{12}C)} \quad (4)$$

Where, $N_i(^{13}C)$ and $N_i(^{12}C)$ were respectively the numbers of heavy isotope (¹³C) and light isotope (¹²C) in the entity (*i*).

R_i could then be expressed *via* the masses of these isotopes pondered by their respective molecular-weights as:

$$R_i = \frac{m_i(^{13}\text{C}) \times 12}{m_i(^{12}\text{C}) \times 13} \quad (5)$$

Where, $m_i(^{13}\text{C})$ and $m_i(^{12}\text{C})$ were respectively the overall masses of heavy isotope (^{13}C) and light isotope (^{12}C) in the entity (i).

According to the relative natural abundances of ^{13}C and ^{12}C , it was approximated that $m_i(^{12}\text{C})$ was equal to $m_i(\text{C})$, the total mass of carbon in the entity (i). $m_i(\text{C})$ was then calculated knowing the percentage of carbon (TOC or Total Organic Carbon) in this entity and the subsequent total mass:

$$m_i(\text{C}) = m_i \times \text{TOC}_i \quad (6)$$

Where m_i and TOC_i were respectively the total mass and the TOC of the entity (i).

The mass $m_i(^{13}\text{C})$ of heavy isotope (^{13}C) in a entity (i) was then written as:

$$m_i(^{13}\text{C}) = \frac{13}{12} \times R_{VPDB} \times \left(\frac{\delta^{13}\text{C}_i}{1000} + 1 \right) \times m_i \times \text{TOC}_i \quad (7)$$

Where R_{VPDB} is the stable carbon isotope ratio of the international standard Vienna PDB, $R_{VPDB} = 11,237 \text{ ppm}$.

However, if for individually identified products the TOC was immediately deduced from the chemical formula, the TOC of molecular fractions such as C_{14+} compounds soluble in *n*-pentane, non-volatile compounds insoluble in *n*-pentane but soluble in dichloromethane, and the solid residue were unknown. In this case they were respectively taken equal to 0.941, 0.953, and 0.967, after the study of Al Darouich (2005).

Overall ^{13}C -mass balances $^{13}\text{C}_{mb}$ were eventually established using equation (8):

$$^{13}\text{C}_{mb} = \frac{\sum_i m_i(^{13}\text{C})}{m_{IR}(^{13}\text{C})} \times 100 \quad (8)$$

Where $m_{IR}(^{13}\text{C})$ was the mass of heavy isotope (^{13}C) in the initial reactant.

PART B: CHOICE OF THE INITIAL CHEMICAL SYSTEM

1. C₁₄ aromatics: first step to a kinetic model predicting $\delta^{13}\text{C}$ of secondary gases

The scope of the present study was to validate an original integrated approach that could be applied to elaborate a model that would predict the $\delta^{13}\text{C}$ of the gases generated during secondary thermal cracking of oil.

Despite the huge variety of chemical components constituting crude oils, the development of kinetic models describing their thermal degradation passes through the simplification of the system by 'lumping' individual molecules bearing similar structural features and thermal reactivity, into same chemical classes. The choice of the initial chemical system for such kinetic studies is critical. Indeed, model compounds constituting these chemical systems have to be reactive enough to generate realistic quantities of gas compared to that generated *via* thermal cracking of the entire oil. At the same time these model compounds also have to allow the experimental identification of a maximum number of their products to accurately constrain pathways leading to gas generation in the kinetic scheme.

Standard crude oils mainly comprise saturated hydrocarbons, aromatic hydrocarbons, and polar compounds (NSO) (Tissot and Welte, 1984). Recent studies have demonstrated that in sedimentary basins, aromatic hydrocarbons are thermally less stable than saturated hydrocarbons (Behar and Vandenbroucke, 1996; Behar et al., 1999 and 2002). NSO compounds and heavy aromatics (C₁₄₊) are known to produce significant quantities of methane during thermal cracking (*e.g.* Behar et al., 2008a). However, the high-molecular-weight of NSOs makes it difficult to characterize their chemical structure. Regarding C₁₄₊ aromatics, current routine analysis techniques still do not allow identification of the majority of their thermal cracking products since many of them are of higher molecular weight than the reactant itself (Smith and Savage, 1992; Behar et al., 1999; Lorant et al., 2000).

Consequently, as a first step in describing the stable carbon isotope fractionation of gases generated during secondary cracking of oil, the initial chemical system considered in this study was taken among the low-molecular-weight aromatic hydrocarbons (*i.e.* C₁₄₋) of oil.

2. A chemical system composed of methylaromatics and alkylaromatics

As stated above, the focus for this study was the light aromatic fraction of oil *i.e.* C₆-C₁₄ aromatic hydrocarbons. A previous study by Al Darouich et al (2005) had revealed that the light aromatic fraction of standard Type-II oil (Safaniya, Saudi Arabia) could be divided into the molecular classes reported in Table II.1.

Class	Compounds	Rel. Ab. (wt %)
BTXN	benzene, toluene, xylenes, naphthalene	14.3
Methylaromatics	trimethylbenzenes, tetramethylbenzenes, pentamethylbenzene, hexamethylbenzene methylnaphthalenes, di and trimethylnaphthalenes	18.6
Alkylaromatics	C ₂ -C ₇ alkylbenzenes, ethylnaphthalenes	48.1
Naphtenoaromatics	indane, C ₁ -C ₄ indanes, C ₁ -C ₃ tetralins	18.5
Indenes	indene, C ₁ -C ₂ indenenes	0.2
Sulphur-containing aromatics	C ₁ -C ₂ benzothiophenes	0.3

Table II.1. Lumped molecular classes and their relative abundance among the C₆-C₁₄ aromatic fraction of Safaniya oil (After Al Darouich et al., 2005).

Representing respectively only 0.2 wt% and 0.3 wt% of the C₆-C₁₄ aromatic fraction, indenenes and sulphur-containing aromatics were immediately excluded from our study. Moreover, compounds lumped in the molecular class termed BTXN had been demonstrated to be stable under similar conditions by Al Darouich et al (2006a). As these compounds thus did not have a significant impact over the generation of gas during thermal cracking of oil, they were also not considered in our study. On the contrary, naphtenoaromatics could not be considered as stable under our conditions but the difficulty to obtain these compounds in a high purity which was vital for the study lead not to include them in the chemical system. Eventually, the focus was consequently concentrated on the two molecular classes termed methylaromatics and alkylaromatics. Considering the stability of BTXN, the initial chemical system was thus representative of 81 wt% of unstable classes leading to gas generation during thermal cracking of the light aromatic fraction of this Type-II oil.

Seven model compounds were selected (Table II.2) as on the one hand they represented the various cases of side-chains positions, degrees of substitution of the aromatic ring, and side-chains lengths that could be found among the unstable compounds with substantial abundances in the two considered classes of methylaromatics and alkylaromatics and as they were commercially available in high purity (> 99%) on the other hand. These seven selected model compounds were all monoaromatics since the abundance of diaromatics was shown to be less than 1 wt% (Al Darouich et al., 2005). They include two ethyltoluenes, two ethylxylenes, two trimethylbenzenes, and a tetramethylbenzene.

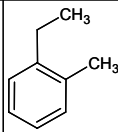
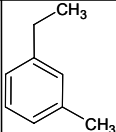
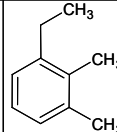
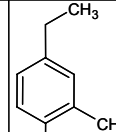
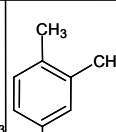
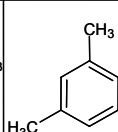
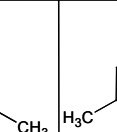
Compound							
Wt %	3.16	3.57	2.15	1.14	5.67	1.36	0.90
	Alkylaromatics				Methylaromatics		

Table II.2. Selected model compounds and their relative abundance (After Al Darouich et al., 2005) among the C₆-C₁₄ aromatic fraction of Safaniya oil.

Since the previous system represented around 27 wt% of {methylaromatics + alkylaromatics} of the oil, the yield of gas (CH₄ and C₂H₆) generated during pyrolysis of this mixture (in same proportions, normalized to 100%) was compared to the yield of gas predicted by the model of Al Darouich et al (2006a) thermal cracking of similar proportions of {methylaromatics + alkylaromatics}. Despite the uncertainty on the real proportions in the experimental mixture due to the difficulty of loading seven volatile compounds in specific proportions in the same tube, results reported in Table II.3 are relatively consistent to consider that the system seemed adequate to study thermal cracking of C₆-C₁₄ methylaromatics and alkylaromatics.

	425 °C / 120 h	425 °C / 404 h
Model of Al Darouich et al (2006a)	CH ₄ : 8.8 C ₂ H ₆ : 2.6	CH ₄ : 10.4 C ₂ H ₆ : 2.6
Mixture 7 compounds	CH ₄ : 6.0 C ₂ H ₆ : 1.5	CH ₄ : 10.7 C ₂ H ₆ : 2.6

Table II.3. Compared yields of methane and ethane generated during thermal cracking of C₆-C₁₄ {methylaromatics + alkylaromatics} predicted by the model of Al Darouich et al. (2006a) and generated during pyrolysis of the mixture of the seven selected model compounds.

3. From a chemical system of 7 model compounds to a system of 2 model compounds

The necessity to determine specific cracking pathways for each class as well as the time needed (about 2h per tube) to load the gold tubes with the seven model compounds in adequate proportions lead to consider a potential downscaling to two model compounds.

In that purpose, 1,2,4-trimethylbenzene and 2-ethyltoluene were selected. The gas generated during pyrolysis of their mixture as well as the yield of gas calculated with the appropriate linear combination of the gas generated during their individual pyrolyses was compared to results obtained on the mixture of seven compounds (Table II.4). Comparison

between results for the two mixtures reveals that the system is also well represented by only two compounds. Moreover, comparison between results for the mixture of the 1,2,4-trimethylbenzene and 2-ethyltoluene and results of the calculations from individual yields does not reveal any significant mixture effect that would request to only study compounds in a mixture rather than individually.

	425 °C / 120 h	425 °C / 404 h
Mixture 7 compounds	CH ₄ : 6.0 C ₂ H ₆ : 1.5	CH ₄ : 10.7 C ₂ H ₆ : 2.6
Mixture 2 compounds	CH ₄ : 5.4 C ₂ H ₆ : 1.9	CH ₄ : 11.6 C ₂ H ₆ : 2.6
Calculated from individual yields of 2 compounds	CH ₄ : 4.0 C ₂ H ₆ : 1.6	CH ₄ : 9.3 C ₂ H ₆ : 2.9

Table II.4. Compared yields of methane and ethane generated during pyrolysis of the mixture of the seven selected model compounds, generated during pyrolysis of the mixture of 1,2,4-trimethylbenzene and 2-ethyltoluene, and calculated by linear combination of the yields generated during individual pyrolysis of 1,2,4-trimethylbenzene and 2-ethyltoluene.

As a consequence of the preliminary results shown above, the decision was taken to study individually the model compounds representative of C₆-C₁₄ methylaromatics (*i.e.* 1,2,4-trimethylbenzene) and representative of C₆-C₁₄ alkylaromatics (*i.e.* 2-ethyltoluene). This would allow the identification of the thermal cracking pathways specific to each of these classes.

Despite experiments were conducted for both model compounds, the timing issue only enabled the development of the integrated approach for one model compound. Since methylaromatics could be generated during thermal cracking of alkylaromatics, the earlier had to be studied first. Consequently, the following three chapters will present how the whole the research strategy presented in Chapter I was applied to 1,2,4-trimethylbenzene.

CHAPTER III:

Mechanistic kinetic model for thermal cracking of 1,2,4-trimethylbenzene

This chapter is extracted from a submitted paper (ref below) and inserted in the thesis report as such, with the exception of the references which have been moved to AppendixIII and the acknowledgements which have been removed.

Fusetti, L., Behar, F., Bounaceur, R., Marquaire, P.M., Grice, K., Derenne, S., 2009a. New insights into secondary gas generation from oil thermal cracking: methylated monoaromatics. A kinetic approach using 1,2,4-trimethylbenzene. Part I: A free-radical mechanism. Organic Geochemistry, accepted and revision in progress.

ABSTRACT:

The scope of the present study was to follow methane generation during thermal cracking of a model compound representative of methylated monoaromatic hydrocarbons present in reservoir crude oils. 1,2,4-trimethylbenzene was selected and subjected to pyrolysis experiments between 395 °C and 450 °C, at 100 bar. The whole range of conversion (2%-97%) was studied to discriminate primary products (*i.e.* those starting to be generated at low conversion) from non-primary products (*i.e.* those generated at higher conversion) in order to elucidate a maximum number of elementary processes involved in methane generation. All pyrolysis fractions were recovered and quantified. Mass-balances were established to ensure that all materials were recovered. Experiments with less than 98% recovery were discarded to ensure that the quantitative data were accurately constrained. All products that could be quantified individually were identified. On this basis, a free-radical mechanism of 122 reversible chemical transformations involving 47 species was proposed to model thermal cracking of 1,2,4-trimethylbenzene. The model prediction was satisfying for the yields of methane, hydrogen, residual reactant, xylenes, toluene, benzene, dimers (containing two aromatic rings coupled *via* an aliphatic bridge) below 70% conversion. The model was then used to characterize some methane generation pathways at 425 °C and 200 °C. In both cases it was demonstrated that methane was generated *via*: (i) The 'monoaromatic route' *i.e.* the demethylation of trimethylbenzenes into xylenes and in a lesser extent the demethylation of xylenes into toluene. (ii) The dimerization of monoaromatics ('polyaromatic route', step 1), (iii) The intramolecular ring closure reaction of dimers into triaromatic precursors (polyaromatic route, step 2).

1. Introduction

The renewing interest around the energy potential of natural gas requires a better characterization of all the pathways leading to its generation. In sedimentary basins, gas can be generated *via* bacterial and thermal processes. Thermal processes can be further divided into primary processes, *i.e.* the generation of gas during thermal cracking of kerogen; and secondary processes, *i.e.* gas generation from thermal cracking of the reservoir oil. The purpose of this study is to better understand thermal processes leading to secondary-gas generation.

Thermal cracking of oil in sedimentary basins generally occurs at temperatures and pressures ranging from 160 °C to 220 °C, and 200 bar to 1000 bar, respectively. It was

demonstrated that the thermal evolution of oil is controlled by the kinetics of cracking reactions (*e.g.* Tissot and Welte, 1984). This allows petroleum geochemists to simulate such processes with laboratory experiments, in particular using pyrolysis at high temperatures generally in the 250 °C to 550 °C range. Due to the huge variety of chemical structures found in crude oil, the development of comprehensive mathematical models requires simplifying the system by 'lumping' individual molecules bearing similar structural features and thermal reactivity, into same chemical classes (*e.g.* Dominé et al., 2002; Behar et al., 2008b). Thus, model compounds representative of the main components present in oil are generally chosen for pyrolysis experiments. Kinetic schemes based on free-radical mechanisms derived from these experiments point out the nature and occurrence of chemical processes involved in natural crude oils.

The choice of model compounds for such kinetic studies is critical. Indeed, those compounds have to be reactive enough to generate realistic quantities of gas compared to that generated *via* thermal cracking of the entire oil. At the same time these model compounds also have to allow the experimental identification of a maximum number of their products to accurately constrain pathways leading to gas generation in the kinetic scheme. Standard crude oils mainly comprise saturated (aliphatic and cycloaliphatic) hydrocarbons, aromatic hydrocarbons (naphthoenaromatics, alkylated aromatics and methylated aromatics), and NSO compounds which are polar compounds containing heteroatomic elements (mainly nitrogen, sulfur and oxygen) in addition to carbon and hydrogen (Tissot and Welte, 1984). Recent studies have demonstrated that in sedimentary basins, aromatic hydrocarbons are thermally less stable than saturated hydrocarbons (Behar and Vandenbroucke, 1996; Behar et al., 1999 and 2002). NSO compounds and heavy aromatics (C₁₄₊) are known to produce significant quantities of methane during thermal cracking (*e.g.* Behar et al., 2008a). However, the high-molecular-weight of NSOs makes it difficult to characterize their chemical structure and it is thus impossible to establish a free-radical mechanism for their thermal degradation. Regarding C₁₄₊ aromatics, current routine analysis techniques still do not allow identification of the majority of their thermal cracking products since many of them are of higher molecular weight than the reactant itself (Smith and Savage, 1992; Behar et al., 1999; Lorant et al., 2000). Consequently, compounds that can be considered to establish a free-radical mechanism rather are the low-molecular-weight aromatic hydrocarbons (*i.e.* C₁₄). Among those compounds, methylated aromatics have the particularity to be present in crude oils both as reactants and as products of thermal degradation of naphthoenaromatics (Leininger et al., 2006) and alkylated aromatics (Savage, 2000; Burklé-Vitzthum et al., 2003; Al Darouich et

al., 2006a). When considering the light-aromatic fraction of a standard Type II crude-oil (Al Darouich et al., 2005), it appeared that 31 wt% of the fraction consisted of trimethylbenzenes. With an abundance of 5.67 wt%; 1,2,4-trimethylbenzene was thus chosen as the model compound for the present study on methylated monoaromatics.

Free-radical mechanisms describing chemical processes occurring during thermal cracking of a model compound and assigning kinetic parameters to all elementary steps were proposed for *n*-hexane (Dominé et al., 1990), butylbenzene (Freund and Olmstead, 1989), 1-ethylpyrene and 1-methylpyrene (Smith and Savage, 1992), 1-dodecylpyrene (Smith and Savage, 1994), Decylbenzene (Burklé-Vitzthum et al., 2003), toluene (Pamidimukkala et al., 1987; Lannuzel, 2007) and tetralin (Bounaceur et al., 2000; Poutsma, 1990 and 2002). Those publications have constituted a source of inspiration to guide our present work.

Studying the entire range of conversion (0%-100%) *via* experiments below 250 °C being impossible on a human scale, our strategy consisted to extrapolate a free-radical mechanism elaborated on the basis of high-temperature laboratory pyrolysis experiments (and at 100 bar). However, considering experimental data which derive from experiments at too elevated temperatures would be irrelevant. Indeed processes and products involved at such high temperatures may be modified by reactions that do not occur at lower temperature. Our literature review on the pyrolysis of methylated aromatics was thus driven by the need to answer three main questions regarding the future elaboration of the free-radical mechanism:

- (i) Which initiation reactions need to be considered according to the range of pressure at which the experiments are performed?
- (ii) At which temperature does the aromatic nucleus of monoaromatic hydrocarbons start to be degraded?
- (iii) Which products of lower and higher molecular-weight than the degraded compound have been previously observed according to the chosen experimental conditions? Which propagation reactions have been considered to explain their formation?

Initiation reactions

Extensive kinetic studies on pyrolysis of toluene and xylenes were initiated in the 1940s by Szwarc (1948) who worked with a silica flow-reactor at temperatures between 680 °C and 850 °C, and at pressures comprised between 2 mm Hg and 15 mm Hg. The author

interpreted the formation of hydrogen as indicative that the determining step was the initiation reaction of homolysis of the benzylic C-H bonds yielding hydrogen atoms and benzyl radicals. Smith and Savage (1992) derived a kinetic scheme to account for the thermal degradation of 1-methylpyrene at temperatures ranging from 400 °C to 450 °C in a stainless steel batch micro reactor of a constant volume. The model showed that bimolecular reactions of Reverse Radical Disproportionation (RRD) played an important role in engendering hydrogenolysis directly and also indirectly through the generation of alkylhydropyrenyl radicals, which subsequently transferred hydrogen. Leininger et al (2006) published a kinetic study on thermal cracking of 1-methylnaphthalene between 380 °C and 450 °C at 100 atmospheres in a batch reactor (gold tubes). They also considered RRD as bimolecular initiation reactions in addition to unimolecular initiation reactions resulting from the homolysis of the benzylic C-H bonds, in order to properly model their experimental results. Lannuzel (2007) proposed an updated free-radical mechanism for thermal decomposition of toluene at 700 bar and 10 mbar based on pyrolysis experiments performed between 350 °C and 450 °C in gold sealed-tubes. For elevated pressures, the author pointed out the necessity to consider bimolecular initiations like RRD as key reactions to generate benzyl radicals whereas at low pressures unimolecular reactions were favoured and bimolecular reactions were negligible.

Bimolecular reactions proceeding through reverse radical disproportionation (RRD) are thus favoured for high pressure conditions in which our pyrolysis experiments were performed (100 bar).

Opening of the aromatic ring

Errede and DeMaria (1962) followed the kinetics for the over-all pyrolysis reaction of *p*-xylene between 940 °C and 1110 °C at pressures mostly below 5 mm Hg in a fast flow-reactor and showed that thermal degradation of the benzene ring became significant above 1050 °C. Pamidimukkala et al (1987) investigated thermal decomposition of toluene under temperatures ranging from 1550 K to 2200 K (1277 °C to 1927 °C) at pressures ranging from 0.2 atmosphere to 0.5 atmosphere in shock-tubes. Under such conditions, not was only methane generated but products resulting from the decomposition of the benzene ring were also observed. Jess (1996) investigated the thermal stability of aromatic hydrocarbons such as naphthalene, toluene and benzene between 700 °C and 1400 °C at 160 kPa. For high thermal stress, toluene mainly generated methane and benzene by demethylation reactions rather than decomposing. McClaine and Wornat (2007) studied reaction pathways leading to the

formation of Polycyclic Aromatic Hydrocarbons (PAH) during supercritical pyrolysis of toluene (100 atm., 535 °C) in a silica flow-reactor. Under these conditions, they found no evidence for rupture of the aromatic ring. No acetylene cyclopenta-fused PAH nor ethynyl substituted PAH products were found, showing that acetylene was never generated under these temperatures.

Degradation of the benzene ring is thus not significant for the range of temperature in which our pyrolysis experiments will be performed ($T < 600$ °C).

Pyrolysis products

Szwarc (1948) pyrolysed xylenes and toluene in a silica flow-reactor at temperatures between 680 °C and 850 °C, and pressures comprised between 2 mm Hg and 15 mm Hg. He identified bibenzyl, benzene, methane and hydrogen as main products of toluene. Regarding the pyrolysis of xylenes, he observed hydrogen and methane assumed that dimethylbibenzyl isomers were the main heavy products. Under similar experimental conditions, Blades et al (1954) confirmed the products reported by Szwarc (1948) for the pyrolysis of toluene and also identified a large variety of higher molecular-weight products such as dimethylbiphenyl isomers and anthracene. They postulated that dimethylbiphenyl isomers were produced by side reactions of either benzyl radical or bibenzyl. Schaeffgen (1955) studied the pyrolysis of *p*-xylene for a series of temperatures ranging from 795 °C to 920 °C at pressures comprised between 2 mm Hg and 12 mm Hg in a quartz flow-reactor. He reported toluene as being the main liquid product, and hydrogen and methane were the main gases formed. He also identified dimethylbibenzyl dimers and methylated anthracenes in the higher-molecular-weight fraction. He postulated that their formation originated from the ring closure and loss of hydrogen atoms after two methylbenzyl radicals had coupled and rearranged into dimers like *o*-methylated diphenylmethane isomers. Takahasi (1960) performed high-temperature pyrolysis experiments on toluene between 737 °C and 953 °C at pressures between 4 mm Hg and 10 mm Hg in a silica flow-reactor. For such high temperatures, the author noted that abstraction reactions of H-atoms not only occurred on benzylic methyl groups but also involved H-atoms located on the benzene ring. Consequently, the formation of other combination products like dimethylbiphenyls or methyl diphenylmethane isomers could be explained. Following the idea of Schaeffgen (1955), Errede and Cassidy (1960) proposed a stepwise mechanism for thermal conversion of benzylic radicals to anthracenes *via* bibenzyl type molecules during toluene and *p*-xylene pyrolysis in a silica fast-flow reactor at $T = 970$ °C / $P = 0.5$ mmHg and $T = 1065$ °C / $P = 4.0$ mmHg, respectively. Isomers of *o*-methylated

diphenylmethane were proposed as intermediate compounds during the ring closure process. Thermal rupture of benzylic C-H bonds was thought to generate benzylic radicals that could couple to form bibenzyl type molecules. The latter reaction being reversible (Schaeffgen, 1955), recombination eventually occurred irreversibly affording dimers like *o*-methylated diphenylmethane isomers. These in turn, underwent ring closure and dehydrogenation yielding anthracenes (methylated or not) as stable end products. To understand the influence of hydrogen over the demethylation reaction, Gräber and Hüttinger (1982) added large quantities of this compound to the reaction medium (hydro gasification) during thermal cracking of toluene, 1- and 2-methylnaphthalenes and diphenylmethane between 600 °C and 1000 °C in a flow-reactor. When concentration of molecular hydrogen was artificially increased in significant proportions, methylene bridges were completely split off from the aromatic nuclei (engendering noticeable increase in methane yield) and condensation reactions leading to solid products became of minor importance. It demonstrated that substantial demethylation reactions observed for 'traditional' pyrolysis experiments (no hydrogen artificially added) occur *via* a more complex mechanism than the sole *ipso*-addition of hydrogen as this compound is generated in low concentration. Smith and Savage (1992) derived a kinetic scheme accounting for 1-methylpyrene thermal degradation at temperatures ranging from 400 °C to 450 °C in a stainless steel batch micro reactor of a constant volume. Demethylation pathways leading to pyrene and methyl addition pathways leading to dimethylpyrenes isomers were characterized. The authors did not identify the gaseous products nor the heavy fraction. They assumed this latter was mainly constituted of 1,2-dipyrenylethane, generated by recombination of two methylpyrenyl radicals β . Methane generation through demethylation of the reactant was only one of the multiple possible pathways as other methylated compounds (isomers, dimers) were produced. In 1993, the same authors (Smith and Savage, 1993) performed pyrolysis experiments on 1-, 2- and 9-methylanthracenes at temperatures between 350 °C and 450 °C. They concluded that thermal cracking proceeded through three primary parallel-reaction pathways whose relative importance varied according to which isomer was involved. The first reaction pathway led to anthracene *via* demethylation, the second to dimethylantracenes through methyl-addition and the third to methyl-9,10-dihydroanthracenes *via* hydrogenation. In the work of Behar et al (1999), the thermal decomposition of 9-methylphenanthrene was studied in a batch reactor (gold sealed-tubes) at temperatures between 375 °C and 450 °C at a pressure of 120 bar. A kinetic scheme based on stoichiometric reactions associated to bulk kinetic parameters was established. Methane generated during primary and secondary cracking of the reactant was

quantified. Lorant et al (2000) established a kinetic scheme for thermal cracking of 1-methylpyrene in gold sealed-tubes at temperatures ranging from 400 °C to 475 °C at a pressure of 150 bar. Two main processes of methane formation were reported: one related to the loss of the methyl group and another one corresponding to the opening of the aromatic system. Leininger et al (2006) proposed a kinetic study on thermal cracking of 1-methylnaphthalene in gold-sealed tubes between 380 °C and 450 °C at a pressure of 100 atmospheres. All gases as well as some products soluble in *n*-pentane were identified and quantified. Heavier fractions were quantified by weight. The authors concluded that below 2% of conversion, the rate of decomposition of 1-methylnaphthalene was accelerated by the formation of dimers assumed to be dimethylbinaphthalenes. At such conversions, 1-methylnaphthalene was reported to be mostly converted into naphthalene, methylated dimers, methane and molecular hydrogen. Above 10% conversion, secondary products were identified as dimethylnaphthalenes, 2-methylnaphthalene and heavier dehydrogenated polyaromatics. The global conversion (10%-80%) was modelled. Regarding relative similarities with products distribution and kinetic parameters in studies of Behar et al (1999) on 9-methylphenanthrene and Lorant et al (2000) on 1-methylpyrene, Leininger et al (2006) concluded that methylaromatic hydrocarbons containing from two up to four benzene rings behaved similarly during thermal cracking. Lannuzel (2007) proposed an updated free-radical mechanism for toluene thermal decomposition at 700 bar and 10 mbar based on pyrolysis experiments in gold sealed tubes performed between 350 °C and 450 °C at a pressure of 700 bar. The importance of the formation of dimers through the reaction of benzyl radicals with the reactant was demonstrated *via* a sensibility analysis. Unfortunately, the limited experimental data did not allow a very precise calibration of the model.

Research Strategy:

As previously stated, temperatures considered for our experiments had to be high enough to enable acceptable durations of pyrolysis experiments (a few hours to a few months) but also had to be reasonable in order not to lead to unrealistic chemical phenomena compared to lower temperature conditions. The compromise was found for pyrolysis experiments performed between 395 °C and 450 °C (at a pressure of 100 bar).

To the best of our knowledge, with the exception of the work of Lannuzel (2007) on toluene, no experimental and kinetic study of processes governing thermal-cracking of a methylated monoaromatic hydrocarbons in the range 250 °C-550 °C have been performed. As

a consequence we propose the following work related to methane generation *via* thermal cracking of 1,2,4-trimethylbenzene.

The following research strategy has been conducted:

(1) *Identification of generated products*

It was necessary to discriminate primary products (*i.e.* those starting to be generated at low conversion) from non-primary products (*i.e.* those generated at higher conversion) in order to elucidate a maximum number of elementary processes involved in methane generation during thermal cracking of 1,2,4-trimethylbenzene. Consequently, we performed pyrolysis experiments with experimental conditions covering the widest range of reactant conversions. All pyrolysis fractions were recovered and quantified. Mass-balances were established to ensure all materials were recovered and experiments with less than 98% recovery were discarded to ensure the quantitative data were accurately constrained. All products that could be identified were quantified individually.

(2) *Elaboration of a free-radical mechanism*

Based on primary products experimentally observed and on the evolution of their yield, an exhaustive primary free-radical mechanism was elaborated. Then, according to the evolution of primary and non-primary products, the primary mechanism was completed by other reactions to account for chemical processes occurring on a maximum range of conversion.

(3) *Extrapolation of the free-radical mechanism to lower temperature*

Once validated on experimental data of high-temperature laboratory experiments, an attempt of extrapolation of the mechanism was performed to compare the relative importance of identified chemical pathways yielding methane with those predicted by the model at low temperature (200 °C).

2. Experimental

2.1 Pyrolysis of 1,2,4-trimethylbenzene

1,2,4-trimethylbenzene, or Pseudocumene, (99.5% pure) was purchased from Sigma-Aldrich (ref: 82540). The purity was checked by GC. The impurities were a series of trimethylbenzene isomers.

T (°C)	t (h)
395	72; 144; 216; 312; 432; 550; 648
425	3; 9.5; 72; 120; 216; 648
450	24; 50; 72; 144; 195; 336; 432; 648

Table 1: Pyrolysis conditions for thermal cracking of 1,2,4-trimethylbenzene at 100 bar. Pyrolysis times *t* are indicated in hours.

As displayed in Table 1, pyrolysis experiments were performed between 395 °C and 450 °C for heating durations ranging from 1 h to 648 h, at a constant pressure of 100 bar.

Pyrolyses were performed in gold sealed-tubes (65 mm length, 9 mm i.d. and 0.5 mm thickness). Filling and ultrasonic-welding of the tubes were carried out under a nitrogen atmosphere in a glove-box to prevent contamination by oxygen and carbon dioxide (whose concentrations did not exceed 10 ppm). A charge of approximately 50 mg of 1,2,4-trimethylbenzene was loaded in each tube with a syringe and the exact mass of compound was accurately calculated by subtracting the weight of the tube before loading (one extremity being already welded) to the weight after loading it and welding the second extremity. The pyrolysis oven was pre-heated prior to each experiment at the chosen temperature. Gold tubes were then placed in pressurized autoclaves at 100 bar. Temperature (measured by a calibrated thermocouple, accuracy ± 1 °C) and pressure were maintained constant and continuously recorded. The pyrolysis time was initiated when the desired isothermal temperature was reached (± 1 °C), *i.e.* about 15 min to 20 min after placing the autoclaves in the oven. At the end of the desired reaction time, the autoclaves were cooled in a water bath, and slowly depressurized in order not to rupture the gold tubes.

Two tubes were used for each pyrolysis (temperature/time) experiment: one for molecular analysis of gaseous products and one for analysis of liquid and solid products. Special attention was paid to mass balances using different fractions: a gaseous fraction (H₂; C₁-C₄ gases), a pentane extract (C₆-C₁₃ and C₁₄₊ compounds), a dichloromethane extract and the residue insoluble in dichloromethane. In our experimental procedure, C₅ compounds were not recovered and thus, not quantified.

2.2 Analysis of Pyrolysis Products

2.2.1 Gaseous Products

Gold tubes were pierced in a vacuum line equipped with a primary vacuum pump, a secondary vacuum pump and a Toepler pump. The latter pump was employed to isolate and measure the total quantity of gas (Behar et al., 1989). Condensable gases (C₂-C₄ alkanes) were trapped in a programmable-temperature cold trap filled with liquid nitrogen while permanent gases (N₂ from the glove-box, H₂ and C₁ products) remained volatilized in the line. Permanent gases were then transferred into a calibrated ampoule. The volume, pressure and temperature of the permanent gases were measured in order to estimate the recovered amount (total number of moles *n*). Thereafter, the programmable-temperature cold trap was warmed to -90 °C, allowing condensable gases to volatilize in the line (water remaining trapped). Their recovery and quantification was achieved as above for permanent gases. The whole gas fraction was transferred into a vacuumed ampoule for subsequent molecular analyses.

The molecular characterization and quantification of all individual gases generated were performed by gas chromatography (GC). A Varian 3800 GC equipped with two thermal conductivity detectors (TCD) was used. The gas sample was introduced simultaneously into two 250 µl loops connected to a vacuum pump. Three columns were used during the same run: 1 (molecular sieve 13X, 80-100 mesh, 1.5 m x 1/8"), 2 (Porapak N, 60-80 mesh, 3.30 m x 1/8"), 3 (molecular sieve 13X, 45-60 mesh, 1 m x 1/8"). The first channel (carrier gas nitrogen) was used to analyze hydrogen. The second channel (carrier gas helium) was used to analyze the other permanent gases and the condensable gases. The GC was calibrated using a reference gas mixture (H₂, N₂, methane, ethane, propane, *iso*-butane and *n*-butane) to calculate relative response factors. When some oxygen was detected (due to an imperfect vacuum in the line during the previously described recovery of gaseous effluents or due to a leak in the connection between the ampoule and the GC), a correction was made on the nitrogen peak (using the ratio of response factors of N₂ and O₂ and their relative proportions in the atmosphere) to only take into account the nitrogen issued from the glove-box.

2.2.2 Liquid and solid Products

The volatile nature of some pyrolysis products required special care. Refrigeration was used and concentration/evaporation procedures were avoided whenever possible, or used under mild conditions.

Tube opening was carried out at low temperature by cooling in dry ice under atmospheric pressure. Two successive extractions were performed by stirring under reflux for 1h before filtering. The first extraction was carried out with *n*-pentane. Three aliquots were sub-sampled. Such procedure allowed concentrations of the residual reactant and different

products to be adjusted adequately in order to enable accurate quantification by GC. The first aliquot was used for molecular identification of the C₆-C₁₃ compounds on a GC coupled to a mass-spectrometer (GC/MS). An internal standard (C₂₅ *n*-alkane) was added to the second aliquot prior to GC-FID analysis for quantification of the above C₆-C₁₃ compounds. Solvent was evaporated from the third aliquot to quantify the total amount of C₁₄₊ compounds soluble in *n*-pentane by weight. A minimum quantity of *n*-pentane was then re-added to the third fraction and an aliquot was analysed by GC-FID and GC-MS to individually quantify and identify C₁₄-C₁₈ products soluble in *n*-pentane. Thereafter, the fraction insoluble in *n*-pentane and the pieces of gold tube underwent a second extraction, carried out in dichloromethane (DCM) under a 1h reflux. The filtrate then underwent solvent evaporation and the remaining fraction was weighed. If no residue had been observed on the walls when looking at pieces of the gold tube after opening, zero was assigned to the value of the residue. If a black deposit of residue had been observed, quantification was performed by weighing the gold tube pieces (left to dry 1h at 60 °C in an oven) after the second extraction.

Regarding the quantification of C₆-C₁₈ products soluble in *n*-pentane a Varian 3800 GC was used. The programmable temperature vaporizing (PTV) injector was programmed from 20 to 320 °C at a heating rate of 200 °C/min. A DB-1 capillary column (60 m length, 0.32 mm i.d., 0.25 µm film thickness) was used. Helium was used as the carrier gas with a flow rate of 2.0 ml/min at the column outlet. CO₂ was used as a cryogenic gas to maintain the oven at 20°C for 10 min, before heating to 320 °C at a rate of 3 °C/min and holding this temperature for 30 min. The temperature of the flame ionization detector (FID) was 320 °C. Flame conditions were: air: 300 ml/min, H₂: 30ml/min and nitrogen was employed as a make-up gas with a flow rate of 25 ml/min. A volume of 1 µl was injected with a 10 µl syringe *via* a Varian 8400 auto-sampler (split/splitless injector) using pulsed-splitless mode.

Regarding the identification of C₆-C₁₃ products soluble in *n*-pentane, GC-MS was performed using a HP 5973 mass-selective detector (MSD) interfaced to HP 6890 GC fitted with a 60 m x 0.25 mm i.d. fused silica open tubular capillary column coated with a 0.25 µm (5%-phenyl, 95%-methyl)polysiloxane stationary phase (HP-5MS, Agilent J&W). The GC was programmed from 35 °C to 280 °C at 3 °C/min with initial and final hold times of 1 min and 10 min, respectively. Samples dissolved in *n*-pentane were injected (split/splitless injector) by a HP 6890 series auto-sampler using pulsed-splitless mode. Ultra-high purity (UHP) helium (further purified using an in-line OMI™ Indicating purifier, Supelco, Bellefonte, PA) was used as the carrier gas at a flow rate of 1.5 ml/min with the injector operating at a constant flow. In full-scan mode, the MS was typically operating at ionisation

energy of 70 eV, a source temperature of 230 °C, an electron multiplier voltage of 1800 V and a mass range of 20 Dalton to 550 Dalton.

Regarding the identification of C₁₄-C₁₈ products soluble in *n*-pentane, GC-MS was performed using a Thermo Fisher MS DSQ (Dual Single Quadrupole) detector interfaced to a Thermo Fisher GC Trace gas chromatograph (GC) fitted with a 30 m x 0.25 mm i.d. fused silica open tubular capillary column coated with a 0.5 µm (5%-diphenyl, 95%-dimethyl)polysiloxane stationary phase (RTX-5Sil MS, Restek). The GC was programmed from 50 °C to 320 °C at 3 °C/min with a final hold time of 60 min. Samples dissolved in *n*-pentane were manually injected (split/splitless injector) in splitless mode. Ultra-high purity (UHP) helium (Alphagaz 1) was used as the carrier gas at a flow rate of 1.0 ml/min with the injector operating at a constant flow. In full-scan mode, the MS was typically operating at ionisation energy of 70 eV, a source temperature of 220 °C, an electron multiplier voltage of 1100 V and a mass range of 40 Dalton to 600 Dalton.

2.3 Calculation of mass balances

T (°C)	t (h)	Conversion (%)	residual reactant	gases	C ₆ -C ₁₃ in <i>n</i> -C ₅	C ₁₄₊ in <i>n</i> -C ₅	DCM fraction	estimated residue	mass balance
425	3	2.7	972.5	0.2	2.7	6.6	18.0	0.0	1000.0
425	9.5	3.0	970.1	0.5	3.0	9.4	16.8	0.0	999.8
395	144	4.7	945.5	2.5	7.0	25.6	18.7	0.0	999.3
395	432	22.2	771.0	27.8	62.5	101.0	20.8	16.9	993.9
425	120	30.9	681.0	43.2	90.9	114.3	20.2	50.4	989.0
450	50	46.5	515.6	66.5	172.1	103.2	20.0	122.6	980.2
450	72	62.3	350.5	102.7	231.7	91.1	19.9	204.1	982.2
450	144	76.2	210.7	146.7	268.1	79.1	20.9	274.5	989.4
450	195	86.7	113.5	167.5	297.2	63.3	20.5	338.0	982.1
450	432	97.4	17.6	212.5	272.3	49.8	21.4	426.4	986.2

Table 2: Mass-balances obtained for thermal cracking of 1,2,4-trimethylbenzene at 100 bar (ratios in mg/g of initial reactant).

In the above recovery and analytical process, six molecular fractions were distinguished (Table 2): the residual reactant (reported separately to illustrate the conversion),

the gas fraction, C₆-C₁₃ compounds (excluding the reactant) which were soluble in *n*-pentane (*n*-C₅), C₁₄₊ compounds which were soluble in *n*-pentane, non-volatile compounds which were insoluble in *n*-pentane but soluble in dichloromethane (DCM) and the estimated solid residue. Mass-balances (in mg/g of initial charge) were calculated for all experiments as below (equation 1):

$$MassBalance(mg / g) = \frac{\sum \text{fractions masses (mg)}}{\text{initial mass of reactant (g)}} \quad (1)$$

All experiments with mass balances of less than 980 mg/g recovery were discarded in order to make sure that pyrolysis products had been all quantitatively recovered before considering data. If no residue had visually been observed on the walls when looking at the inside of the gold tube after the opening, a value of zero was assigned to the 'estimated residue' (Table 2). When residue had been quantified experimentally, the value termed 'estimated residue' was calculated by adding the difference between 1000 mg/g and the mass balance (in mg/g) to the yield of the experimental residue (equation 2).

$$'estimated\ residue' = 'experimental\ residue' + (1000 - \text{mass balance}) \quad (2)$$

2.4 Calculation of conversion

At low thermal stress (*i.e.* below 5% conversion), the reactant global conversion was derived from the overall mass of recovered pyrolysis products according to equation (3). Indeed, the experimental uncertainty on the quantification of residual 1,2,4-trimethylbenzene by GC-FID could generate a substantial error at such low conversions.

$$Conv1(\%) = \frac{\sum \text{products masses}}{\text{initial mass of reactant}} * 100 \quad (3)$$

For higher thermal stress, the reactant global conversion was calculated as the average value between the conversion calculated using equation (3) and the reactant conversion derived from the estimation of its residual quantity using GC-FID (equation 4).

$$Conv2(\%) = 100 - \%(residual\ reactant) \quad (4)$$

3. Experimental results and discussion

As shown in Table 2, nearly the entire range of 1,2,4-trimethylbenzene conversion was studied with values ranging from 2.7% to 97.4%, corresponding to the residual reactant decreasing from 972.5 mg/g to 17.6 mg/g of initial charge.

Conv. (%)	2.7	3.0	4.7	22.2	30.9	46.5	62.3	76.2	86.7	97.4
Products										
CH ₄	0.7	1.5	15.8	195.8	302.3	470.3	733.5	1056.0	1209.0	1552.5
C ₂ H ₆	0.4	1.2	1.3	6.0	10.3	13.2	17.6	21.6	23.6	20.4
H ₂	0.4	0.6	3.0	12.0	16.8	27.0	31.2	27.0	26.4	21.0
Xylenes	0.8	1.5	4.9	64.8	95.7	177.2	228.4	243.7	241.3	142.4
Toluene	0.0	0.0	0.0	1.4	2.6	14.6	33.0	62.8	99.7	158.0
Benzene	0.0	0.0	0.0	0.0	0.0	0.4	1.5	3.1	8.5	37.0
Dimers238	0.9	1.9	3.3	3.3	3.0	1.6	1.0	0.6	0.5	0.2
Dimers224	0.1	0.3	3.5	3.7	3.4	2.8	2.0	1.3	1.1	0.9
Dimers210	0.0	0.0	0.0	0.4	0.7	1.0	0.8	0.6	0.4	0.1
Dimers196	0.0	0.0	0.0	0.3	0.5	1.1	1.7	1.9	2.2	2.6
Dimers182	0.0	0.0	0.0	0.1	0.1	0.2	0.2	0.4	0.6	1.7
Triaro206	0.0	0.2	0.9	4.1	4.2	3.9	2.5	1.7	1.1	0.4
Triaro192	0.0	0.0	0.0	4.3	5.2	6.0	4.4	3.2	2.0	1.0
Triaro178	0.0	0.0	0.0	1.9	3.1	5.2	5.2	4.4	3.2	2.1

Table 3: Molar yields obtained for thermal cracking of 1,2,4-trimethylbenzene at 100 bar (ratios in mmol/mol of initial reactant).

The composition of the free-radical reactions involved products both identified and quantified (see Table 3: molar yields are in mmol/mol of the initial reactant). These included methane, ethane and hydrogen for the gaseous fraction; monoaromatics, dimers and triaromatics for the *n*-pentane fraction. C₁₈₊ products soluble in *n*-pentane, non-volatile products soluble in dichloromethane and the solid residues were classified as 'unidentified heavy products'. The latter products were used in the mass-balance calculations (in mg/g in Table 2) but were not used in the free-radical mechanism.

3.1 Gaseous products

3.1.1 Methane

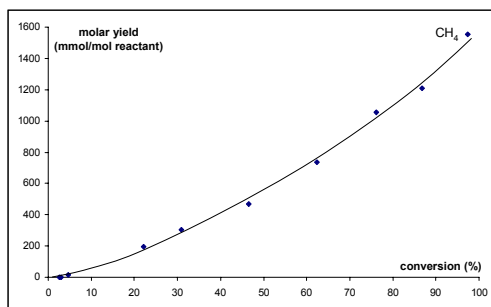


Figure 1: Molar yield of methane (in mmol/mol of initial reactant) versus conversion (curve suggests a trend line).

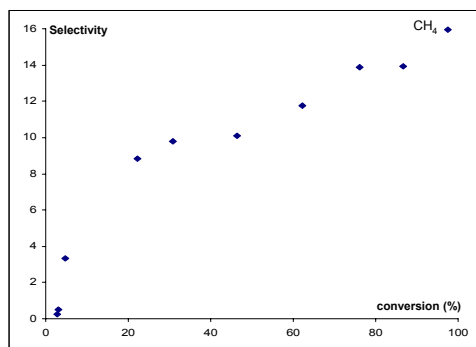


Figure 2: Selectivity diagram of methane.

Methane (Figure 1 and Table 3) started to be generated at low conversion (2.7%). Methane being a stable product, its yield then increased continuously reaching 1552.5 mmol/mol at 97.4% conversion (no infinity value was observed). On Figure 2, the Delplot methodology (Bhore et al., 1990) is illustrated in its simplest form. It involves inspection of plots of the product selectivity as a function of the reactant conversion (Smith and Savage, 1993). Selectivity was calculated as the ratio of the product molar yield to the conversion. Despite the inherent uncertainty of experimental quantifications, Figure 2 enables interesting observations related to methane generation pathways. The intercept on the Delplot appears to be positive, showing that there were primary contributions to methane generation. Indeed, one common pathway of methane generation has been identified as demethylation reactions of methylated aromatics (e.g. Smith and Savage, 1992 and 1993; Leininger et al.; 2006, Lannuzel, 2007). However, the continuous increase of methane selectivity with conversion (Figure 2) supports the idea that methane also originated from several non-primary sources (e.g. Behar et al., 1999). Such sources will now be characterized by examining all experimental data regarding the generation and degradation of identified products.

3.1.2 Ethane and hydrogen

Among the gas fraction, in addition to methane, hydrogen was identified together with ethane. No significant amounts of C₃ and C₄ hydrocarbon gases were observed. Moreover, as might be anticipated in regard to our previous literature review (*e.g.* McClaine and Wornat, 2007), decomposition of the aromatic nucleus did not occur in our range of temperatures since there was no evidence of acetylene being formed.

Ethane increased proportionally reaching 23.6 mmol/mol at 86.7% conversion before decreasing to 20.4 mmol/mol at 97.4% conversion (Table 3). The thermal instability of ethane was due to the relatively high thermal stress of pyrolysis conditions ($T > 400\text{ }^{\circ}\text{C}$) and only contributed in minor amount to methane generation due to the discrepancy between respective molar yields of those two gases. Indeed, when conversion increased the ethane yield quickly became much lower than the methane yield (already 1.3 mmol/mol and 15.8 mmol/mol at 4.7% conversion, respectively). It has been reported that when the aromatic ring remains stable, methane and ethane generation pathways are related to the presence of methyl and ethyl moieties, respectively (Smith and Savage, 1992 and 1993; Lorant et al., 2000; Leininger et al., 2006; Lannuzel, 2007). To the best of our knowledge, as 1,2,4-trimethylbenzene did not contain any ethyl group, ethane might thus only result from termination reactions (Smith and Savage, 1992), justifying its low yield. This point will be discussed further.

Due to its low molecular-weight, the quantification of hydrogen was quite challenging and values obtained were considered with some caution. Hydrogen started to be generated (Table 3) at low conversion (0.4 mmol/mol at 2.7%) and its formation was thus incorporated into the primary mechanism. It reached a maximum of around 31 mmol/mol at 62.3% conversion before decreasing to around 21 mmol/mol at 97.4%. Coupling reactions of molecules to form dimers (see below) and more extensively, all the condensation reactions leading to char have been shown to release hydrogen (*e.g.* Smith and Savage, 1992; Poutsma, 2002). It can explain the increase of hydrogen molar yield meanwhile *ipso*-additions leading to the release of methyl radicals consume hydrogen (*e.g.* Smith and Savage, 1992 and 1993; Lannuzel, 2007).

3.2 Identified products soluble in *n*-pentane

The chemical structures of those products are listed in Table 4.

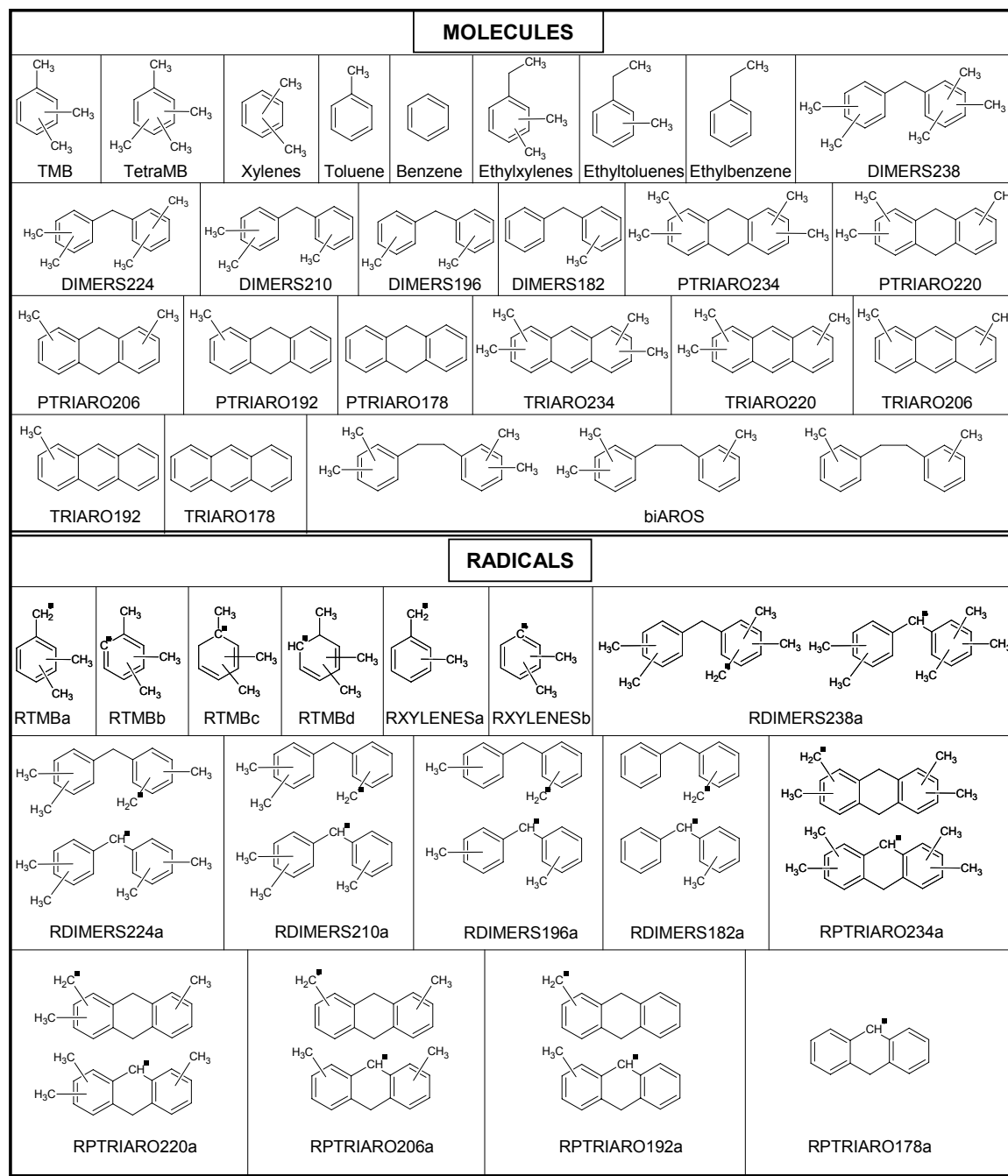


Table 4: Chemical structures of molecules and radicals

3.2.1 Monoaromatics

Apart from the residual reactant, other monoaromatics were detected experimentally. Xylenes, toluene and benzene were quantified (Figure 3 and Table 3) and traces of tetramethylbenzenes, ethylxylenes, ethyltoluenes and ethylbenzene were only detected. No ethynyl substituted monoaromatic products were observed, confirming that no acetylene was produced during methylmonoaromatics thermal cracking under such temperatures (*e.g.*

McClaine and Wornat, 2007). The opening of the benzene ring does not occur in the 400 °C to 500 °C range contrary to what has been reported previously for the aromatic system of polyaromatic hydrocarbons (Smith and Savage, 1993; Lorant et al., 2000).

The traces of tetramethylbenzene isomers which were detected result from methylation reactions of the reactant. As opposed to polyaromatic hydrocarbons (Smith and Savage, 1992 and 1993; Leininger et al., 2006) this methylation reaction does not seem to play an important role for monoaromatics as already observed by Lannuzel (2007) on toluene. However, as tetramethylbenzene isomers are primary products, their formation was taken into account in the primary free-radical mechanism.

All isomers of xylenes (*o*-, *m*- and *p*-xylenes) were identified and quantified but they were 'lumped' under the term xylenes. Xylenes were produced throughout the entire range of conversion and reached a maximum value of 243.7 mmol/mol at 76.2% conversion before decreasing to 142.4 mmol/mol at 97.4% (Figure 3 and Table 3). Toluene started to be generated at 22.2% conversion and its yield reached 158.0 mmol/mol at 97.4%. Benzene started to be generated at 46.5% conversion and its yield increased to reach 37.0 mmol/mol at 97.4%.

Xylenes, toluene and benzene result from successive demethylation reactions of 1,2,4-trimethylbenzene similar to those which have been observed on other methylated aromatic hydrocarbons (*e.g.* Smith and Savage, 1992; Leininger et al., 2006; Lannuzel, 2007). Trimethylbenzenes generate xylenes which in turn undergo demethylation reactions yielding toluene. As benzene was generated in very low quantities, toluene was found to be fairly stable under our experimental conditions.

Such demethylation pathways account for a first source of methane that was implemented into the free-radical mechanism. Methane is generated together with xylenes through a primary process as opposed to methane generated together with toluene and benzene through non-primary processes.

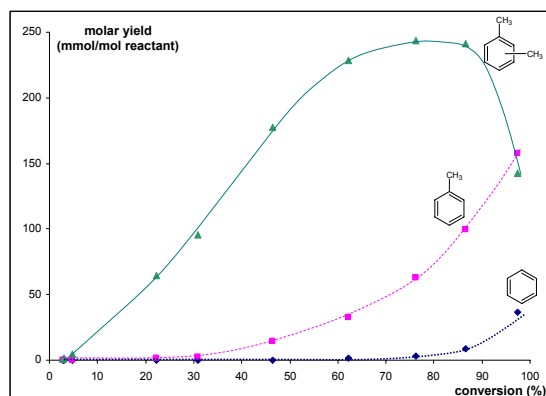


Figure 3: Molar yields of xylenes, toluene and benzene (in mmol/mol of initial reactant) versus conversion (curves suggest the trend lines).

3.2.2 Dimers

Dimers containing two aromatic rings coupled *via* an aliphatic bridge were detected. They range from C₁₃ to C₁₈ and are labelled according to their molecular-weight (for example dimers_238 have a molecular weight of 238 g/mol). Smith and Savage (1992) did not characterized heavy products of 1-methylpyrene pyrolysis but assumed those to be 1,2-dipyrenylethane. However, our GC-MS analyses showed that for 1,2,4-trimethylbenzene pyrolysis, methylated 1,2-diphenylethane isomers were minor dimers. This result is a consequence of the chemical instability of such bonds between two benzylic carbon atoms (Poutsma, 1990). Dimers are represented (Table 4) as methylated diphenylmethane isomers (Lannuzel, 2007) rather than methylated biphenyl isomers even if our GC-MS analysis did not enable discrimination. With no further analytical evidence, Leininger et al (2006) have chosen in contrast a direct bonding between aromatic rings to represent dimers obtained during the pyrolysis of 1-methylnaphthalene. We justify our representation according to the presence of anthracene type structures also detected experimentally (see below: triaromatic compounds for further justification).

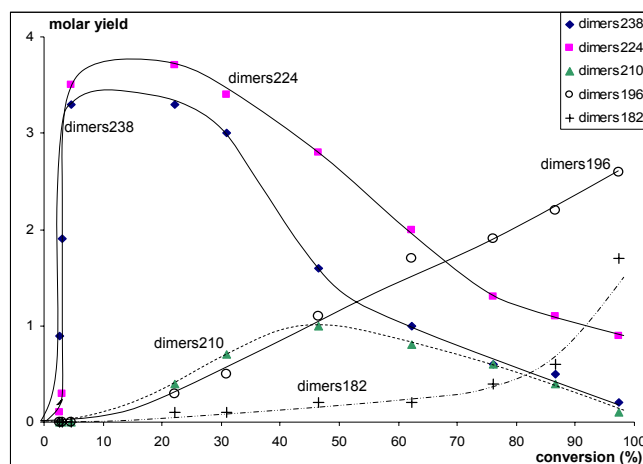


Figure 4: Molar yields of dimers (in mmol/mol of initial reactant) versus conversion (curves suggest the trend lines).

Dimers₂₃₈ were formed at low conversions (below 3%) and started to be degraded nearly immediately, reaching a maximum yield of 3.3 mmol/mol between 4.7% and 22.2% conversion before decreasing to 0.2 mmol/mol at 97.4% (Figure 4 and Table 3). Dimers₂₂₄ were also generated and degraded in early stages of the global reaction reaching a maximum of 3.7 mmol/mol at 22.2% conversion before decreasing to 0.9 mmol/mol at 97.4%. Dimers₂₁₀ started to be generated at 22.2% conversion, reached a maximum of 1.0 mmol/mol at 46.5% and decreased to 0.1 mmol/mol at 97.4%. Regarding dimers₁₉₆ and dimers₁₈₂, only an apparent increase of their molar yield was observed with values of 2.6 mmol/mol and 1.7 mmol/mol at 97.4% conversion, respectively. Only traces of dimers₁₆₈ were observed at high conversion (> 85%) and their quantification was not possible.

Regarding initial slopes for molar yields of dimers₂₃₈ and dimers₂₂₄ (Figure 4), it appears that secondary cracking of such compounds already takes place at low conversion. Generation and secondary cracking of dimers account for two additional identified pathways of early methane generation that were implemented into the free-radical mechanism.

3.2.3 Triaromatic hydrocarbons

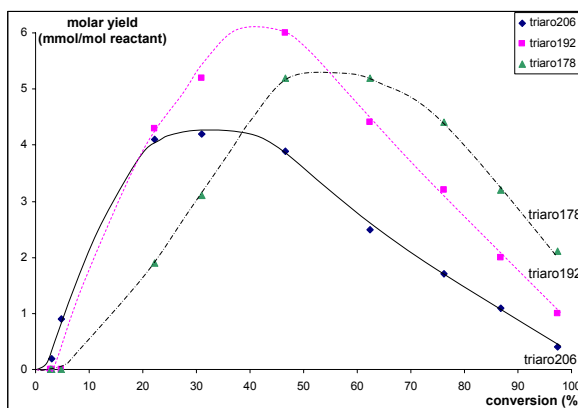


Figure 5: Molar yields of triaromatics (in mmol/mol of initial reactant) versus conversion (curves suggest the trend lines).

Triaromatic hydrocarbons such as methylated anthracene isomers and anthracene itself were detected experimentally. They range from C₁₄ to C₁₈ and are labelled according to their molecular-weight (for example triaro_206 have a molecular weight of 206 g/mol).

Triaro_220 and triaro_234 have been observed experimentally but their accurate quantification could not be performed. Indeed for each of these compounds, the isomers eluted in multiple tiny peaks and it was impossible to quantify them by gas-chromatography. Consequently, only molar yields of triaro_206, triaro_192 and anthracene (triaro_178) have been quantified and reported. Triaro_206 were generated at low conversion (3%) and reached a maximum molar yield of 4.2 mmol/mol at 30.9% conversion before decreasing to 0.4 mmol/mol at 97.4% (Figure 5 and Table 3). Triaro_192 and triaro_178 started to be generated at 22.2% conversion, and reached maximum molar yields of 6.0 mmol/mol and 5.2 mmol/mol at 46.5% and 55% conversion, respectively. They then decreased to 1.0 mmol/mol and 2.1 mmol/mol at 97.4 % conversion, respectively.

The formation of methylated anthracenes upon pyrolysis of methylated monoaromatics has already been reported (*e.g.* Szwarc, 1948; Blades et al., 1954; Schaeffgen, 1955; Errede and Cassidy, 1960). Detecting compounds with such a central 6-carbon-atoms ring convinced us to represent dimers as methylated diphenylmethane isomers rather than methylated biphenyl isomers. Indeed, coupling reactions can also occur intramolecularly within dimers (*e.g.* Errede and Cassidy, 1960). Such intramolecular reactions form intermediate species (termed p_{triaro} for triaromatic precursors) which dehydrogenate immediately (Poutsma, 1990) yielding triaromatic hydrocarbons. Traces of triaromatic precursors such as 9,10-dihydroanthracene were indeed detected experimentally within the *n*-pentane soluble fraction. The closure to a central 6-C-atoms ring is impossible for methylated biphenyl isomers which can only close into a central 5-C-atoms ring. The generation of

triaromatic products *via* secondary cracking of dimers thus accounts for an additional identified pathway of methane generation that was implemented into the free-radical mechanism.

3.3 Unidentified heavy products

No molecular identification of C₁₈₊ products which were soluble in *n*-pentane, of products soluble in dichloromethane (and not in *n*-pentane) and of the solid residue could be performed resulting in the exclusion of these species from molar yield calculations. Consequently, reactions leading to those species were not implemented in the free-radical mechanism. However, as their formation and degradation to generate char have been debated to constitute potential pathways of methane generation at high conversion (Smith and Savage, 1992; Behar et al., 1999; Lorant et al., 2000), the evolution of their yields is discussed in the following lines.

As shown in Table 2, the yield of heavy products which were soluble in *n*-pentane reached a maximum of 114.3 mg/g at 30.9% conversion and then decreased to 49.8 mg/g at 97.4%. After increasing sharply to around 18 mg/g at low conversion (< 5%), products which were soluble in dichloromethane remained fairly constant around 20 mg/g on the entire range of conversion. Solid residue was not observed at low conversion before being generated in significant quantity to reach 426.4 mg/g at 97.4%.

Condensation reactions have been a matter of debate due to the difficulty to characterize chemical structures of components in such heavy fractions. For example, Leininger et al (2006) proposed that polymerisation would continue with dimers of methylanthalene becoming trimers. McClaine and Wornat (2007) proposed a series of coupling reactions between PAH and radicals followed by ring closures and dehydrogenations to give larger PAH. In any case, according to their increasing molecular-weight, such products became less soluble in *n*-pentane and dichloromethane and might have generated char as soon as they started to disappear from the C₁₄₊ *n*-pentane fraction. Indeed, the solid residue started to be generated in significant quantity around 20% conversion (16.9 mg/g) while the yield of C₁₄₊ compounds which were soluble in *n*-pentane started to decline.

3.4 Guidelines for composing the free-radical mechanism

- (i) Our experiments were performed at a pressure of 100 bar. In such conditions, our literature review emphasized the need to consider bimolecular initiations in addition to unimolecular ones,

- (ii) In our temperature conditions, experimental results confirmed previous studies showing that the opening of the benzene ring did not occur and would not need to be modelled,
- (iii) Methane can be generated *via* successive demethylation reactions of the reactant,
- (iv) As such demethylation reactions occurred for monoaromatics they would also be considered for other methylated products such as dimers, triaromatic precursors and triaromatics,
- (v) Competitive pathways for methane production can be the generation of dimers and their degradation to form tricyclic compounds (triaromatic precursors).

4. Composition of the free-radical mechanism

On the basis of the previous guidelines, a free-radical mechanism for thermal cracking of 1,2,4-trimethylbenzene has been established (Table 5). It comprises more than 100 reversible reactions and has been written in the format of software CHEMKIN II (Kee et al., 1989), used for validation. Kinetic parameters involved in rate constants k ($k = A.T^b \cdot \exp(-Ea/R.T)$) are given in cubic centimetre, mole, second, calorie units. A represents the frequency factor, Ea the activation energy and b the curvature of the Arrhenius plot versus temperature (when given in the kinetic database). Initial guesses for kinetic parameters are those published for simple model reactions with molecules having similar structural features and thus supposedly similar reactivity to our compounds. Most of those parameters are referenced in updated version of N.I.S.T. (c.f. references) chemical kinetics database. Some adjustments F ($F = k(\text{fitted}) / k(\text{estimated})$) have been made on frequency factors when needed to fit experimental results at best and are reported in the last column of Table 5. Such modifications never exceed a multiplication or division factor of 10 to remain chemically reliable.

Regarding presentation of Table 5, each numbered reaction is followed by the related kinetic parameters. Kinetic parameters corresponding to the reverse reaction are indicated below the latter, following the word 'reverse'. For the reader, most species are represented by abbreviations. The real chemical structures are listed in Table 4. In most cases, abbreviations (including the reactant) correspond to a group of possible isomers differing from each other by the locations of methyl moieties on the ring(s). Consequently methyl groups are not drawn in specific positions. Abbreviations for radicals start with the letter R. Letters 'a' and 'b' stand for radicals resulting from the abstraction in the subsequent molecule of benzylic and phenylic H-atoms, respectively. Letters 'c' and 'd' stand for radicals resulting from the

addition of an H-atom on the aromatic nucleus of the reactant. Each abbreviation of radical corresponds to a group of isomers regarding locations of methyl moieties and locations of the resonance delocalized single electron. To reduce the size of Table 4, only one or two examples of possible isomers (underlining the main types of structures involved) are represented for each abbreviation of radical.

The general idea of the mechanism is that, apart from initiation reactions which have been considered only for the reactant (trimethylbenzenes), all reaction types have been composed with the reactant, the xylenes, and their corresponding radicals (according to the substantial abundance of xylenes observed experimentally). Major types of reactions leading to the formation of the main pyrolysis products will be described in the following lines.

4.1 Initiation reactions

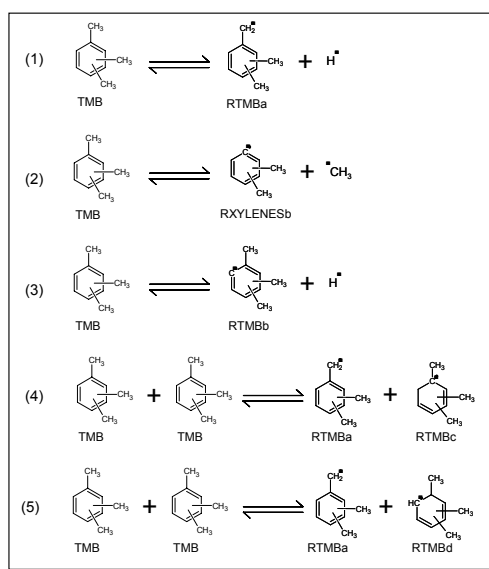


Figure 6: Unimolecular and bimolecular initiation reactions considered for modelling thermal cracking of trimethylbenzene.

As already stated above, according to our elevated pressure conditions (100 bar), we had to consider both unimolecular and bimolecular initiation reactions (Figure 6).

Unimolecular initiations of trimethylbenzene molecules give either dimethylbenzyl radicals and H-atoms (reaction 1), xylil isomers and methyl radicals (reaction 2) or trimethylphenyl radicals and H-atoms (reaction 3). Despite they were respectively published for toluene and phenyl radicals, kinetic parameters of Bounaceur et al (2005) and Tokmakov

et al (1999) have been used without the need of adjustment to fit our experimental data (Table 5).

Bimolecular initiations of trimethylbenzene molecules proceed through reverse radical disproportionation RRD (Smith and Savage, 1992; Leininger et al., 2006; Lannuzel, 2007). The transfer of H-atoms from benzylic carbons to the aromatic nucleus affords dimethylbenzyl radicals and trimethylcyclohexadienyl radicals with an H-atom in α - (reaction 4) or *ipso*- (reaction 5) positions of a methyl group. Kinetic parameters of Lannuzel (2007) which were estimated for toluene have been used without the need of adjustment to fit our experimental data (Table 5).

4.2 Propagation reactions

4.2.1 *Ips*o-additions

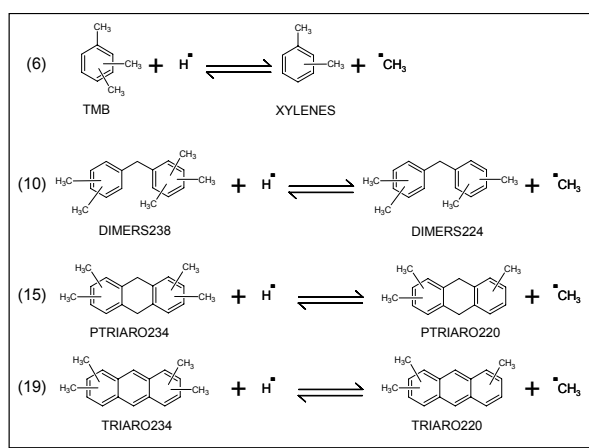


Figure 7: Examples of ipso-additions considered for modelling thermal cracking of trimethylbenzene.

As part of propagation reactions, molecules can undergo *ipso*-additions of H-atoms which release CH₃ radicals (Figure 7).

*Ips*o-additions of H-atoms on monoaromatics (reactions 6, 8, 9 and reverse-reaction of 7) are illustrated by reaction 6 in which trimethylbenzenes undergo *ipso*-additions of H-atoms yielding methyl radicals and xylenes. *Ips*o-additions of H-atoms on dimers (reactions 10 to 14) are illustrated by reaction 10 in which dimers₂₃₈ undergo *ipso*-additions of H-atoms to give dimers₂₂₄ and methyl radicals. *Ips*o-additions of H-atoms on precursors of triaromatics (reactions 15 to 18) and on triaromatics themselves (reactions 19 to 22) are illustrated by

reactions 15 and 19 in which ptriaro_234 and triaro_234 are demethylated into ptriaro_220 and triaro_220, respectively.

Regarding kinetic parameters, the rate constant published by Baulch et al (1994) for the *ipso*-additions of H-atoms on toluene has been adjusted to better fit our experimental results. Chosen multiplication factors are $F = 10$ for molecules containing two or more methyl moieties and $F = 3$ for molecules with only one methyl group (Table 5).

4.2.2 Additions of benzylic radicals

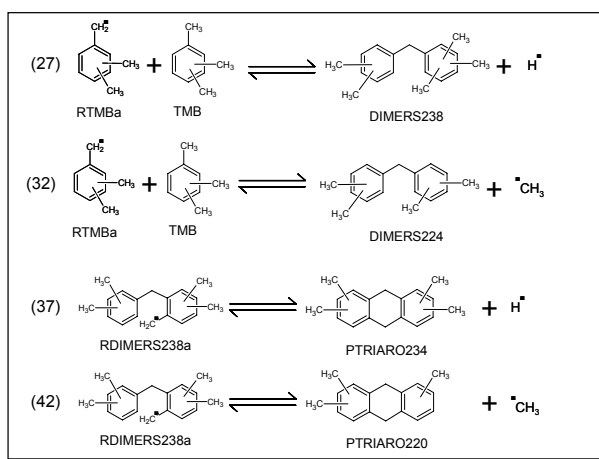


Figure 8: Examples of additions of benzylic radicals considered for modelling thermal cracking of trimethylbenzene.

Lannuzel (2007) demonstrated that coupling reactions of toluene and benzyl radicals generate diphenylmethane isomers and CH₃ radicals. We have thus written the same type of reactions for species detected in our experiments.

Benzylic radicals such as RTMBa and RXYLENESa can react with monoaromatics (Figure 8) to form dimers and release either H-atoms (as illustrated by reaction 27 in which dimers_238 are formed) or methyl radicals (as illustrated by reaction 32 in which dimers_224 are formed). The initial guess for kinetic parameters has been taken from Brioukov et al (1999) for the coupling reaction between benzene and benzyl radicals which forms diphenylmethane and H-atoms. When additions necessitated the breaking of C-H bonds (reactions 27 to 31), multiplication factors F have been chosen equal to 2, 3 and 5 for the series of respectively trimethylbenzenes, xylenes and toluene in which the number of hydrogen-atoms increases. When additions necessitated the breaking of C-C bonds (reactions 32 to 36), multiplication factors F have been chosen equal to 5, 3 and 2 for the series of respectively trimethylbenzenes, xylenes and toluene in which the number methyl of moieties

decreases (Table 5). The model showing no much difference when the coupling reactions of toluene with RTMBa, benzene with RTMBa and benzene with RXYLENESa were considered, those additions have not been kept in the final version.

Coupling reactions can also occur *via* intramolecular pathways (reactions 37 to 45) after one H-atom has been abstracted on the -CH- group located in β -position of the bridge of dimers. Consequently, triaromatic precursors ptriaro can be formed by such intramolecular addition and, either further elimination (Figure 8) of H-atoms (reactions 37 to 41 illustrated by reaction 37) or further elimination of methyl radicals (reactions 42 to 45 illustrated by reaction 42). The best fit with our experimental data was obtained by dividing the frequency factor by 2 compared to Brioukov et al (1999) for reactions 37 to 41 (Table 5).

Rate constants are thus slower for intramolecular additions (reactions 37 to 45) than for intermolecular ones (reactions 27 to 36). The sterical hindrance is indeed relatively high for intramolecular reactions in which the closure into a central 6-C-ring is possible for only a limited range of bond angles and locations. On the contrary, for bimolecular reactions the collision between a molecule and a benzylic radical yielding a dimer can occur more easily. Moreover, for a given type of addition (intermolecular or intramolecular), rate constants are faster when methyl radicals are released rather than H-atoms. It demonstrates that despite the sterical hindrance being higher for an approach in the neighbourhood of a methyl group than an H-atom, the kinetic of the reaction is in fact determined by the difference in bond energies being 10 kcal/mol (≈ 41.9 kJ/mol) in favour of the breaking of the C-C bond rather than the C-H one (*e.g.* Luo, 2003).

4.2.3 Metatheses

H-abstractions on trimethylbenzenes, xylenes, dimers and triaromatic precursors by H-atoms (reactions 46 to 57), methyl radicals (reactions 58 to 69) and benzylic radicals (reactions 70 to 90) have been written as potential metatheses (*i.e.* reactions of H-transfer). They all lead to the formation of benzylic radicals. Adjustments *via* the factor F (Table 5) follow the general idea that the formation of benzylic radicals from dimers and triaromatic precursors had to be very much emphasized. Indeed, those structures allow the localisation of the single electron to be also on the -CH- group of the bridge (see Table 4) which enables the writing of mesomeric formulae with the two aromatic nuclei, enhancing tremendously the stability of such radicals.

Metatheses by H-atoms yielding molecular hydrogen are illustrated by reactions 46, 48 and 53, and metatheses by methyl radicals yielding methane are illustrated by reactions 58, 60

and 65 (Figure 9). The lack of appropriate kinetic parameters for reverse reactions has forced us to attempt an estimation after the work of Tsang (1991) on the reaction ‘propenyl radical + CH₄ = propene + CH₃’. We have divided the frequency factor by 10 to account for cyclic radicals which are more stabilized than a propenyl radical (Table 5).

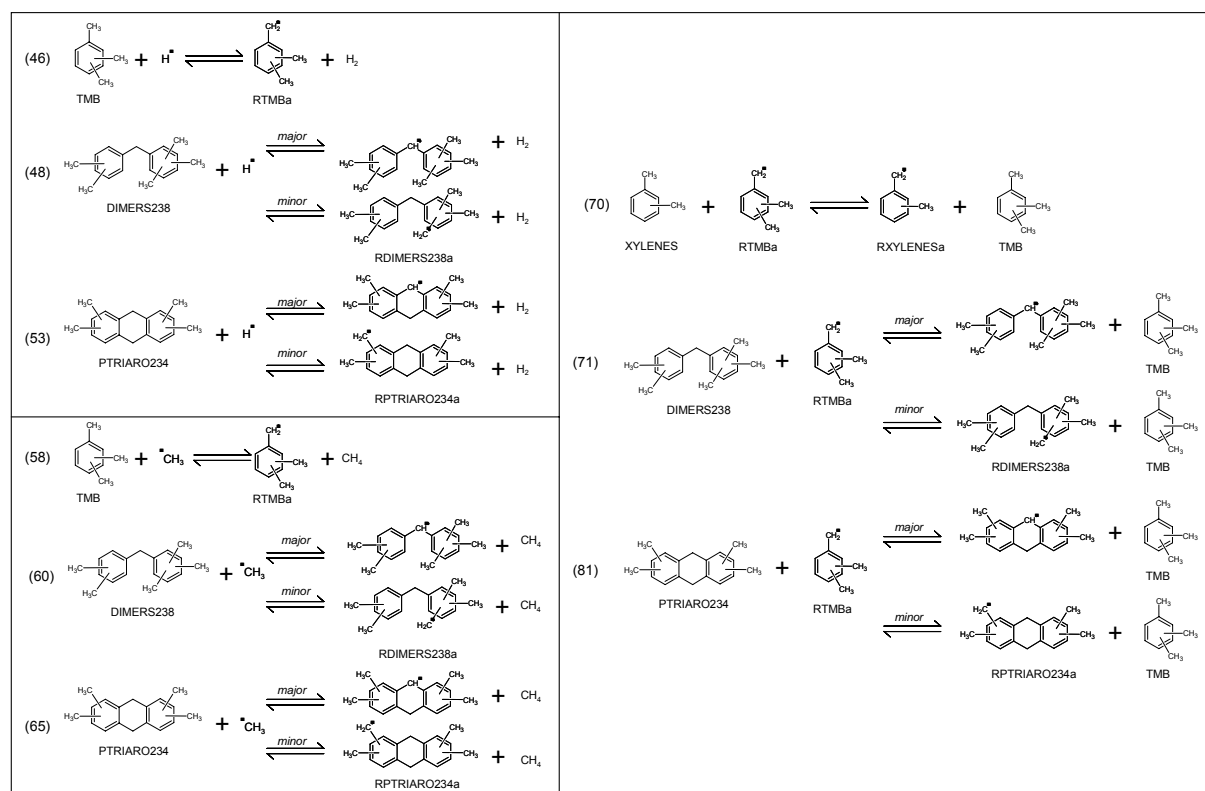


Figure 9: Examples of metatheses considered for modelling thermal cracking of trimethylbenzene.

Metatheses by benzylic radicals RTMBa and RXYLENESa are illustrated by reactions 70, 71 and 81 (Figure 9). Benzylic radicals can react with methylated aromatics to lead to other methylated aromatics and other benzylic radicals. To the best of our knowledge, no kinetic parameters have been published for such type of reaction. Estimation has thus been attempted after the reaction ‘toluene + CH₃ = benzyl + CH₄’ (N.I.S.T. fit: A = 1.6e¹¹ cm³.mol⁻¹.s⁻¹ and Ea = 8800 cal.mol⁻¹). We have divided the frequency factor by 10 to account for cyclic radicals and the activation energy has been taken 4 kcal/mol higher to account for resonance stabilised radicals. Then, frequency factors for direct and reverse reactions have been respectively multiplied and divided by 10 to emphasize the enhanced stability of radicals with a ‘double mesomeric stabilization’ (Table 5).

4.2.4 Decompositions

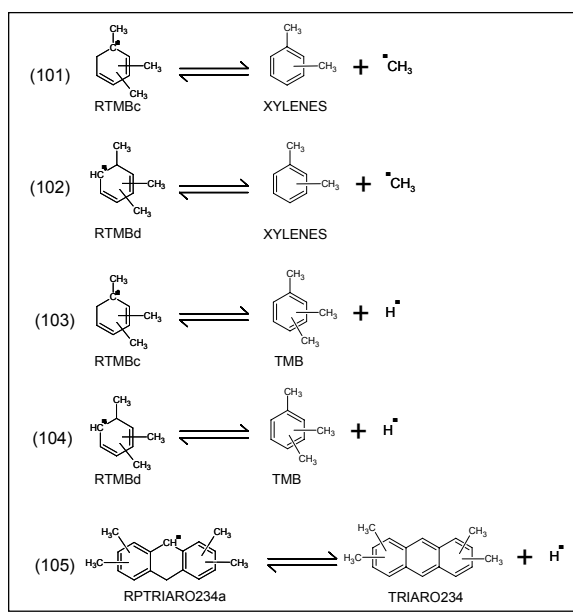


Figure 10: Examples of decompositions considered for modelling thermal cracking of trimethylbenzene.

The last type of propagation reactions which have been taken into account in the mechanism are decompositions of radicals generating aromatic rings. They occur (Figure 10) *via* β -eliminations of H-atoms or β -eliminations of methyl radicals (reactions 101 to 104), and *via* more complex dehydrogenation reactions yielding triaromatics (reactions 105 to 109).

4.2.5 Termination reactions

To compare the model prediction with experimental data which revealed only traces of methylated 1,2-diphenylethane isomers (termed biaros in the mechanism), ethylxylenes, ethyltoluenes and ethylbenzene, we took into account all the termination reactions (reactions 110 to 115) between main types of benzylic radicals (RTMBa and RXYLENESa) as well as non-aromatic radicals (H, CH₃).

The established free-radical mechanism is summarized on Figures 11a and 11b, not including reactions and products relying on termination reactions. It models 122 chemical transformations involving 47 species. In addition to the reactant, 27 molecular products are represented including: 3 non-aromatic molecules (H₂, CH₄, and C₂H₆), 7 monoaromatic compounds (benzene and substituted counterparts), 12 diaromatic compounds (dimers, biaros and ptiaros) and 5 triaromatic compounds (triaros). This mechanism is also based on 19

radical species including: 3 non-aromatic radicals (H, CH₃, C₂H₅), 6 monoaromatic radicals (2 benzylic, 2 phenylic and 2 non-aromatic) and 10 diaromatic benzylic radicals.

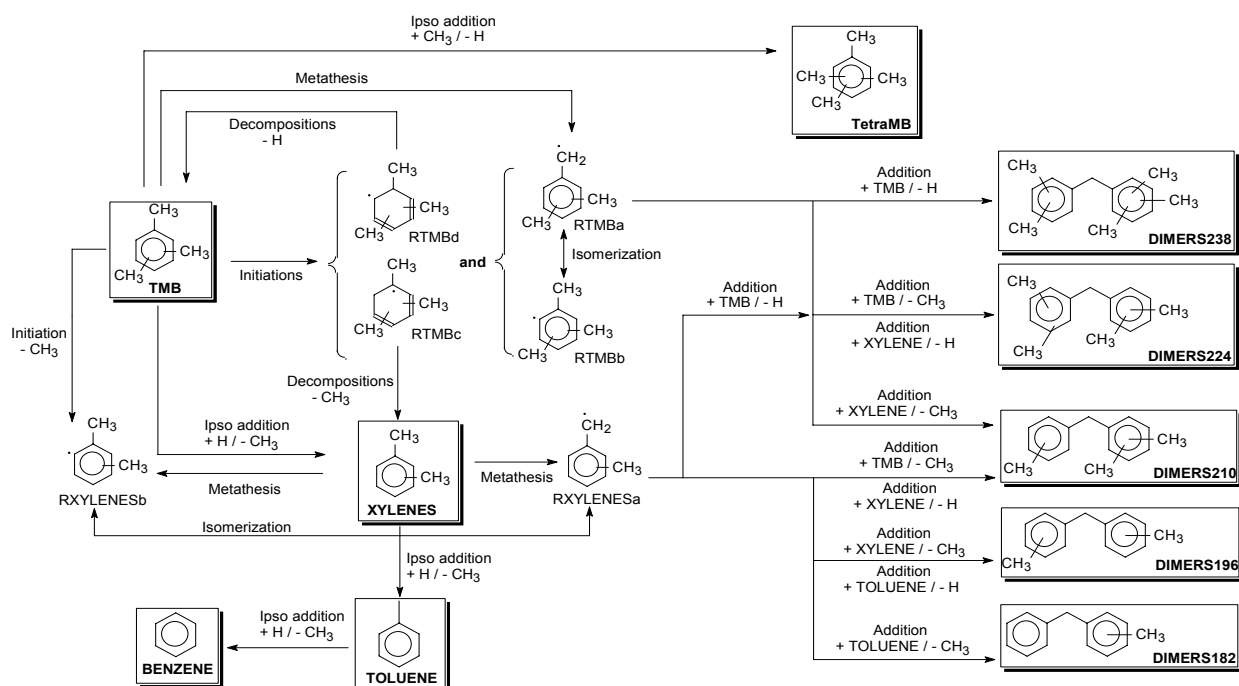


Figure 11a: Summary of the free-radical mechanism for thermal cracking of trimethylbenzene. Reactions up to dimers.

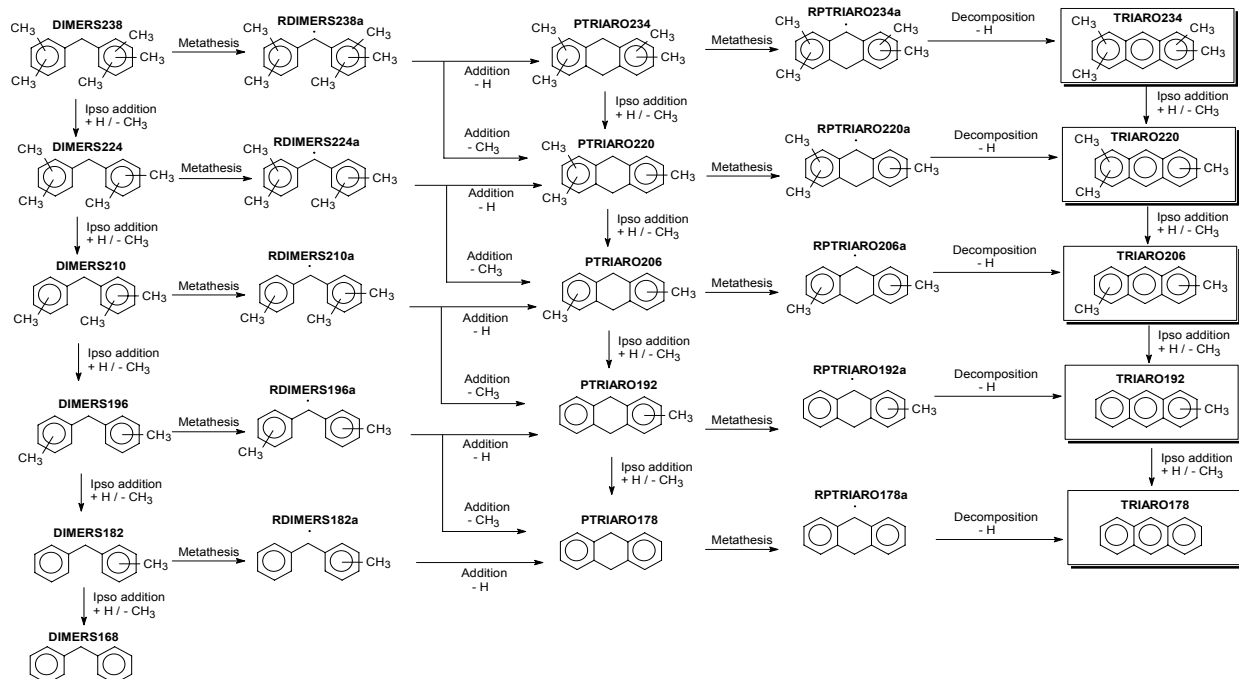


Figure 11b: Summary of the free-radical mechanism for thermal cracking of trimethylbenzene. Reactions from dimers to triaromatics.

The scope of the paper being to identify chemical pathways leading to methane generation, such potential pathways are illustrated on Figure 12. It is interesting to note that methane is produced at every major stage. We can however distinguish 2 main routes. The 'monoaromatic route' is constituted of successive demethylations of the reactant. This route also accounts for the generation of xylenes, toluene and benzene. The 'polyaromatic route' represents condensation reactions which successively lead to dimers (step 1), triaromatic precursors (step 2), triaromatics (step 3) and also generates hydrogen in addition to methane. It also comprises demethylation reactions of dimers, triaromatic precursors, and triaromatics. As represented with dashed lines, triaromatics may be involved in further condensation reactions (step 4). Such reactions have the potential to generate methane as well as prechar, char and hydrogen (Smith and Savage, 1992; Behar et al., 1999; Lorant et al., 2000). However, as justified above, reactions of step 4 could not be taken into account in the free-radical model.

Next stage is then to validate the model by comparing its predictions to experimental observations before using it to quantitatively assess the various potential pathways identified for methane generation.

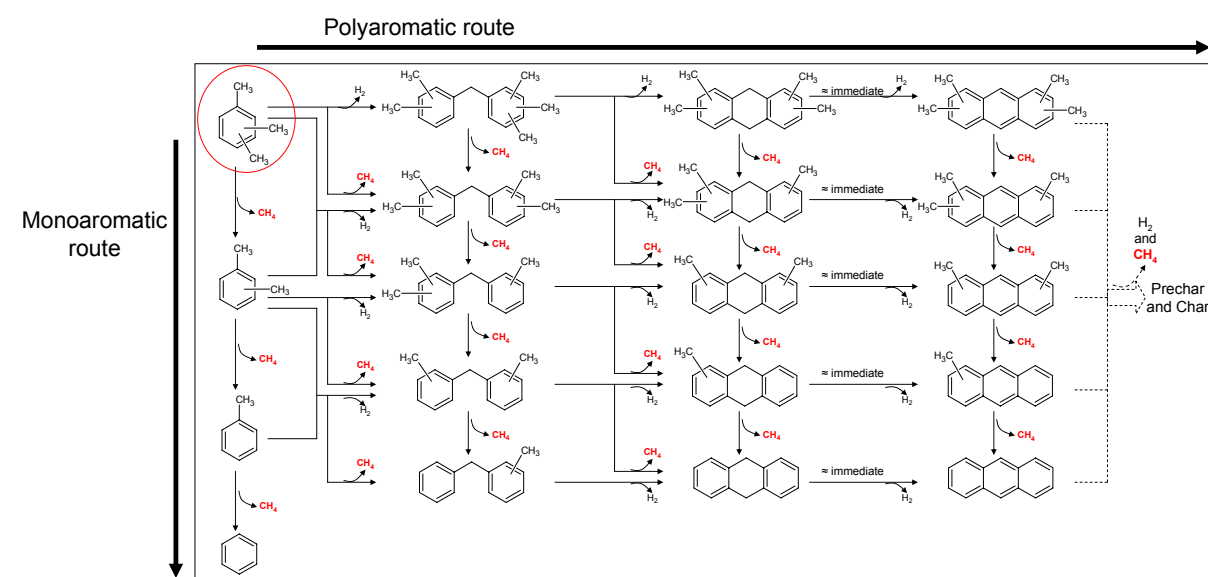


Figure 12: Methane potential generation pathways during thermal cracking of trimethylbenzene.

5. Validation of the model

We simulated the pyrolysis of 1,2,4-trimethylbenzene at 395 °C, 425 °C, and 450 °C and a pressure of 100 bar using the software CHEMKIN II (Kee et al., 1989). Chemical reactions and kinetic parameters were entered as they are reported in Table 5. CHEMKIN II,

enables to follow molar ratios (X_i) of yields (n_i) of species to the total yield ($n_t = \sum n_i$) of all species as shown in equation 5.

$$X_i = n_i / n_t \quad (5)$$

Consequently, apart from the reactant conversion (Figure 14), charts displayed on Figures 13 to 17 report molar ratios and enable comparison between model predictions and experimental results.

5.1 Methane

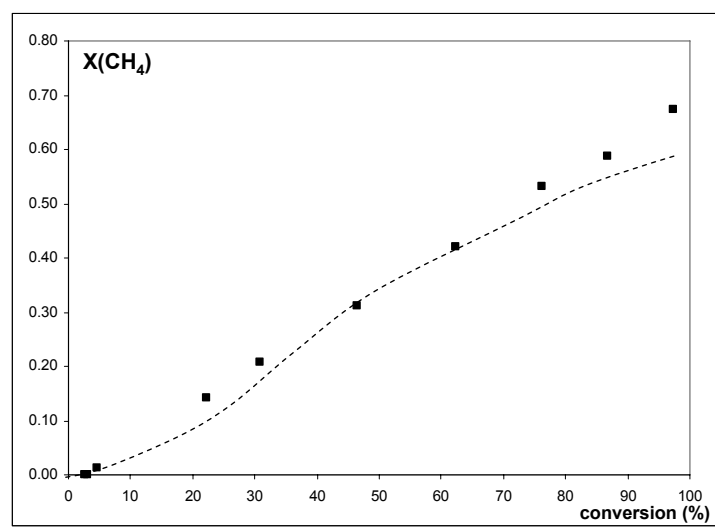


Figure 13: Computer-predicted (dashed line) and experimental (dots) molar ratios $X(CH_4)$ for methane versus conversion.

As shown on Figure 13, the prediction for methane is accurate on nearly the entire range of conversion but starts to diverge significantly from experimental data around 90% conversion. Two explanations can be proposed to explain such result. Indeed, when conversion increases, condensation reactions may generate methane but are not taken into account in the model, leading to an underestimation for this gas. Moreover, as heavy compounds could not be identified individually, they are not taken into account in the total molar yield n_t for the calculation of experimental molar ratios X_i . It can thus lead to an overestimation of experimental molar ratio X_i (including methane one) when heavy species are produced significantly *i.e.* at conversions above 50% (Table 2).

5.2 Reactant conversion

Despite the mechanism being validated on methane, its accuracy to predict the reactant conversion is also an aspect to consider with attention. Figure 14 shows 1,2,4-

trimethylbenzene conversion versus time at 395 °C, 425 °C, and 450 °C. Computer predicted results reproduce the general trend of the conversion at all temperatures and remain in the same order of magnitude as experimental results. The overestimation becomes significant at 450 °C for conversions above 70% (above 75h).

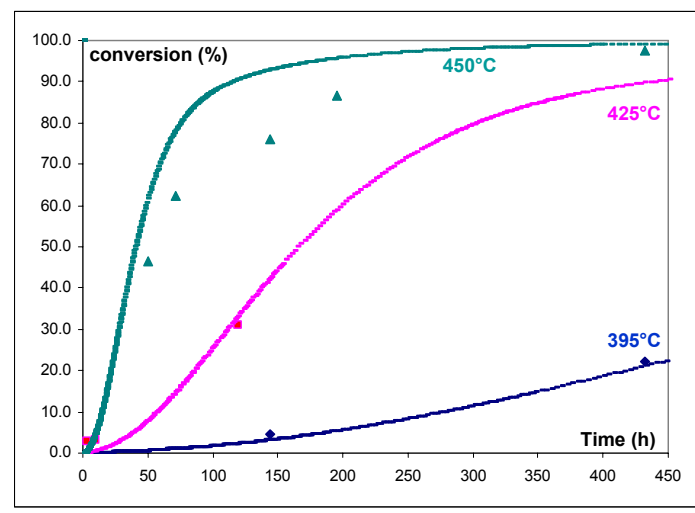


Figure 14: Computer-predicted (lines) and experimental (dots) conversion of trimethylbenzene versus time at 395°C, 425°C and 450°C.

5.3 Other gaseous products

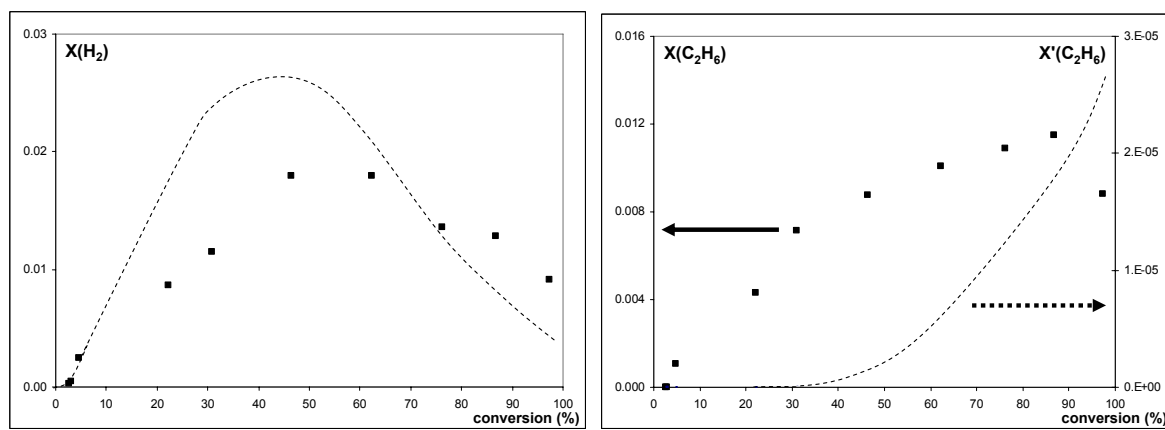


Figure 15a and 15b: Computer-predicted (dashed line) and experimental (dots) molar ratios X_i for hydrogen and ethane versus conversion.

Regarding hydrogen, the increase and decrease are predicted by the model in the same order of magnitude as experimental results even if the maximum is overestimated (Figure 15a). It must be noted that molecular hydrogen having a molecular-weight of only 2 g/mol, its molar ratio is the most sensitive to variations. Despite our efforts, ethane prediction remained inaccurate as shown in Figure 15b. The two scales of the y-axis reveal at least a two orders of magnitude underestimation by the model. With a reactant being a methylated aromatic, the

generation of ethane in the model can indeed only rely on termination reactions either *via* recombinations of CH₃ radicals or *via* termination reactions leading to ethyl substituted monoaromatics (ethylxylenes, ethyltoluenes and ethylbenzene) which in turn undergo *ipso*-additions of hydrogen to release C₂H₅. High-pressure conditions (100 bar) of our experiments may have induced other processes rather than elementary free-radical reactions. The misestimating of ethane cracking to give methane is anyway not the cause to methane underestimation at high conversion according to the discrepancy between ethane and methane molar ratios.

5.4 Monoaromatics

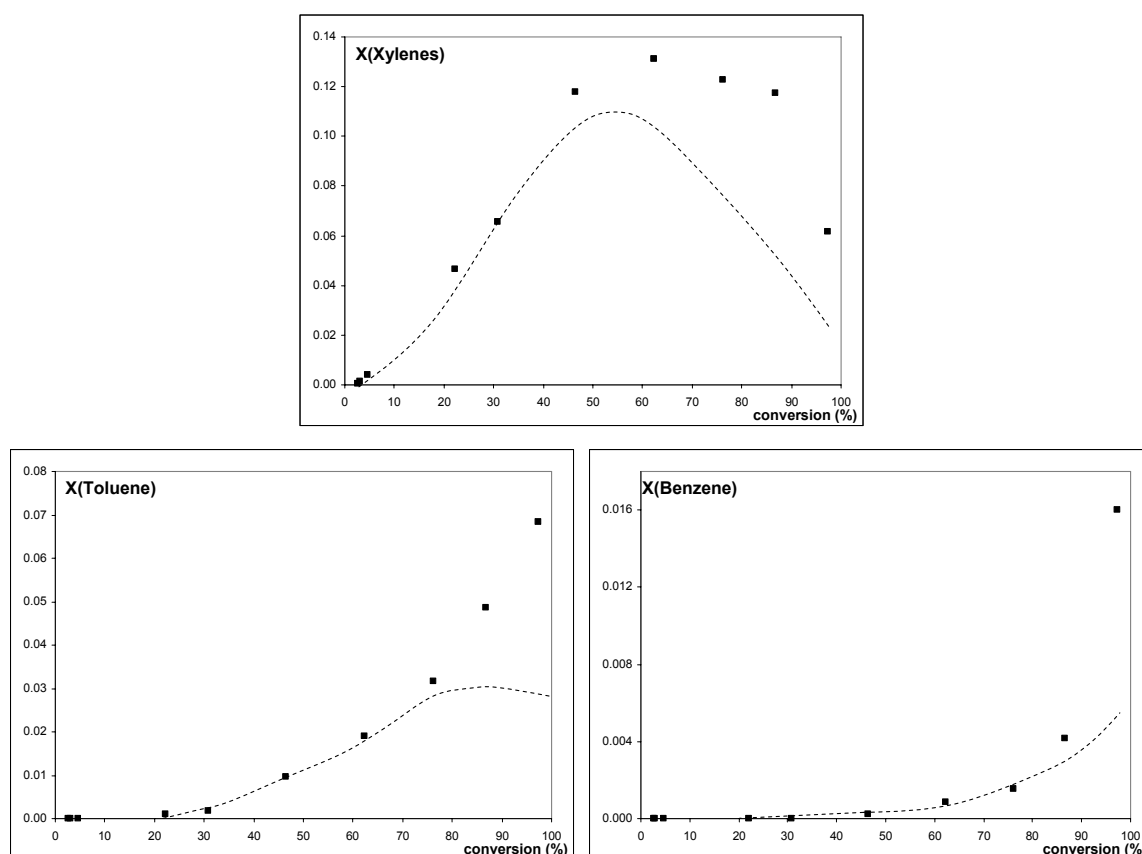


Figure 16a, 16b and 16c: Computer-predicted (dashed lines) and experimental (dots) molar ratios X_i for xylenes, toluene and benzene versus conversion.

Products of the aforementioned 'monoaromatic route' (xylenes, toluene and benzene) are also accurately modelled below 70% conversion before showing the same underestimation as other species (Figure 16a, 16b and 16c). Regarding xylenes (Figure 16a), the inversion observed experimentally between 50% and 70% conversion is also predicted by the model.

Tetramethylbenzenes, ethylxylenes, ethyltoluenes and ethylbenzene are not predicted in significant amount by the model which is in agreement with traces observed experimentally.

5.4 Dimers

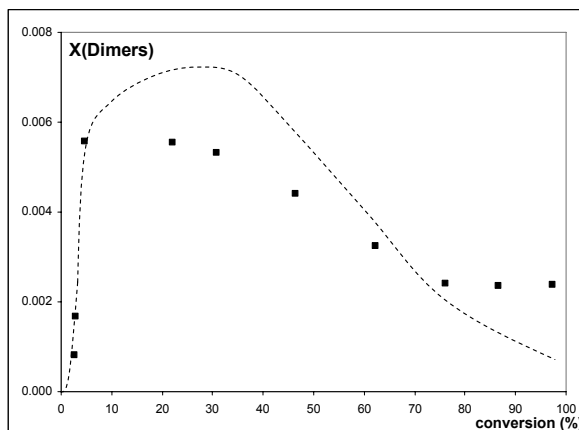


Figure 17: Computer-predicted (dashed line) and experimental (dots) molar ratios $X(\text{dimers})$ for the sum of dimers versus conversion.

For the reader, only the total yields of dimers are represented in Figure 17. Increase and decrease are accurately modelled predicting the inversion between 10% and 30% conversion, and remaining in the same order of magnitude as experimental data. Dimers_168, 1,2-diphenylethane isomers (biaros) and triaromatic precursors (ptriaro) are not predicted in significant amount by the model, a result which is in agreement with traces observed experimentally for those compounds.

As already stated, degradation reactions of triaromatics have not been accounted in the model and thus predictions obtained for those compounds can not be compared with our experiments.

As detailed above, the model has been validated at high temperature (395 °C-450 °C) and at a pressure of 100 bar. Studies regarding the effect of pressure are rare and sometimes controversial. For example, Dominé (1991) pyrolysed *n*-butyl benzene at 305 °C and 357 °C with pressure ranging between 210 bar and 15,400 bar. He found out that increasing pressure hindered the cracking process. However, this conclusion was not confirmed by Al Darouich et al (2006b) when they pyrolysed a mixture of light aromatic compounds at 375 °C and at pressures of 400 bar, 800 bar and 1200 bar. They indeed observed a slight acceleration of the global rates when increasing pressure. Consequently and by precaution, we will consider that the prediction given by our model is only valid at a pressure of 100 bar.

Our model will now be used to assess the relative contributions of potential identified pathways of methane generation.

6. Methane generation pathways

Figure 13 has demonstrated that the model is accurate to predict methane generation at high temperature (395 °C-450 °C) until around 70% conversion. Figures 14 to 17 have confirmed such prediction is based on chemically reliable reactions. On Figure 12 we have illustrated that methane potential sources described by the model are:

- (i) Successive demethylation reactions of the reactant trimethylbenzene,
- (ii) Intermolecular additions of monoaromatics yielding dimers,
- (iii) Intramolecular additions of dimers yielding precursors of triaromatics,
- (iv) Demethylation reactions of either dimers, triaromatic precursors, and triaromatics.

In the following part we will quantify the contributions of these sources to methane global yield. Such sensibility analysis will enable to check whether the relative importance of these sources depends on temperature or not.

6.1 Sensibility analysis of the mechanism at high temperature

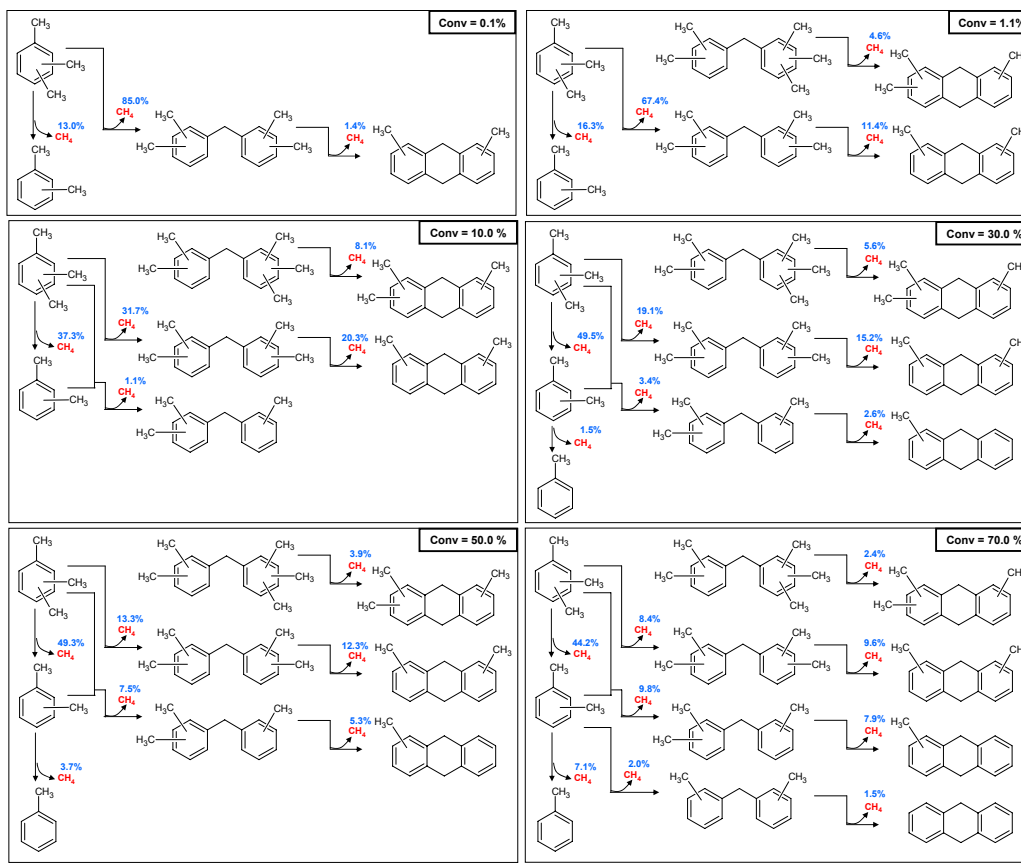


Figure 18: Methane generation pathways according to conversion during thermal cracking of trimethylbenzene at 425 °C.

Simulations have been performed at 425 °C as it was the medium temperature of our pyrolysis experiments. For each reaction generating methane at a given conversion, percentages (Figure 18) have been calculated as the ratio of the rate of production of methyl radicals by the reaction to the global rate of generation of methyl radicals. Values of less than 1% have not been reported. Low conversions (0.1% and 1.1%) have been tested to quantify the sources of primary methane (*e.g.* Leininger et al., 2006). Then, simulations have been performed at 10%, 30%, 50%, and 70% of conversion to estimate the evolution in the distribution of methane sources with conversion. No simulations have been performed at conversions higher than 70% for which the model has been shown to be less accurate.

At low conversion (0.1% and 1.1%) it appears that methane is mainly (65% - 85%) generated by the aforementioned 'polyaromatic route' (Figure 12) especially with the formation of dimers₂₂₄. The 'monoaromatic route' is not negligible anyway, as the demethylation of trimethylbenzene into xylenes contributes by around 15% to the global methane yield.

When conversion increases, the contribution of the 'monoaromatic route' becomes of greater importance regarding methane generation and represents around 50% of its global

yield at 70% conversion. The demethylation of toluene into benzene contributes by less than 1% to methane global yield at 70% conversion. Toluene can thus be reasonably considered as the terminal monoaromatic product of the monoaromatic route. Within the 'polyaromatic route', the formation of dimers exhibits merely the same contribution to methane generation as the generation of triaromatic precursors above 10% of conversion. For example, at 70% conversion those contributions to methane global yield are 20.2% and 21.4%, respectively. Whatever the conversion, the demethylation reactions of either dimers, triaromatic precursors or triaromatics do not show any significant contribution to methane global yield, accounting for less than 1%.

6.2 Sensibility analysis of the mechanism at low temperature

Except the opening of the benzene ring, all possible free-radical reactions have been taken into account in the model at high temperature (395 °C-450 °C). As such reaction is even more unlikely to occur at lower temperature, no additional reaction has been added for performing simulations at 200 °C. We chose the same series of conversions (0.1%, 1.1%, 10%, 30%, 50%, 70%) as those at 425 °C to estimate whether the distribution of predicted methane sources changes when temperature is lower. Results are reported in Figure 19 and once again values of less than 1% are not displayed.

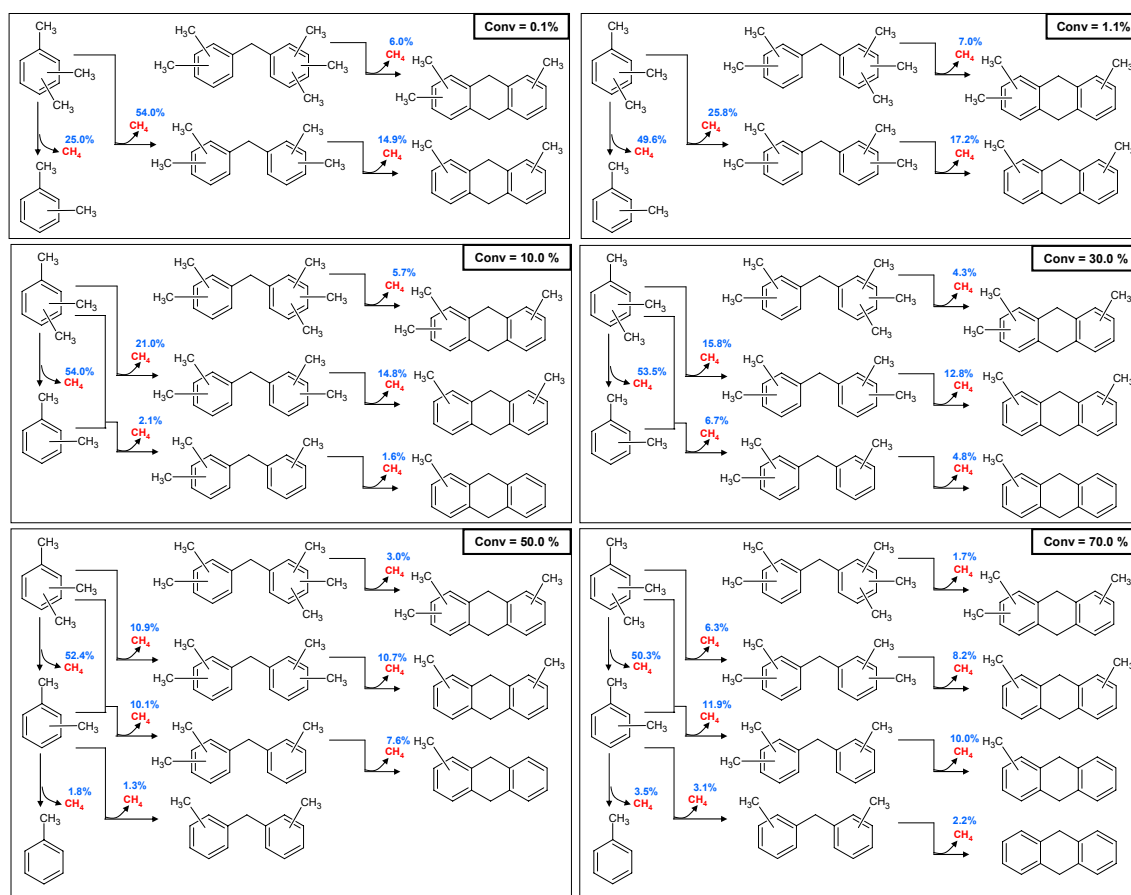


Figure 19: Methane generation pathways according to conversion during thermal cracking of trimethylbenzene at 200 °C.

At very low conversion (0.1%) it appears that methane is in majority (75%) generated by the 'polyaromatic route' but compared to 425 °C the formation of triaromatic precursors seems to occur earlier, already accounting for around 21% of the total methane. The 'monoaromatic route' is more emphasized with 25% of the total methane generated by the demethylation of trimethylbenzenes into xylenes compared to the 13% at 425 °C.

When conversion increases, the proportion of methane generated by the 'monoaromatic route' expands faster at 200 °C than at 425 °C, representing around 50% at 1.1% conversion but remains stable afterwards. The demethylation of toluene into benzene is once again negligible whatever the conversion regarding its contribution to methane generation. The relative contributions of the 'polyaromatic' and 'monoaromatic' routes remain fairly similar until 70% conversion with a slight advantage in the favour of the 'monoaromatic route'. Within the 'polyaromatic route', the formation of dimers (step 1) exhibits merely the same contribution to methane generation as the generation of triaromatic precursors (step 2) above 1.1% conversion. For example, at 70% conversion, the contributions of those two pathways to methane global yield are 21.3% and 22.1%, respectively. Those proportions are

in the same range as those observed at 425 °C. The demethylation reactions of either dimers, triaromatic precursors or triaromatics are once again negligible whatever the conversion regarding their contribution to methane generation.

When comparing the sensibility analyses at 425 °C and at 200 °C (until 70% conversion), it has thus been demonstrated that when a pathway is negligible (respectively substantial) at high temperature it remains the same at low temperature.

The pathways relevant for methane generation are:

- (i) The 'monoaromatic route' *i.e.* the demethylation of trimethylbenzenes into xylenes and to a lesser extent the demethylation of xylenes into toluene,
- (ii) The formation of dimers ('polyaromatic route', step 1),
- (iii) The intramolecular ring closure reaction of dimers into triaromatic precursors 'polyaromatic route', step 2).

At low temperature (200 °C) the contribution of the 'monoaromatic route' expands faster than at high temperature (425 °C). However, at both temperatures the equilibrium reached is a fairly equal contribution for the 'monoaromatic route' and the 'polyaromatic route'. Eventually, demethylation reactions of toluene, dimers, triaromatic precursors and triaromatics are no relevant pathways to consider regarding methane generation in both ranges of temperature.

7. Conclusion

1,2,4-trimethylbenzene was chosen as a model compound to study thermal cracking of methylated monoaromatic hydrocarbons present in reservoirized petroleum. It was necessary to discriminate primary products from non-primary products in order to elucidate a maximum of elementary processes involved in methane generation. Consequently, we performed pyrolysis experiments choosing experimental conditions in order to cover the widest range of reactant conversion (between 395 °C and 450 °C, at a pressure of 100 bar). All pyrolysis fractions were recovered and quantified. Mass-balances were established to ensure that the whole materials were recovered and experiments with less than 98% recovery were discarded to ensure that quantitative data were accurately constrained. All products that could be identified individually were quantified.

According to experimental results, methane could potentially be generated *via*:

- (i) The demethylation reactions of the reactant into successively xylenes, toluene and benzene,

- (ii) The formation of dimers issued from intermolecular coupling reactions of methylated monoaromatics,
- (iii) The intramolecular ring closure reactions of dimers into 'triaromatic precursors' releasing methane. Those triaromatic precursors were only detected as traces since they might have dehydrogenated quasi immediately into triaromatics,
- (iv) The demethylation reactions of dimers, triaromatic precursors and triaromatics,
- (v) The generation of heavy fractions such as pre-char and char.

On the basis of experimental observations and detailed free-radical mechanisms published for other model compounds, a free-radical mechanism for thermal cracking of trimethylbenzene was proposed. According to the high pressure (100 bar) of our experiments, bimolecular initiation reactions were taken into account. Because pre-char and char had not been molecularly characterized experimentally, related reactions were not implemented in the model and triaromatics were thus taken as ultimo species. The obtained mechanism described 122 chemical transformations involving 47 species. In addition to the reactant, 27 molecular products and 19 radical species were represented.

The model was validated on experimental results obtained between 395 °C and 450 °C and at 100 bar. Strictly in, it is thus only valid at pressures in the surrounding of 100 bar and our study could be completed by experiments at a few mbar, 400 bar and 2000 bar to quantify the effect of pressure. The model failed to properly predict the low yield of generated ethane. However, the results were satisfying for the yields of methane, residual trimethylbenzene, hydrogen, xylenes, toluene, benzene, and dimers below 70%. At higher conversions those yields were underestimated compared to experimental data. The condensation reactions into heavier species than triaromatics which were not taken into account in the model may be one reason to explain this deviation.

The model was then used to assess the relative contributions of identified potential methane generation pathways below 70% conversion at 425 °C and 200 °C. It was demonstrated that when a pathway was negligible (respectively substantial) at high temperature it remained the same at low temperature.

The pathways relevant for methane generation were identified as:

- (i) The 'monoaromatic route' *i.e.* the demethylation of trimethylbenzenes into xylenes and to a lesser extent the demethylation of xylenes into toluene (above 50% conversion),

- (ii) The formation of dimers ('polyaromatic route', step 1) which is very substantial at low conversion,
- (iii) The ring closure reaction of dimers into triaromatic precursors ('polyaromatic route', step 2).

At low temperature (200 °C) the contribution of the 'monoaromatic route' has been demonstrated to expand faster than at high temperature (425 °C). However, at both temperatures the equilibrium reached was a fairly equal contribution for the 'monoaromatic route' and the 'polyaromatic route'. Eventually, demethylation reactions of toluene, dimers, triaromatic precursors and triaromatics have been shown to be no relevant pathways to consider regarding methane generation in both ranges of temperature.

Since basin simulators only comprise a limited number of equations, we plan in a future work to 'translate' the three main pathways for methane generation characterized in the present work into a kinetic model based on stoichiometric equations. Sources of methane resulting from all condensation reactions explaining the formation of heavy fractions such as pre-char and char will also be included in order to be able to account for methane generation on the whole range of conversion. As this next model will derive from a validated free-radical model, the extrapolation of its prediction to geological conditions will offer more scientific confidence.

n°	Reactions	A	b	Ea	References	F
<i>Units: cm³, mol, s, cal</i>						
Unimolecular initiations						
1	TMB = RTMBa + H	2.2E ¹⁶	0	87200	Brand et al., 1990	
	reverse	7.8E ¹³	0	139	Brand et al., 1990	
2	TMB = RXYLENESb + CH ₃	1.0E ¹⁷	0	97000	Bounaceur et al., 2005	
	reverse	1.4E ¹³	0	45.7	Tokmakov et al., 1999	
3	TMB = RTMBb + H	3.2E ¹⁵	0	105000	N.I.S.T. fit for benzene	
	reverse	1.0E ¹⁴	0	17.2	N.I.S.T. fit for phenyl	
Bimolecular initiations						
4	TMB + TMB = RTMBa + RTMBc	2.5E ¹⁴	0	68800	Lannuzel, 2007	
	reverse	1.0E ¹²	0	1600	Estimated ^a	
5	TMB + TMB = RTMBa + RTMBd	2.5E ¹⁴	0	71300	Lannuzel, 2007	
	reverse	1.0E ¹²	0	1600	Estimated ^a	
Ipsso additions						
6	TMB + H = XYLENES + CH ₃	58E ¹³	0	8100	Baulch et al., 1994	*10
	reverse	1.2E ¹²	0	15900	Robaugh and Tsang, 1986	
7	TMB + CH ₃ = TetraMB + H	1.2E ¹²	0	15900	Robaugh and Tsang, 1986	
	reverse	58E ¹³	0	8100	Baulch et al., 1994	*10
8	XYLENES + H = TOLUENE + CH ₃	58E ¹³	0	8100	Baulch et al., 1994	*10
	reverse	1.2E ¹²	0	15900	Robaugh and Tsang, 1986	
9	TOLUENE + H = BENZENE + CH ₃	17E ¹³	0	8100	Baulch et al., 1994	*3
	reverse	1.2E ¹²	0	15900	Robaugh and Tsang, 1986	
10	DIMERS238 + H = DIMERS224 + CH ₃	58E ¹³	0	8100	Baulch et al., 1994	*10
	reverse	1.2E ¹²	0	15900	Robaugh and Tsang, 1986	
11	DIMERS224 + H = DIMERS210 + CH ₃	58E ¹³	0	8100	Baulch et al., 1994	*10
	reverse	1.2E ¹²	0	15900	Robaugh and Tsang, 1986	
12	DIMERS210 + H = DIMERS196 + CH ₃	58E ¹³	0	8100	Baulch et al., 1994	*10
	reverse	1.2E ¹²	0	15900	Robaugh and Tsang, 1986	
13	DIMERS196 + H = DIMERS182 + CH ₃	58E ¹³	0	8100	Baulch et al., 1994	*10
	reverse	1.2E ¹²	0	15900	Robaugh and Tsang, 1986	
14	DIMERS182 + H = DIMERS168 + CH ₃	17E ¹³	0	8100	Baulch et al., 1994	*3
	reverse	1.2E ¹²	0	15900	Robaugh and Tsang, 1986	
15	PTRIARO234 + H = PTRIARO220 + CH ₃	58E ¹³	0	8100	Baulch et al., 1994	*10
	reverse	1.2E ¹²	0	15900	Robaugh and Tsang, 1986	
16	PTRIARO220 + H = PTRIARO206 + CH ₃	58E ¹³	0	8100	Baulch et al., 1994	*10
	reverse	1.2E ¹²	0	15900	Robaugh and Tsang, 1986	
17	PTRIARO206 + H = PTRIARO192 + CH ₃	58E ¹³	0	8100	Baulch et al., 1994	*10
	reverse	1.2E ¹²	0	15900	Robaugh and Tsang, 1986	
18	PTRIARO192 + H = PTRIARO178 + CH ₃	17E ¹³	0	8100	Baulch et al., 1994	*3
	reverse	1.2E ¹²	0	15900	Robaugh and Tsang, 1986	
19	TRIARO234 + H = TRIARO220 + CH ₃	58E ¹³	0	8100	Baulch et al., 1994	*10
	reverse	1.2E ¹²	0	15900	Robaugh and Tsang, 1986	
20	TRIARO220 + H = TRIARO206 + CH ₃	58E ¹³	0	8100	Baulch et al., 1994	*10
	reverse	1.2E ¹²	0	15900	Robaugh and Tsang, 1986	
21	TRIARO206 + H = TRIARO192 + CH ₃	58E ¹³	0	8100	Baulch et al., 1994	*10
	reverse	1.2E ¹²	0	15900	Robaugh and Tsang, 1986	
22	TRIARO192 + H = TRIARO178 + CH ₃	17E ¹³	0	8100	Baulch et al., 1994	*3
	reverse	1.2E ¹²	0	15900	Robaugh and Tsang, 1986	
23	ETHYLXYLENES + H = ETHYLTOLUENES + CH ₃	58E ¹³	0	8100	Baulch et al., 1994	*10
	reverse	1.2E ¹²	0	15900	Robaugh and Tsang, 1986	
24	ETHYLTOLUENES + H = ETHYLBENZENE + CH ₃	17E ¹³	0	8100	Baulch et al., 1994	*3
	reverse	1.2E ¹²	0	15900	Robaugh and Tsang, 1986	
25	ETHYLXYLENES + H = XYLENES + C ₂ H ₅	52E ¹²	0	4100	Ellis et al., 2003	*10
	reverse	0.12E ¹²	0	15900	Robaugh and Tsang, 1986	/10
26	ETHYLTOLUENES + H = TOLUENE + C ₂ H ₅	52E ¹²	0	4100	Ellis et al., 2003	*10
	reverse	0.12E ¹²	0	15900	Robaugh and Tsang, 1986	/10
Additions of benzylic radicals						
Intermolecular additions						
27	RTMBa + TMB = DIMERS238 + H	17E ¹¹	0	23500	Brioukov et al., 1999	*2
	reverse	5.8E ¹³	0	29400	Estimated ^b	
28	RXYLENESa + TMB = DIMERS224 + H	17E ¹¹	0	23500	Brioukov et al., 1999	*2
	reverse	5.8E ¹³	0	29400	Estimated ^b	
29	RTMBa + XYLENES = DIMERS224 + H	25E ¹¹	0	23500	Brioukov et al., 1999	*3
	reverse	5.8E ¹³	0	29400	Estimated ^b	

30	RXYLENESa + XYLENES = DIMERS210 + H		25E ¹¹	0	23500	Brioukov et al., 1999	*3
		reverse	5.8E ¹³	0	29400	Estimated ^b	
31	RXYLENESa + TOLUENE = DIMERS196 + H		42E ¹¹	0	23500	Brioukov et al., 1999	*5
		reverse	5.8E ¹³	0	29400	Estimated ^b	
32	RTMBa + TMB = DIMERS224 + CH3		42E ¹¹	0	23500	Brioukov et al., 1999	*5
		reverse	1.2E ¹²	0	29400	Estimated ^c	
33	RXYLENESa + TMB = DIMERS210 + CH3		42E ¹¹	0	23500	Brioukov et al., 1999	*5
		reverse	1.2E ¹²	0	29400	Estimated ^c	
34	RTMBa + XYLENES = DIMERS210 + CH3		25E ¹¹	0	23500	Brioukov et al., 1999	*3
		reverse	1.2E ¹²	0	29400	Estimated ^c	
35	RXYLENESa + XYLENES = DIMERS196 + CH3		25E ¹¹	0	23500	Brioukov et al., 1999	*3
		reverse	1.2E ¹²	0	29400	Estimated ^c	
36	RXYLENESa + TOLUENE = DIMERS182 + CH3		17E ¹¹	0	23500	Brioukov et al., 1999	*2
		reverse	1.2E ¹²	0	29400	Estimated ^c	
	Intramolecular additions						
37	RDIMERS238a = PTRIARO234 + H		4.2E ¹¹	0	23500	Brioukov et al., 1999	/2
		reverse	5.8E ¹³	0	29400	Estimated ^b	
38	RDIMERS224a = PTRIARO220 + H		4.2E ¹¹	0	23500	Brioukov et al., 1999	/2
		reverse	5.8E ¹³	0	29400	Estimated ^b	
39	RDIMERS210a = PTRIARO206 + H		4.2E ¹¹	0	23500	Brioukov et al., 1999	/2
		reverse	5.8E ¹³	0	29400	Estimated ^b	
40	RDIMERS196a = PTRIARO192 + H		4.2E ¹¹	0	23500	Brioukov et al., 1999	/2
		reverse	5.8E ¹³	0	29400	Estimated ^b	
41	RDIMERS182a = PTRIARO178 + H		4.2E ¹¹	0	23500	Brioukov et al., 1999	/2
		reverse	5.8E ¹³	0	29400	Estimated ^b	
42	RDIMERS238a = PTRIARO220 + CH3		8.4E ¹¹	0	23500	Brioukov et al., 1999	
		reverse	1.2E ¹²	0	29400	Estimated ^c	
43	RDIMERS224a = PTRIARO206 + CH3		8.4E ¹¹	0	23500	Brioukov et al., 1999	
		reverse	1.2E ¹²	0	29400	Estimated ^c	
44	RDIMERS210a = PTRIARO192 + CH3		8.4E ¹¹	0	23500	Brioukov et al., 1999	
		reverse	1.2E ¹²	0	29400	Estimated ^c	
45	RDIMERS196a = PTRIARO178 + CH3		8.4E ¹¹	0	23500	Brioukov et al., 1999	
		reverse	1.2E ¹²	0	29400	Estimated ^c	
	Metatheses with abstraction of a benzylic H-atom						
46	TMB + H = RTMBa + H2		40E ¹⁴	0	8400	Hippler et al., 1994	*10
		reverse	0.70E ¹²	0	14500	Brooks et al., 1971	/4
47	XYLENES + H = RXYLENESa + H2		40E ¹⁴	0	8400	Hippler et al., 1994	*10
		reverse	0.47E ¹²	0	14500	Brooks et al., 1971	/6
48	DIMERS238 + H = RDIMERS238a + H2		40E ¹⁴	0	8400	Hippler et al., 1994	*10
		reverse	0.28E ¹²	0	14500	Brooks et al., 1971	/10
49	DIMERS224 + H = RDIMERS224a + H2		40E ¹⁴	0	8400	Hippler et al., 1994	*10
		reverse	0.28E ¹²	0	14500	Brooks et al., 1971	/10
50	DIMERS210 + H = RDIMERS210a + H2		40E ¹⁴	0	8400	Hippler et al., 1994	*10
		reverse	0.28E ¹²	0	14500	Brooks et al., 1971	/10
51	DIMERS196 + H = RDIMERS196a + H2		40E ¹⁴	0	8400	Hippler et al., 1994	*10
		reverse	0.28E ¹²	0	14500	Brooks et al., 1971	/10
52	DIMERS182 + H = RDIMERS182a + H2		40E ¹⁴	0	8400	Hippler et al., 1994	*10
		reverse	0.28E ¹²	0	14500	Brooks et al., 1971	/10
53	PTRIARO234 + H = RPTRIARO234a + H2		40E ¹⁴	0	8400	Hippler et al., 1994	*10
		reverse	0.28E ¹²	0	14500	Brooks et al., 1971	/10
54	PTRIARO220 + H = RPTRIARO220a + H2		40E ¹⁴	0	8400	Hippler et al., 1994	*10
		reverse	0.28E ¹²	0	14500	Brooks et al., 1971	/10
55	PTRIARO206 + H = RPTRIARO206a + H2		40E ¹⁴	0	8400	Hippler et al., 1994	*10
		reverse	0.28E ¹²	0	14500	Brooks et al., 1971	/10
56	PTRIARO192 + H = RPTRIARO192a + H2		40E ¹⁴	0	8400	Hippler et al., 1994	*10
		reverse	0.28E ¹²	0	14500	Brooks et al., 1971	/10
57	PTRIARO178 + H = RPTRIARO178a + H2		40E ¹⁴	0	8400	Hippler et al., 1994	*10
		reverse	0.28E ¹²	0	14500	Brooks et al., 1971	/10
58	TMB + CH3 = RTMBa + CH4		4.8E ¹¹	0	8800	N.I.S.T. fit for toluene	*3
		reverse	6.6E ¹¹	0	27500	Estimated ^d	
59	XYLENES + CH3 = RXYLENESa + CH4		1.6E ¹¹	0	8800	N.I.S.T. fit for toluene	
		reverse	6.6E ¹¹	0	27500	Estimated ^d	
60	DIMERS238 + CH3 = RDIMERS238a + CH4		16E ¹¹	0	8800	N.I.S.T. fit for toluene	*10
		reverse	6.6E ¹¹	0	27500	Estimated ^d	
61	DIMERS224 + CH3 = RDIMERS224a + CH4		16E ¹¹	0	8800	N.I.S.T. fit for toluene	*10
		reverse	6.6E ¹¹	0	27500	Estimated ^d	
62	DIMERS210 + CH3 = RDIMERS210a + CH4		16E ¹¹	0	8800	N.I.S.T. fit for toluene	*10
		reverse	6.6E ¹¹	0	27500	Estimated ^d	
63	DIMERS196 + CH3 = RDIMERS196a + CH4		16E ¹¹	0	8800	N.I.S.T. fit for toluene	*10
		reverse	6.6E ¹¹	0	27500	Estimated ^d	
64	DIMERS182 + CH3 = RDIMERS182a + CH4		16E ¹¹	0	8800	N.I.S.T. fit for toluene	*10
		reverse	6.6E ¹¹	0	27500	Estimated ^d	
65	PTRIARO234 + CH3 = RPTRIARO234a + CH4		16E ¹¹	0	8800	N.I.S.T. fit for toluene	*10

66	PTRIAO220 + CH ₃ = RPTRIAO220a + CH ₄	reverse	6.6E ¹¹	0	27500	Estimated ^d	
			1.6E ¹¹	0	8800	N.I.S.T. fit for toluene	*10
67	PTRIAO206 + CH ₃ = RPTRIAO206a + CH ₄	reverse	6.6E ¹¹	0	27500	Estimated ^d	
			1.6E ¹¹	0	8800	N.I.S.T. fit for toluene	*10
68	PTRIAO192 + CH ₃ = RPTRIAO192a + CH ₄	reverse	6.6E ¹¹	0	27500	Estimated ^d	
			1.6E ¹¹	0	8800	N.I.S.T. fit for toluene	*10
69	PTRIAO178 + CH ₃ = RPTRIAO178a + CH ₄	reverse	6.6E ¹¹	0	27500	Estimated ^d	
			1.6E ¹¹	0	8800	N.I.S.T. fit for toluene	*10
70	XYLENES + RTMBa = RXYLENESa + TMB	reverse	6.6E ¹¹	0	27500	Estimated ^d	
			4.8E ¹⁰	0	12800	Estimated ^e	*3
71	DIMERS238 + RTMBa = RDIMERS238a + TMB	reverse	1.6E ¹⁰	0	12800	Estimated ^e	*10
			0.16E ¹⁰	0	12800	Estimated ^e	/10
72	DIMERS238 + RXYLENESa = RDIMERS238a + XYLENES	reverse	1.6E ¹⁰	0	12800	Estimated ^e	*10
			0.16E ¹⁰	0	12800	Estimated ^e	/10
73	DIMERS224 + RTMBa = RDIMERS224a + TMB	reverse	1.6E ¹⁰	0	12800	Estimated ^e	*10
			0.16E ¹⁰	0	12800	Estimated ^e	/10
74	DIMERS224 + RXYLENESa = RDIMERS224a + XYLENES	reverse	1.6E ¹⁰	0	12800	Estimated ^e	*10
			0.16E ¹⁰	0	12800	Estimated ^e	/10
75	DIMERS210 + RTMBa = RDIMERS210a + TMB	reverse	1.6E ¹⁰	0	12800	Estimated ^e	*10
			0.16E ¹⁰	0	12800	Estimated ^e	/10
76	DIMERS210 + RXYLENESa = RDIMERS210a + XYLENES	reverse	1.6E ¹⁰	0	12800	Estimated ^e	*10
			0.16E ¹⁰	0	12800	Estimated ^e	/10
77	DIMERS196 + RTMBa = RDIMERS196a + TMB	reverse	1.6E ¹⁰	0	12800	Estimated ^e	*10
			0.16E ¹⁰	0	12800	Estimated ^e	/10
78	DIMERS196 + RXYLENESa = RDIMERS196a + XYLENES	reverse	1.6E ¹⁰	0	12800	Estimated ^e	*10
			0.16E ¹⁰	0	12800	Estimated ^e	/10
79	DIMERS182 + RTMBa = RDIMERS182a + TMB	reverse	1.6E ¹⁰	0	12800	Estimated ^e	*10
			0.16E ¹⁰	0	12800	Estimated ^e	/10
80	DIMERS182 + RXYLENESa = RDIMERS182a + XYLENES	reverse	1.6E ¹⁰	0	12800	Estimated ^e	*10
			0.16E ¹⁰	0	12800	Estimated ^e	/10
81	PTRIAO234 + RTMBa = RPTRIAO234a + TMB	reverse	1.6E ¹⁰	0	12800	Estimated ^e	*10
			0.16E ¹⁰	0	12800	Estimated ^e	/10
82	PTRIAO234 + RXYLENESa = RPTRIAO234a + XYLENES	reverse	1.6E ¹⁰	0	12800	Estimated ^e	*10
			0.16E ¹⁰	0	12800	Estimated ^e	/10
83	PTRIAO220 + RTMBa = RPTRIAO220a + TMB	reverse	1.6E ¹⁰	0	12800	Estimated ^e	*10
			0.16E ¹⁰	0	12800	Estimated ^e	/10
84	PTRIAO220 + RXYLENESa = RPTRIAO220a + XYLENES	reverse	1.6E ¹⁰	0	12800	Estimated ^e	*10
			0.16E ¹⁰	0	12800	Estimated ^e	/10
85	PTRIAO206 + RTMBa = RPTRIAO206a + TMB	reverse	1.6E ¹⁰	0	12800	Estimated ^e	*10
			0.16E ¹⁰	0	12800	Estimated ^e	/10
86	PTRIAO206 + RXYLENESa = RPTRIAO206a + XYLENES	reverse	1.6E ¹⁰	0	12800	Estimated ^e	*10
			0.16E ¹⁰	0	12800	Estimated ^e	/10
87	PTRIAO192 + RTMBa = RPTRIAO192a + TMB	reverse	1.6E ¹⁰	0	12800	Estimated ^e	*10
			0.16E ¹⁰	0	12800	Estimated ^e	/10
88	PTRIAO192 + RXYLENESa = RPTRIAO192a + XYLENES	reverse	1.6E ¹⁰	0	12800	Estimated ^e	*10
			0.16E ¹⁰	0	12800	Estimated ^e	/10
89	PTRIAO178 + RTMBa = RPTRIAO178a + TMB	reverse	1.6E ¹⁰	0	12800	Estimated ^e	*10
			0.16E ¹⁰	0	12800	Estimated ^e	/10
90	PTRIAO178 + RXYLENESa = RPTRIAO178a + XYLENES	reverse	1.6E ¹⁰	0	12800	Estimated ^e	*10
			0.16E ¹⁰	0	12800	Estimated ^e	/10
91	TMB + RXYLENESb = RTMBa + XYLENES	reverse	1.6E ⁹	3.95	-879	Estimated ^f	
			7.9E ⁶	0	30300	Leininger et al., 2007	
92	XYLENES + RXYLENESb = RXYLENESa + XYLENES	reverse	1.6E ⁹	3.95	-879	Estimated ^f	
			7.9E ⁶	0	30300	Leininger et al., 2007	
93	TMB + RTMBb = RTMBa + TMB	reverse	1.6E ⁹	3.95	-879	Estimated ^f	
			7.9E ⁶	0	30300	Leininger et al., 2007	
94	XYLENES + RTMBb = RXYLENESa + TMB	reverse	1.6E ⁹	3.95	-879	Estimated ^f	
			7.9E ⁶	0	30300	Leininger et al., 2007	
95	TMB + C ₂ H ₅ = C ₂ H ₆ + RTMBa	reverse	1.8E ¹¹	0	10400	N.I.S.T. fit for toluene	
			6.6E ¹¹	0	27500	Estimated ^d	
96	XYLENES + C ₂ H ₅ = C ₂ H ₆ + RXYLENESa	reverse	1.8E ¹¹	0	10400	N.I.S.T. fit for toluene	
			6.6E ¹¹	0	27500	Estimated ^d	
Metatheses with abstraction of a phenylic H-atom							
97	TMB + H = RTMBb + H ₂		9.8E ¹³	0	12900	Ellis et al., 2003	
		reverse	1.6E ¹³	0	10300	N.I.S.T. fit for phenyl	
98	XYLENES + H = RXYLENESb + H ₂		9.8E ¹³	0	12900	Ellis et al., 2003	
		reverse	1.6E ¹³	0	10300	N.I.S.T. fit for phenyl	
99	TMB + CH ₃ = RTMBb + CH ₄		8.7E ¹²	0	17300	N.I.S.T. fit for benzene	
		reverse	3.0E ¹²	0	10000	N.I.S.T. fit for phenyl	
100	XYLENES + CH ₃ = RXYLENESb + CH ₄		8.7E ¹²	0	17300	N.I.S.T. fit for benzene	
		reverse	3.0E ¹²	0	10000	N.I.S.T. fit for phenyl	
Decompositions by β-scission							

101	RTMBc = XYLENES + CH ₃		5.0E ¹³	0	24900	De Bruin et al., 2004	
		reverse	4.0E ⁷	0	9400	De Bruin et al., 2004	
102	RTMBd = XYLENES + CH ₃		5.0E ¹³	0	24900	De Bruin et al., 2004	
		reverse	4.0E ⁷	0	9400	De Bruin et al., 2004	
103	RTMBc = TMB + H		3.5E ¹³	0	28400	N.I.S.T. fit for hydrophenyl	
		reverse	4.3E ¹³	0	4500	N.I.S.T. fit for benzene	
104	RTMBd = TMB + H		3.5E ¹³	0	28400	N.I.S.T. fit for hydrophenyl	
		reverse	4.3E ¹³	0	4500	N.I.S.T. fit for benzene	
Formation of triaromatics by decomposition							
105	RPTRARIO234a = TRIARIO234 + H		3.5E ¹³	0	28400	N.I.S.T. fit for hydrophenyl	
		reverse	4.3E ¹³	0	4500	N.I.S.T. fit for benzene	
106	RPTRARIO220a = TRIARIO220 + H		3.5E ¹³	0	28400	N.I.S.T. fit for hydrophenyl	
		reverse	4.3E ¹³	0	4500	N.I.S.T. fit for benzene	
107	RPTRARIO206a = TRIARIO206 + H		3.5E ¹³	0	28400	N.I.S.T. fit for hydrophenyl	
		reverse	4.3E ¹³	0	4500	N.I.S.T. fit for benzene	
108	RPTRARIO192a = TRIARIO192 + H		3.5E ¹³	0	28400	N.I.S.T. fit for hydrophenyl	
		reverse	4.3E ¹³	0	4500	N.I.S.T. fit for benzene	
109	RPTRARIO178a = TRIARIO178 + H		3.5E ¹³	0	28400	N.I.S.T. fit for hydrophenyl	
		reverse	4.3E ¹³	0	4500	N.I.S.T. fit for benzene	
Main Termination Reactions							
110	RTMBa + RTMBa = biAROS		7.9E ¹²	0	0	Tsang and Walker, 1992	
		reverse	9.9E ¹⁴	0	60600	Korobkov and Kalechits, 1991	
111	RXYLENESa + RXYLENESa = biAROS		0.79E ¹²	0	0	Tsang and Walker, 1992	/10
		reverse	9.9E ¹⁴	0	60600	Korobkov and Kalechits, 1991	
112	RXYLENESa + RTMBa = biAROS		1.6E ¹²	0	0	Tsang and Walker, 1992	/5
		reverse	9.9E ¹⁴	0	60600	Korobkov and Kalechits, 1991	
113	RTMBa + CH ₃ = ETHYLXYLENES		2.0E ¹³	0	0	Tsang and Walker, 1992	
		reverse	2.8E ¹⁴	0	67200	Estimated ^g	
114	RXYLENESa + CH ₃ = ETHYL TOLUENES		2.0E ¹³	0	0	Tsang and Walker, 1992	
		reverse	2.8E ¹⁴	0	67200	Estimated ^g	
115	RXYLENESa + H = XYLENES		7.8E ¹³	0	139	Brand et al., 1990	
		reverse	2.2E ¹⁶	0	87200	Brand et al., 1990	
C₀-C₂ Reactions							
116	H+H+M=H ₂ +M CH ₄ /3.0/ H ₂ /0.0/ C ₂ H ₆ /3.0/ N ₂ /0.4/		1.9E ¹⁸	-1.0	0	(1,-1) Baulch et al., 1994	
117	CH ₃ +CH ₃ (+M)=>C ₂ H ₆ (+M) CH ₄ /3.0/ C ₂ H ₆ /3.0/ N ₂ /0.4/ LOW / 3.63E41 -7.0 2.76E3 / TROE / 0.62 73 1180 /		3.66E ¹³	0	0	(14) Baulch et al., 1994	
118	C ₂ H ₆ (+M)=>CH ₃ +CH ₃ (+M) CH ₄ /3.0/ C ₂ H ₆ /3.0/ N ₂ /0.4/ LOW / 1.89E49 -8.24 93.7E3/ TROE / 0.62 73 1180 /		1.8E ²¹	-1.24	90900	(-14) Baulch et al., 1994	
119	H+CH ₃ (+M)=>CH ₄ (+M) CH ₄ /3.0/ C ₂ H ₆ /3.0/ N ₂ /0.4/ LOW / 1.408E24 -1.8 0.0 / TROE / 0.37 3315 61 /		1.7E ¹⁴	0	0	(17) Baulch et al., 1994	
120	CH ₄ (+M)=>CH ₃ +H(+M) CH ₄ /0.0/ C ₂ H ₆ /3.0/ N ₂ /0.4/ LOW / 1.29E18 0.00 90.9E3 / TROE / 0 1350 1 7830 /		2.4E ¹⁶	0	105000	(-17) Baulch et al., 1994	
121	CH ₄ (+CH ₄)=>CH ₃ +H(+CH ₄) LOW / 8.43E17 0.00 90.9E3 / TROE / 0.69 90 2210 /		2.4E ¹⁶	0	105000	(-17 ^g) Baulch et al., 1994	
122	CH ₄ +H=CH ₃ +H ₂		1.3E ⁰⁴	3	8000	(18,-18) Baulch et al., 1994	

^a Zhu et al (2004) with A taken equal to 1.0E¹² cm³.mol⁻¹.s⁻¹

^b Ea taken from Ritter et al (1990) and A taken from Baulch et al (1994)

^c Ea taken from Ritter et al (1990) and A taken from Robaugh and Tsang (1986)

^d Tsang, 1991 for 'propenyl radical + CH₄ = propene + CH₃' with A divided by 10 for a cyclic radical

^e As 'toluene + CH₃' (N.I.S.T. fit: A=1.6E¹¹ cm³.mol⁻¹.s⁻¹ and Ea=8800 cal.mol⁻¹) with A divided by 10 for a cyclic radical and with Ea taken 4 kcal/mol higher for a resonance stabilised radical

^f N.I.S.T. fit for 'toluene + phenyl'

^g Fit for values of Barton and Stein (1980) as 2-ethyl-1,3-dimethylbenzene

Table 5: Free-radical mechanism for trimethylbenzene thermal cracking. Kinetic parameters are in cubic centimetre, mole, second, calorie units.

CHAPTER IV:

Lumped kinetic model for thermal cracking of 1,2,4-trimethylbenzene

This chapter is extracted from a submitted paper (ref below) and inserted in the thesis report as such, with the exception of the references which have been moved to Appendix III and the acknowledgements which have been removed.

Fusetti, L., Behar, F., Grice, K., Derenne, S., 2009b. New insights into secondary gas generation from oil thermal cracking: methylated monoaromatics. A kinetic approach using 1,2,4-trimethylbenzene. Part II: A lumped kinetic scheme. *Organic Geochemistry*, *accepted and revision in progress*.

ABSTRACT:

The scope of the present study was to develop a lumped kinetic model predicting methane generation during thermal cracking of a model methylated monoaromatic (1,2,4-trimethylbenzene), whose further implementation into a basin simulator would be possible, and whose prediction would be reliable under laboratory and geological conditions.

The chemistry of the global kinetic scheme was constrained by an initial study in which a free radical mechanism was proposed (*Fusetti, L., Behar, F., Bounaceur, R., Marquaire, P.M., Grice, K., Derenne, S., 2009a. New insights into secondary gas generation from oil thermal cracking: methylated monoaromatics. A kinetic approach using 1,2,4-trimethylbenzene. Part I: A free-radical mechanism. Organic Geochemistry OG-713, accepted and revision in progress*).

The resulting scheme presented here is composed of four pathways for CH₄ generation which account for the decomposition of the reactant 1,2,4-trimethylbenzene *via*: **Reactant** → **Dimers** (pathway P_a), **Reactant** → **Xylenes** (pathway P_b), **Dimers** → {**Prechar + Char**} (pathway P_c), and **Xylenes** → **Dimers + Toluene** (pathway P_d).

Optimization of the scheme was performed at 395 °C, 425 °C, 450 °C, and 475 °C yielding activation energies (E_a) in the range 50-60 kcal/mol, and frequency factors (A) in the neighbourhood of 10¹² s⁻¹. Simulations revealed that the reactant's demethylation pathway (P_b) and the condensation pathway (P_c) led to the greatest amounts of CH₄ below 5% conversion, followed by the reactant's dimerization pathway (P_a). Above 5% conversion, CH₄ generated *via* the condensation pathway (P_c) became dominant but the contributions of the reactant's demethylation (P_a) and dimerization (P_b) pathways were also found to be of importance. Contribution from the decomposition of xylenes (pathway P_d) was found to be negligible, except for when 100% conversion was almost reached.

CH₄ yield was also modelled using a unique stoichiometric equation (CH_{4max} = 7.6 wt% per methyl group) associated with E_a = 58.5 kcal/mol and A = 10^{11.96} s⁻¹, showing relative similarities to other reported values for methylated polyaromatics.

Then, the four equations-scheme was used to perform simulations under geological heating rates. These simulations revealed that significant amounts of CH₄ were generated by methylated monoaromatics in deeply buried reservoirs and that methylated monoaromatics thus had a higher thermal stability than their polyaromatic counterparts but lower than the saturated hydrocarbons.

1. Introduction

The renewed interest of natural gas (*i.e.* methane) as an energy source requires a better understanding of the pathways leading to its formation. In sedimentary basins, methane can be generated *via* bacterial and/or thermal processes. Thermal processes can be further divided into (i) primary, *i.e.* the generation of gas associated with the thermal cracking of kerogens, (ii) secondary, *i.e.* the generation of gas from the thermal cracking of reservoired oils.

Whether they are formed through primary or secondary processes, accumulations of thermogenic gases are thought to be the result of a combination of thermal cracking reactions from several sources within the organic matter matrix. The aim of basin simulators used in the oil and gas industry is to predict the occurrence of such processes taking place in sedimentary basins over geological time-scales (million of years at less than 250 °C). The kinetic schemes implemented in basin simulators both require a limited number of reactions and the possibility to be confidently extrapolated at low temperatures met under geological conditions. Despite the huge variety of chemical components constituting kerogens or crude oils, the development of such models thus passes through the simplification of the system by 'lumping' individual molecules bearing similar structural features and thermal reactivity, into same chemical classes which are very often represented by a single model compound. Two types of kinetic models are however generally proposed:

- (i) Mechanistic models are based on free-radical reactions (*e.g.* Dominé et al., 2002; Leininger et al., 2006; Dartiguelongue et al., 2006). These models describe chemical phenomena using elementary reactions (involving known compounds) associated with kinetic parameters which can thus be extrapolated to other temperatures, including those that occur under geological conditions. Unfortunately, despite simplification *via* the 'lump' of species of similar reactivity, the numerous free-radical chemical equations involved do not facilitate the implementation of these models into basin simulators.
- (ii) Empirical models are based on global stoichiometric equations associated with kinetic parameters calibrated on the basis of global observations obtained from laboratory experiments (*e.g.* Behar et al., 2008b). These models consist of a limited number of chemical equations which facilitate their implementation into basin simulators. However, the extrapolation of these models' prediction to geological conditions is controversial since the stoichiometric equations and their associated kinetic parameters represent global experimental results observed at high temperatures which are the sum of elementary processes. Consequently, if some chemical processes are

inactive at high temperatures, this global description is unable to account for these processes' influence at low temperatures even though they might be of critical importance to properly model thermal cracking phenomena under geological conditions.

The aim of the present study was to develop a lumped kinetic model predicting methane generation during thermal cracking of 1,2,4-trimethylbenzene, whose further implementation into a basin simulator would be possible, and whose prediction would be reliable under laboratory and geological conditions. 1,2,4-trimethylbenzene was chosen as a model compound since it was representative of methylated monoaromatic hydrocarbons present in most reservoir crude oils (Al Darouich et al., 2005).

In an initial study on the thermal cracking of 1,2,4-trimethylbenzene (Fusetti et al., 2009a) we proposed a free-radical mechanism involving 122 reversible chemical transformations and 47 species. Unlike many free-radical mechanisms, this model showed accuracy in predicting the evolutions of the reactant and all products up to C₁₈ over a wide range of reactant conversions (0%-70%). At both high (425 °C) and low (200 °C) temperatures, the following pathways (Figure 1) of methane generation were identified:

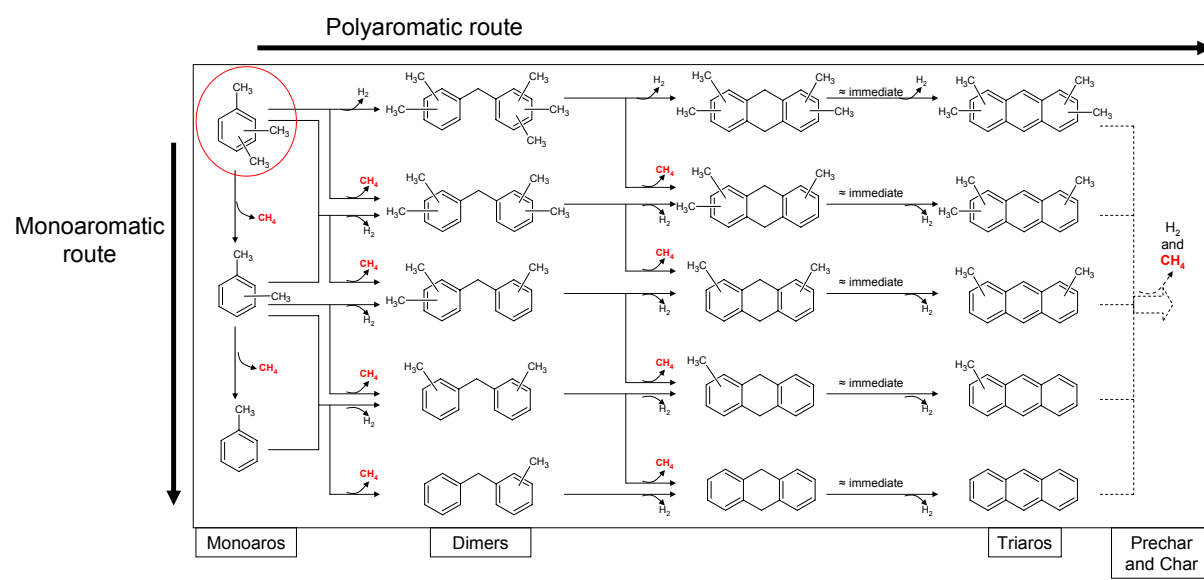


Figure 1: Methane generation pathways during thermal cracking of 1,2,4-trimethylbenzene.

- (i) The 'monoaromatic route' *i.e.* the demethylation reactions of monoaromatic compounds (**1,2,4-trimethylbenzene** → **xylenes** and to a lesser extent **xylenes** → **toluene**),
- (ii) The dimerization reactions of monoaromatic compounds ('polyaromatic route', step 1)
- (iii) The condensation reactions of dimers into triaromatics ('polyaromatic route', steps 2 and 3).

All primary and non-primary reactions generating C₁₈ products (including methane) at both high and low temperatures being identified until 70% conversion, this free-radical model thus constituted a substantial chemical constraint to the development of a lumped global model that could also be extrapolated to geological conditions.

Based on previous observations, the following research strategy was conducted in the present study:

- A.** Lumped stoichiometric equations were derived from the demethylation and dimerization pathways of the reactant 1,2,4-trimethylbenzene and product xylenes, identified and constrained by the aforementioned free-radical mechanism.
- B.** Sources of methane resulting from condensation reactions were extended to the formations of compounds heavier than triaromatics. Indeed, the impossibility to extensively consider all the condensation reactions in the initial free-radical model might have led to an overestimation of methane yield *via* the demethylation and dimerization pathways.

Steps **A** and **B** led us to consider the lumped scheme for methane generation presented in Figure 2 in which toluene is the ultimo aromatic product of the 'monoaromatic route'. Within the 'polyaromatic route', all the dimers formed from monoaromatics (1,2,4-trimethylbenzene, xylenes, toluene) are lumped into the same chemical class. Dimers can in turn degrade yielding higher molecular-weight species lumped in the chemical class {Prechar + Char}.

- C.** Optimization of the kinetic scheme was performed after constraining initial guesses in regards to other studies and experimental results.
- D.** Prediction of the optimized lumped model was extrapolated to geological conditions.

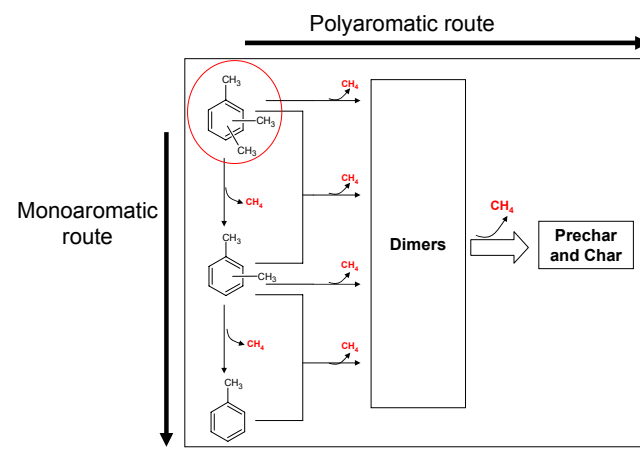


Figure 2: Ideal lumped kinetic scheme to consider for modelling methane generation during thermal cracking of 1,2,4-trimethylbenzene.

2. Experimental and kinetic modelling

2.1 Experimental

1,2,4-trimethylbenzene was subjected to isothermal pyrolysis experiments (395 °C, 425 °C, and 450 °C) previously described (Fusetti et al., 2009a). The scope of the present study was to understand the generation of methane and thus to better constrain the optimization, additional pyrolysis experiments were performed at 475 °C to extend the range of temperatures at which methane data was collected. Results are summarized in Table 1.

T (°C)	t (h)	Conversion (%)	H ₂	CH ₄	C ₂ H ₆	Residual reactant	Xylenes	Toluene	Dimers	Prechar + Char
395	72	ND	0.0	1.3	0.1	ND	ND	ND	ND	ND
395	144	4.7	0.1	2.1	0.3	945.5	4.3	0.0	13.1	31.2
395	216	ND	0.1	5.9	0.7	ND	ND	ND	ND	ND
395	312	ND	0.2	17.0	1.1	ND	ND	ND	ND	ND
395	432	22.2	0.2	26.1	1.5	771.0	57.2	1.1	14.8	123.9
395	550	ND	0.3	34.5	1.9	ND	ND	ND	ND	ND
395	648	ND	0.2	43.2	2.2	ND	ND	ND	ND	ND
425	3	2.7	0.0	0.1	0.1	972.5	0.7	0.0	2.0	22.6
425	9.5	3.0	0.0	0.2	0.3	970.1	1.3	0.0	4.3	21.9
425	72	ND	0.2	22.8	1.9	ND	ND	ND	ND	ND
425	120	30.9	0.3	40.3	2.6	681.0	84.5	2.0	14.5	170.4
425	216	ND	0.4	67.1	3.4	ND	ND	ND	ND	ND
425	648	ND	0.3	139.4	5.8	ND	ND	ND	ND	ND
450	24	ND	0.3	23.9	1.5	ND	ND	ND	ND	ND
450	50	46.5	0.5	62.7	3.3	515.6	156.5	11.2	12.2	233.6
450	72	62.3	0.5	97.8	4.4	350.5	201.8	25.3	10.2	304.9
450	144	76.2	0.5	140.8	5.4	210.7	215.3	48.1	8.4	366.1
450	195	86.7	0.4	161.2	5.9	113.5	213.1	76.4	8.2	413.6
450	336	ND	0.4	191.2	5.5	ND	ND	ND	ND	ND
450	432	97.4	0.4	207.0	5.1	17.6	125.8	121.1	9.1	488.5
450	648	ND	0.3	229.5	4.1	ND	ND	ND	ND	ND
475	3	ND	0.2	4.9	0.5	ND	ND	ND	ND	ND
475	9	ND	0.5	51.9	3.0	ND	ND	ND	ND	ND
475	24	ND	0.6	117.7	4.8	ND	ND	ND	ND	ND
475	72	ND	0.5	190.1	5.5	ND	ND	ND	ND	ND
475	133	ND	0.5	225.9	5.5	ND	ND	ND	ND	ND

Table 1: Experimental results obtained for thermal cracking of 1,2,4-trimethylbenzene at 100 bar (ratios in mg/g of initial reactant). The chemical class {Prechar + Char} 'lumps' the compounds collected via the fractions referred in our previous study (Fusetti et al., 2009a) as: {C₁₄₊ compounds soluble in n-pentane (less the dimers)} + {non-volatile compounds insoluble in n-pentane but soluble in dichloromethane (DCM)} + {the estimated solid residue}.

2.2 Kinetic modelling

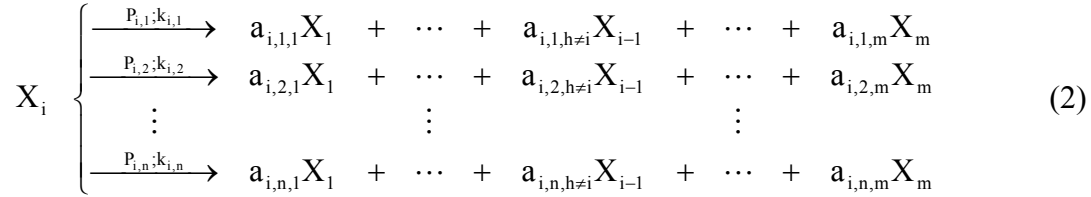
As opposed to elementary processes in which the order assigned to each reactant is by definition equal to its stoichiometric coefficient (in mol), when working with global equations the order of the reaction needs to be assigned. We thus assumed that the thermally unstable components decomposed through first-order processes.

Rate constants were derived from the Arrhenius equation:

$$k = A \exp\left(-\frac{Ea}{RT}\right) \quad (1)$$

Where k = rate constant, A = frequency factor, Ea = activation energy, $R = 8.314 \text{ J.mol}^{-1}.\text{K}^{-1}$, and T = temperature.

The average rate of decomposition of a chemical species can be accounted for by a set of independent, parallel reactions, *i.e.*:



Where X_i is the reacting specie and $X_{j \neq i}$ are generated products, $k_{i,j}$ is the rate constant of reaction j , $P_{i,j}$ is the weight fraction of X_i that reacts through reaction j , $a_{i,j,h}$ is the stoichiometric coefficient for the conversion of X_i into X_h in reaction j , m is the number of chemical classes in the model, and n is the number of reactions involved in the thermal decomposition of X_i .

For equations (2), mass conservation implies that:

$$\sum_{j=1}^n P_{i,j} = 1 \quad (3)$$

And for each reaction j :

$$\sum_{\substack{h=1 \\ h \neq i}}^m a_{i,j,h} = 1 \quad (4)$$

Noting $c_{i,j}$ the conversion of reaction j during the decomposition of X_i , the global rate (q_i) of thermal cracking of X_i is finally given by:

$$q_i = \sum_{j=1}^n P_{i,j} \frac{dc_{i,j}}{dt} \quad (5)$$

With

$$\frac{dc_{i,j}}{dt} = k_{i,j}(1 - c_{i,j}) \quad (6)$$

Kinetic parameters (E_a and A for each reaction in the model) and stoichiometric coefficients ($P_{i,j}$ and $a_{i,j,h}$) were numerically optimized according to mass-balances obtained from pyrolysis experiments. Optimization was achieved with GeoKin Compositional software, an IFP kinetic simulator that allows rate parameters to be adjusted by finding the minimum of an error function F , corresponding to the sum of squared differences between measured and computed amounts :

$$F = \sum_{i=1}^s \sum_{j=1}^m r_{ij}^2 \quad (7)$$

Where s = the number of experiments, m = the number of chemical classes of the model, and r_{ij} = residual, i.e. difference between measured and calculated amounts for compound j in experiment i ($X_{ij \text{ measured}} - X_{ij \text{ calculated}}$).

3. Results and discussion

3.1 Initial guesses for the lumped kinetic scheme

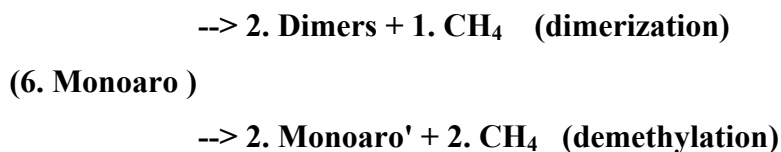
a) Composition of pathways

Despite being vital to explain the decrease of hydrogen in the reaction medium, the *ipso*-additions $\{H_2 + 1,2,4\text{-trimethylbenzene (TMB)}\}$ and $\{H_2 + \text{xylene}\}$ were demonstrated to be minor contributors to the methane yield (Fusetti et al., 2009a). The scope of the present study was therefore to focus on methane generation, the above reactions were thus not considered in the pathways derived from Figure 2 and hydrogen was never accounted for in the stoichiometric equations. The influence of this latter approximation over stoichiometric coefficients is acceptable since molecular-weight of hydrogen is small.

Moreover, as the intrinsic construction of the software GeoKin Compositional used for the optimization did not enable the composition of bimolecular reactions involving two distinct species, cross bimolecular additions $\{1,2,4\text{-trimethylbenzene} + \text{xylene}\}$ and $\{\text{xylene} + \text{toluene}\}$ yielding dimers could not be accounted for. An underestimation of the production of dimers can therefore be anticipated.

Another constraint imposed by the software GeoKin Compositional was the impossibility of having the same reactant named in two different pathways. However, according (not considering H_2) to our initial free-radical mechanism, 6 mol of a same

monoaromatic react *via* two parallel pathways (4 mol *via* the dimerization pathway and 2 mol *via* the demethylation pathway):



Where the couple (Monoaro, Monoaro') is either (1,2,4-trimethylbenzene, xylene) or (xylene, toluene).

Consequently, in the software GeoKin Compositional, 1,2,4-trimethylbenzene (TMB) was split into two 'virtual' reactants TMB1 and TMB2 for the dimerization (P_a) and demethylation (P_b) pathways, respectively. According to the relative contributions of pathways P_a and P_b discussed above to the decrease of TMB, the corresponding initial starting compositions were thus set as:

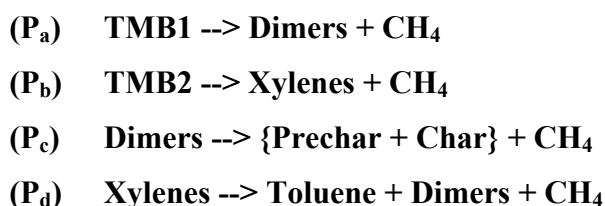
$$\text{TMB1}_0 = 0.666 * \text{TMB}_0$$

$$\text{TMB2}_0 = 0.334 * \text{TMB}_0$$

Moreover, since xylenes were products and not reactants, the above splitting procedure could not be applied to these components in the software. The approximation was thus made to lump their demethylation and dimerization reactions into the same pathway (P_d).

Eventually, regarding higher molecular-weight species we showed in our initial study that the yield of the chemical fraction termed Prechar successively increased and decreased above 30% conversion, whereas the yield of the chemical fraction termed Char always increased. No additional information regarding the pathways linking these two molecular fractions could be provided since their intrinsic compositions could not be determined. We thus decided to lump {Prechar + Char} components into the same chemical fraction that would result from condensation reactions of dimers *via* pathway (P_c).

As a consequence, the following pathways were extracted from Figure 2:



Where toluene, methane, and {Prechar + Char} are thermally stable entities and TMB1, TMB2, Dimers, and Xylenes are reactive entities.

b) Kinetic parameters

Since the optimization of the kinetic scheme relied on a mathematical algorithm, initial guesses had to be constrained to lead to chemically realistic results and not only to one local minimum of the error function.

Kinetic parameters of global equations could not be estimated directly from those of elementary free-radical reactions. Kinetic parameters proposed in previous empirical models to predict thermal cracking of aromatic compounds present in oils were thus examined (Table 2). Results show that, activation energies (E) and frequency factors (A) range from 47 kcal/mol to 62 kcal/mol and from 10^9 s^{-1} to 10^{14} s^{-1} , respectively. A detailed study performed on the thermal cracking of the light aromatic fraction from a natural oil (Al Darouich et al., 2006a) was also examined. By fractionating the initial C₆-C₁₄ aromatic fraction into alkyl aromatics (48 wt%), methyl aromatics (19 wt%), Benzene + Toluene + Xylene + Naphthalene (BTXN, 14 wt%) and naphtheno aromatics (19 wt%) fractions, the authors established a kinetic scheme for each individual class. Ranging from 10^{11} s^{-1} to 10^{13} s^{-1} and 49 kcal/mol to 60 kcal/mol, the respectively optimised A and E values were in the same range as those previously proposed from model aromatic compounds.

Consequently, initial guesses for kinetic parameters of the lumped scheme were constrained to the range 45-65 kcal/mol and 10^{11} - 10^{13} s^{-1} for the activation energies and the frequency factors, respectively.

Compound	Reference	E (kcal/mol)	A (s ⁻¹)
Tetralin	Yu and Eser, 1998b	58.0	$3.5 \cdot 10^{12}$
2-Ethyltetralin	Savage and Klein, 1988	53.5	$5.0 \cdot 10^{12}$
2-Dodecyl-9,10-dihydrophenanthrene	Savage and Baxter, 1996	54.5	$4.0 \cdot 10^{13}$
Ethylbenzene	Domke et al., 2001	62.3	$4.7 \cdot 10^{13}$
Butylbenzene	Freund and Olmstead, 1989	52.9	$1.1 \cdot 10^{12}$
Dodecylbenzene	Behar et al., 2002	53.3	$1.3 \cdot 10^{13}$
Pentadecylbenzene	Savage and Klein, 1987	55.5	$1.1 \cdot 10^{14}$
1-Methylnaphthalene	Leininger et al., 2006	47.4	$7.9 \cdot 10^9$
9-Methylphenanthrene	Behar et al., 1999	49.0	$4.5 \cdot 10^{10}$
Dibenzothiophene	Dartiguelongue et al., 2006	59.0	$1.9 \cdot 10^{11}$

Table 2: Global E and A obtained on various model aromatic compounds.

c) Stoichiometric coefficients

To allow the optimization procedure, stoichiometric coefficients in mol of pathways P_a , P_b , P_c , and P_d , had to be converted into stoichiometric equations relying on mass-balances (wt%). However, in the case of lumped chemical classes (dimers, {Prechar + Char}) the subsequent molecular-weight was not known *a priori*. For example, when written in mole the pathway (P_a) of dimerization of 1,2,4-trimethylbenzene was:



In our initial study we showed that the molecular-weight of individual dimers ranged from 238 g/mol to 182 g/mol. Accordingly, the evolution of the respective experimental yields of dimers, led to an average molecular-weight for the chemical class dimers ranging from 236.9 g/mol to 199.3 g/mol at 2.7% and 97.4% conversions, respectively. The stoichiometric coefficient of the chemical class dimers was thus constrained between 96.8 wt% and 96.1 wt%, and the subsequent stoichiometric coefficient of methane between 3.2 wt% and 3.9 wt%. The same approach was applied for the pathway (P_b) of demethylation of 1,2,4-trimethylbenzene and the pathway (P_d) of degradation of xylenes.

Since no complete molecular identification had been performed regarding the chemical class {Prechar + Char}, its stoichiometric coefficient could not be constrained as above. However, this chemical class containing only heavy compounds, its stoichiometric coefficient was constrained between 80 wt% and 100 wt%, and the subsequent stoichiometric coefficient of methane between 0 wt% and 20 wt%.

3.2 Optimization

The optimization was performed on the experimental data reported in Table 1, with the exception of the yields of dimers above 75% conversion. Indeed, cross bimolecular additions {1,2,4-trimethylbenzene + xylene} and {xylene + toluene} could not be composed in the software and taking into account yields of dimers above 75% conversion would have faked the optimization since these dimers mainly resulted from the aforementioned unaccounted reactions (Fusetti et al., 2009a).

Initially, the optimization was performed using a distribution of activation energies between 45 kcal/mol and 65 kcal/mol for each pathway and frequency factors were left to vary between 10^{11} s^{-1} and 10^{13} s^{-1} with an initial value of 10^{12} s^{-1} . Pathways were considered to be better described by independent parallel reactions when, using the same frequency factor, the difference between activation energies was greater than 1 kcal/mol. The results of the optimization are presented in Table 3. The resulting optimized scheme was only

composed of simple stoichiometric equations as no relevant set of independent parallel reactions was found. Activation energies ranged from 52.84 kcal/mol to 60.53 kcal/mol and frequency factors were all around 10^{12} s^{-1} . The frequency factors thus only slightly shifted from their initial value.

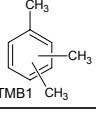
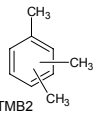
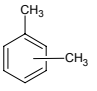
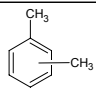
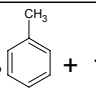
Stoichiometric equations	Ea (kcal/mol)	log A(s ⁻¹)
P_a :  \longrightarrow 96.73 % Dimers + 3.27 % CH ₄	58.02	12.006
P_b :  \longrightarrow  + 13.04 % CH ₄	57.87	12.106
P_c : Dimers \longrightarrow 82.84 % { Prechar + Char } + 17.16 % CH ₄	52.84	11.921
P_d :  \longrightarrow 64.37 % Dimers + 28.12 %  + 7.51 % CH ₄	60.53	12.015

Table 3: Optimized kinetic scheme and associated kinetic parameters for thermal cracking of 1,2,4-trimethylbenzene .

The lower activation energy (52.84 kcal/mol) was found for the equation associated with the condensation of dimers (pathway P_c), translating their *quasi*-immediate decrease when generated in substantial amounts at very low conversion (Table 1). The resulting optimized infinite value for methane generated through this condensation pathway was 17.16 wt%. The values of activation energies found for the dimerization pathway (P_a) of 1,2,4-trimethylbenzene and its demethylation pathway (P_b) were 58.02 kcal/mol and 57.87 kcal/mol, respectively. These very close values justified the approximation which was made to lump equivalent dimerization and demethylation pathways into a unique pathway (P_d) in the case of xylenes because of the software constraint (*c.f.* 3.1.a). The high corresponding activation energy (60.53 kcal/mol) of pathways P_d demonstrated the higher stability of xylene compared to 1,2,4-trimethylbenzene and could explain why xylenes were included in a stable chemical class in previous kinetic studies with similar experimental conditions (*e.g.* Al Darouich et al., 2006a).

3.3 Comparison with experimental data

a) Gases

Comparison of model predictions and experimental data for methane yields are presented in Figure 3 at 395 °C, 425 °C, 450 °C, and 475 °C against time. The model prediction was accurate for the four temperatures and the 0-100% range of reactant conversions (100% and 99.7% conversions are reached at 450 °C/600 h and 475 °C/133 h, respectively). Above 100% conversion, the model showed an underestimated yield of methane pointing to a new source of methane which was not taken into account. Two pathways could be potential candidates for this new source of methane above 100% conversion:

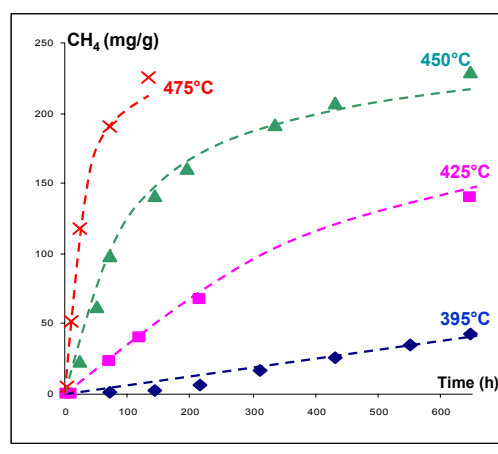


Figure 3: Computer-predicted (dashed lines) and experimental (dots) yields (in mg/g of initial reactant) versus time (in h) for methane at 395 °C, 425 °C, 450 °C, and 475 °C.

- (i) The deviation between the model and the experiments may be associated with the degradation of the aromatic rings of the polyaromatic condensed structures lumped in the chemical class {Prechar + Char}. Indeed, under similar experimental conditions, polyaromatic hydrocarbons have been reported to undergo partial ring degradation as shown for 1-methylnaphthalene (Leininger et al., 2006) and 1-methylpyrene (Lorant et al., 2000). This assumption is compatible with the presence of trace amounts of C₃ and C₄ hydrocarbon gases detected experimentally above 100% conversion of 1,2,4-trimethylbenzene (Fusetti et al., 2009a).
- (ii) An alternative explanation could be the secondary cracking of ethane. Based on experimental data (Table 1) a set of kinetic parameters was calibrated and the yield of ethane simulated (Figure 4) for having a mere estimation of the contribution of ethane cracking to the global yield of methane. This was achieved using two stoichiometric equations (Table 4), (P₁) accounting for the generation of ethane from unidentified precursors termed C₂Prec., and (P₂) accounting for the

degradation of ethane into methane. Simulations indicated that methane yield resulting from the degradation of ethane was about 2.5 mg/g at 450 °C / 648 h and 3.6 mg/g at 475 °C / 133 h. It could thus not compensate for the underestimated methane yield (underestimations of 18.3 mg/g at 450 °C / 648 h and 19.3 mg/g at 475 °C / 133 h) obtained from the previous lumped scheme (Table 3) above 100% conversion.

Stoichiometric equations	Ea (kcal/mol)	log A(s ⁻¹)
P ₁ : C ₂ Prec. → 0.68 % C ₂ H ₆ + 99.32 % Other compounds	57.46	12.017
P ₂ : C ₂ H ₆ → 100.00 % CH ₄	90.64	20.741

Table 4: Optimized kinetic scheme and associated kinetic parameters for ethane generation and degradation during thermal cracking of 1,2,4-trimethylbenzene .

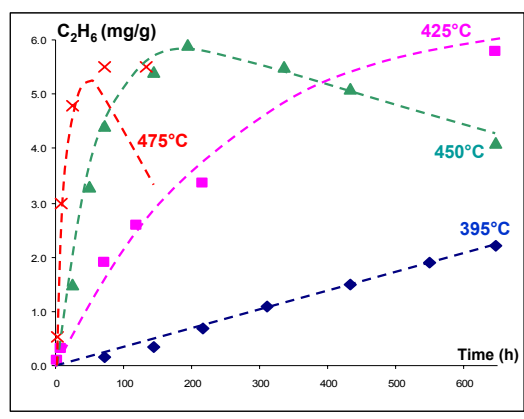


Figure 4: Computer-predicted (dashed lines) and experimental (dots) yields (in mg/g of initial reactant) versus time (in h) for ethane at 395 °C, 425 °C, 450 °C, and 475 °C.

The degradation of condensed structures of the molecular fraction {Prechar + Char} might thus be the most likely new source of gas above 100 % reactant conversion. The existence of such process(es) which were also not taken into account in the two equations of Table 4 could explain the 2.3 mg/g underestimation of ethane yield at 475°C/133h (Figure 4).

Below 100% conversion, the pathways yielding methane during thermal cracking of 1,2,4-trimethylbenzene are thus (Table 3):

- (i) Decomposition of the reactant *via* dimerization (pathway P_a),
- (ii) Decomposition of the reactant *via* demethylation (pathway P_b),

- (iii) Condensation reactions of dimers into higher molecular-weight products (pathway P_c),
- (iv) Decomposition of xylenes *via* demethylation and dimerization (pathway P_d).

Figure 5 shows that below 5% conversion, demethylation of the reactant (pathway P_b) and condensation reactions (pathway P_c) dominated methane generation, followed by dimerization of the reactant (pathway P_a). Above 5% conversion, condensation reactions (P_c) were the main source of methane, followed by demethylation (P_b) and dimerization (P_a) of the reactant, respectively. The decomposition of xylenes (pathway P_d) showed negligible methane yields, except above 95% conversion.

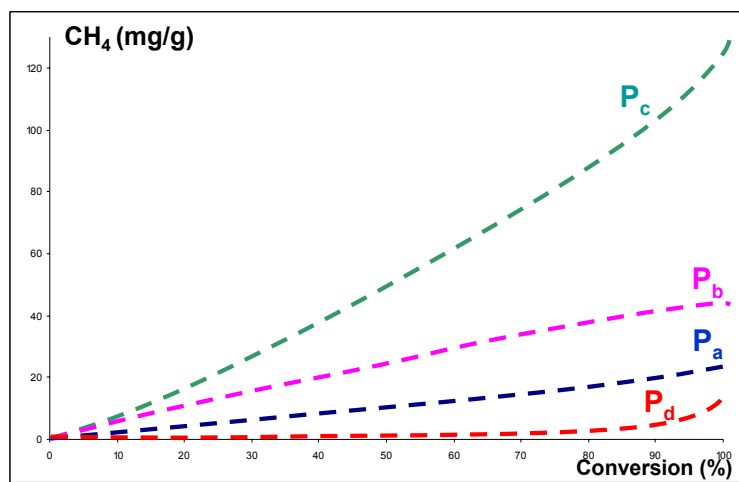


Figure 5: Simulated yields (in mg/g of initial reactant) versus conversion (in %) of the four identified pathways of methane generation.

It was also interesting to compare the methane generation potential of 1,2,4-trimethylbenzene with that previously reported for other methylated aromatics (Behar et al., 1999; Lorant et al., 2000), with respect to an equivalent number of methyl groups in the degraded molecule. Other empirical models often provide only one set of kinetic parameters for the generation of methane. Consequently, we also attempted to model methane generation across the whole range of reactant conversions using a unique stoichiometric equation in which methane was produced together with other compounds from precursors termed C₁Prec:

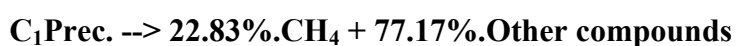


To fix the initial of the stoichiometric coefficient (x) of methane, we used the previous lumped scheme of methane generation (Table 3). In this scheme, the maximum yield of

methane (in mg/g) produced from pathway P_a was $(0.666*3.27)$ wt% since $TMB_{1o}=0.666*TMB_o$. Using the same approach, the maximum yield of methane produced from pathways P_b , P_c , and P_d were $(0.334*13.04)$ wt%, $(0.666*0.9673 + 0.334*0.8696*0.6437)*17.16$ wt%, and $(0.334*0.8696*7.51)$ wt%, respectively. Accordingly, the total infinite yield of methane produced during thermal degradation of 1,2,4-trimethylbenzene *via* the scheme of Table 3 was 22.98 wt%. This value was thus taken as the initial guess for the stoichiometric coefficient (x) of methane, and $y = 77.02$ wt% was taken as the initial guess for the stoichiometric coefficient of co-generated compounds. Optimization was then performed using a distribution of activation energies between 45 kcal/mol and 65 kcal/mol and frequency factors left to vary between $10^{11} s^{-1}$ and $10^{13} s^{-1}$ with an initial value of $10^{12} s^{-1}$.

The resulting optimized set of kinetic parameters $E = 58.5$ kcal/mol and $A = 10^{11.96} s^{-1}$ was in the same range as parameters calibrated for methane generation (before occurrence of the degradation of the polyaromatic structure) during thermal cracking of 9-methylphenanthrene ($E_a = 54.5$ kcal/mol and $A = 1.1*10^{12} s^{-1}$, Behar et al., 1999) and 1-methylpyrene ($E_a = 55.6$ kcal/mol and $A = 4.2*10^{12} s^{-1}$, Lorant et al., 2000).

The resulting optimized stoichiometric equation showed an infinite value of 22.83 wt% for methane which thus remained close to the 22.98 wt% of the initial guess:



Since there are three methyl groups in 1,2,4-trimethylbenzene, this gave an average of 7.6 wt% of methane per methyl. Such infinity value was close to the methane yields previously found for the degradation of 9-methylphenanthrene (6.4 wt%, Behar et al., 1999) and 1-methylpyrene (4.6 wt%, Lorant et al., 2000). It confirmed that despite being based directly on an empirical scheme, the kinetic studies of Behar et al (1999) and Lorant et al (2000) were predictive of the global chemistry of methane under laboratory conditions.

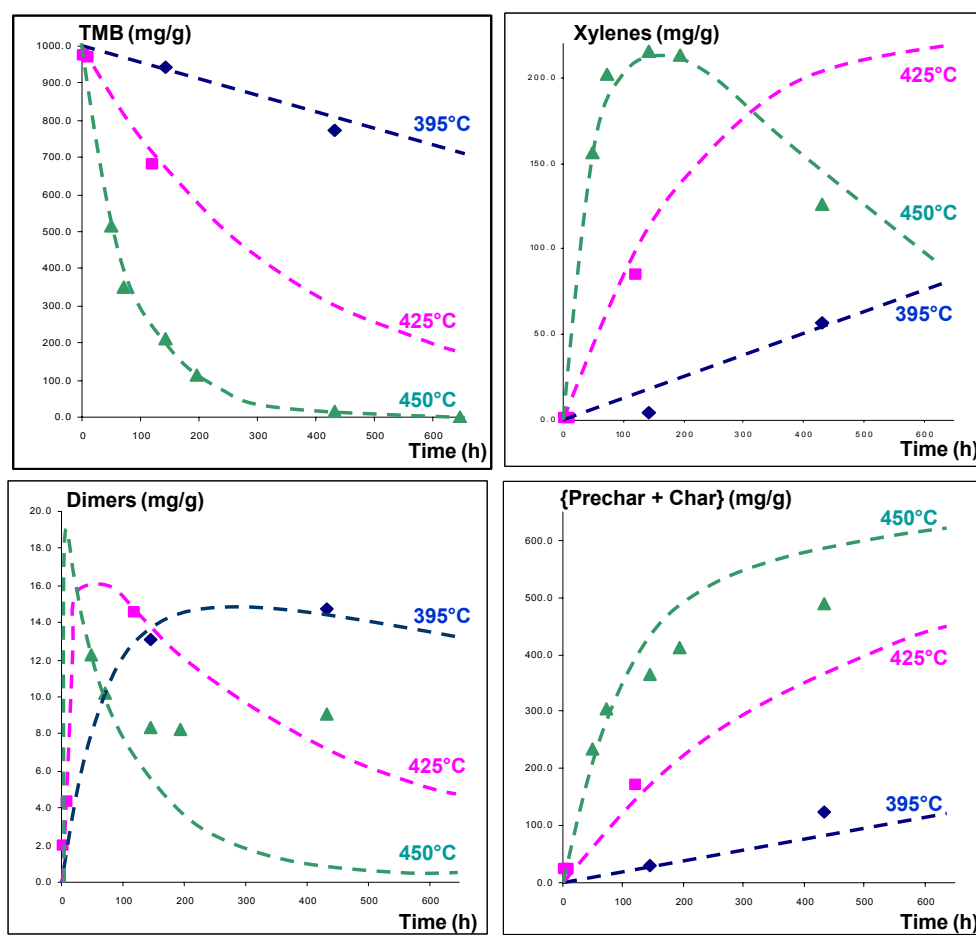
b) Other compounds

Comparison of model predictions and experimental data at 395 °C, 425 °C, and 450 °C for the yields of 1,2,4-trimethylbenzene (TMB), xylenes, and the chemical classes dimers and {Prechar + Char} are reported in Figures 6, 7, 8, and 9.

The decrease in the reactant 1,2,4-trimethylbenzene was accurately modelled at the three temperatures and for the whole range of conversions (0-100%), attesting that the principal reactions of degradation of this compound had been taken into account.

The yield of xylenes was also correctly predicted on nearly the entire range of conversion but was overestimated at 450 °C / 432 h (97.4% conversion). Such result was anticipated as cross bimolecular additions {1,2,4-trimethylbenzene + xylene} and {xylene + toluene} yielding dimers at high conversion (>75% conversion) could not be accounted by the mechanism. Accordingly, the experimental yield of dimers was underestimated by 4.6 mg/g at 450 °C / 195 h (86.7% conversion).

The predicted yield of the chemical class {Prechar + Char} remained in the same order of magnitude as experimental data. The greatest difference between the model prediction and experimental data was an overestimation by 114.6 mg/g observed at 450 °C / 432 h. Such precision was however satisfying, regarding approximations made concerning reactions of condensations in the scheme.



Figures 6, 7, 8, and 9: Computer-predicted (dashed lines) and experimental (dots) yields (in mg/g of initial reactant) versus time (in h) for 1,2,4-trimethylbenzene (TMB), xylenes, dimers, and {Prechar + Char} at 395 °C, 425 °C, 450 °C, and 475 °C.

3.4 Extrapolation to geological conditions

a) Geothermal gradient

As the present lumped model (Table 3) derived from a free-radical model which had enabled the identification of chemical processes at both high and low temperatures, its prediction was extrapolated to low temperature conditions met in sedimentary basins. As an example, simulations were performed using a geothermal heating rate of 2 °C/Ma.

b) Methane generation

In these simulations methane started to be generated significantly above 180 °C to reach 170 mg/g of initial charge at 220 °C (Figure 10). Similar simulations performed on 9-methylphenanthrene (Behar et al., 1999) and on 1-methylpyrene (Lorant et al., 2000), revealed that those two latter methylated polyaromatics started to generate methane between 170 °C and 180 °C. The generation temperature of methane is thus only slightly lower for methylated polaromatics than for methylated monoaromatics and both classes are methane prone compounds under conditions met in deeply buried reservoirs (high temperature especially).

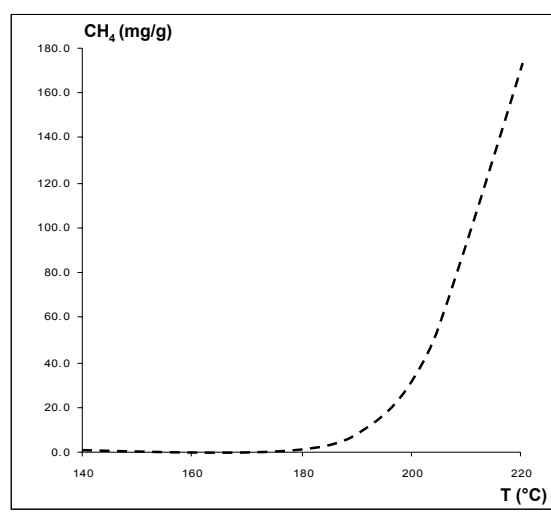


Figure 10: Simulated yield (in mg/g of initial reactant) of methane under geological conditions for a geothermal gradient of 2 °C/Ma.

c) Relative thermal stability of methylated aromatics

In simulations with the same geothermal heating rate of 2 °C/Ma, 1,2,4-trimethylbenzene started degradation at around 180 °C and was nearly completely decomposed at 220 °C (Figure 11).

We then performed simulations under the same conditions using previously reported kinetic parameters for methylated polyaromatics and saturates (other ubiquitous compounds in crude oils). Results revealed that 1-methylnaphthalene (Leininger et al., 2006) and 9-methylphenanthrene (Behar et al., 1999) started to degrade at around 130 °C. Such higher stability of methylated monoaromatics compared to methylated polyaromatics at low geological temperatures was also confirmed in regards to the work of Al Darouich et al (2006a). These authors indeed found that the molecular class termed methyl aromatics, composed of both mono- and diaromatics, started to decompose at an intermediate temperature of around 150 °C.

Similar simulations performed for saturated hydrocarbons such as *n*-C₂₅ (Behar and Vandenbroucke, 1996) and *n*-C₁₆ (Ford, 1986; Khorasheh and Gray, 1993; Jackson et al., 1995) revealed that these compounds started to be altered in the range 170 °C-210 °C.

At low temperatures usually met in sedimentary basins, the order of thermal stability was thus methylated polyaromatics < methylated monoaromatics < saturates. These results emphasized the need to consider these chemical classes separately in basin simulators.

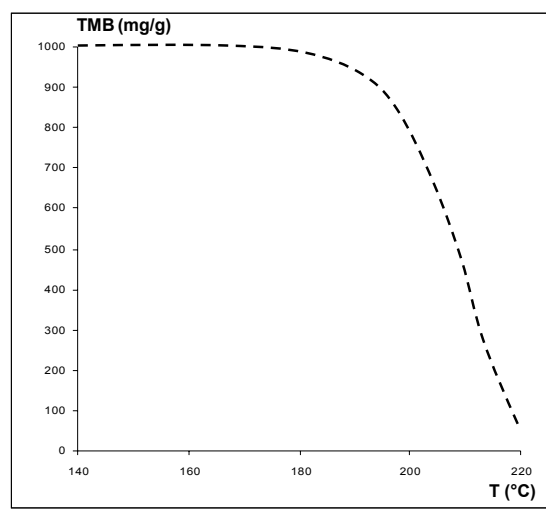


Figure 11: Simulated yield (in mg/g of initial reactant) of 1,2,4-trimethylbenzene (TMB) for a geothermal gradient of 2 °C/Ma.

d) Evolution of other fractions

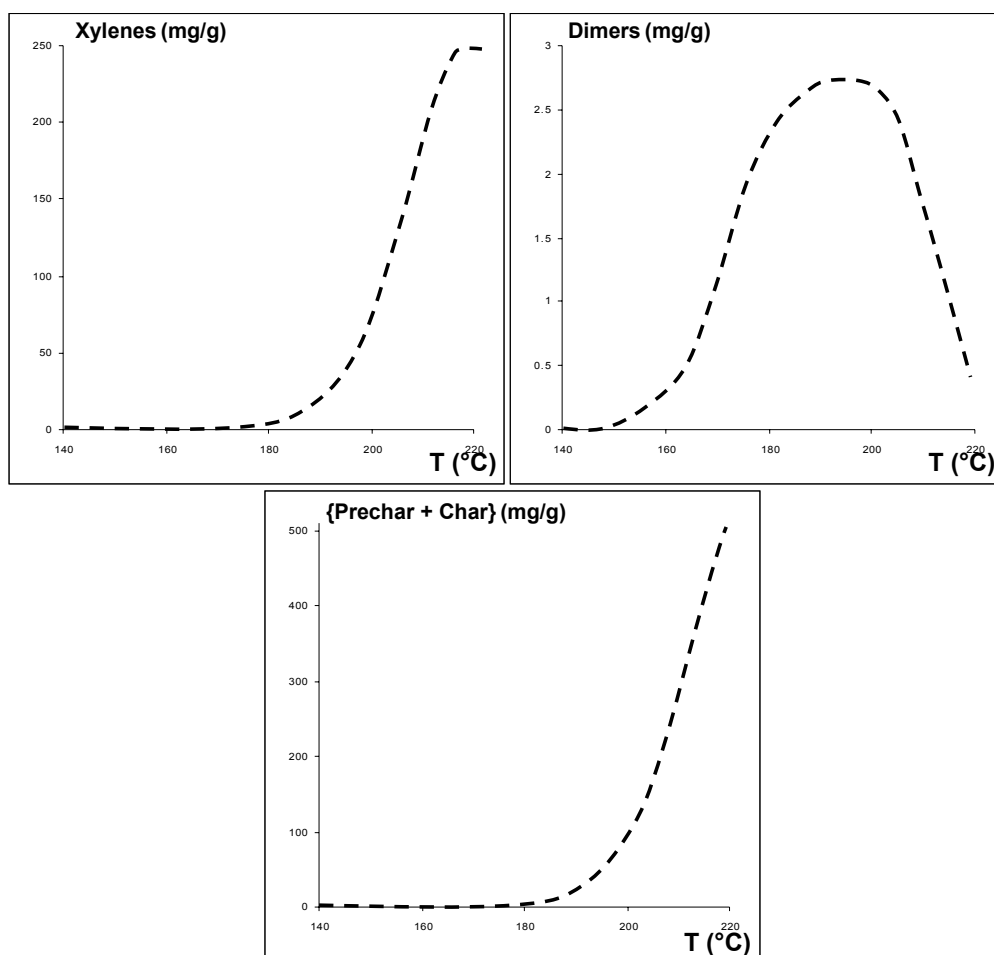
The simulation of the yields of xylenes, dimers, and {Prechar + Char} using the same geothermal gradient of 2°C/Ma are represented in Figures 12, 13, and 14.

In these simulations, xylenes started to be generated significantly above 180 °C and remained stable until above 200 °C reaching 245 mg/g at 220 °C. This result was in

agreement with the stability postulated by Al Darouich et al (2006a) for xylenes over the same range of temperatures.

Dimers started to be generated at 150 °C, their yield reached a maximum of 2.7 mg/g between 190 °C and 200 °C and they had nearly completely disappeared at 220 °C.

The estimation of the yield of a heavy fraction such as {Prechar + Char} was also of tremendous importance in regards to exploration prospects since it can cause problems by decreasing the porosity of the reservoir. In our simulations, condensed compounds lumped in the chemical class {Prechar + Char} were the most abundant products above 190 °C and reached 500 mg/g at 220 °C, *i.e.* half of the original charge. The model of Al Darouich et al (2006a) also predicted a sharp increase of insoluble residue above 190 °C during thermal cracking of the C₆-C₁₄ aromatic fraction of a Type II crude oil.



Figures 12, 13, and 14: Simulated yields (in mg/g of initial reactant) of xylenes, dimers, and {Prechar + Char} for a geothermal gradient of 2 °C/Ma.

4. Conclusions

In the present work we presented a lumped kinetic scheme for thermal cracking of 1,2,4-trimethylbenzene. The chemistry of the stoichiometric equations was constrained on the basis of an initial free-radical mechanism (Fusetti et al., 2009a) which predicted the generation and degradation of compounds up to C₁₈ until 70% conversion of 1,2,4-trimethylbenzene.

Sources of methane resulting from the condensation reactions of dimers into heavier molecular-weight compounds (lumped in the chemical fraction {Prechar + Char}) were added in the present study since they could not be taken into account in the previous free-radical mechanism. Because of the constraint imposed by the software used for the optimization, cross bimolecular additions were not taken into account.

The new model thus resulted in a scheme involving four stoichiometric equations *i.e.* the decomposition of the reactant *via* dimerization (pathway P_a) or *via* demethylation (pathway P_b), the condensation reactions of dimers (pathway P_c), and the decomposition of xylenes *via* dimerization and demethylation (pathway P_d).

The optimization was constrained by an extended pool of experimental data at 395 °C, 425 °C, 450 °C, and 475 °C. Resulting activation energies ranged between 50-60 kcal/mol and frequency factors were all close to 10¹² s⁻¹.

The model presented here satisfyingly predicted the yields of methane, 1,2,4-trimethylbenzene, xylenes, dimers, and higher molecular-weight compounds {Prechar + Char} over the whole range of 1,2,4-trimethylbenzene conversions (0-100 %).

The relative importance of the four pathways of methane generation was assessed. Results revealed that below 5% conversion, demethylation of the reactant (pathway P_b) and condensation reactions (pathway P_c) led to the most methane, followed by dimerization of the reactant (pathway P_a). Above 5% conversion, condensation reactions (P_c) were the main source of methane, followed by demethylation (P_b) and dimerization (P_a) of the reactant, respectively. The decomposition of xylenes (pathway P_d) showed negligible methane yields, except above 95% conversion.

The yield of methane was also successfully modelled with a unique stoichiometric equation and associated set of kinetic parameters ($E = 58.5$ kcal/mol, and $A = 10^{11.96}$ s⁻¹) yielding to an infinite yield of 7.6 wt% of methane per methyl group of 1,2,4-trimethylbenzene. These results values were relatively similar to those obtained during the study of methane generation from thermal cracking of 9-methylphenanthrene (Behar et al., 1999) and 1-methylpyrene (Lorant et al., 2000).

Eventually the lumped model of four equations (P_a , P_b , P_c , and P_d) was extrapolated to conditions met in usual sedimentary basins. These simulations revealed that significant amounts of CH_4 were generated by methylated monoaromatics in deeply buried reservoirs and that methylated monoaromatics thus had a higher thermal stability than their polyaromatic counterparts but lower than the saturated hydrocarbons. This last conclusion emphasized the need to consider the three chemical classes (methylated monoaromatics, methylated polyaromatics, saturated hydrocarbons) separately in basin simulators. Regarding products of the degradation of 1,2,4-trimethylbenzene, simulations also reported that xylenes started to be generated significantly above 180 °C and remained stable until above 200 °C. Dimers were generated at 150 °C, reached a maximum between 190 °C and 200 °C and had nearly completely disappeared at 220 °C. Condensed compounds {Prechar + Char} were the most abundant products above 190 °C and reached 500 mg/g at 220 °C, *i.e.* half of the original charge which would significantly decrease the porosity of a reservoir.

To the best of our knowledge, the present study constitutes the first attempt to establish a global kinetic scheme whereby the majority of the chemistry is constrained by a free-radical mechanism. Such strategy allows obtaining a model that can be both implemented easily in a basin simulator and whose prediction can be extrapolated with a relative confidence to geological conditions. However, we are aware that, if on the one hand the study of a single compound such as 1,2,4-trimethylbenzene enables such strategy, on the other hand dealing with complex system to describe kerogens or oils composition is far more complex and approximations on the nature of the chemical reactions and species lumped in the scheme are still a necessity at this stage.

CHAPTER V:

Stable carbon isotope fractionation model for methane generated during thermal cracking of 1,2,4-trimethylbenzene

This chapter is extracted from a submitted paper (ref below) and inserted in the thesis report as such, with the exception of the references which have been moved to Appendix III and the acknowledgements which have been removed.

Fusetti, L., Behar, F., Lorant, F., Grice, K., Derenne, S., 2009c. New insights into secondary gas generation from oil thermal cracking: methylated monoaromatics. A kinetic approach using 1,2,4-trimethylbenzene. Part III: A stable carbon isotope fractionation model. *Submitted to Organic Geochemistry.*

ABSTRACT:

The scope of the present study was to establish a model to predict the stable carbon isotope composition of methane generated during the thermal cracking of 1,2,4-trimethylbenzene. The chemistry of the model was extracted from a previous study (*Fusetti, L., Behar, F., Grice, K., Derenne, S., 2009b. New insights into secondary gas generation from oil thermal cracking: methylated monoaromatics. A kinetic approach using 1,2,4-trimethylbenzene. Part II: A lumped kinetic scheme. Organic Geochemistry OG-772, accepted and revision in progress*). Kinetics for the generation of $^{12}\text{CH}_4$ and $^{13}\text{CH}_4$ were expressed separately, the temperature dependent nature of isotopic fractionation phenomena being taken into consideration. Optimization was constrained by experimental data for $\delta^{13}\text{C}_{\text{CH}_4}$ above 30% conversion at 425 °C, 450 °C, and 475 °C, yielding a ratio of frequency factors $\Omega = 1.028$ and variations of activation energy ΔE_i ranging from 36 cal/mol to 79 cal/mol. Simulations performed under geological heating rates illustrated the greater isotopic fractionation of CH_4 generated under geological conditions compared with laboratory conditions. The comparison at high maturity with $\delta^{13}\text{C}_{\text{CH}_4}$ during thermal cracking of 1-methylpyrene and mature kerogen under the same simulation conditions emphasized the need to determine the magnitude of the precursor effect for natural compounds.

1. Introduction

The growing interest for natural gas (*i.e.* methane) as an energy source still requires an improved understanding of the pathways leading to its formation. In sedimentary basins, commercial accumulations of methane found in reservoir rocks can originate from bacterial and/or thermal processes. Regarding thermogenic methane, a further differentiation is traditionally made between (i) primary methane, *i.e.* the migrated gas generated from the direct thermal cracking of organic matter within source rocks, (ii) secondary methane, *i.e.* the gas generated within reservoir rocks from the thermal cracking of the reservoir oil. The discovery of gas during exploration campaigns therefore raises questions related to source tracking such as: bacterial *vs.* thermal origin for shallow methane, primary *vs.* secondary thermal origin for methane in deeply buried reservoirs.

The $\delta^{13}\text{C}$ analysis of individual gases such as methane has been regarded as a key analytical tool to classify natural gas with respect to its origin and post genetic history. Retracing the origin of gas would therefore be accurate if isotopic ranges of variation could be linked with specific generation processes. Previous studies have showed that thermogenic gases were less depleted in ^{13}C than biogenic gases which their $\delta^{13}\text{C}$ ranging from -60‰ to -

25‰ and -90‰ to -55‰, respectively (Schoell, 1988; Rice and Claypool, 1981; Whiticar, 1994). Pioneering models have attempted to increase the precision of the correlation by empirically linking $\delta^{13}\text{C}$ of thermogenic gases to maturity (vitrinite reflectance R_o) of respective source rocks (e.g. Stahl and Carey, 1975; Chung and Sackett, 1979; Schoell, 1983; Faber, 1987; Berner and Faber, 1996). These results have provided the backbone of natural gas interpretation carried out in the oil and gas industry. However, such empirical models faced limitations because they were not generally applicable to all types of sedimentary basins, gas sources, and thermal histories. The development of a fundamental understanding of what governed isotopic fractionation became a necessity.

Variations in stable isotopic composition or 'isotopic fractionations' were demonstrated to occur in nature as a result of chemical and physical processes, due to different isotopes of an element having subtly different chemical and physical properties (Urey, 1947; Bigeleisen and Mayer, 1947; Bigeleisen, 1949). Under steady state conditions, the magnitude of isotopic fractionations is governed by thermodynamic equilibrium principles whereas under transitional conditions, isotopic fractionations are induced by the kinetic isotopic effect *i.e.* the difference between reaction velocities of individual isotopes. According to Bigeleisen (1949), the phenomenon of isotope partitioning during chemical reactions without any further rearrangement is then caused by such kinetic effect. In a reaction where a reactant A yields products B and C, there may be two (or more) competing unidirectional isotopic reactions to describe the isotopic fractionation between B and A:



Where k_l and k_h are the rate constants of the reactions yielding to the isotopically light (B_l) and heavy (B_h) forms of B, respectively.

In such kinetic approach, the isotopic fractionation factor α between A and B is then defined as the ratio:

$$\alpha = k_h / k_l$$

Regarding the generation of thermogenic gases, it has been demonstrated that the evolution of $\delta^{13}\text{C}$ as a function of temperature and time was due to the kinetic isotopic effect (Sackett et al., 1966; Sackett, 1968; Frank and Sackett, 1969). Moreover, it was shown (Galimov, 1975) that another effect may influence the $\delta^{13}\text{C}$ of such gases, the 'precursor isotopic effect'. The evidence of this effect is to be found when the stable carbon isotope composition of the cumulated gas at the end of the reaction ($\delta^{13}\text{C}_\infty$) differs from the bulk

initial stable carbon isotope composition of the reactant ($\delta^{13}\text{C}_o$). The $\delta^{13}\text{C}$ of the generated gas indeed tends to reach the initial stable carbon isotope composition $\delta^{13}\text{C}_p$ of its precursor within the reactant. However, according to their genetic history, molecules are not isotopically homogeneous and it was for example demonstrated that in substituted aromatics, ^{13}C is preferentially concentrated in the aromatic rings rather than in the substituents (Galimov, 1975). Consequently, the initial stable carbon isotope composition $\delta^{13}\text{C}_p$ of the gas precursor differs from the bulk initial stable carbon isotope composition $\delta^{13}\text{C}_o$ of the reactant, causing the so called precursor effect at the end of the reaction.

During the past three decades, various models based on a kinetic approach were proposed to predict the $\delta^{13}\text{C}$ of hydrocarbon gases generated from thermal cracking of organic matter. Initially, these models were based on a stochastic formalism (Waples and Tornheim, 1978) or on the Rayleigh (1896) distillation theory (Clayton, 1991a; Berner et al., 1992 and 1995; Rooney et al., 1995). However, due to their intrinsic hypotheses, these approaches failed to account for the temperature dependency of the isotopic fractionation factor α . A new type of kinetic approach was then developed, combining the kinetic concept commonly used to describe gas generation and the fundamentals of the isotopic fractionation phenomenon. The temperature dependence of α was however still not accounted by several models. Indeed, Smith et al (1971), Galimov (1988), and Lorant et al (1998) fixed α as a constant which was thus somehow equivalent to a distillation model combined with a compositional approach (Rooney et al., 1995). Xiong et al (2004) studied the $\delta^{13}\text{C}$ evolution of methane generated during coalification. They assumed either a uniform $\delta^{13}\text{C}_p$ for all methane precursors or a constant α during the whole gas formation process. Sundberg and Bennet (1983) and Poljakov (1996) did consider α as temperature-dependent and used respectively a second order polynomial function $\log(\alpha) = f(1/T)$ and complex mathematical equations to account for this dependency. Tang et al (2000) developed the Arrhenius-like formalism to mathematically model the $\delta^{13}\text{C}$ of methane generated during thermal cracking of several simple model compounds. Variation of activation energies ΔE were calculated using zero-point energy differences resulting from quantum mechanical calculation of a previous work (Tang and Jenden, 1995). Tang et al (2000) then calibrated their model on data obtained during laboratory pyrolysis of *n*-octadecane and emphasized the need to well constrain the precision of such experimental $\delta^{13}\text{C}$ values since α was known to undergo greater variations under geological conditions rather than under laboratory conditions. Lorant and co-workers extended this formalism to predict the $\delta^{13}\text{C}$ of methane generated during the thermal cracking of 1-methylpyrene (Lorant et al., 2000) and the late primary cracking of kerogen (Lorant and

Behar, 2001). An extended contribution to the development of theoretical principles governing stable carbon isotope fractionations was also brought by Cramer and co-workers (Cramer et al., 1998 and 2001; Cramer, 2004). Modelling the $\delta^{13}\text{C}$ of methane generated from the thermal maturation of coal during non-isothermal pyrolysis experiments, their approach was successfully extrapolated to geological heating rates. Their studies concluded that the influences of the kinetic (α) and precursor ($\delta^{13}\text{C}_p$) effects over the $\delta^{13}\text{C}$ of generated gases should not be accounted separately and should instead be both included in a reaction kinetic picture of isotopic fractionation claiming any reference to reality.

In our previous study (Fusetti et al., 2009b) we demonstrated that methylated monoaromatics were gas prone components in deeply buried reservoirs. Their contribution could thus have a significant impact on the carbon isotopic signature of methane generated in such conditions. As a consequence, the purpose of the present study was to establish a model that isotopically characterize the generation of methane ($\delta^{13}\text{C}_{\text{CH}_4}$) during the thermal cracking of 1,2,4-trimethylbenzene, a methylated monoaromatic found in the light aromatic fraction of most crude oils. The aforementioned literature review has emphasized the necessity to link the description of the isotopic fractionation of methane to the mechanisms leading to its generation since chemical and isotopic modifications during a reaction are related to the same genetic pathways. Consequently, to accurately predict $\delta^{13}\text{C}_{\text{CH}_4}$ our isotopic fractionation model had to be based on a validated kinetic model describing thermal cracking of 1,2,4-trimethylbenzene. Based on previous observations, the following research strategy was thus conducted:

- A. Stable carbon isotope data ($\delta^{13}\text{C}$) was collected for methane generated during thermal cracking of 1,2,4-trimethylbenzene.
- B. On the basis of a lumped kinetic scheme (Fusetti et al., 2009b) reported in Table 1, kinetic equations describing stable carbon isotope fractionation of the generated methane were elaborated.
- C. Optimization of the model was performed and its prediction was extrapolated to geological conditions.

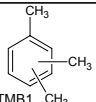
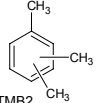
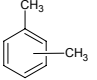
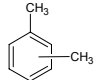
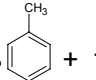
Stoichiometric equations	Ea (kcal/mol)	log A(s ⁻¹)
P_a :  \longrightarrow 96.73 % Dimers + 3.27 % CH ₄	58.02	12.006
P_b :  \longrightarrow 86.96 %  + 13.04 % CH ₄	57.87	12.106
P_c : Dimers \longrightarrow 82.84 % { Prechar + Char } + 17.16 % CH ₄	52.84	11.921
P_d :  \longrightarrow 64.37 % Dimers + 28.12 %  + 7.51 % CH ₄	60.53	12.015

Table 1: Optimized kinetic scheme and associated kinetic parameters for thermal cracking of 1,2,4-trimethylbenzene (Fusetti et al., 2009b).

2. Experimental

2.1 Pyrolysis of 1,2,4-trimethylbenzene

T (°C)	t (h)	Conversion (%)	H ₂	CH ₄	C ₂ H ₆	C ₆ -C ₁₃ in n-C ₅	C ₁₄₊ in n-C ₅	DCM fraction	Residue
395	144	6.0	0.1	2.1	0.3	952.5	25.6	18.7	0.0
395	432	17.0	0.2	26.1	1.5	833.5	101.0	20.8	16.9
425	3	0.8	0.0	0.1	0.1	975.2	6.6	18.0	0.0
425	9.5	2.7	0.0	0.2	0.3	973.1	9.4	16.8	0.0
425	120	28.6	0.3	40.3	2.6	771.9	114.3	20.2	50.4
425	216	45.3	0.4	67.1	3.4	ND	ND	ND	ND
425	648	83.1	0.3	139.4	5.8	ND	ND	ND	ND
450	24	24.9	0.3	23.9	1.5	ND	ND	ND	ND
450	50	44.7	0.5	62.7	3.3	687.7	103.2	20.0	122.6
450	72	57.3	0.5	97.8	4.4	582.2	91.1	19.9	204.1
450	144	81.3	0.5	140.8	5.4	478.8	79.1	20.9	274.5
450	195	89.5	0.4	161.2	5.9	410.7	63.3	20.5	338
450	336	97.8	0.4	191.2	5.5	ND	ND	ND	ND
450	432	99.2	0.4	207.0	5.1	289.9	49.8	21.4	426.4
450	648	99.9	0.3	229.5	4.1	ND	ND	ND	ND
475	9	33.9	0.5	51.9	3.0	ND	ND	ND	ND
475	24	66.3	0.6	117.7	4.8	ND	ND	ND	ND
475	72	95.8	0.5	190.1	5.5	ND	ND	ND	ND

Table 2: Experimental mass-balances obtained (Fusetti et al., 2009a and 2009b) for thermal cracking of 1,2,4-trimethylbenzene at 100 bar (ratios in mg/g of initial reactant).

1,2,4-trimethylbenzene was subjected to pyrolysis experiments at 395 °C, 425 °C, 450 °C, and 475 °C (Fusetti et al., 2009a and 2009b). Mass-balances of the different fractions

(gases, C₆-C₁₃ compounds soluble in *n*-pentane, C₁₄₊ compounds soluble in *n*-pentane, C₁₄₊ compounds insoluble in *n*-pentane but soluble in dichloromethane, and solid residue) are reported in Table 2.

2.2 $\delta^{13}\text{C}$ measurements of methane

2.2.1 Standards and notation

Stable carbon isotope composition is determined not as an absolute isotopic abundance, but as a ratio of heavy isotope (¹³C) to light isotope (¹²C) relative to a standard: the international standard Pee Dee Belemnite (PDB), a marine limestone from the Pee Dee formation in South Carolina (USA). Stable carbon isotope composition is expressed as a delta ($\delta^{13}\text{C}$) in units of per mil (‰) or parts per thousand, and calculated using equation (1):

$$\delta^{13}\text{C} = \left[\left(\frac{R_{\text{sample}}}{R_{\text{standard}}} \right) - 1 \right] \times 1000 \quad (1)$$

Where *R* is the ratio of heavy to light isotope.

The PDB international standard is thus assigned the value $\delta^{13}\text{C}_{\text{PDB}} = 0\text{‰}$. However, it should be noted that PDB went exhausted and was replaced by calibrating another carbonate (NBS-19) relative to PDB (Urey et al., 1951; Craig, 1957). The new calibration was termed 'VPDB' (Vienna PDB) and $R_{\text{VPDB}} = 11,237$ ppm.

2.2.2 GC-irMS conditions

Gas chromatography-isotope ratio mass spectrometry (GC-irMS) of methane was performed on a Micromass IsoPrime mass spectrometer interfaced to a HP GC for determination of compound-specific stable carbon-isotope compositions ($\delta^{13}\text{C}$).

$\delta^{13}\text{C}$ values were calculated by integration of the *m/z* 44, 45 and 46 ion currents of the CO₂ peaks produced of the chromatographically separated compounds using copper oxide pellets (4mm x 0.5 mm, isotope grade, Elemental Microanalysis Ltd.) at 850°C. Compositions were reported relatively to CO₂ reference-gas pulses (Coleman Instrument grade, BOC Gases Australia Ltd.) of known ¹³C/¹²C content into the spectrometer. The ¹³C/¹²C content of the CO₂ reference gas was monitored daily *via* analysis of the gas mixture of reference compounds. At least three analyses were performed per sample. Carbon-isotope compositions were given in the delta notation relative to Vienna Peedee Belemnite (VPDB).

3. Experimental results and discussion

3.1 Experimental values observed for the $\delta^{13}\text{C}$ of methane

T (°C)	t (h)	Conversion (%)	$\delta^{13}\text{C}$ (CH ₄)
395	144	6.0	ND
395	432	17.0	ND
425	3	0.8	ND
425	9.5	2.7	ND
425	120	28.6	ND
425	216	45.3	-35.0
425	648	83.1	-33.8
450	24	24.9	ND
450	50	44.7	-35.0
450	72	57.3	-34.8
450	144	81.3	-34.0
450	195	89.5	-33.6
450	336	97.8	-33.1
450	432	99.2	-32.8
450	648	99.9	-32.5
475	9	33.9	-35.0
475	24	66.3	-34.5
475	72	95.8	-33.2

Table 3: Stable carbon isotope compositions ($\delta^{13}\text{C}$ in ‰) of methane obtained during thermal cracking of 1,2,4-trimethylbenzene at 100 bar. The initial $\delta^{13}\text{C}$ of the reactant 1,2,4-trimethylbenzene was measured at -29.6‰. All $\delta^{13}\text{C}$ are given with a precision of $\pm 0.6\%$, the maximum observed standard deviation being 0.3‰.

As shown in Table 3, reproducible $\delta^{13}\text{C}$ values of methane were obtained for conversions of the reactant 1,2,4-trimethylbenzene being greater than 30%. Indeed, according to the charge (≈ 50 mg) of 1,2,4-trimethylbenzene pyrolysed during each experiment, the corresponding methane generated at conversions lower than 30% was less than 160 μmol . Despite using small sampling ampoules, the concentration of methane in such experiments was still very low due to the much larger quantity of nitrogen, the inert gas used during the experiments. Sampling with the syringe before injection into the GC-irMS, then induced the quantity of methane to be not sufficient for obtaining a reproducible value below 30% conversion.

Observed $\delta^{13}\text{C}_{\text{CH}_4}$ were more depleted in ^{13}C than the initial 1,2,4-trimethylbenzene for which $\delta^{13}\text{C}_0 = -29.6\%$. Between 30% and 100% conversion, the $\delta^{13}\text{C}$ of methane increases from -35.0‰ to -32.5‰ *i.e.* an enrichment in ^{13}C . These results illustrate the kinetic

effect (Sackett et al., 1966; Sackett, 1968; Frank and Sackett, 1969) *i.e.* ^{12}C - ^{12}C bonds were broken faster than ^{12}C - ^{13}C bonds generating a methane which was always more depleted in ^{13}C than the reactant and whose stable carbon isotope composition increased with conversion.

When approaching 100% conversion, $\delta^{13}\text{C}$ values of methane reached a plateau in the neighbourhood of $\delta^{13}\text{C}_\infty = -32.5\text{‰}$, illustrating the precursor effect since such stable carbon isotope composition of methane precursor groups (*i.e.* methyl moieties, *c.f.* Fusetti et al., 2009a) $\delta^{13}\text{C}_{\text{methyl}} = \delta^{13}\text{C}_p = \delta^{13}\text{C}_\infty$ differs from the bulk initial stable carbon isotope composition of the reactant $\delta^{13}\text{C}_0 = -29.6\text{‰}$.

3.2 Elaboration of the isotopic fractionation model

a) Pathways of methane generation

The lumped kinetic scheme (Table 1) elaborated in our previous study (Fusetti et al., 2009b) was composed of four pathways of methane generation which accounted for the decomposition of the reactant 1,2,4-trimethylbenzene *via* **Reactant** --> **Dimers** (pathway P_a), **Reactant** --> **Xylenes** (pathway P_b), **Dimers** --> **{Prechar + Char}** (pathway P_c), and **Xylenes** --> **Dimers + Toluene** (pathway P_d). We had assumed that P_a involved 2/3 of the initial reactant while the remaining 1/3 had been associated to P_b. Optimized activation energies E were comprised between 50 kcal/mol and 60 kcal/mol, and frequency factors A were in the neighbourhood of 10^{12} s^{-1} . Simulations had revealed that the reactant demethylation pathway (P_b) and the condensation pathway (P_c) led to the greatest amount of methane below 5% conversion, followed by the reactant dimerization pathway (P_a). Above 5% conversion, methane generated *via* the condensation pathway (P_c) was dominant but the contributions of the reactant demethylation (P_a) and dimerization (P_b) were non negligible. The contribution of the decomposition of xylenes (pathway P_d) to methane generation had been demonstrated to be always negligible except when approaching 100% conversion. Consequently, we only kept the reactions: **Reactant** --> **Dimers** (pathway P_a), **Reactant** --> **Xylenes** (pathway P_b), **Dimers** --> **{Prechar + Char}** (pathway P_c) as relevant contributions to $\delta^{13}\text{C}_{\text{CH}_4}$ until 100% conversion of 1,2,4-trimethylbenzene.

b) Generation kinetics of $^{12}\text{CH}_4$

The kinetic scheme represented in Table 1, had been elaborated to predict the yield of total methane *i.e.* $\{^{12}\text{CH}_4 + ^{13}\text{CH}_4\}$. However, according to the natural abundances of the

heavy (^{13}C) and light (^{12}C) isotopes (1.109% and 99.891%, respectively), the approximation was made to consider that the kinetics for the generation of $^{12}\text{CH}_4$ were the same as those of the total CH_4 . The yield of $^{12}\text{CH}_4$ was thus expressed by solving the system of equations (2) in which all reactions rates were assumed to be of first order relative to each individual reactant.

$$(2) \quad \begin{cases} \frac{d[\text{TMB}_1]}{dt} = -k_a[\text{TMB}_1] \\ \frac{d[\text{TMB}_2]}{dt} = -k_b[\text{TMB}_2] \\ \frac{d[\text{Dimers}]}{dt} = (1-x_a)k_a[\text{TMB}_1] - k_c[\text{Dimers}] \\ \frac{d[^{12}\text{CH}_4]}{dt} \approx \frac{d[\text{CH}_4]}{dt} = x_a k_a[\text{TMB}_1] + x_b k_b[\text{TMB}_2] + x_c k_c[\text{Dimers}] \end{cases}$$

Where k_a , k_b , and k_c are the rate constants for methane generation in pathways P_a , P_b and P_c , respectively. Where $x_a = 3.27 \text{ wt}\%$, $x_b = 13.04 \text{ wt}\%$, and $x_c = 17.16 \text{ wt}\%$ are the stoichiometric coefficients of methane in pathways P_a , P_b and P_c , respectively (c.f. Table 1).

The integration (for isothermal conditions) gave equation (3) (in wt% of initial 1,2,4-trimethylbenzene).

$$(3) \quad \begin{aligned} [^{12}\text{CH}_4] = & [\text{TMB}_1]_0 \left(x_a - \frac{k_c}{k_a - k_c} (1 - x_a) x_c \right) (1 - \exp(-k_a t)) \\ & + [\text{TMB}_1]_0 \frac{k_a}{k_a - k_c} (1 - x_a) x_c (1 - \exp(-k_c t)) + [\text{TMB}_2]_0 x_b (1 - \exp(-k_b t)) \end{aligned}$$

Where $[\text{TMB}_1]_0 = (2/3)$ and $[\text{TMB}_2]_0 = (1/3)$.

c) Generation kinetics of $^{13}\text{CH}_4$

The kinetics for the generation of $^{13}\text{CH}_4$ were then expressed relatively to those of $^{12}\text{CH}_4$. The isotopic fractionation factor α_i of methane was defined for each pathway P_i ($i = a, b$ or c) using the Arrhenius-like formalism (equation (4)) developed by Tang et al (2000) in order to account for the temperature dependency of isotopic fractionations.

$$\alpha_i(T) = \frac{k_{h,i}}{k_{l,i}} = \Omega_i \cdot \exp(-\Delta E_i / R.T) \quad (4)$$

Where for the pathway P_i , ($\Omega_i = A_{h,i}/A_{l,i}$) and ($\Delta E_i = E_{h,i} - E_{l,i}$) are respectively the ratio of frequency factors and the variation of activation energy representing the shift between the generation kinetics of $^{13}\text{CH}_4$ and $^{12}\text{CH}_4$.

Under the approximation that CH_4 was the only product to undergo a significant isotopic fractionation compared to each of its sources; generation kinetics of $^{13}\text{CH}_4$ were thus expressed according to the system of equations (5).

$$(5) \quad \begin{cases} \frac{d[^{13}\text{TMB}_1]}{dt} = -\tilde{\alpha}_a k_a [^{13}\text{TMB}_1] & \text{with } \tilde{\alpha}_a = x_a \alpha_a + (1 - x_a) \\ \frac{d[^{13}\text{TMB}_2]}{dt} = -\tilde{\alpha}_b k_b [^{13}\text{TMB}_2] & \text{with } \tilde{\alpha}_b = x_b \alpha_b + (1 - x_b) \\ \frac{d[^{13}\text{Dimers}]}{dt} = (1 - x_a) k_a [^{13}\text{TMB}_1] - \tilde{\alpha}_c k_c [^{13}\text{Dimers}] & \text{with } \tilde{\alpha}_c = x_c \alpha_c + (1 - x_c) \\ \frac{d[^{13}\text{CH}_4]}{dt} = x_a \alpha_a k_a [^{13}\text{TMB}_1] + x_b \alpha_b k_b [^{13}\text{TMB}_2] + x_c \alpha_c k_c [^{13}\text{Dimers}] \end{cases}$$

Where $^{13}\text{TMB}_1$, $^{13}\text{TMB}_2$, and $^{13}\text{Dimers}$ are respectively a molecule of TMB_1 , TMB_2 , and Dimers that contains a $^{13}\text{CH}_3$ group that will become $^{13}\text{CH}_4$ during the degradation of the molecule in the subsequent reaction.

With ^{13}TMB representing a molecule of 1,2,4-trimethylbenzene that contained at least a $^{13}\text{CH}_3$ group (yielding $^{13}\text{CH}_4$), a similar integration procedure as the one leading to equation (3) gave equation (6) (in wt% of initial ^{13}TMB).

$$(6) \quad \begin{aligned} [^{13}\text{CH}_4] = & [\text{TMB}_1]_0 \left(\alpha_a x_a - \frac{\alpha_c k_c}{\tilde{\alpha}_a k_a - \tilde{\alpha}_c k_c} (1 - x_a) x_c \right) \frac{(1 - \exp(-\tilde{\alpha}_a k_a t))}{\tilde{\alpha}_a} \\ & + [\text{TMB}_1]_0 \frac{\alpha_c k_a}{\tilde{\alpha}_a k_a - \tilde{\alpha}_c k_c} (1 - x_a) x_c \frac{(1 - \exp(-\tilde{\alpha}_c k_c t))}{\tilde{\alpha}_c} \\ & + [\text{TMB}_2]_0 \alpha_b x_b \frac{(1 - \exp(-\tilde{\alpha}_b k_b t))}{\tilde{\alpha}_b} \end{aligned}$$

d) Theoretical $\delta^{13}\text{C}$ of methane

As shown in equation (1), the expression of the stable carbon isotope composition $\delta^{13}\text{C}$ of methane is linked to the ratio R (of the heavy carbon isotope $^{13}\text{CH}_4$ to the light carbon isotope $^{12}\text{CH}_4$) which is proportional to the ratio of equation (6) to equation (3). Moreover, we

already mentioned that as a consequence of the precursor effect, $\delta^{13}\text{C}_{\text{CH}_4}$ reached $\delta^{13}\text{C}_\infty = \delta^{13}\text{C}_p$ when approaching 100% conversion of 1,2,4-trimethylbenzene. The stable carbon isotope composition of the cumulative methane at the reaction time t and for a temperature T could thus be expressed as shown in equation (7).

$$\delta^{13}\text{C}_{\text{CH}_4}(t, T) = \left[\left(\frac{\delta^{13}\text{C}_p}{1000} + 1 \right) \cdot \frac{{}^{13}\text{CH}_4(t) / {}^{12}\text{CH}_4(t)}{{}^{13}\text{CH}_4(\infty) / {}^{12}\text{CH}_4(\infty)} - 1 \right] \times 1000 \quad (\text{in } \text{‰}) \quad (7)$$

Where ${}^{13}\text{CH}_4(t) / {}^{12}\text{CH}_4(t)$ is the instantaneous ratio of equation (6) to equation (3) at a reaction time t , and ${}^{13}\text{CH}_4(\infty) / {}^{12}\text{CH}_4(\infty)$ is the ratio of equation (6) to equation (3) at 100% conversion.

In equation (7), seven parameters were thus to be calibrated *i.e.* $\delta^{13}\text{C}_p$ and the couples $(\Omega_i / \Delta E_i)$ for the three considered pathways P_i ($i = a, b, c$) of methane generation. The usual approximation (*e.g.* Lorant et al., 2000) was made to fix $\Omega_a = \Omega_b = \Omega_c = \Omega$ in order to reduce the number of free parameters. $\delta^{13}\text{C}_p$, Ω , ΔE_a , ΔE_b , and ΔE_c thus remained to be calibrated.

3.3 Optimization

The five parameters were calibrated by numerical optimization using equations (7), (6) and (3) to calculate the $\delta^{13}\text{C}$ of methane at each experimental condition. The obtained values were compared to the experimental $\delta^{13}\text{C}$ of methane by finding the minimum of a standard quadratic error function F , defined as:

$$F = \frac{1}{2} \cdot \sum_{j=1}^N \left(\delta^{13}\text{C}_j^{\text{exp}} - \delta^{13}\text{C}_j^{\text{calc}} \right)^2$$

Where N was the total number of experimental values for the $\delta^{13}\text{C}$ of methane.

According to previously reported values (Tang and Jenden, 1995; Cramer et al., 1998; Tang et al., 2000; Lorant et al., 2000), initial guesses were $\Omega = 1.020$ with a variation range between 0.990 and 1.050, and $\Delta E_i = 50$ cal/mol ($i = a, b, c$) with a variation range between 0 and 100 cal/mol. Since we had observed experimentally that $\delta^{13}\text{C}_p \approx -32.5\text{‰}$, this latter value was taken as initial guess with a variation range of $\pm 0.6\text{‰}$ (the maximum experimental uncertainty).

Pathways	ΔE_i (cal/mol)	Ω	$\delta^{13}C_p$ (‰)
TMB \rightarrow Dimers + CH ₄	77	1.028	- 32.7
TMB \rightarrow Xylenes + CH ₄	79		
Dimers \rightarrow {Prechar + Char} + CH ₄	36		

Table 4: Optimized parameters for the model of stable carbon isotope fractionation of methane during thermal cracking of 1,2,4-trimethylbenzene.

Optimized parameters were reported in Table 4. Optimized precursor effect $\delta^{13}C_p = -32.7\text{‰}$ which is very close to the initial guess, as anticipated. Regarding the ratio of frequency factors, an optimized value $\Omega = 1.028$ was obtained. Comparable variations in activation energies $\Delta E_a = 77$ cal/mol and $\Delta E_b = 79$ cal/mol were obtained for the dimerization of 1,2,4-trimethylbenzene and its demethylation into xylene. This result does not seem illogical since these reactions both yield to the formation of methane *via* the release of a methyl group from 1,2,4-trimethylbenzene. $\Delta E_c = 36$ cal/mol was obtained for the condensation pathway of dimers. Such result is difficult to justify on a theoretical point of view but qualitatively it would mean that the structure of higher molecular-weight compounds with a higher number of methyl groups would have an inhibiting effect over the kinetic discrimination between the degradation of ^{12}C - ^{12}C and ^{12}C - ^{13}C bonds.

All these results are comparable with previously reported literature data. Indeed, for the demethylation of toluene, Tang et al (2000) calculated global $\Delta E = 52$ cal/mol and $\Omega = 1.034$, meanwhile for the demethylation of 1-methylpyrene, Lorant et al (2000) obtained global $\Delta E = 43$ cal/mol and $\Omega = 1.024$ which are in the same range as our values. Moreover for thermal cracking of *n*-alkanes, Tang et al (2000) calculated average values $\Delta E = 42$ cal/mol and $\Omega = 1.021$, and Poljakov (1996) calculated an average $\Omega = 1.017$. This comparison seems to emphasize the fact that $\delta^{13}C_{CH_4}$ during thermal cracking of *n*-alkanes and methylated aromatics would be governed by similar kinetic effects, thus implying that differences in the respective domains of variation would be due to the precursor effect.

3.4 Comparison with experimental data

Comparison of the model prediction with experimental data was illustrated on Figures 1 and 2. According to the error bars provided for the experimental data and due to the fact that no data has been obtained below 30% conversion (Figure 2), some comments about the relative confidence in the obtained optimized parameters should be made. Figure 1 reveals that the model prediction was accurate for the three temperatures (425 °C, 450 °C, and 475

°C), falling into the range of experimental error bars. Such result confirms that the temperature dependence of isotopic fractionation factors α_i ($i = a, b, c$) was correctly taken into account using the Arrhenius-like formalism. This conclusion offers more confidence for the future extrapolation of the prediction to geological conditions.

We demonstrated in our previous study (Fusetti et al., 2009b), that the pathway P_a of dimerization of 1,2,4-trimethylbenzene was significant in terms of methane generation at low conversion. Then, as might expected, when in our present model the value $\Delta E_a = 0$ cal/mol is assigned, we indeed do not observe much change above 30% conversion and the prediction remains within the range of experimental error bars. A more accurate value for ΔE_a would thus be obtained using experimental values below 30% conversion. Moreover, according to the range of variation allowed by the experimental error bars, the values $\Delta E_b = 79$ cal/mol and $\Delta E_c = 36$ cal/mol resulting from the optimization should be given with a precision of ± 5 cal/mol.

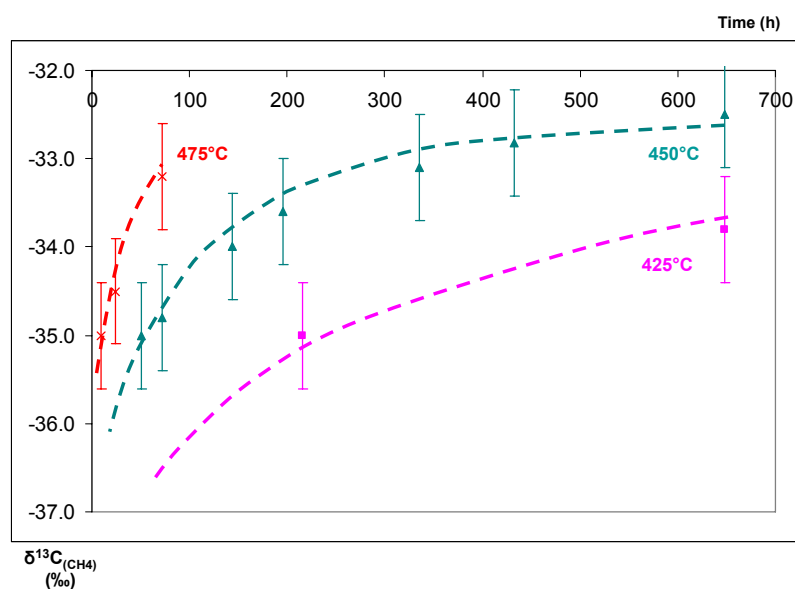


Figure 1: Computer-predicted (dashed lines) and experimental (dots + error bars) stable carbon isotope composition (in ‰) of methane versus time (in h) at 425 °C, 450 °C, and 475 °C.

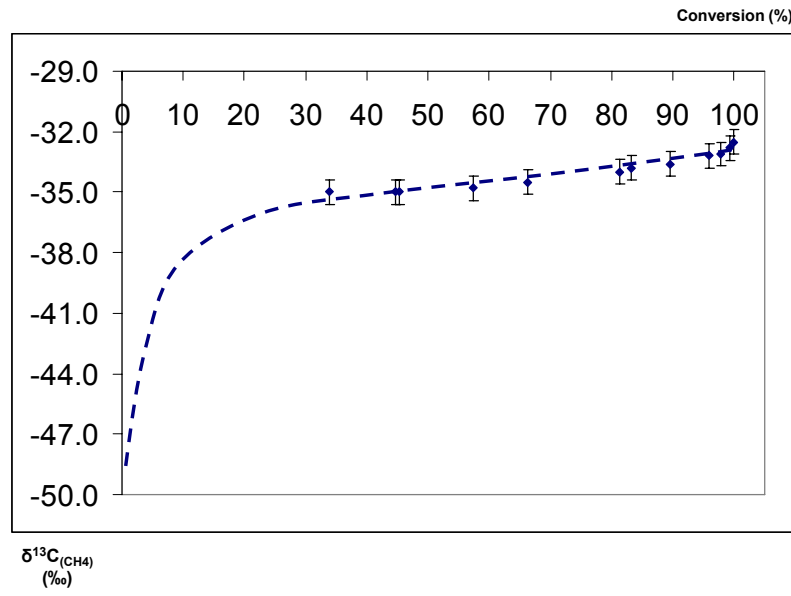


Figure 2: Computer-predicted (dashed line) and experimental (dots + error bars) stable carbon isotope composition (in ‰) of methane versus 1,2,4-trimethylbenzene conversion (in %).

3.5 Extrapolation to geological conditions

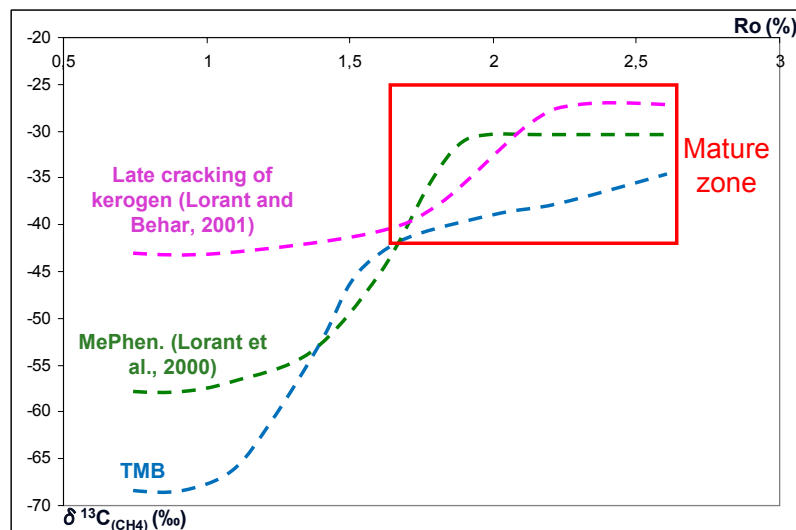


Figure 3: Simulated stable carbon isotope composition (in ‰) of methane versus Ro (in %) during thermal cracking of 1,2,4-trimethylbenzene (TMB), 1-methylphenanthrene (MePhen) and mature kerogen under geological conditions (burial 50m/Ma, gradient 25°C/Km).

The prediction of the present model was extrapolated to low temperature conditions met in sedimentary basins. As an example, simulations were performed using a burial rate of 50m/Ma and geothermal gradient of 25 °C/Km (Figure 3). Results were plotted versus the Ro values which were calculated using the EasyRo model (Burnham and Sweeney, 1989).

The first observation is that our model for 1,2,4-trimethylbenzene reveals a greater isotopic fractionation for the methane generated under geological conditions (Figure 3) than under laboratory conditions (Figure 2). This result illustrates once again the fact that the temperature dependency of α has been taken into account and emphasizes the need to have laboratory isotopic experimental data as accurate as possible to calibrate the models before extrapolation to geological conditions is performed.

These simulations were then compared to those given by the models for the $\delta^{13}\text{C}$ of methane generated during thermal cracking of 1-methylpyrene (Lorant et al., 2000) and late primary cracking of kerogen (Lorant and Behar, 2001) under the same conditions (Figure 3). Despite methane generated from thermal cracking of 1,2,4-trimethylbenzene being slightly more depleted in ^{13}C than others, the comparison between the three models in the mature zone (*i.e.* above approximately $R_o = 1.6\%$) which is of interest for deeply buried reservoirs, does not reveal any substantial discrimination between the three $\delta^{13}\text{C}_{\text{CH}_4}$. This observation should however be moderated by considering the origin of the samples used for the three studies. Indeed, if the kerogen used Lorant and Behar (2001) was a natural sample, on the contrary the 1-methylpyrene used by Lorant et al (2000) and our 1,2,4-trimethylbenzene were commercial synthetic compounds. As mentioned in the introduction, $\delta^{13}\text{C}_{\text{CH}_4}$ in such high maturity zone is governed by the precursor effect. However, the magnitude of the precursor effect depends on the synthetic history of the molecule and it is thus difficult to compare results obtained using natural compounds with results obtained using synthetic compounds. Before any definitive conclusion, a quantification of the precursor effect for a natural 1-methylpyrene and a natural 1,2,4-trimethylbenzene should thus be performed.

4. Conclusions

In the present work we presented the elaboration of a model predicting the stable carbon isotope composition of methane generated during thermal cracking of 1,2,4-trimethylbenzene. From a lumped kinetic scheme describing methane generation during thermal cracking of 1,2,4-trimethylbenzene (Fusetti et al., 2009b), the reactions: **Reactant** --> **Dimers** (pathway P_a), **Reactant** --> **Xylenes** (pathway P_b), **Dimers** --> **{Prechar + Char}** (pathway P_c) were selected as relevant contributions to stable carbon isotope composition of methane until 100% conversion of 1,2,4-trimethylbenzene. On this basis and in order to predict the $\delta^{13}\text{C}$ of the generated methane, kinetics for the generation of $^{12}\text{CH}_4$ and $^{13}\text{CH}_4$ were expressed separately for the pathways P_i ($i = a, b, c$) using free parameters such as a unique ratio of frequency

factors $\Omega = A_h/A_l$, three variations of activation energy $\Delta E_i = E_{h,i} - E_{l,i}$ with $i = a, b, \text{ or } c$, and the stable carbon isotope composition of methane precursor groups $\delta^{13}\text{C}_p$. The optimization was constrained by experimental data for $\delta^{13}\text{C}$ of generated methane above 30% conversion at 425 °C, 450 °C, and 475 °C. The optimized model yielded $\Omega = 1.028$ and showed accuracy to predict experimental $\delta^{13}\text{C}_{\text{CH}_4}$ at the three temperatures. If a more accurate value than $\Delta E_a = 77$ cal/mol should be obtained using data below 30% conversion, the values $\Delta E_b = 79$ cal/mol and $\Delta E_c = 36$ cal/mol were determined with a precision of ± 5 cal/mol. The extrapolation of the model prediction at a burial rate of 50m/Ma and geothermal gradient of 25 °C/Km illustrated the greater isotopic fractionation of CH_4 generated under geological conditions compared with laboratory conditions. The comparison at high maturity with $\delta^{13}\text{C}_{\text{CH}_4}$ during thermal cracking of 1-methylpyrene and mature kerogen under the same simulation conditions emphasized the need to determine the magnitude of the precursor effect for natural compounds.

Further work will focus on calibrating the model below 30% conversion, on determining the magnitude of the precursor isotope effect for natural compounds and on establishing similar stable carbon isotope fractionation models for gases generated during thermal cracking of alkylated monoaromatics.

CHAPTER VI:

Conclusions and Perspectives

PART A: CONCLUSIONS

The scope of the present study was to validate an original integrated approach that could be applied to elaborate a model that would predict the $\delta^{13}\text{C}$ of the gases generated during the thermal cracking of oil. To the best of our knowledge such an approach has never been elaborated. Consequently, the chemical system for this thesis was kept simple. It was taken among the low-molecular-weight aromatic hydrocarbons (*i.e.* C_{14}) of oil, the focus being on methylaromatics and alkylaromatics.

In a first round, seven model compounds were selected representing various cases of side-chains positions, degrees of substitution of the aromatic ring, and side-chains lengths that could be found among the unstable compounds having significant abundances in the two classes of methylaromatics and alkylaromatics. These seven model compounds included two ethyltoluenes, two ethylxylenes, two trimethylbenzenes, and a tetramethylbenzene.

The chemical system was then successfully reduced to one methylaromatic *i.e.* 1,2,4-trimethylbenzene and one alkylaromatic *i.e.* 2-ethyltoluene. Despite the fact that experiments were conducted for both model compounds, the timing issue only enabled the development of the integrated approach for the methane generated during thermal cracking of 1,2,4-trimethylbenzene.

In the first step of the methodology, it was necessary to discriminate primary from non-primary products in order to elucidate a maximum number of elementary processes involved in methane generation during the thermal cracking of 1,2,4-trimethylbenzene. Consequently, we performed pyrolysis experiments choosing experimental conditions representing the widest range of reactant conversion (between 395 °C and 450 °C, at a pressure of 100 bar). All pyrolysis fractions were collected and quantified. Mass-balances were established to ensure that the whole materials were recovered and experiments with less than 98% recovery were discarded to ensure that quantitative data were accurately constrained. All products that could be identified individually were quantified.

On the basis of experimental observations and detailed free-radical mechanisms published for other model compounds, a free-radical mechanism for thermal cracking of 1,2,4-trimethylbenzene was proposed. According to the high pressure (100 bar) of our experiments, bimolecular initiation reactions were taken into account. Because pre-char and char had not been molecularly characterized experimentally, related reactions were not implemented in the model and triaromatics were taken as ultimo species. The obtained

mechanism described 122 chemical transformations involving 47 species. In addition to the reactant, 27 molecular products and 19 radical species were represented.

The model satisfyingly predicted the experimental yields of methane, residual 1,2,4-trimethylbenzene, hydrogen, xylenes, toluene, benzene, and dimers until 70% conversion. The condensation reactions which could not be taken into account in the model were considered as the cause of its deviation at higher conversions.

The model was then used to characterize methane generation pathways at 425 °C and 200 °C until 70% conversion. It was demonstrated that when a pathway was negligible (respectively substantial) at high temperature it remained the same at low temperature. At both temperatures, the identified pathways were:

- (i) The 'monoaromatic route' *i.e.* the demethylation of trimethylbenzenes into xylenes and to a lesser extent the demethylation of xylenes into toluene,
- (ii) The dimerization of monoaromatics ('polyaromatic route', step 1),
- (iii) The ring closure reaction of dimers into triaromatic precursors ('polyaromatic route', step 2).

At low temperature the contribution of the 'monoaromatic route' was demonstrated to expand faster than at high temperature. However, at both temperatures the equilibrium reached was a fairly equal contribution for the 'monoaromatic route' and the 'polyaromatic route'. Eventually, demethylation reactions of toluene, dimers, triaromatic precursors and triaromatics were shown not to be relevant pathways to consider regarding methane generation in both ranges of temperature.

Since a further implementation of the model into basin simulators would require a limited number of equations, the previous free-radical mechanism for thermal cracking of 1,2,4-trimethylbenzene was used to constrain the chemistry of a simpler lumped kinetic scheme. Sources of methane resulting from the condensation reactions of dimers into heavier molecular-weight compounds (chemical fraction termed {Prechar + Char}) were added since they had not been taken into account in the previous free-radical mechanism. Because of the constraint imposed by the software used for the optimization, cross bimolecular additions were not taken into account.

The new model resulted in a scheme involving four stoichiometric equations *i.e.* the decomposition of the reactant *via* dimerization (pathway P_a) or *via* demethylation (pathway P_b), the condensation reactions of dimers (pathway P_c), and the decomposition of xylenes *via* dimerization and demethylation (pathway P_d).

The optimization was performed using experimental data at 395 °C, 425 °C, 450 °C, and 475 °C. Resulting activation energies ranged between 50-60 kcal/mol and frequency factors were all close to 10^{12} s^{-1} .

The new model predicted the yields of methane, 1,2,4-trimethylbenzene, xylenes, dimers, and higher molecular-weight compounds {Prechar + Char} over the whole range of 1,2,4-trimethylbenzene conversions (0-100 %).

The relative importance of the four pathways of methane generation was assessed. Results revealed that below 5% conversion, demethylation of the reactant (P_b) and condensation reactions (P_c) led to the most methane, followed by dimerization of the reactant (P_a). Above 5% conversion, condensation reactions (P_c) were the main source of methane, followed by demethylation (P_b) and dimerization (P_a) of the reactant, respectively. The decomposition of xylenes (P_d) showed negligible methane yields, except above 95% conversion.

The yield of methane was also successfully modelled with a unique stoichiometric equation ($\text{CH}_{4\text{max}} = 7.6 \text{ wt\%}$ of methane per methyl group of 1,2,4-trimethylbenzene). This stoichiometric equation was associated to the set of kinetic parameters $E = 58.5 \text{ kcal/mol}$ and $A = 10^{11.96} \text{ s}^{-1}$. These results were relatively similar to those reported for previous studies of methane generation during thermal cracking of methylated polyaromatic hydrocarbons.

Eventually the lumped model of four equations (P_a , P_b , P_c , and P_d) was extrapolated to geological heating rates. These simulations revealed that in sedimentary basins, the thermal stability increased in the series methylated polyaromatics < methylated monoaromatics < saturates, emphasizing the need to consider these three chemical classes separately in basin simulators. Moreover, it demonstrated that in addition to methylated polyaromatics, methylated monoaromatics were other methane prone compounds under temperature conditions met in deeply buried reservoirs. Regarding products of the degradation of 1,2,4-trimethylbenzene, these simulations also reported that xylenes started to be generated significantly above 180 °C and remained stable until above 200 °C. Dimers were generated at 150 °C, reached a maximum between 190 °C and 200 °C and had nearly completely disappeared at 220 °C. Condensed compounds {Prechar + Char} were the most abundant products above 190 °C and reached 500 mg/g at 220 °C, *i.e.* half of the original charge which could significantly decrease the porosity of a reservoir.

In the third and final stage of the methodology, the reactions: (P_a) **Reactant** --> **Dimers**, (P_b) **Reactant** --> **Xylenes**, (P_c) **Dimers** --> **{Prechar + Char}** were kept as relevant

contributions to $\delta^{13}\text{C}_{\text{CH}_4}$ until 100% conversion during thermal cracking of 1,2,4-trimethylbenzene. Kinetics for the generation of $^{12}\text{CH}_4$ and $^{13}\text{CH}_4$ were then expressed separately for each pathway P_i ($i = a, b, c$) using free parameters such as a unique ratio of frequency factors $\Omega = A_h/A_l$, three variations of activation energy $\Delta E_i = E_{h,i} - E_{l,i}$ ($i = a, b, c$), and the stable carbon isotope composition of methane precursor groups $\delta^{13}\text{C}_p$. The optimization was constrained by experimental $\delta^{13}\text{C}_{\text{CH}_4}$ above 30% conversion at 425 °C, 450 °C, and 475 °C.

The optimized model showed accuracy to predict experimental $\delta^{13}\text{C}_{\text{CH}_4}$ at the three temperatures, demonstrating that the theoretical temperature dependence of isotope fractionation factor α_i ($i = a, b, c$) had correctly been taken into account. Resulting optimized parameters were $\Omega = 1.028$, $\Delta E_a = 77$ cal/mol, $\Delta E_b = 79$ cal/mol, $\Delta E_c = 36$ cal/mol, and $\delta^{13}\text{C}_p = -32.7\text{‰}$. The existence of a precursor effect was thus confirmed since $\delta^{13}\text{C}_p$ differed from the bulk initial stable carbon isotope composition of the reactant $\delta^{13}\text{C}_o = -29.6\text{‰}$. The values of the average ΔE (64 cal/mol) and Ω being in the same order of magnitude than those reported for the methane generated during thermal cracking of *n*-alkanes and other methylated aromatics, revealing similar kinetic isotope effects. It thus demonstrated that the variations between the domains of $\delta^{13}\text{C}_{\text{CH}_4}$ according to which class of starting compounds was considered were due to the precursor isotope effect rather than the kinetic isotope effect.

The extrapolation of the model prediction to geological heating rates illustrated the greater isotopic fractionation of CH_4 generated under geological conditions compared with laboratory conditions. The comparison at high maturity with $\delta^{13}\text{C}_{\text{CH}_4}$ during thermal cracking of 1-methylpyrene and mature kerogen under the same simulation conditions emphasized the need to determine the magnitude of the precursor effect for natural compounds.

PART B: SUGGESTIONS FOR FURTHER WORK

Influence of pressure

All experiments performed to calibrate the different models in this study were performed at 100 bar and strictly in, the range of application of the results is consequently for pressures in the surrounding this pressure. It would thus be interesting to complete this study with experiments at a few mbar, 400 bar and 2000 bar to quantify the effect of pressure.

Isotopic fractionations below 30% conversion

The isotopic fractionation model was validated only for conversions in 1,2,4-trimethylbenzene above 30%. Indeed, according to the charge (≈ 50 mg) of 1,2,4-trimethylbenzene pyrolysed during each experiment, the corresponding methane generated at conversions lower than 30% was less than 160 μmol . Despite using small sampling ampoules, the concentration of methane in such experiments was still very low due to the much larger quantity of nitrogen, the inert gas used during the experiments. Sampling with the syringe before injection into the GC-irMS, then induced the quantity of methane to be not sufficient for obtaining a reproducible value below 30% conversion.

It would thus be interesting to perform new experiments below 30% conversion with a larger amount of starting material in order to validate the isotopic fractionation model on the whole range of conversion.

Models for alkylated aromatics

Once all models will be fully constrained for 1,2,4-trimethylbenzene (methylated aromatic), it would be interesting to extend the approach to alkylated aromatics. Indeed, some experimental data for 2-ethyltoluene has already been obtained during this study (*c.f.* Appendix I). On the theoretical aspect, methylated aromatics being products of the thermal degradation of alkylated aromatics, the extension will require to add the reactions specific to the presence of the ethyl moiety of 2-ethyltoluene to the models for 1,2,4-trimethylbenzene. To quantify the influence of this ethyl group, additional experiments with ethylbenzene have also been performed during this study (*c.f.* Appendix I).

Precise comparison of the kinetic isotope effects for methylaromatics and alkylaromatics

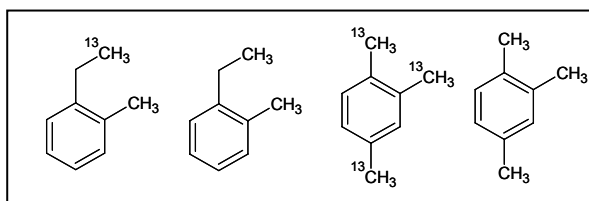
As mentioned above in the conclusions, this study seemed to show a similarity of kinetic isotope effects for the formation of methane during thermal cracking of *n*-alkanes and

methylaromatics. A precise comparison of the kinetic isotope effect for methylaromatics and alkylaromatics could be performed. To constrain the accuracy of this comparison, we imagined a way to fix the other free parameter: the precursor isotope effect. Indeed, this latter effect depending on the formation history of the molecule it can be adjusted by controlling the initial carbon isotope composition of the moieties that are of interest in terms of gas generation. Such control is obviously impossible for natural products. Moreover, it is far to be easy with commercial compounds for which the chemicals and the pathway from which they have been synthesized are often not disclosed. However, it can be done by controlling the synthesis route of the model compounds. We thus synthesized new 1,2,4-trimethylbenzene and 2-ethyltoluene (*c.f.* Appendix II for experimental conditions of the syntheses).

As demonstrated in this study, precursors of the methane generated during thermal cracking of 1,2,4-trimethylbenzene are the methyl moieties. New, 1,2,4-trimethylbenzene was thus synthesized so the initial carbon isotope composition of the methyl groups could be controlled. In fact, ^{13}C -labelled and unlabelled 1,2,4-trimethylbenzene were synthesized in order to adjust the magnitude of the 'precursor effect' to any desired $\delta^{13}\text{C}_p$ with an appropriate mixture of the labelled and the unlabelled component.

Regarding 2-ethyltoluene no mechanistic model was established during this study. To confirm ethane would originate in majority from the ethyl group, the same way methane was originating from the methyl groups of 1,2,4-trimethylbenzene, 2-ethyltoluene with a ^{13}C -label in the β -position was synthesized. This compound will also enable discrimination between the contributions to methane generation of the β -scission in the ethyl group and the α -scission in the methyl group. Unlabelled 2-ethyltoluene was also synthesized to be able to adjust the magnitude of $\delta^{13}\text{C}_p$ of the generated gases to any desired range.

The 4 types of synthesized compounds are represented below:



The precursor isotope effects for natural products

Domains of variations observed in this study for $\delta^{13}\text{C}_{\text{CH}_4}$ should be considered with precaution since they have been obtained on commercial compounds whose synthetic history,

and consequently precursor isotope effect, was different than that of natural compounds. An interesting approach would be to determine the extent of the ‘true’ precursor isotope effect *i.e.* the one of natural products.

We concluded on a rough similarity of the kinetic isotope effects for the formation of methane during thermal cracking of some chemical classes of molecules (*n*-alkanes and methylaromatics). We could also postulate the constant character of such effect whatever the genetic history within the same chemical class, since the kinetic isotope effect is due to the relative shift between the breaking kinetics of ^{12}C - ^{12}C and ^{12}C - ^{13}C bonds. The kinetic isotope effect being determined for a given chemical class of compounds using the approach presented in this study, the calibration of an isotopic fractionation model for the pyrolysis of natural products would then enable the precise calibration of their precursor isotope effect.

This work presented a fastidious but necessary method for the characterization of the kinetic and precursor isotope effects for analytically well identified fractions such as C_{14} -methylated monoaromatics. Since the determination of these parameters for all unstable chemical classes found in oil is necessary, this approach could be used for other analytically well identified fractions such as C_{14} -alkylated monoaromatics. In the case of analytically more challenging fractions such as resins and asphaltenes, a more global approach similar to that presented by Lorant et al (2000) for late primary gas could be used. Overall, it can be expected that the combination of these two types of approaches will enable the elaboration of a kinetic model predicting the individual $\delta^{13}\text{C}$ of natural gases generated during thermal cracking of oil in sedimentary basins.

APPENDIX I:

Experimental data

1. 1,2,4-trimethylbenzene

T (°C)	t (h)	Conversion (%)	residual reactant	Gases (C ₁ -C ₄ + H ₂)	C ₆ -C ₁₃ in n-C ₅	C ₁₄₊ in n-C ₅	DCM fraction	estimated residue	mass balance
425	3	2.7	972.5	0.2	2.7	6.6	18.0	0.0	1000.0
425	9.5	3.0	970.1	0.5	3.0	9.4	16.8	0.0	999.8
395	144	4.7	945.5	2.5	7.0	25.6	18.7	0.0	999.3
395	432	22.2	771.0	27.8	62.5	101.0	20.8	16.9	993.9
425	120	30.9	681.0	43.2	90.9	114.3	20.2	50.4	989.0
450	50	46.5	515.6	66.5	172.1	103.2	20.0	122.6	980.2
450	72	62.3	350.5	102.7	231.7	91.1	19.9	204.1	982.2
450	144	76.2	210.7	146.7	268.1	79.1	20.9	274.5	989.4
450	195	86.7	113.5	167.5	297.2	63.3	20.5	338.0	982.1
450	432	97.4	17.6	212.5	272.3	49.8	21.4	426.4	986.2

Mass-balances of molecular fractions recovered from thermal cracking of 1,2,4-trimethylbenzene at 100 bar for various temperatures (ratios in mg/g of initial reactant).

Conv. (%)	2.7	3.0	4.7	22.2	30.9	46.5	62.3	76.2	86.7	97.4
Products										
CH ₄	0.7	1.5	15.8	195.8	302.3	470.3	733.5	1056.0	1209.0	1552.5
C ₂ H ₆	0.4	1.2	1.3	6.0	10.3	13.2	17.6	21.6	23.6	20.4
H ₂	0.4	0.6	3.0	12.0	16.8	27.0	31.2	27.0	26.4	21.0
Xylenes	0.8	1.5	4.9	64.8	95.7	177.2	228.4	243.7	241.3	142.4
Toluene	0.0	0.0	0.0	1.4	2.6	14.6	33.0	62.8	99.7	158.0
Benzene	0.0	0.0	0.0	0.0	0.0	0.4	1.5	3.1	8.5	37.0
Dimers238	0.9	1.9	3.3	3.3	3.0	1.6	1.0	0.6	0.5	0.2
Dimers224	0.1	0.3	3.5	3.7	3.4	2.8	2.0	1.3	1.1	0.9
Dimers210	0.0	0.0	0.0	0.4	0.7	1.0	0.8	0.6	0.4	0.1
Dimers196	0.0	0.0	0.0	0.3	0.5	1.1	1.7	1.9	2.2	2.6
Dimers182	0.0	0.0	0.0	0.1	0.1	0.2	0.2	0.4	0.6	1.7
Triaro206	0.0	0.2	0.9	4.1	4.2	3.9	2.5	1.7	1.1	0.4
Triaro192	0.0	0.0	0.0	4.3	5.2	6.0	4.4	3.2	2.0	1.0
Triaro178	0.0	0.0	0.0	1.9	3.1	5.2	5.2	4.4	3.2	2.1

Molar yields of individually quantified species generated from thermal cracking of 1,2,4-trimethylbenzene at 100 bar for various conversions (ratios in mmol/mol of initial reactant).

T (°C)	t (h)	H ₂	CH ₄	C ₂ H ₆
395	72	0.0	1.3	0.1
395	144	0.1	2.1	0.3
395	216	0.1	5.9	0.7
395	312	0.2	17.0	1.1
395	432	0.2	26.1	1.5
395	550	0.3	34.5	1.9
395	648	0.2	43.2	2.2
425	3	0.0	0.1	0.1
425	9.5	0.0	0.2	0.3
425	72	0.2	22.8	1.9
425	120	0.3	40.3	2.6
425	216	0.4	67.1	3.4
425	648	0.3	139.4	5.8
450	24	0.3	23.9	1.5
450	50	0.5	62.7	3.3
450	72	0.5	97.8	4.4
450	144	0.5	140.8	5.4
450	195	0.4	161.2	5.9
450	336	0.4	191.2	5.5
450	432	0.4	207.0	5.1
450	648	0.3	229.5	4.1
475	3	0.2	4.9	0.5
475	9	0.5	51.9	3.0
475	24	0.6	117.7	4.8
475	72	0.5	190.1	5.5
475	133	0.5	225.9	5.5

Experimental yields of individual gases generated from thermal cracking of 1,2,4-trimethylbenzene at 100 bar at all pyrolysis conditions (ratios in mg/g of initial reactant).

T (°C)	t (h)	$\delta^{13}\text{C}$ of CH_4	$\delta^{13}\text{C}$ of $\text{C}_6\text{-C}_{13}$ in $n\text{-C}_5$	$\delta^{13}\text{C}$ of C_{14+} in $n\text{-C}_5$	$\delta^{13}\text{C}$ of DCM fraction	$\delta^{13}\text{C}$ of residue	^{13}C Balance (%)
395	144	ND	-28.8	-29.7	-27.9	ND	101.0
395	432	ND	-28.7	-29.5	-28.5	ND	101.1
425	3	ND	-28.8	-30.5	-27.5	ND	101.0
425	9.5	ND	-28.7	-30.2	-27.5	ND	101.0
425	120	ND	-28.6	-29.2	-27.7	ND	101.3
425	216	-35.0	ND	ND	ND	ND	ND
425	648	-33.8	ND	ND	ND	ND	ND
450	50	-35.0	-27.9	-29.4	-28.2	ND	99.3
450	72	-34.8	-27.4	-28.5	-27.6	-30.0	99.0
450	144	-34.0	-27.5	-27.7	-27.8	-29.9	99.5
450	195	-33.6	-27.4	-27.4	-27.6	-29.7	98.7
450	336	-33.1	ND	ND	ND	ND	ND
450	432	-32.8	ND	-28.5	-27.6	-29.6	99.6
450	648	-32.5	ND	ND	ND	ND	ND
475	9	-35.0	ND	ND	ND	ND	ND
475	24	-34.5	ND	ND	ND	ND	ND
475	72	-33.2	ND	ND	ND	ND	ND

Stable carbon isotope compositions ($\delta^{13}\text{C}$ in ‰) of fractions recovered from thermal cracking of 1,2,4-trimethylbenzene at 100 bar. The initial $\delta^{13}\text{C}$ of the reactant 1,2,4-trimethylbenzene was measured at - 29.6‰. All $\delta^{13}\text{C}$ are given with a precision of ± 0.6 ‰, the maximum observed standard deviation being 0.3‰.

2. 2-ethyltoluene

T (°C)	t (h)	Conversion (%)	residual reactant	Gases ($\text{C}_1\text{-C}_4 + \text{H}_2$)	$\text{C}_6\text{-C}_{13}$ in $n\text{-C}_5$	C_{14+} in $n\text{-C}_5$	DCM fraction	estimated residue	mass balance
425	3	3.5	972.1	2.5	18.9	3.2	13.0	0.0	1009.7
450	1	3.8	967.5	2.3	23.5	3.6	11.0	0.0	1007.9
425	9.5	4.9	958.7	3.6	33.3	5.1	10.4	0.0	1011.1
395	144	10.6	894.2	8.6	51.8	29.1	16.5	0.0	1000.2
450	10	24.0	759.7	21.1	139.3	62.3	17.7	0.0	1000.1
395	432	45.2	548.1	43.2	254.9	111.0	21.1	21.7	994.3
425	120	53.9	460.9	64.0	303.1	118.0	18.3	35.7	994.8
450	50	72.2	278.3	94.7	396.3	119.0	18.4	93.3	999.7
450	72	81.1	188.9	125.5	423.7	111.3	14.0	136.6	999.2
450	195	97.4	26.0	191.0	422.8	84.5	13.5	262.2	992.8

Mass-balances of molecular fractions recovered from thermal cracking of 2-ethyltoluene at 100 bar for various temperatures (ratios in mg/g of initial reactant).

T (°C)	t (h)	H ₂	CH ₄	C ₂ H ₆
395	72	0.1	2.1	2.7
395	144	0.1	3.3	3.7
395	216	0.2	7.6	7.7
395	312	0.3	14.7	10.3
395	432	0.4	23.4	17.4
395	550	0.5	31.4	22.6
395	648	0.6	38.6	27.6
425	3	0.0	0.2	0.6
425	9.5	0.1	1.2	1.2
425	72	0.4	22.8	15.1
425	120	0.5	36.5	24.6
425	216	0.7	61.3	39.2
425	648	0.7	105.3	56.5
450	1	0.0	0.2	0.7
450	10	0.3	10.7	9.1
450	24	0.5	28.1	17.7
450	50	0.7	54.6	35.7
450	72	0.7	73.4	43.4
450	144	0.6	105.5	53.9
450	195	0.6	127.4	58.4
450	336	0.5	149.9	57.7
450	648	0.4	184.3	48.1
475	3	0.3	11.7	8.6
475	9	0.7	49.2	29.0
475	24	0.7	91.1	50.3
475	72	0.5	166.8	55.7
475	105	0.4	175.4	53.8

Experimental yields of main gases generated from thermal cracking of 2-ethyltoluene at 100 bar at all pyrolysis conditions (ratios in mg/g of initial reactant).

T (°C)	t (h)	$\delta^{13}\text{C}$ of CH_4	$\delta^{13}\text{C}$ of C_2H_6	$\delta^{13}\text{C}$ of $\text{C}_6\text{-C}_{13}$ in $n\text{-C}_5$	$\delta^{13}\text{C}$ of C_{14+} in $n\text{-C}_5$	$\delta^{13}\text{C}$ of DCM fraction	$\delta^{13}\text{C}$ of residue	^{13}C Balance (%)
395	144	ND	ND	-27.3	-29.4	-27.5	ND	100.5
395	432	ND	ND	-26.7	-28.8	-28.4	ND	100.0
425	3	ND	ND	-27.5	ND	-27.5	ND	101.4
425	9.5	ND	ND	-27.4	ND	-27.5	ND	101.6
425	120	ND	ND	-26.5	-28.8	-28.5	ND	99.9
425	648	-35.6	-31.4	ND	ND	ND	ND	ND
450	1	ND	ND	-27.6	ND	-27.4	ND	101.2
450	10	ND	ND	-27.0	-29.4	-27.2	ND	100.5
450	50	-39.0	-34.1	-26.5	-28.2	-27.9	-29.5	99.9
450	72	ND	ND	-26.5	-28.2	-27.9	-29.1	ND
450	144	-35.9	-30.9	ND	ND	ND	ND	ND
450	195	ND	ND	-26.5	-26.6	-27.7	-28.4	ND
450	432	-34.4	-28.5	ND	ND	ND	ND	ND
450	648	-33.8	-26.6	ND	ND	ND	ND	ND
475	9	-38.6	-33.7	ND	ND	ND	ND	ND
475	24	-36.4	-31.6	ND	ND	ND	ND	ND
475	72	-34.5	-28.6	ND	ND	ND	ND	ND
475	105	-33.9	-27.6	ND	ND	ND	ND	ND

Stable carbon isotope compositions ($\delta^{13}\text{C}$ in ‰) of fractions recovered from thermal cracking of 2-ethyltoluene at 100 bar. The initial $\delta^{13}\text{C}$ of the reactant 2-ethyltoluene was measured at -28.9‰ . All $\delta^{13}\text{C}$ are given with a precision of $\pm 0.6\text{‰}$, the maximum observed standard deviation being 0.3‰ .

3. Ethylbenzene

T (°C)	t (h)	H_2	CH_4	C_2H_6
475	3	0.2	7.0	6.8
475	9	0.3	34.0	18.9
475	24	0.4	59.5	29.2
475	72	0.5	98.6	39.0
475	105	0.6	116.2	39.7

Experimental yields of main gases generated from thermal cracking of ethylbenzene at 100 bar and 475 °C (ratios in mg/g of initial reactant).

T (°C)	t (h)	$\delta^{13}\text{C}$ of CH_4	$\delta^{13}\text{C}$ of C_2H_6
475	9	-38.7	-30.3
475	24	-37.3	-28.5
475	72	-36.0	-25.4
475	105	-35.4	-24.1

Stable carbon isotope compositions ($\delta^{13}\text{C}$ in ‰) of methane and ethane generated from thermal cracking of ethylbenzene at 100 bar and 475 °C. $\delta^{13}\text{C}$ are given with a precision of $\pm 0.6\text{‰}$, the maximum observed standard deviation being 0.3‰ .

APPENDIX II:

Synthesis of new model compounds

Syntheses were performed in Münster Universität, Germany, under the supervision of Professor Jan Andersson.

1. Catalysed synthesis of substituted aromatic hydrocarbons

The best synthesis pathway for such compounds involved a cross-coupling reaction of an aromatic halide with a Grignard reagent. However, such reaction is induced by a variety of transition metal halides (Kharasch and Reinmuth, 1954; Tamura and Kochi, 1971). Those reactions without the presence of a catalyst are seldom employed in synthetic chemistry, due to the formation of homo coupling products and a variety of other side compounds produced in substantial amounts (Tamao et al., 1972).

Tamura and Kochi (1971) demonstrated that "soluble catalysts" consisting of silver, copper or iron in tetrahydrofuran (THF) were extremely effective for coupling Grignard reagents with alkyl halides; silver being useful for homo coupling and copper or iron for cross-coupling (*e.g.* Fürstner et al., 2002; Martin and Fürstner, 2004; Shinokubo and Oshima, 2004), especially the iron catalyst, being only for alkenyl halides. The influence of the catalyst on catalysed cross-coupling reactions was also widely studied with palladium (*e.g.* Merrill and Negishi, 1974; Kataoka et al., 2002; Milstein and Stille, 1979; Hatanaka and Hiyama, 1990; Saa et al., 1992; Vedejs et al., 1992; Rai et al., 1995; Roshchin et al., 1995) and nickel complexes (*e.g.* Tamao et al., 1972; Hayashi et al., 1981; Eapen et al., 1984; Yuan and Scott, 1991; Percec et al., 1995). Moreover, Π -allylnickel compounds (Corey and Semmelhack, 1967) and lithium diorganocuprates (Corey and Posner, 1967 and 1968; Withesides et al., 1969) were proven to be excellent reagents in terms of coupling organometallic compounds with organic halides. Palladium complexes were shown to be much inferior to nickel in such related reactions (Klingstedt and Fredj, 1983).

2. Synthesis pathways

a) 1,2,4-trimethylbenzenes

1,2,4-trimethylbenzenes were prepared from 1,2,4-trichlorobenzene using a method (Eapen et al., 1984) based on Tamao et al (1972) involving the selective cross-coupling of a Grignard reagent with an aryl halide, catalyzed by a nickel-phosphine complex. This reaction is enabled by two properties of nickel-phosphine complexes. First, as shown with reactions (b) and (d) on Figure A.II.1, two organic groups of the nickel-phosphine complex are released

by the action of an organic halide to undergo coupling, while the complex itself is converted to the corresponding (halo)(organo)nickel complex (Uchino et al., 1970; Miller et al., 1968; Miller and Kuhlman, 1971; Dobson et al., 1971). In addition, such a halogen-nickel bond readily reacts with a Grignard reagent to form the corresponding (organo) nickel bond (Chatt and Shaw, 1960; Yamazaki et al., 1966; Moss and Shaw, 1966; Miller et al., 1970; Rausch and Tibbetts, 1970) suggesting the catalytic ability of dihalodiphosphenickel complex for the coupling of a Grignard reagent with an organic halide (Tamao et al., 1972). Indeed, the dihalodiphosphenickel L_2NiX_2 reacts with the Grignard reagent $RMgX'$ to form the diorganonickel intermediate complex (I) which is subsequently converted into the (halo)-(organo) nickel complex (II) by reacting with the organic halide $R'X''$. Successive reactions of (II) with the Grignard reagent forms a new diorgano complex (III) from which the cross-coupling product is released by the attack of the organic halide and thereby (II) is regenerated to complete the catalytic cycle (Figure A.II.1).

However, neither Tamao et al (1972 and 1976) nor Kumada (1980) who extended the method to organometallic reagents containing lithium, zinc, boron, aluminium and zirconium, worked on substrates containing more than two halogen atoms. Successful studies on the nickel-phosphine complex catalysing cross-coupling of trichlorobenzenes with *n*-alkyl magnesium bromides were reported for the first time by Eapen et al (1984). However, methyl iodide was used instead of a methyl bromide to graft methyl groups in our synthesis. Indeed, methyl bromide is a gaseous reactant and so doing a reaction in solution was much more convenient. The Grignard reagent was prepared first by reaction of methyl iodide with magnesium. Then, this Grignard reagent was reacted with 1,2,4-trichlorobenzene in the presence of a catalytic quantity of [1,3-Bis(diphenylphosphino)propane]dichloronickel(II). This synthesis route is illustrated in Figure A.II.2 for labelled 1,2,4-trimethylbenzene.

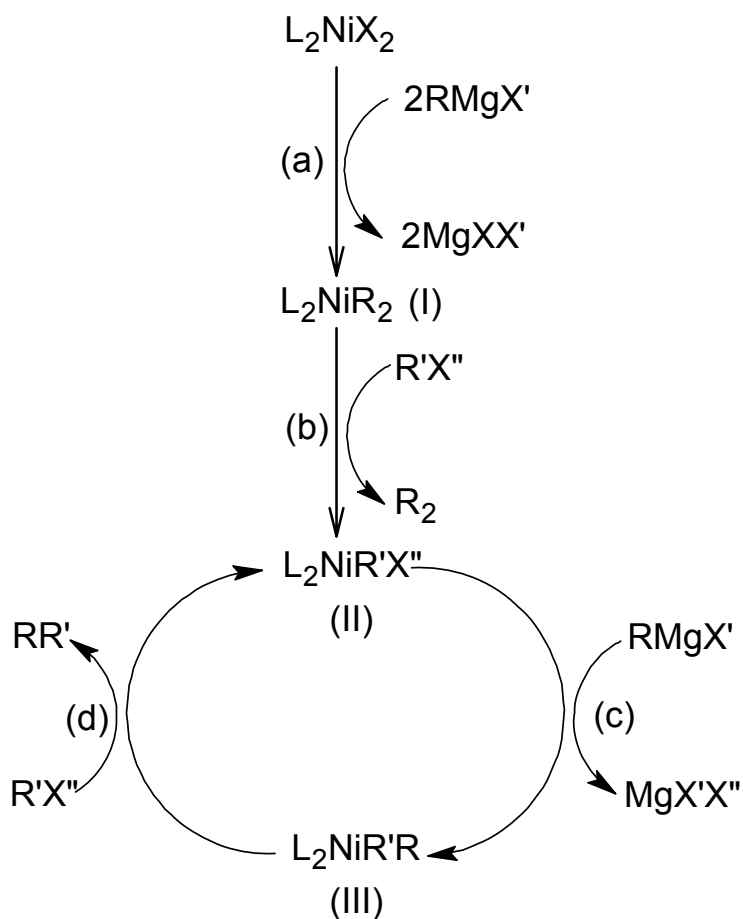


Figure A.II.1. Selective cross-coupling of a Grignard reagent with an aryl halide, catalyzed by a nickel-phosphine complex. After Tamao et al. (1972).

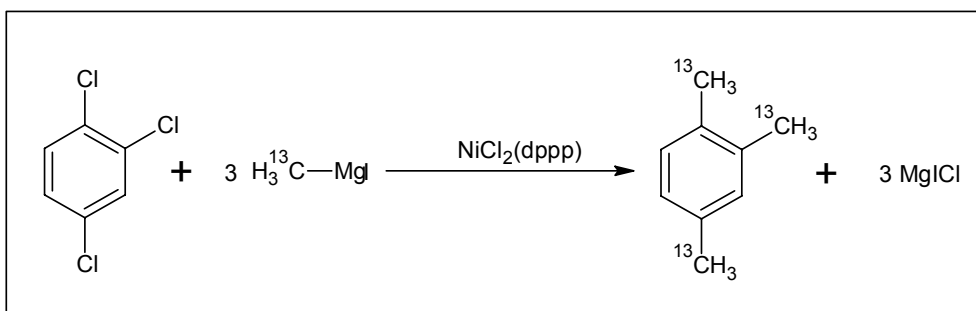


Figure A.II.2. Synthesis route for labelled 1,2,4-trimethylbenzene.

b) 2-Ethyltoluenes

2-ethyltoluenes were prepared from α -chloro-ortho-xylene. However, as the chlorine atom was in a β -position and not in the α -position, the above synthesis method using [1,3-Bis(diphenylphosphino)propane]dichloronickel(II) as a catalyst could not be used.

Moreover, there is a risk when one wants to activate a benzylic position is Wurtz-coupling, leading to "bibenzyl". Indeed, Wurtz-coupling is a prominent side reaction when benzyl chloride is, for example, treated with metallic lithium (Gilman and Gorsich, 1955). To avoid such side reaction, attempts were made to follow the procedure of Gilman et al (1929a and 1929b) by mixing α -chloro-o-xylene with magnesium. However, even cooled down with dry ice, the Grignard reagent obtained immediately reacted with remaining α -chloro-o-xylene in a dimerization reaction to lead to a bibenzyl type bonding. Thus, a "home made" procedure was set up. It was based on the complementary reaction pathway, transforming methyl iodide rather than α -chloro-ortho-xylene, into a Grignard reagent. The reagent was reacted with α -chloro-ortho-xylene. Such synthesis route is illustrated for labelled 2-ethyltoluene in Figure A.II.3.

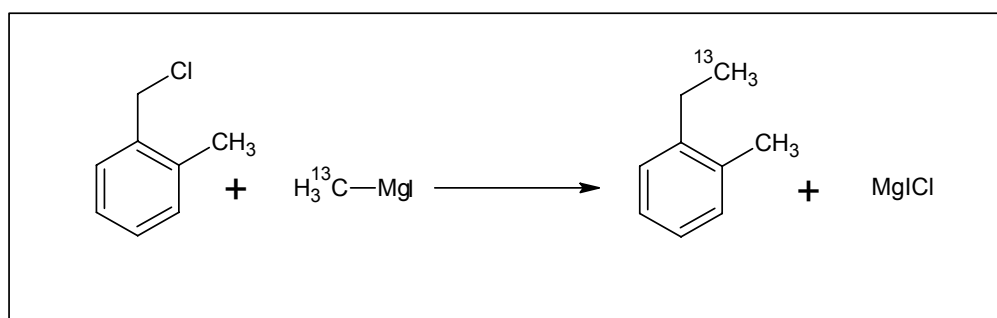


Figure A.II.3. Synthesis route for labelled 2-ethyltoluene.

3. Experimental

a) Reactants and solvents

All reactants were high purity commercial compounds (Table A.II.1). All solvents were analytical grade and redistilled before use.

Name	Formula	Provider	Purity
1,2,4-Trichlorobenzene	C ₆ H ₃ Cl ₃	Sigma-Aldrich	≥99%
Methyl Iodide (¹³ C labelled)	¹³ CH ₃ I	Cambridge Isotope Laboratories, Inc.	99% ¹³ C
Methyl Iodide	CH ₃ I	Acros Organics	99%
Methyl Magnesium Iodide (≈3M in diethylether)	CH ₃ MgI	Fluka	Purum
[1,3-Bis(diphenylphosphino)propane]dichloronickel(II)	C ₂₇ H ₂₆ Cl ₂ NiP ₂	Sigma-Aldrich	-
α -chloro-o-xylene	C ₈ H ₈ Cl	Acros Organics	99%
Magnesium purum for Grignard reaction	Mg	Fluka	≥99.5%

Table A.II.1. Reactants used for the synthesis of labelled and unlabelled compounds.

b) Synthesis of ¹³C-labelled and unlabelled 1,2,4-trimethylbenzenes

The reaction (Figure A.II.2) consisted of the permethylation of 1,2,4-trichlorobenzene, in the presence of a nickel catalyst, by a methylated Grignard reagent.

Labelled and non-labelled compounds were synthesized using the same route replacing labelled methyl iodide with a non-labelled one. The procedure for synthesizing labelled 1,2,4-trimethylbenzene is only reported.

A three-necked flask equipped with a magnetic stirrer, a pressure-equalizing dropping funnel, and a reflux condenser and a nitrogen inlet, was charged with one equivalent (897 mg) of fresh magnesium turnings. The magnesium was dried under a rapid stream of nitrogen with a heat gun. After the flask had cooled down to room temperature, the rate of nitrogen flow was reduced to the minimum and 15 ml of anhydrous diethyl ether was added. Then, 4 ml of a solution of one equivalent of ¹³C-labelled methyl iodide (5.20 g) in anhydrous ether was added drop wise. When addition was complete, the mixture was stirred at room temperature, and within a few minutes an exothermic reaction occurred. The flask was immediately immersed in an ice bath for five minutes. The mixture was then gently refluxed and stirred for 30 minutes and cooled to room temperature.

Meanwhile, another three-necked flask, equipped like the previous one was charged with a catalytic quantity (≈ 20 mg) of dichloro[1,3-bis(diphenylphosphino)propane]nickel (II), 1.86 g of 1,2,4-trichlorobenzene and 8 ml of anhydrous diethyl ether. The Grignard reagent prepared in the first flask was transferred into the dropping funnel and added drop wise while stirring, the mixture being cooled in an ice bath. A note from Tamao et al (1972), advised to use an excess of at least 20% of Grignard reagent in order to compensate loss through undesirable side-reactions.

The nickel complex reacted immediately with the Grignard reagent and the resulting clear-tan reaction mixture, while still stirring, was allowed to warm to room temperature. After stirring for two hours at room temperature, the mixture was gently refluxed and stirred for twenty hours.

It was then cooled in an ice bath and carefully hydrolysed with a 2 mol.L⁻¹ hydrochloric acid solution, the reaction being very exothermic.

The nearly colourless organic layer was separated from the aqueous one. The latter was extracted with two successive portions of diethyl ether. The combined organic layers were then successively washed with water, a saturated solution of sodium hydrogen carbonate and water again. The resulting solution was dried on anhydrous sodium sulphate and filtered.

An aliquot of the obtained solution was analysed by GC-MS. It was revealed that a mixture of the desired compound 1,2,4-trimethylbenzene together with residual reagents and all mono/di methylation isomers was formed through the synthesis procedure. Purification to isolate 1,2,4-trimethylbenzene is reported below.

c) Synthesis of ¹³C-labelled and unlabelled 2-ethyltoluenes

The reaction (Figure A.II.3) was performed to methylate the benzylic position of α -chloro-ortho-xylene with a methylated Grignard reagent synthesized above.

Labelled and non-labelled compounds were synthesized using the same route replacing the labelled methyl iodide with a non-labelled one. The procedure for synthesizing labelled 2-ethyltoluene is only reported.

A three-necked flask equipped with a magnetic stirrer, a pressure-equalizing dropping funnel, and a reflux condenser and a nitrogen inlet, was charged with one equivalent (996 mg) of fresh magnesium turnings. The magnesium was dried under a rapid stream of nitrogen with a heat gun. After the flask has cooled down to room temperature, the rate of nitrogen flow was reduced to the minimum and 16.5 ml of anhydrous diethyl ether were added. Then, 4 ml of a solution of one equivalent of ¹³C-labelled methyl iodide (5.86 g) in anhydrous ether were added drop wise. When addition was complete, the mixture was stirred at room temperature, and within a few minutes an exothermic reaction started. The flask was immediately immersed in an ice bath for five minutes. The mixture was gently refluxed and stirred for thirty minutes and then cooled to room temperature.

Meanwhile, another three-necked flask, equipped like the previous one was charged with 21.1 g of α -chloro-ortho-xylene and 150 ml of anhydrous diethyl ether. This solution was transferred into the dropping funnel of the first three-necked flask and added drop wise to the Grignard reagent solution while stirring and cooling with an ice bath.

Several hours later, when addition was complete, the mixture was allowed to warm to room temperature. After stirring for two hours at room temperature, the mixture was gently refluxed and stirred for twenty hours.

It was then cooled in an ice bath and hydrolysed with a 2 mol.L⁻¹ hydrochloric acid.

The nearly colourless organic layer was separated from the aqueous one. The latter was extracted with two successive portions of diethyl ether. The combined organic layers were then successively washed with water, a saturated solution of sodium hydrogen carbonate and water again. The resulting solution was dried on anhydrous sodium sulphate and filtered.

An aliquot of the obtained solution was analysed by GC-MS. It was revealed that a mixture of the desired compound 2-ethyltoluene together with residual reagents and a compound resulting from the dimerisation reaction of α -chloro-ortho-xylene was obtained through the synthesis procedure. The dimer crystallised at room temperature and was easily removed from other reagents by filtering. Purification to isolate 2-ethyltoluene from α -chloro-ortho-xylene is described below.

d) Purification

Mixtures containing 2-ethyltoluene were obtained in a higher yield than the mixtures containing 1,2,4-trimethylbenzene. The purification process is thus described below for mixtures containing 2-ethyltoluene on which it was elaborated. However, once validated, this process was also used to purify mixtures containing 1,2,4-trimethylbenzene.

Purification of the 2-ethyltoluene from α -chloro-ortho-xylene was performed using liquid chromatography. The chosen stationary phase was silica gel and the solvent pure *n*-pentane. Silica gel was successively washed three times with dichloromethane, left to dry and activated overnight at 80 °C. The glass-column (which had also been dried overnight in an oven) was loaded with approximately 100 g of activated silica. The silica gel was then impregnated with *n*-pentane. Four millilitres of the mixture to purify were carefully deposited at the top of the column before being eluted with *n*-pentane. Fractions collected at the bottom of the column were analysed by gas-chromatography (GC). Three types of fractions were recovered:

- (i) Fractions containing only 2-ethyltoluene from which solvent was gently removed,
- (ii) Fractions still containing a mixture of 2-ethyltoluene and α -chloro-ortho-xylene were then subjected again to the above purification process,
- (iii) Fractions containing only α -chloro-ortho-xylene were not kept.

The following extraction process allowed a complete removal of the chlorine reactant in the mixture. However, a pink-coloured impurity suspected to be an iodine complex was still present along with 2-ethyltoluene (or 1,2,4-trimethylbenzene). This component needs to be removed before further studies can proceed.

APPENDIX III:

References

- Al Darouich, T., Behar, F., Largeau, C., Budzinski, H., 2005. Separation and characterisation of the C₁₅- aromatic fraction of Safaniya crude oil. *Oil and Gas Science and Technology* 60, 681-695.
- Al Darouich, T., 2005. Stabilité thermique de la fraction aromatique de l'huile brute Safaniya (Moyen-Orient) : étude expérimentale, schéma cinétique par classes moléculaires et implications géochimiques. PhD Dissertation, Université Pierre et Marie Curie, Paris, France.
- Al Darouich, T., Behar, F., Largeau, C., 2006a. Thermal cracking of the light aromatic fraction of Safaniya crude oil - experimental study and compositional modelling of molecular classes. *Organic Geochemistry* 37, 1130-1154.
- Al Darouich, T., Behar, F., Largeau, C., 2006b. Pressure effect on the thermal cracking of the light aromatic fraction of Safaniya crude oil – Implications for deep prospects. *Organic Geochemistry* 37, 1154-1169.
- Baronnet, F., Dzierzynski, M., Côme, G.M., Martin, R., Niclaude, M., 1971. The pyrolysis of neopentane at small extents of reaction. *International Journal of Chemical Kinetics* 3, 197-213.
- Barton, B.D., Stein, S.E., 1980. Pyrolysis of alkyl benzenes. Relative stabilities of methyl-substituted benzyl radicals. *Journal of Physical Chemistry* 84(17), 2141-2145.
- Baulch, D.L., Cobos, C.J., Cox, R.A., Frank, P., Hayman, G., Just, Th., Kerr, J.A., Murrells, T., Pilling, M.J., Troe, J., Walker, R.W., Warnatz, J., 1994. Evaluated kinetic data for combustion modelling. Supplement I. *Journal of Physical and Chemical Reference Data* 23, 847-1033.
- Behar, F., Leblond, C., Saint-Paul, C., 1989. Analyse quantitative des effluents de pyrolyse en milieu ouvert et fermé. *Revue de l'Institut Français du Pétrole* 44, 387-411.
- Behar, F., Ungerer, P., Kressmann, S., Rudkiewicz, J. L., 1991a. Thermal evolution of crude oils in sedimentary basins: experimental simulation in a confined system and kinetic modelling. *Oil and Gas Science and Technology* 46, 151-181.
- Behar, F., Kressmann, S., Rudkiewicz, J.L., Vandenbroucke, M., 1991b. Experimental simulation in a confined system and kinetic modelling of kerogen and oil cracking. *Organic Geochemistry* 19, 173-189.
- Behar, F., Vandenbroucke, M., 1996. Experimental determination of rate constants of the *n*-C₂₅ thermal cracking at 120, 400, and 800 bar: Implications for the high pressure/high temperature prospects. *Energy and Fuels* 10, 932-940.

- Behar, F., Budzinski, H., Vandenbroucke, M., Tang, Y., 1999. Methane Generation from Oil Cracking: Kinetics of 9-Methylphenanthrene Cracking and Comparison with Other Pure Compounds and Oil Fractions. *Energy and Fuels* 13, 471-481.
- Behar, F., Lorant, F., Budzinski, H., Desavis, E., 2002. Thermal stability of alkylaromatics in natural systems: Kinetics of thermal decomposition of dodecylbenzene. *Energy and Fuels* 16, 831-841.
- Behar, F., Lorant, F., Lewan, M., 2008a. Role of NSO compounds during primary cracking of a Type II kerogen and a Type III lignite. *Organic Geochemistry* 39, 1-22.
- Behar, F., Lorant, F., Mazeas, L., 2008b. Elaboration of a new compositional kinetic schema for oil cracking. *Organic Geochemistry* 39, 764-782.
- Berkaloff, C., Casadevall, E., Largeau, C., Metzger, P., Peracca, S., Virlet, J., 1983. The resistant biopolymer of the walls of the hydrocarbon-rich alga *Botryococcus braunii*. *Photochemistry* 22, 389-397.
- Berner, U., Faber, E., Stahl, W., 1992. Mathematical simulation of the carbon isotopic fractionations in coals and related methane. *Chemical Geology* 94, 315-319.
- Berner, U., Faber, E., Scheeder, G., Panten, D., 1995. Primary cracking of algal and land plant kerogens: kinetic modeling of kerogen and oil cracking. *Chemical Geology* 126, 233-245.
- Berner, U., Faber, E., 1996. Empirical carbon isotope/maturity relationships for gases from algal kerogens and terrigenous organic matter, based on dry, open-system pyrolysis. *Organic Geochemistry* 24, 947-955.
- Bhore, N.A., Klein, M.T., Bischoff, K.B., 1990. The Delplot Technique: A New Method for Reaction Pathway Analysis. *Industrial and Engineering Chemistry Research* 29, 313-316.
- Bigeleisen, J., Mayer, M.G., 1947. Calculation of equilibrium constants for isotopic exchange reactions. *Journal of Chemical Physics* 15, 261-267.
- Bigeleisen, J., 1949. The relative reaction velocities of isotopic molecules. *Journal of Chemical Physics* 17(8), 675-678.
- Billaud, F., Ajot, H., Freund, E., 1983. Unité micropilote pour l'étude de charges de vapocraquage. Exemple d'un mélange de normales paraffines. *Revue de l'Institut Français du Pétrole* 38(6), 763-781.
- Bjørøy, M., Hall, K., Gillyon, P., Jumeau, J., 1991. Carbon isotope variations in *n*-alkanes and isoprenoids of whole oils. *Chemical Geology* 93, 13-20.
- Blades, H., Blades, A.T., Steacie, E.W.R., 1954. The kinetics of the Pyrolysis of Toluene. *Canadian Journal of Chemistry* 32, 298-311.

- Bonnier, J.M., Gaudemaris, G., 1962. Stabilité thermique des hydrocarbures *Revue de l'Institut Français du Pétrole* 17(6), 852-882.
- Botao, G., Casanova, G., 1964. Separation factors in isotopic phase equilibria. In: Craig, H., Miller, S.L., Wasserburg, G.J. (Eds.). *Isotopic and Cosmic Chemistry*, North-Holland Publishing, Amsterdam, pp. 16-33.
- Bounaceur, R., Scacchi, G., Marquaire, P.M., 2000. Mechanistic Modeling of the Thermal Cracking of Tetralin. *Industrial and Engineering Chemistry Research* 39, 4152-4165.
- Bounaceur, R., Warth, V., Marquaire, P.M., Scacchi, G., Dominé, F., Dessort, D., Pradier, B., Brévar, O., 2002a. Modeling of hydrocarbons pyrolysis at low temperature. Automatic generation of free radicals mechanisms. *Journal of Analytical and Applied Pyrolysis* 64, 103-122.
- Bounaceur, R., Scacchi, G., Marquaire, P.M., Dominé, F., Brévar, O., Dessort, D., Pradier, B., 2002b. Inhibiting effect of tetralin on the pyrolytic decomposition of hexadecane. Comparison with toluene. *Industrial and Engineering Chemistry Research* 41, 4689-4701.
- Bounaceur, R., Da Costa, I., Fournet, R., Billaud, F., Battin-Leclerc, F., 2005. Experimental and modeling study of the oxidation of toluene. *International Journal of Chemical Kinetics* 37(1), 25-49.
- Brand, U., Hippler, H., Lindemann, L., Troe, J., 1990. C-C and C-H bond splits of laser-excited aromatic molecules. 1. Specific and thermally averaged rate constants. *Journal of Physical Chemistry* 94, 6305-6316.
- Brand, W.A., Tegtmeier, A.R., Hilkert, A.W., 1994. Compound-specific isotope analysis: extending toward $^{15}\text{N}/^{14}\text{N}$ and $^{18}\text{O}/^{16}\text{O}$. *Organic Geochemistry* 21, 585-594.
- Braun, R.L., Burnham, A.K., 1990. Mathematical model of oil generation, degradation and expulsion. *Energy and Fuels* 4, 132-146.
- Braun, R.L., Burnham, A.K., 1992. PMOD: a flexible model of oil and gas generation, cracking and expulsion. *Organic Geochemistry* 19, 161-172.
- Brioukov, M.G., Park, J., Lin, M.C., 1999. Kinetic Modeling of Benzene Decomposition Near 1000 K: The Effect of Toluene Impurity. *International Journal of Chemical Kinetics* 31(8), 577-582.
- Brooks, C.T., Cummins, C.P.R., Peacock, S.J., 1971. Pyrolysis of Toluene Using a Static System. *Transactions of the Faraday Society* 67, 3265-3274.
- Brooks, C.T., Peacock, S.J., Reuben, B.G., 1979. Pyrolysis of benzene. *Journal of the Chemical Society Faraday Transactions I*. 75, 652-662.

- Brooks, C.T., Peacock, S.J., Reuben, B.G., 1982. Pyrolysis of ethylbenzene. *Journal of the Chemical Society Faraday Transactions I.* 78, 3187-3202.
- Brouwer, L.D., Mueller-Markgraf, W., Troe, J., 1988. Thermal decomposition of toluene: a comparison of thermal and laser-photochemical activation experiments. *Journal of Physical Chemistry* 92(17), 4905-4914.
- Bruinsma, S.L.O., Geertsma, R.S., Moulijn, P.K., 1988. Gas phase pyrolysis of coal-related aromatic compounds in a coiled tube flow reactor. I: Benzene and derivatives. *Fuel* 67, 327-333.
- Burgoyne, T.W., Hayes, J.M., 1998. Quantitative production of H₂ by pyrolysis of gas chromatographic effluents. *Analytical Chemistry* 70, 5136-5141.
- Burklé-Vitzthum, V., 2001. Etude expérimentale et modélisation cinétique de la pyrolyse d'hydrocarbures présents dans les pétroles. Extrapolation aux conditions géologiques. PhD Dissertation, Institut National Polytechnique de Lorraine, Nancy, France.
- Burklé-Vitzthum, V., Michels, R., Scacchi, G., Marquaire, P.M., 2003. Mechanistic Modeling of the Thermal Cracking of Decylbenzene. Application to the Prediction of Its Thermal Stability at Geological Temperatures. *Industrial and Engineering Chemistry Research* 42, 5791-5808.
- Burklé-Vitzthum, V., Michels, R., Scacchi, G., Marquaire, P.M., Dessort, D., Pradier, B., Brevart, O., 2004. Kinetic effect of alkylaromatics on the thermal stability of hydrocarbons under geological conditions. *Organic Geochemistry* 35, 3-31.
- Burnham, A.K., Sweeney, J.J., 1989. A chemical kinetic model of vitrinite maturation and reflectance. *Geochimica et Cosmochimica Acta* 53, 2649-2657.
- Burnham, A.K., 1991. Oil evolution from a self-purging reactor: kinetics and composition at 2°C/min and 2°C/h. *Energy and Fuels* 5, 205-214.
- Burnham, A.K., Sanborn, R.H., Braun, R.L., 1995. Unravelling the kinetics of petroleum destruction by using 1,2 ¹³C isotopically labelled dopants. *Energy and Fuels* 9, 190-191.
- Burnham, A.K., Gregg, H.R., Ward, R.L., Knauss, K.G., Copenhaver, S.A., Reynolds, J.G., Sanborn, R.H., 1998. Decomposition kinetics and mechanism of *n*-hexadecane-1,2 ¹³C₂ and dodec-1-en-1,2 ¹³C₂ doped in petroleum and *n*-hexadecane. *Geochimica et Cosmochimica Acta* 61, 3725-3737.
- Chatt, J., Shaw, B.L., 1960. Alkyls and Aryls of Transition Metals. Part III. Nickel (II) Derivatives. *Journal of the Chemical Society* 345, 1718-1729.

- Chung, H.M., Sackett, W.M., 1979. Use of stable isotope compositions of pyrolytically derived methane as maturity indices for carbonaceous materials. *Geochimica et Cosmochimica Acta* 43(12), 1979-1988.
- Chung, H.M., Rooney, M.A., Toon, M.B., Claypool, G.E., 1992. Carbon isotope composition of marine crude oils. *The American Association of Petroleum Geologists Bulletin* 76, 1000-1007.
- Clark, W.D., Price, S.J., 1970. Free-radical and molecular processes in the pyrolysis of ethylbenzene. *Canadian Journal of Chemistry* 48 (7), 1059-1064.
- Clayton, C., 1991a. Carbon isotope fractionation during natural gas generation from kerogen. *Marine Petroleum Geology* 8, 232-240.
- Clayton, C., 1991b. Effect of maturity on carbon isotope ratios of oils and condensates. *Organic Geochemistry* 17, 887-899.
- Clayton, C., Bjorøy, M., 1994. Effect of maturity on $^{13}\text{C}/^{12}\text{C}$ ratios of individual compounds in North-Sea oils. *Organic Geochemistry* 21, 737-750.
- Corey, E.J., Semmelhack, M.F., 1967. Organonickel Compounds as Reagents for Selective Carbon-Carbon Bond Formation between Unlike Groups. *Journal of the American Chemical Society* 89(11), 2755-2757.
- Corey, E.J., Posner, G.H., 1967. Selective Formation of Carbon-Carbon Bonds between unlike Groups Using Organocopper Reagents. *Journal of the American Chemical Society* 89(15), 3911-3912.
- Corey, E.J., Posner, G.H., 1968. Carbon-Carbon Bond Formation by Selective Coupling of *n*-Alkylcopper Reagents with Organic Halides. *Journal of the American Chemical Society* 90(20), 5615-5616.
- Craig, H., 1957. Isotopic standards for carbon and oxygen and correction factors for mass-spectrometric analysis of carbon dioxide. *Geochimica et Cosmochimica Acta* 12, 133-149.
- Cramer, B., Krooss, B.M., Littke, R., 1998. Modelling isotope fractionation during primary cracking of natural gas: a reaction kinetic approach. *Chemical Geology* 149, 235-250.
- Cramer, B., Faber, E., Gerling, P., Krooss, B.M., 2001. Reaction Kinetics of Stable Carbon Isotopes in Natural Gas-Insights from Dry, Open System Pyrolysis Experiments. *Energy and Fuels* 15, 517-532.
- Cramer, B., 2004. Methane generation from coal during open system pyrolysis investigated by isotope specific, Gaussian distributed reaction kinetics. *Organic Geochemistry* 35, 379-392.

- Crowne, C.W.P., Grigulis, V.J., Throssell, J.J., 1969. Pyrolysis of ethylbenzene by the toluene carrier method. *Transactions of the Faraday Society* 65, 1051.
- Dartiguelongue, C., 2006. Réactivité thermique des aromatiques soufrés dans les pétroles. Etude expérimentale et cinétique. PhD Dissertation, Université Bordeaux I, Bordeaux, France.
- Dartiguelongue, C., Behar, F., Budzinski, H., Scacchi, G., Marquaire, P.M., 2006. Thermal stability of dibenzothiophene in closed system pyrolysis: Experimental study and kinetic modelling. *Organic Geochemistry* 37, 98-116.
- Davis, H.G., 1983. Rate of formation of toluene from ethylbenzene. *International Journal of Chemical Kinetics* 15(5), 469-474.
- Dawson, D., Grice, K., Alexander, R., Edwards, D., 2007. Evaluation of the source and maturity of sedimentary organic matter from the Vulcan Sub-basin (Timor Sea) using stable hydrogen isotope ratios of individual hydrocarbons. *Organic Geochemistry* 38, 1015-1038.
- De Bruin, T. J. M., Lorant, F., Toulhoat, H., Goddard, W. A. III., 2004. Reaction Kinetics of a Selected Number of Elementary Processes Involved in the Thermal Decomposition of 9-Methylphenanthrene Using Density Functional Theory. *Journal of Physical Chemistry A* 108(46), 10302-10310.
- De Leeuw, J.W., Largeau, C., 1993. A review of macromolecular organic compounds that comprise living organisms and their role in kerogen, coal and petroleum formation. In: Engel, M.H., Macko, S.A. (Eds.), *Organic Geochemistry*, Plenum Publishing Group, New York, pp. 23-72.
- Demaison, G.J., Moore, G.T., 1980. Anoxic Environments and Oil Source Bed Genesis. *The American Association of Petroleum Geologists Bulletin* 64, 1179-1209.
- Derenne, S., Largeau, C., Casadevall, E., Berkaloff, C., Rousseau, B., 1991. Chemical evidence of kerogen formation in source rocks and oil shales *via* selective preservation of thin resistant outer walls of microalgae: origin of ultralaminae. *Geochimica et Cosmochimica Acta*, 55, 1041-1050.
- Dieckmann, V., Horsfield, B., Schenk, H.J., 2000. Heating rate dependency of petroleum-forming reactions: implications for compositional kinetic prediction. *Organic Geochemistry* 31, 1333-1348.
- Dobson, J., Miller, R.G., Wiggen, J.P., 1971. Synthesis of a Nickel Heterocycle. *Journal of the American Chemical Society* 93(2), 554-556.

- Dominé, F., 1989. Kinetics of hexane pyrolysis at very high pressure. 1. Experimental study. *Energy and Fuels* 3, 89-96.
- Dominé, F., Marquaire, P.M., Muller, C., Côme, G.M., 1990. Kinetics of Hexane Pyrolysis at Very High Pressure. 2: Computer Modeling. *Energy and Fuels* 4, 2-10.
- Dominé, F., 1991. High pressure pyrolysis of *n*-hexane, 2-4 dimethylpentane and 1-phenylbutane. Is pressure an important geochemical parameter ? *Organic Geochemistry* 17, 619-634.
- Dominé, F., Enguehard, F., 1992. Kinetics of hexane pyrolysis at very high pressure. 3. Application to geochemical modelling. *Organic Geochemistry* 18, 41-49.
- Dominé, F., Dessort, D., Brevart, O., 1998. Towards a new method of geochemical kinetic modelling: implications for the stability of crude oils. *Organic Geochemistry* 28, 597-612.
- Dominé, F., Bounaceur, R., Scacchi, G., Marquaire, P.M., Dessort, D., Pradier, B., Brevart, O., 2002. Up to what temperature is petroleum stable? New insights from a 5200 free radical reactions model. *Organic Geochemistry* 33, 1487-1499.
- Domke, S.B., Pogue, R.F., Van Neer, F.J.R., Smith, C.M., Wojciechowski, B.W., 2001. Investigation of the kinetics of ethylbenzene pyrolysis using a temperature-scanning reactor. *Industrial and Engineering Chemistry Research* 40(25), 5878-5884.
- Doué, F., Guiochon, G., 1968. Etude théorique et expérimentale de la cinétique de décomposition thermique du *n*-hexadecane, de son mécanisme et de la composition du mélange de produits obtenus. *Journal de Chimie Physique et Chimie Biologique* 64, 395-409.
- Durand, B., Espitalié, J., 1973. Evolution de la matière organique au cours de l'enfouissement des sédiments, *Compte Rendu de l'Académie des Sciences* 276, Paris, pp 2253-2256.
- Durand, B., 1980. Sedimentary organic matter and kerogen. Definition and quantitative importance of kerogen. In: Durand, B (Ed), *Kerogen-insoluble organic matter from sedimentary rocks*. Editions Technip, Paris, pp. 13-33.
- Durand B., Monin J.C., 1980. Elemental analysis of kerogen (C, H, O, N, S, Fe). In: Durand, B (Ed), *Kerogen-insoluble organic matter from sedimentary rocks*. Editions Technip, Paris, pp. 113-142.
- Durand, B., 2003. A History of Organic Geochemistry. *Oil and Gas Science and Technology* 58(2), 203-231.
- Eapen, K.C., Dua, S.S, Tamborski, C., 1984. Regiospecific Synthesis of Aromatic Compounds *via* Organometallic Intermediates. 3. *n*-Alkyl-Substituted Benzene. *Journal of Organic Chemistry* 49(3), 478-482.

- Ehleringer, J.R., Hall, A.E., Farquhar, G.D., 1993. Stable isotopes and plant carbon-water relations. Academic Press, San Diego, California.
- Ellis, C., Scott, M.S., Walker, R.W., 2003. Addition of toluene and ethylbenzene to mixture of H₂ and O₂ at 772 K: Part 2: Formation of products and determination of kinetic data for H plus additive and for other elementary reactions involved. *Combustion and Flame* 132, 291-304.
- Errede, L.A., Cassidy, J.P., 1960. The Chemistry of Xylylenes. V. The Formation of Anthracenes *via* Fast Flow Pyrolysis of Toluenes and Related Compounds. *Journal of the American Chemical Society* 82, 3653-3658.
- Errede, L.A., DeMaria, F., 1962. The Chemistry of Xylylenes. XV. The Kinetics of Fast Flow Pyrolysis of *p*-Xylene. *Journal of Physical Chemistry* 66, 2664-2672.
- Faber, E., 1987. Zur Isotopengeochemie gasförmiger Kohlenwasserstoffe. *Erdöl Erdgas Kohle* 103, 210-218.
- Fabuss, B.M., Smith, J.O., Lait, R.I., Borsanyi, A.S., Satterfield, C.N. 1962. Rapid thermal cracking of n-hexadecane at elevated pressures. *Industrial and Engineering Chemistry Research* 1, 293-299.
- Fabuss, B.M., Smith, J.O., Satterfield, C.N., 1964. Thermal cracking of pure saturated hydrocarbons. In: Mc Ketta J. (Ed.), *Advances in Petroleum Chemistry and Refining*. Wiley and Sons, New-York, pp. 156-201.
- Ford, T. J., 1986. Thermal decomposition of hexadecane: reaction mechanism. *Industrial and Engineering Chemistry Research* 25, 240-243.
- Frank, D.J., Sackett, W.M., 1969. Kinetic isotope effects in the thermal cracking of neopentane. *Geochimica et Cosmochimica Acta* 33, 811-820.
- Freeman, K.H., Hayes, J.M., Trendel, J.M., Albrecht, P., 1990. Evidence from carbon isotope measurements for diverse origins of sedimentary hydrocarbons. *Nature* 343, 254-256.
- Freund, H., Olmstead, W.N., 1989. Detailed Chemical Modeling of Butylbenzene Pyrolysis. *International Journal of Chemical Kinetics* 21, 561-574.
- Fürstner, A., Leitner, A., Méndez, M., Krause, H., 2002. Iron-Catalyzed Cross-Coupling Reactions. *Journal of the American Chemical Society* 124(46), 13856-13863.
- Fusetti, L., Behar, F., Bounaceur, R., Marquaire, P.M., Grice, K., Derenne, S., 2009a. New insights into secondary gas generation from oil thermal cracking: methylated monoaromatics. A kinetic approach using 1,2,4-trimethylbenzene. Part I: A free-radical mechanism. *Organic Geochemistry*, *accepted and revision in progress*.

- Fusetti, L., Behar, F., Grice, K., Derenne, S., 2009b. New insights into secondary gas generation from oil thermal cracking: methylated monoaromatics. A kinetic approach using 1,2,4-trimethylbenzene. Part II: A lumped kinetic scheme. *Organic Geochemistry*, *accepted and revision in progress*.
- Fusetti, L., Behar, F., Lorant, F., Grice, K., Derenne, S., 2009c. New insights into secondary gas generation from oil thermal cracking: methylated monoaromatics. A kinetic approach using 1,2,4-trimethylbenzene. Part III: A stable carbon isotope fractionation model. *Submitted to Organic Geochemistry*.
- Galimov, E.M., Posyagin, V.I., Prokhorov, V.S., 1972. Carbon isotope fractionation as a function of temperature in the CH₄-C₂H₆-C₃H₈-C₄H₁₀ system. *Geokhimiya* 8, 977-987.
- Galimov, E.M., Ivlev, A.A., 1973. Thermodynamic isotope effects in organic compounds: I. Carbon isotope effects in straight-chain alkanes. *Russian Journal of Physical Chemistry* 47, 1564-1566.
- Galimov, E.M., 1975. Carbon isotopes in oil-gas geology. NASA Technical Translation. NASA TT F-682, Washington DC, 395 pp.
- Galimov, E.M., 1988. Sources and mechanisms of formation of gaseous hydrocarbons in sedimentary rocks. *Chemical Geology* 71, 77-95.
- Gilman, H., Zoellner, E. A., Dickey, J.B., 1929a. The Yields of Some Grignard Reagents. Alternating Properties of Normal Alkyl Bromides. *Journal of the American Chemical Society* 51(5), 1576-1583.
- Gilman, H., Zoellner, E. A., Dickey, J.B., 1929b. The Effect of Rapid Addition of Halide on the Yields of Some Grignard Reagents. *Journal of the American Chemical Society* 51(5), 1583-1587.
- Gilman, H., Gorsich, R.D., 1955. The Direct Preparation of Benzylolithium. *Journal of the American Chemical Society* 77(11), 3134 -3135.
- Goericke, R., Montoya, J.P., Fry, B., 1994. Physiology of isotope fractionation in algae and cyanobacteria. In: Lajtha, K., Micener, R.H., (Eds), *Stable Isotopes in Ecology and Environmental Science*, Blackwell Scientific Publications, Oxford, pp. 187-221.
- Gräber, W.D., Hüttinger, K.J., 1982. Chemistry of methane formation in hydrogasification of aromatics. 2. Aromatics with Aliphatic Groups. *Fuel* 61, 505-509.
- Grice, K., Cao, C., Love, G.D., Böttcher, M.E., Twitchett, R.J., Grosjean, E., Summons, R.E., Turgeon, S.C., Dunning, W., Jin, Y., 2005. Photic Zone Euxinia During the Permian-Triassic Superanoxic Event. *Science* 307, 706-709.

- Grigor'eva, E.N., Panchenko, S.S., Korbkov, V.Yu., Kalechits, I.V., 1991. Kinetic model of liquid-phase thermolysis of tetralin. *Solid Fuel Chemistry* 25, 101-106.
- Groenendyk, H., Levy, E.J., Sarnier, S.F., 1970. Controlled thermolytic dissociation of hexadecane and methyl decanoate. *Journal of Chromatographic Science* 8, 115-121.
- Harris, S. A., Whiticar, M.J., Fowler, M.G., 2003. Classification of Duvernay sourced oils from central and southern Alberta using Compound Specific Isotope Correlation (CSIC). *Bulletin of Canadian Petroleum Geology* 51 (2), 99-125.
- Hatanaka, Y., Hiyama, T., 1990. A Wide Range of Organosilicon Compounds Couples with Enol and Aryl Triflates in the Presence of Pd Catalyst and Fluoride Ion. *Tetrahedron Letters* 31(19), 2719-2722.
- Hayashi, T., Katsuro, Y., Okamoto, Y., Kumada, M., 1981. Nickel-Catalyzed Cross-Coupling of Aryl Phosphates With Grignard and Organoaluminium Reagents. Synthesis of Alkyl-, Alkenyl-, and Arylbenzenes from Phenols. *Tetrahedron Letters* 22(44), 4449-4452.
- Hayes, J.M., 1993. Factors controlling the ^{13}C contents of sedimentary organic compounds: principles and evidence. *Marine Geology* 113, 111-125.
- Hill, R.J., Tang, Y., Kaplan, I.R., Jenden, P.D., 1996. The influence of pressure on the thermal cracking of oil. *Energy and Fuels* 10, 873-882.
- Hill, R.J., Tang, Y., Kaplan, I.R., 2003. Insight into oil cracking based on laboratory experiments. *Organic Geochemistry* 34, 1651-1672.
- Hippler, H., Seisel, S., Troe, J., 1994. Pyrolysis of p-xylene and of 4-methylbenzyl radicals. 25th Symposium International on Combustion Proceedings 25, pp. 875-882.
- Hoefs, J., 1987. *Stable Isotope Geochemistry*, Springer-Verlag, Berlin.
- Hood, A., Gutjahr, C.C.M., Heacock, R.L., 1975. Organic metamorphism and generation of petroleum. *The American Association of Petroleum Geologists Bulletin* 59(6), 986-996.
- Horsfield, B., Schenk, H.J., Mills, N., Welte, D.H., 1992. An investigation of the in-reservoir conversion of oil to gas: compositional and kinetic findings from closed-system programmed-temperature pyrolyses. *Organic Geochemistry* 19, 191-204.
- Huc, A.Y., 1980. Origin and formation of organic matter in recent sediments and its relation to kerogen. In: *Kerogen*. Durand, B. (Ed.), Technip, Paris, pp 475-474.
- Hunt, J.M., 1996. *Petroleum Geochemistry and Geology*, Freeman, J.H. (Ed.), New York.
- Jackson, K.J., Burnham, A.K., Braun, R.L., Knauss, K.G., 1995. Temperature and pressure dependence of *n*-hexadecane cracking. *Organic Geochemistry* 23(10), 941-953.

- James, A.T., 1983. Correlation of natural gas by use of carbon isotopic distribution between hydrocarbon components. *The American Association of Petroleum Geologists Bulletin* 67(7), 1176-1191.
- Jenden, P.D., Newell, K.D., Kaplan, I.R., Watney, W.L., 1988. Composition and stable-isotope geochemistry of natural gases from Kansas, Midcontinent, U.S.A. *Chemical Geology* 71, 117-147.
- Jenden, P.D., Kaplan, I.R., 1989. Origin of natural gas in the Sacramento Basin, California. *The American Association of Petroleum Geologists Bulletin* 73, 431-453.
- Jess, A., 1996. Mechanisms and kinetics of thermal reactions of aromatic hydrocarbons from pyrolysis of solid fuels. *Fuel* 75(12), 1441-1448.
- Kataoka, N., Shelby, Q., Stambuli, J.P., Hartwig, J.F., 2002. Air Stable, Sterically Hindered Ferrocenyl Dialkylphosphines for Palladium-Catalyzed C-C, C-N, and C-O Bond-Forming Cross-Couplings. *Journal of Organic Chemistry* 67(16), 5553-5566.
- Kee, R.J., Rupley, F.M., Miller, J.A., 1989. CHEMKIN II: a Fortran chemical kinetics package for the analysis of gase-phase chemical kinetics. Sandia National Laboratories, Albuquerque, New-Mexico, U.S.A. Report SAND89-8009.
- Kharasch, M.S., Reinmuth, O., 1954. "Grignard Reactions of Non-metallic Substances", In: Englewood Cliffs, N.J. (Ed.), Prentice Hall, pp.122 and 1056.
- Khorasheh, F., Gray, M.R., 1993. High-pressure thermal cracking of n-hexadecane. *Industrial and Engineering Chemistry Research* 32(9), 1853-1863.
- Klingstedt, T., Fredj, T., 1983. Nickel-Catalyzed Synthesis of Arylacetic Esters from Arylzinc Chlorides and Ethyl Bromoacetate. *Organometallics* 2(5), 598-600.
- König, H., 1992. Microbiology of methanogens. *Bacterial Gas*, Vially, R. (Ed.), Editions Technip, Paris, pp. 3-11.
- Korobkov, V.Y., Kalechits, I.V., 1991. Kinetics of the thermolysis of para-substituted 1,2-diarylethanes. Effect of substituents on the strength of the CH₂-CH₂-bond. *Russian Journal of Physical Chemistry* 65, 346-351.
- Kossiakoff, A., Rice, F.O., 1943. Thermal Decomposition of Hydrocarbons, Resonance Stabilization and Isomerization of Free Radicals. *Journal of the American Chemical Society* 65(4), 590-595.
- Kressmann, S., 1991. Craquage thermique de mélanges d'hydrocarbures à haute pression: Etude cinétique expérimentale et modélisation numérique, implication pour la géochimie pétrolière. PhD dissertation, Université Paris-VI, Paris, France.

- Kumada, M., 1980. Nickel and Palladium Complex Catalyzed Cross-Coupling Reactions of Organometallic Reagents with Organic Halides. *Pure and Applied Chemistry* 52, 669-679.
- Kuo, L.C., Michael, G.E., 1994. A multicomponent oil-cracking model for modelling preservation and composition of reservoired oil. *Organic Geochemistry* 21, 911-925.
- Lannuzel, F., 2007. Influence des aromatiques sur la stabilité thermique des pétroles dans les gisements. PhD Dissertation, Institut National Polytechnique de Lorraine, Nancy, France.
- Largeau, C., Derenne, S., Casadevall, E., Kadouri, A., Sellier, N., 1986. Pyrolysis of immature Torbanite and of the resistant biopolymer (PRBA) isolated from extant alga *Botryococcus braunii*. Mechanism of formation and structure of Torbanite. *Organic Geochemistry* 10, 1023-1032.
- Laws, E.A., Popp, B.N., Bidigare, R.R., Kennicutt, M.C., Macko, S.A., 1995. Dependence of phytoplankton isotopic composition on growth rate and $[\text{CO}_2]_{\text{aq}}$: Theoretical considerations and experimental results. *Geochimica et Cosmochimica Acta* 59, 1131-1138.
- Leininger, J.P., Lorant, F., Minot, C., Behar, F., 2006. Mechanisms of 1-Methylnaphthalene Pyrolysis in a Batch Reactor. *Energy and Fuels* 20, 2518-2530.
- Leininger, J.P., Minot, C., Lorant, F., Behar, F., 2007. Density Functional Theory Investigation of Competitive Free-Radical Processes during the Thermal Cracking of Methylated Polyaromatics: Estimation of Kinetic Parameters. *Journal of Physical Chemistry A* 111(16), 3082-3090.
- Leyssale, F., 1991. Etude de la pyrolyse d'alkylpolyaromatiques appliquées aux procédés de conversion des produits lourds du pétrole. PhD dissertation, Université Paris-VI, Paris, France.
- Lorant, F., Prinzhofer, A., Behar, F., Huc, Y.A., 1998. Carbon isotopic and molecular constraints on the formation and the expulsion of thermogenic hydrocarbon gases. *Chemical Geology* 147, 249-264.
- Lorant, F., Behar, F., Vandenbroucke, M., McKinney, D.E., Tang, Y., 2000. Methane Generation from Methylated Aromatics: Kinetic Study and Carbon Isotope Modeling. *Energy and Fuels* 14, 1143-1155.
- Lorant, F., Behar, F., 2001. Carbon isotopic characterization of late methane. 20th International Meeting on Organic Geochemistry, Nancy, France.
- Louw, R., Lucas, H.J., 1973. Vapour phase chemistry of arenes. I. Thermolysis of benzene and derivatives; the effect of additives. Evidence for free radical chain processes. *Journal of the Royal Netherlands Chemical Society* 92, 55-71.

- Luo, Y.R., 2003. Handbook of Bond Dissociation Energies in Organic Compounds, CRC Press, Boca Raton, Florida.
- Martin, R., Fürstner, A., 2004. Cross-Coupling of Alkyl Halides with Aryl Grignard Reagents Catalyzed by a Low-Valent Iron Complex. *Angewandte Chemie* 116, 4045-4047.
- Marynowski, L., Rospndek, M.J., Meyer zu Reckendorf, R., Simoneit, B.R.T., 2002. Phenylidibenzofurans and phenylidibenzothiophenes in marine sedimentary rocks and hydrothermal petroleum. *Organic Geochemistry* 33, 701-714.
- Matthews, D.E., Hayes, J.M., 1978. Isotope-ratio-monitoring gas chromatography-mass spectrometry. *Analytical Chemistry* 50, 1465-1473.
- McClaine, J.W., Wornat, M.J., 2007. Reaction Mechanisms Governing the Formation of Polycyclic Aromatic Hydrocarbons in the Supercritical Pyrolysis of Toluene: C₂₈H₁₄ Isomers. *Journal of Physical Chemistry C* 111, 86-95.
- McKinney, D.E., Behar, F., Hatcher, P.G., 1998. Reaction kinetics and *n*-alkane product profile from the thermal degradation of ¹³C-labeled *n*-C₂₅ in two dissimilar oils as determined by SIM/GC/MS. *Organic Geochemistry* 29, 119-136.
- Merrill, R.E., Negishi, E., 1974. Tetrahydrofuran-Promoted Aryl-Alkyl Coupling Involving Organolithium Reagents. *Journal of Organic Chemistry* 39(23), 3452-3453.
- Miller, R.G., Fahey, D.R., Kuhlman, D.P., 1968. Thermolysis of *trans*-chloro(2-allylphenyl)bis(triethylphosphine)nickel(II). *Journal of the American Chemical Society* 90(22), 6248-6250.
- Miller, R.G., Stauffer R.D., Fahey D.R., Parnell D.R., 1970. Alkenylaryl Compounds of Nickel(II) and Palladium(II). Influence of the Transition Metal on Ligand Proton Chemical Shifts. *Journal of the American Chemical Society* 92(6), 1511-1521.
- Miller, R.G., Kuhlman, D.P., 1971. A Carbon-Nickel Addition to Benzyne. *Journal of Organometallic Chemistry* 26(3), 401-406.
- Milstein, D., Stille, J. K., 1979. Palladium-Catalyzed Coupling of Tetraorganotin Compounds with Aryl and Benzyl Halides. Synthetic Utility and Mechanism. *Journal of the American Chemical Society* 101(17), 4992-4998.
- Mizerka, L.J., Kiefer, J.H., 1986. The high temperature pyrolysis of ethylbenzene: evidence for dissociation to benzyl and methyl radicals. *International Journal of Chemical Kinetics* 18(3), 363-378.

- Moss, J.R., Shaw, B.L., 1966. Nuclear Magnetic Resonance Studies on Metal Complexes. Part IV. Arylnickel(II)–Dimethylphenylphosphine Complexes. *Journal of the Chemical Society A*, 1793-1795.
- Murray, A.P., Summons, R.E., Boreham, C.J., Dowling, L.M., 1994. Biomarker and *n*-alkane isotope profiles for Tertiary oils: relationship to source rock depositional setting. *Organic Geochemistry* 22, 521-542.
- N.I.S.T. (National Institute of Standards and Technology) Chemical Kinetics Database, 1998. In: Westley, F., Herron, J.T., Hampson, R.F., Mallard, W.G. (Eds.), *Compilation of chemical kinetic data for combustion chemistry*, U.S. Department of Commerce, Gaithersburg, MD.
- Pallasser, R.J., 2000. Recognising biodegradation in gas/oil accumulations through the $\delta^{13}\text{C}$ compositions of gas components. *Organic Geochemistry* 31, 1363-1373.
- Palmer, S.E., 1993. Effect of biodegradation and water washing on crude oils composition. In: Engel, M.H., Macko, S. (Eds.), *Organic Geochemistry Principles and Applications*, Plenum Press, New York, pp 511-533.
- Pamidimukkala, K.M., Kern, R.D., Patel, M.R., Wei, H.C., Kiefer, J.H., 1987. High-temperature Pyrolysis of Toluene. *Journal of Physical Chemistry* 91, 2148-2154.
- Pelet, R., 1980. Evolution géochimique de la matière organique. In: Durand, B (Ed.), *Kerogen-insoluble organic matter from sedimentary rocks*. Editions Technip, Paris, pp 475-499.
- Pepper, A.S., Dodd, T.A., 1995. Simple kinetic models of petroleum formation. Part II: oil – gas cracking. *Marine and Petroleum Geology* 12, 321-340.
- Percec, V., Bae, J.Y., Hill, D.H., 1995. Aryl Mesylates in Metal Catalyzed Homo- and Cross-Coupling Reactions. 4. Scope and Limitations of Aryl Mesylates in Nickel Catalyzed Cross-Coupling Reactions. *Journal of Organic Chemistry* 60(21), 6895-6903.
- Poljakov, V.B., 1996. The development of the theory of stable isotopes fractionation and its application to geochemistry. PhD Dissertation, Geochemistry and Analytical Chemistry Institute, Russian Academy of Sciences, Moscow, Russia.
- Popp, B.N., Laws, E.A., Bidigare, R.R., Dore, J.E., Hanson, K.L., Wakeham, S.G., 1998. Effect of phytoplankton cell geometry on carbon isotopic fractionation. *Geochimica et Cosmochimica Acta* 62, 69-79.
- Poutsma, M.L., 1990. Free-Radical Thermolysis and Hydrogenolysis of Model Hydrocarbons Relevant to Processing of Coal. *Energy and Fuels* 4(2), 113-131.

- Poutsma, M.L., 2002. Progress toward the Mechanistic Description and Simulation of the Pyrolysis of Tetralin. *Energy and Fuels* 16, 964-996.
- Rai, R., Aubrecht, K.B., Collum, D.B., 1995. Palladium-Catalyzed Stille Couplings of Aryl-, Vinyl-, and Alkyltrichlorostannanes in Aqueous Solution. *Tetrahedron Letters* 36(18), 3111-3114.
- Rao, V.S., Skinner, G.B., 1989. Formation of hydrogen and deuterium atoms in the pyrolysis of toluene-d₈ and toluene- α,α,α -d₃ behind shock waves. *Journal of Physical Chemistry* 93(5), 1864-1869.
- Rausch, M.D., Tibbetts, F.E., 1970. Perhaloarylmethyl chemistry. V. Formation and properties of some sigma-perhaloaryl and methyl derivatives of nickel. *Inorganic Chemistry* 9(3), 512-516.
- Rayleigh, R.S., 1896. Theoretical considerations respecting the separation of gases by diffusion and similar processes. *The London, Edinburgh, and Dublin Philosophical Magazine* 42, 493-498.
- Razafinarivo, N., 2006. Etude cinétique de la pyrolyse du *n*-octane induite par un superoxyde. Application à l'évolution thermique des pétroles dans les gisements. PhD Dissertation, Institut National Polytechnique de Lorraine, Nancy, France.
- Rice, F.O., 1931. The Thermal Decomposition of Organic Compounds from the Standpoint of Free Radicals. I. Saturated Hydrocarbons. *Journal of the American Chemical Society* 53, 1959-1972.
- Rice, F.O., 1933. The thermal decomposition of organic compounds from the standpoint of free radicals. III. The calculations of the products formed from paraffin hydrocarbons. *Journal of the American Chemical Society* 55, 3035-3040.
- Rice, F.O., Hertzfeld, K.F., 1934. The thermal decomposition of organic compounds from the standpoint of free radicals. VI. The mechanism of some chain reactions. *Journal of the American Chemical Society* 56, 284-289.
- Rice, D.D., Claypool, G.E., 1981. Generation, accumulation, and resource potential of biogenic gas. *The American Association of Petroleum Geologists Bulletin* 65, 5-25.
- Ritter, E.R., Bozzelli, J.W., Dean, A.M., 1990. Kinetic study on thermal decomposition of chlorobenzene diluted in H₂. *Journal of Physical Chemistry* 94(6), 2493-2504.
- Robaugh, D.A., Stein, S.E., 1981. Very-low-pressure pyrolysis of ethylbenzene, isopropylbenzene and tert-butylbenzene. *International Journal of Chemical Kinetics* 13(5), 445-462.

- Robaugh, D., Tsang, W., 1986. Mechanism and rate of hydrogen atom attack on toluene at high temperatures. *Journal of Physical Chemistry* 90(17), 4159-4163.
- Rooney, M.A., Claypool, G.E., Chung, H.M., 1995. Modeling thermogenic gas generation using carbon isotope ratios of natural gas hydrocarbons. *Chemical Geology* 126, 219-232.
- Roshchin, A.I., Bumagin, N.A., Beletskaya, I.P., 1995. Palladium-Catalyzed Cross-Coupling Reaction of Organostannoates with Aryl Halides in Aqueous Medium. *Tetrahedron Letters* 36(1), 125-128.
- Saa, J.M., Martorell, G., Garcia-Raso, A., 1992. Palladium-Catalyzed Cross-Coupling Reactions of Highly Hindered, Electron-Rich Phenol Triflates and Organostannanes. *Journal of Organic Chemistry* 57(2), 678-685.
- Sackett, W.M., Nakaparksin, S., Dalrymple, D., 1966. Carbon isotope effects in methane production by thermal cracking. In: Hobson, G.D., Speers, G.G. (Eds.), *Advances in Organic Geochemistry*, Pergamon Press, Oxford, pp. 37-53.
- Sackett, W.M., 1968. Carbon isotope composition of natural methane occurrences. *The American Association of Petroleum Geologists Bulletin* 52, 853-857.
- Sallé C., Debysier J., 1976. Formation des gisements de pétrole, étude des phénomènes géologiques fondamentaux, Editions Technip, Paris.
- Santos Neto, E.V., Hayes, J.M., 1999. Use of hydrogen and carbon stable isotopes characterizing oils from the Potiguar Basin (onshore), Northeastern Brasil. *The American Association of Petroleum Geologists Bulletin* 83, 496-518.
- Savage, P.E., Klein, M.T., 1987. Asphaltene reaction pathways. 2. Pyrolysis of *n*-pentadecylbenzene. *Industrial and Engineering Chemistry Research* 26, 488-494.
- Savage, P.E., Klein, M.T., 1988. Asphaltene reaction pathways. 4. Pyrolysis of tricyclohexane and 2-ethyltetralin. *Industrial and Engineering Chemistry Research* 27(8), 1348-1356.
- Savage, P.E., Korotney, D.J., 1990. Pyrolysis kinetics for long chain *n*-alkylbenzenes: experimental and mechanistic modelling results. *Industrial and Engineering Chemistry Research* 29, 499-502.
- Savage, P.E., 1995. Hydrogen-transfer mechanisms in 1-Dodecylpyrene pyrolysis. *Energy and Fuels* 9, 590-598.
- Savage, P.E., Baxter, K.L., 1996. Pathway, kinetics, and mechanisms for 2-dodecyl-9,10-dihydrophenanthrene pyrolysis. *Industrial and Engineering Chemistry Research* 35, 1517-1523.
- Savage, P.E., 2000. Mechanisms and kinetics models for hydrocarbon pyrolysis. *Journal of Analytical and Applied Pyrolysis* 54, 109-126.

- Schaeffgen, J.R., 1955. The Pyrolysis of *p*-Xylene. *Journal of Polymer Science* 15, 203-219.
- Schenk, H.J., Di Primio, R., Horsfield, B., 1997. The conversion of oil into gas in petroleum reservoirs. Part I: Comparative kinetic investigation of gas generation from crude of lacustrine, marine and fluviodeltaic origin by programmed-temperature closed-system pyrolysis. *Organic Geochemistry* 26, 467-481.
- Schoell, M., 1983. Genetic characterization of natural gases. *The American Association of Petroleum Geologists Bulletin* 67(12), 2225-2238.
- Schoell, M., 1988. Multiple origin of methane in the Earth. *Chemical Geology* 71, 1-10.
- Schouten, S., Klein Breteler, W.C.M., Blokker, P., Schogt, N., Rijpstra, W.I.C., Grice, K., Baas, M., Sinninghe Damsté, J.S., 1998. Biosynthetic effects on the stable carbon isotopic compositions of algal lipids: Implications for deciphering the carbon isotopic biomarker record. *Geochimica et Cosmochimica Acta* 62, 1397-1406.
- Shah, Y.T., Stuart, E.B., Kunzru, D., 1973. Thermal cracking of hydrocarbon mixtures : mixtures of octane-nonane and nonane-2-pentene. *Industrial and Engineering Chemistry Research Process Design and Development* 12, 344-351.
- Shinokubo, H., Oshima, K., 2004. Transition Metal-Catalyzed Carbon-Carbon Bond Formation with Grignard Reagents - Novel Reactions with a Classic Reagent. *European Journal of Organic Chemistry* 10, 2081-2091.
- Sinninghe Damsté, J.S., De Leeuw, J.W., 1990. Analysis, structure and geochemical significance of organically-bound sulphur in the geosphere: State of the art and future research. *Organic Geochemistry* 16, 1077-1101.
- Sinninghe Damsté, J.S., Kohnen, M.E., Horsfield, B., 1998. Origin of low-molecular-weight alkylthiophenes in pyrolysates of sulphur-rich kerogens as revealed by micro-scale sealed vessel pyrolysis. *Organic Geochemistry* 29, 1891-1903.
- Smith, J.E., Erdman, J.G., Morris, D.A., 1971. Migration, accumulation and retention of petroleum in the Earth. 8th World Petroleum Congress, Proceedings 2, pp. 13-26.
- Smith, C.M., Savage, P.E., 1991. Reactions of polycyclic alkylaromatics: Structure and reactivity. *American Institute of Chemical Engineers Journal* 37, 1613-1624.
- Smith, C.M., Savage, P.E., 1992. Reactions of Polycyclic Alkylaromatics. 4. Hydrogenolysis Mechanisms in 1-Alkylpyrene Pyrolysis. *Energy and Fuels* 6, 195-202.
- Smith, C.M., Savage, P.E., 1993. Reactions of Polycyclic Alkylaromatics. 5. Pyrolysis of Methylanthracenes. *American Institute of Chemical Engineers Journal* 39(8), 1355-1362.
- Smith, C.M., Savage, P.E., 1994. Reactions of Polycyclic Alkylaromatics – VI. Detailed Chemical Kinetic Modeling. *Chemical Engineering Science* 49(2), 259-270.

- Sofer, Z., 1984. Stable carbon isotope compositions of crude oils: Application to source depositional environments and petroleum alteration. *The American Association of Petroleum Geologists Bulletin* 68, 31-49.
- Song, C., Lai, W., Schobert, H.H., 1994. Condensed-phase pyrolysis of the n-tetradecane at elevated pressures for long duration. Products and reaction mechanism. *Industrial and Engineering Chemistry Research* 33, 534-547.
- Stahl, W.J., Carey, B.D.Jr., 1975. Source-rock identification by isotope analyses of natural gases from fields in the Val Verde and Delaware Basins, West Texas. *Chemical Geology* 16, 257-267.
- Sundberg, K.R., Bennet, C.R., 1983. Carbon isotope paleothermometry of natural gas. In: Bjoroy, M. (Ed.), *Advances in Organic Geochemistry*, Wiley, pp. 769-774.
- Szwarc, M., 1948. The C-H Bond Energy in Toluene and Xylenes. *Journal of Chemical Physics* 16(2), 128-136.
- Takahasi, M., 1960. Pyrolysis of Organic Compounds. I. Kinetic Study of the Pyrolysis of Toluene. *Bulletin of the Chemical Society of Japan* 33, 801-808.
- Tamao, K., Sumitani, K., Kumada, M., 1972. Selective Carbon-Carbon Bond Formation by Cross-Coupling of Grignard Reagents with Organic Halides. Catalysis by Nickel-Phosphine Complexes. *Journal of the American Chemical Society* 94(12), 4374-4376.
- Tamao, K., Sumitani, K., Kiso, Y., Zembayashi, M., Fujioka, A., Kodama, S., Nakajima, I., Minato, A., Kumada, M., 1976. Nickel-Phosphine Complex-Catalyzed Grignard Coupling. I. Cross-Coupling of Alkyl, Aryl, and Alkenyl Grignard Reagents with Aryl and Alkenyl Halides: General Scope and Limitations. *Bulletin of the Chemical Society of Japan* 49(7), 1958-1969.
- Tamura, M., Kochi, J., 1971. Coupling of Grignard Reagents with Organic Halides. *Synthesis* 6, 303-305.
- Tang, Y., Jenden, P.D., 1995. Theoretical modelling of carbon and hydrogen isotope fractionations in natural gas. In: Grimalt, J.O., Dorronso, C. (Eds.), *Organic Geochemistry: developments and applications to energy, climate, environment and human history*. Donastia-San Sebastian, Spain, pp 1067-1069.
- Tang, Y., Perry, J.K., Jenden, P.D., Schoell, M., 2000. Mathematical modeling of stable carbon isotope ratios in natural gases. *Geochimica et Cosmochimica Acta* 64 (15), 2673-2687.
- Taralas, G., Kontominas, M.G., Kakatsios, X., 2003. Modelling the thermal destruction of toluene (C₇H₈) as tar-related species for fuel gas cleanup. *Energy and Fuels* 17, 329-337.

- Tilicheev, M.D., 1939. Kinetics of cracking hydrocarbons under pressure. First article. Cracking of normal paraffin hydrocarbons. *Foreign Petroleum Technology* 7, 209-224.
- Tissot, B., Durand, B., Espitalié, J., Combaz, A., 1974. Influence of the nature and diagenesis of organic matter in formation of petroleum. *The American Association of Petroleum Geologists Bulletin* 58, 499-506.
- Tissot, B., Welte, D.H., 1984. *Petroleum Formation and Occurrence*, 2nd Edition. Springer Verlag, Berlin.
- Tokmakov, I.V., Park, J., Gheyas, S., Lin, M.C., 1999. Experimental and theoretical studies of the reaction of the phenyl radical with methane. *Journal of Physical Chemistry A* 103, 3636-3645.
- Tsang, W., 1991. Chemical Kinetic Data Base for Combustion Chemistry Part V. Propene. *Journal of Physical and Chemical Reference Data* 20(2), 221-273.
- Tsang, W., Walker, J.A., 1992. Pyrolysis of 1,7-octadiene and the kinetic and thermodynamic stability of allyl and 4-pentenyl radicals. *Journal of Physical Chemistry* 96, 8378-8384.
- Uchino, M., Yamamoto, A., Ikeda, S., 1970. Preparation of a phenyl-nickel complex, phenyl(dipyridyl)nickel chloride, an olefin dimerization catalyst. *Journal of Organometallic Chemistry* 24(3), C63-C64.
- Urey, H.C., 1947. The thermodynamic properties of isotopic substances. *Journal of the Chemical Society* 57, 562-581.
- Urey, H.C., Lowenstam, H.A., Epstein, S., McKinney, C.R., 1951. Measurement of palaeotemperatures and temperatures of the upper Cretaceous of England, Denmark, and Southeastern United States. *The American Association of Petroleum Geologists Bulletin* 62, 399-416.
- Vandenbroucke, M., Behar, F., Rudkiewicz, J.L., 1999. Kinetic modelling of petroleum formation and cracking: Implication from the high pressure/high temperature Elgin Field (UK, North Sea). *Organic Geochemistry* 30, 1105-1125.
- Vandenbroucke, M., Largeau, C., 2007. Review: Kerogen origin, evolution and structure. *Organic Geochemistry* 38, 719-833.
- Van Krevelen, D.W., 1961. *Coal*. Elsevier Editions, Amsterdam.
- Vedejs, E., Haight, A. R., Moss, W. O., 1992. Internal Coordination at Tin Promotes Selective Alkyl Transfer in the Stille Coupling Reaction. *Journal of the American Chemical Society* 114(16), 6556-6558.
- Virk, P.S., Vlastnik, V.J., 1992. Pathways for thermolysis of 9,10-dimethylanthracene. *American Chemical Society Division of Fuel Chemistry* 37, 947.

- Voge, H.H., Good, G.M., 1949. Thermal cracking of higher paraffins. *Journal of the American Chemical Society* 71, 593-597.
- Waples, D.W., Tornheim, L., 1978. Mathematical models for petroleum-forming processes: carbon isotope fractionation. *Geochimica et Cosmochimica Acta* 42(5), 467-472.
- Waples, D.W., 1981. *Organic geochemistry for exploration geologists*, Burgess publishing company, Minneapolis.
- Watanabe, M., Tadafumi, T., Arai, K., 2001. Overall rate constant of pyrolysis of *n*-alkanes at a low conversion level. *Industrial and Engineering Chemistry Research* 40, 2027-2036.
- Whitesides, G.M., Fisher, Jr.W.F., San Filippo, Jr.J., Bashe, R.W., House H.O., 1969. Reaction of Lithium Dialkyl- and Diarylcuprates with Organic Halides. *Journal of the American Chemical Society* 91(17), 4871-4882.
- Whiticar, M.J., Faber, E., Schoell, M., 1986. Biogenic methane formation in marine and freshwater environments: CO₂ reduction vs. acetate fermentation-isotope evidence. *Geochimica et Cosmochimica Acta* 50, 693-709.
- Whiticar, M.J., 1994. Correlation of natural gases with their sources. In: *The Petroleum system – from source to trap*, Magoon, L.B., Dow, W.G. (Eds.). American Association of Petroleum Geologists Memoir 60, pp 261-283.
- Whiticar, M.J., Snowdon, L.R., 1999. Geochemical characterization of selected Western Canada oils by C₅-C₈ Compound Specific Isotope Correlation (CSIC). *Organic Geochemistry* 30 (9), 1127-1161.
- Wu, G., Katsumura, Y., Matsuura, C., Ishigure, K., Kubo, J., 1996. Comparison of liquid-phase and gas-phase pure thermal cracking of *n*-hexadecane. *Industrial and Engineering Chemistry Research* 35, 4747-4754.
- Xiong, Y., Geng, A., Liu, J., 2004. Kinetic-simulating experiment combined with GC-IRMS analysis: application to identification and assessment of coal-derived methane from Zhongba Gas Field (Sichuan Basin, China). *Chemical Geology* 213, 325-338.
- Yamazaki, H., Nishido, T., Matsumoto, Y., Sumida, S., Hagihara, N., 1966. Preparations of σ -Bonded Alkyl-, Aryl- and Alkynylnickel Compounds. *Journal of Organometallic Chemistry* 6(1), 86-91.
- Yang, J., Lu, M., 2005. Thermal growth and decomposition of methylnaphthalenes. *Environmental Science and Technology* 39, 3077-3082.
- Yu, J., Eser, S., 1997a. Thermal decomposition of C₁₀-C₁₄ normal alkanes in near-critical and supercritical regions. Products distribution and reaction mechanisms. *Industrial and Engineering Chemistry Research* 36, 574-584.

- Yu, J., Eser, S., 1997b. Kinetics of supercritical phase thermal decomposition of C₁₀-C₁₄ normal alkanes and their mixtures. Products distribution and reaction mechanisms. *Industrial and Engineering Chemistry Research* 36, 585-591.
- Yu, J., Eser, S., 1998a. Thermal Decomposition of Jet Fuel Model Compounds under Near-Critical and Supercritical Conditions. 1. *n*-Butylbenzene and *n*-Butylcyclohexane. *Industrial and Engineering Chemistry Research* 37(12), 4591-4600.
- Yu, J., Eser, S., 1998b. Thermal Decomposition of Jet Fuel Model Compounds under Near-Critical and Supercritical Conditions. 2. Decalin and tetralin. *Industrial and Engineering Chemistry Research* 37(12), 4601-4608.
- Yuan, K., Scott, W.J., 1991. Nickel-Catalyzed Cross-Coupling of Unactivated Neopentyl Iodides with Grignard Reagents. *Tetrahedron Letters* 32(2), 189-192.
- Zhou, P., Hollis, O.L., Crynes, B.L., 1987. Thermolysis of higher molecular weight straight-chain alkanes. *Industrial and Engineering Chemistry Research* 26, 846-852.
- Zhu, R.S., Xu, Z.F., Lin, M.C., 2004. Ab Initio studies of alkyl radical reactions: combination and disproportionation reactions of CH₃ with C₂H₅, and the decomposition of chemically activated C₃H₈. *Journal of Chemical Physics* 120(20), 6566-6573.
- Zimmerman, C.C., York, R., 1964. Thermal demethylation of toluene. *Industrial and Engineering Chemistry Process Design and Development* 3, 254-258.

APPENDIX IV:

**PhD co-tutelle
agreements between**

***Université Pierre et
Marie Curie***

and

***Curtin University
of Technology***

COOPERATION AGREEMENT ON JOINTLY SUPERVISED Ph.D.

BETWEEN

The University Pierre et Marie Curie, represented by Mr. G. BEREZIAT, President
4, place Jussieu – 75252 Paris cedex 05 - FRANCE

and

Curtin University of Technology represented by Mr L. TWOMEY, Vice-Chancellor
Chancellory Building 100, GPO Box U1987 Perth WA 6845-AUSTRALIA
(that will be designated below as the contracting institution)

have decided the following :

TITLE I Generalities

ARTICLE 1

The Université Pierre et Marie Curie and the contracting institution decide to register Mr, FUSETTI Luc for a Ph.D. thesis preparation, under supervision between the two co-signatory institutions.

ARTICLE 2

Title : Elaboration of a kinetic model in order to predict the molecular and isotopic composition for natural gases produced during hydrocarbon cracking.

ARTICLE 3

Intellectual Property rights relative to the results obtained during the common research programs, will be protected according to the laws in force in each country.

ARTICLE 4

The results obtained in the course of research programs do not allow registration of a patent or commercial exploitation by one University without written permission given by the other. As far as it is possible, eventual patents must be registered jointly. If one party gives no reply within 90 (ninety) days, the other party is entitled to register them under its own name. The publication or free exchange of scientific results will neither give rise to any preliminary permission nor any financial compensation, except if non disclosure statement is attached to the program.

TITLE II Administrative modalities

ARTICLE 5

The enrolment of the Ph.D. student is effective from 2nd November, 2005. The expected length of research is set to 3 years. This length can only be extended in exceptional cases, after a favourable opinion given by the two institutions and on proposition by the Ph.D. advisers. This proposition must be introduced 6 months before the expected date of the end of the Ph.D. thesis set above.

ARTICLE 6

The research will be carried out in both institutions following a calendar which can be found in the enclosed appendix, and approved jointly by the two Ph.D. advisers. Any modification of this calendar must be submitted to the two institutions by the Ph.D. thesis advisers at least 1 month in advance.

ARTICLE 7

The Ph.D. student must be registered in both institutions. The registration fees will be paid to the University Pierre et Marie Curie. The contracting institution, Curtin University of Technology, will not take any registration fees.

ARTICLE 8

The Ph.D. student must take a main insurance in the country where he pays the registration fees. He must also apply for a complementary insurance in the cosignatory country of the convention.

ARTICLE 9

Mrs Kliti GRICE, Associate Professor and Mrs Sylvie DERENNE, Directeur de Recherche CNRS are respectively designated by Curtin University of Technology and the University Pierre et Marie Curie to be Ph.D. advisers. They will ensure the follow up of the student in the conditions required by each institution. They will consult regularly on the research progress of the Ph D. student.

TITLE III
Pedagogical modalities

ARTICLE 10

The authorisation of the thesis submission is given in agreement between both institutions, in conformity with their regulations and after a favourable opinion of their competent departments.

The thesis committee is designated by the legal authorities of the institution where the thesis is submitted, after agreement from the cosignatory institution. It will be equally composed by academic representatives from both countries and will include at least four members, two of whom are the two Ph.D. advisers. It will include at least one professor from each university.

ARTICLE 11

The thesis will be presented at Paris. It will be written in English. A written summary will be written in French and English. The thesis will be presented in English, the written summary will be presented in French.

ARTICLE 12

A short report will be written in English and translated into French. This report will allow the evaluation of the capacity of the Ph.D. student to present his work and show that he masters his research subject.

After the committee has given a favorable advice, the University Pierre et Marie Curie will confer the Ph.D. degree of the University Pierre et Marie Curie and, the contracting institution will confer the Ph.D. degree of Curtin University of Technology.

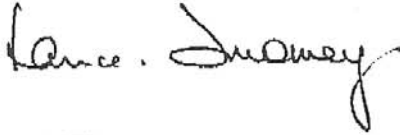
ARTICLE 13

The Ph.D. student must follow the rules of both countries concerning the registering, the description and the reproduction of the thesis.

ARTICLE 14

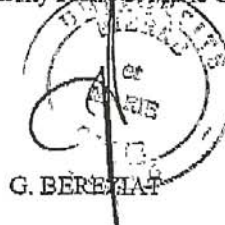
The present convention holds for 3 years. It could be extended following conditions described in article 5.

Perth, 16.12.2005
The Vice-Chancellor of Curtin University of
Technology



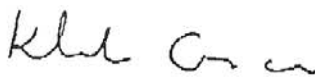
L. TWOMEY

Paris, 5 December 2005
The President of
the University Pierre et Marie Curie



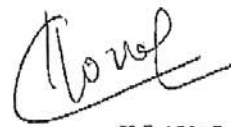
G. BERTHIAT

The Director of the Doctoral School of Sciences de
l'Environnement d'Ile de France (ED n°129)



The PhD adviser of Curtin University of
Technology

K. GRICE



K. LAVAL

Katja LAVAL
Directrice de l'Ecole Doctorale
Sciences de l'Environnement

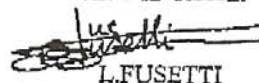
The PhD adviser of the
University Pierre et Marie Curie



S. DERENNE
Directeur de Recherche CNRS

S. DERENNE

The PhD student



L. FUSETTI

CONVENTION DE THÈSE EN COTUTELLE

ENTRE

L'Université Pierre et Marie Curie, représentée par M. G. BEREZIAT, Président
Site 4, place Jussieu – 75252 Paris cedex 05 - FRANCE

ET

Curtin University of Technology représentée par M. L. TWOMEY, Vice-Chancellor
Site, Chancellory Building 100, GPO Box U1987 Perth WA 6845-AUSTRALIE
ci-après désigné l'établissement contractant

sont convenues :

TITRE I

Modalités générales

ARTICLE 1

L'Université Pierre et Marie Curie et l'établissement contractant décident d'inscrire M. FUSSETTI Luc en vue de la préparation d'une thèse en cotutelle entre les deux établissements signataires.

ARTICLE 2

Titre de la thèse : Élaboration d'un modèle cinétique en vue de prédire la composition moléculaire et isotopique des gaz naturels issus du craquage des hydrocarbures.

ARTICLE 3

Les droits de propriété intellectuelle relatifs aux résultats obtenus au cours de programmes communs de recherche sont protégés suivant les lois en vigueur dans les pays des chercheurs impliqués.

ARTICLE 4

Les résultats obtenus au cours de programmes de recherche ne peuvent donner lieu à une prise de brevet ou à une exploitation commerciale par une seule des deux universités sans autorisation préalablement écrite de l'autre. Les prises de brevet éventuelles doivent, dans la mesure du possible, être déposées conjointement. Si l'une d'elles ne répond pas dans les 90 (quatre-vingt-dix) jours à la sollicitation de l'autre, cette dernière est en droit de déposer les prises de brevet en son nom propre. Les deux universités sont soumises aux règles nationales respectives de demande de brevet. La publication ou l'échange gratuit des résultats scientifiques ne donne lieu ni à autorisation préalable ni à contrepartie financière sauf si une confidentialité est attachée à ce programme au titre d'un accord industriel ou des règles de la recherche publique.

TITRE I

Modalités administratives

ARTICLE 5

L'inscription du doctorant prend effet le 2 novembre 2005. La durée prévisionnelle des travaux de recherche est fixée à 3 ans. Cette durée ne pourra être prolongée qu'à titre exceptionnel après avis favorable des deux établissements et sur proposition des directeurs de thèse. Cette demande doit intervenir 6 mois avant la date prévisionnelle de fin de thèse.

ARTICLE 6

Les travaux de recherche seront effectués dans les deux établissements selon un calendrier qui figure en annexe élaboré après avis des deux directeurs de thèse prévus à l'article 9. La modification éventuelle de ce calendrier devra être demandée aux deux établissements signataires par les directeurs de thèse au moins un mois à l'avance.

ARTICLE 7

Le doctorant devra se conformer aux modalités d'inscription prévus dans les deux établissements. Les droits d'inscription seront perçus par l'Université Pierre et Marie Curie.
L'établissement contractant Curtin University of Technology exonère le doctorant des droits d'inscription.

ARTICLE 8

Le doctorant est tenu de prendre une assurance principale dans le pays où il paie ses droits d'inscription. En outre, il doit souscrire une assurance complémentaire dans le pays cosignataire de la convention.

TITRE II
Modalités pédagogiques

ARTICLE 9

Mme Kliti GRICE, Associate Professor et Mme Sylvie DERENNE, Directeur de Recherche CNRS sont respectivement désignées par Curtin University of Technology et l'Université Pierre et Marie Curie comme directeurs de thèse du doctorant. Elles assurent l'encadrement de celui-ci dans les conditions en vigueur dans chaque établissement signataire. Elles se concerteront régulièrement sur l'avancement des travaux de recherche du doctorant.

ARTICLE 10

L'autorisation de soutenance de la thèse est accordée conjointement par les deux établissements, après avis favorable de leurs instances compétentes et selon les modalités prévues par chacun de ces établissements. Le jury de la thèse est désigné par les autorités légales de l'établissement où la thèse sera soutenue, après accord de l'établissement cosignataire. Il est composé à parité par des représentants scientifiques des deux pays et comprend au moins quatre membres dont les deux directeurs de thèse. Il comprend au moins un professeur de chaque université.

ARTICLE 11

La thèse sera soutenue à Paris. Elle sera rédigée en langue anglaise. Un résumé écrit sera rédigé en langues française et anglaise. La thèse sera présentée en langue anglaise, le résumé sera présenté en langue française.

ARTICLE 12

Un rapport de soutenance unique sera établi en langue anglaise. Il sera traduit en langue française. Il devra permettre d'apprécier les aptitudes du candidat à exposer ses travaux et la maîtrise qu'il a de son sujet de recherche.

Après admission prononcée par le jury, l'Université Pierre et Marie Curie décernera le grade de Docteur de l'Université Pierre et Marie Curie et l'établissement contractant décernera le grade de Docteur de Curtin University of Technology.

ARTICLE 13

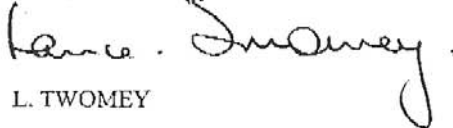
Le doctorant devra se conformer aux règles en vigueur dans les deux pays pour le dépôt, le signalement et la reproduction des thèses.

TITRE III
Dispositions finales

ARTICLE 14

La présente convention est passée pour une durée de 3 ans. Elle peut être prorogée selon les conditions prévues à l'article 5.

Perth, le 16.12.2005
The Vice-Chancellor of Curtin University
of Technology


L. TWOMEY

KL C


Le Directeur de Thèse de
Curtin University of Technology

K.GRICE

PARIS, le 5 de décembre 2005
Le Président de
l'Université Pierre et Marie Curie


Gilbert BEREZIAT


Le Directeur de l'École Doctorale Sciences de
l'Environnement d'Île de France (ED n°129)


K.LAVAL
Directrice de l'École Doctorale
Sciences de l'Environnement

Le Directeur de Thèse de
l'Université Pierre et Marie Curie


S. DERENNE
Directeur de Recherche CNRS
S.DERENNE

Le Doctorant


L.FUSETTI